ESTIMATION & CONTROL IN SPATIALLY DISTRIBUTED CYBER PHYSICAL SYSTEMS

by

SIDDHARTH DESHMUKH

B.E., National Institute of Technology, Raipur, India, 2004
M.Tech., Indian Institute of Technology, Delhi, India, 2006

AN ABSTRACT OF A DISSERTATION

submitted in partial fulfillment of the
requirements for the degree

DOCTOR OF PHILOSOPHY

Department of Electrical and Computer Engineering
College of Engineering

KANSAS STATE UNIVERSITY
Manhattan, Kansas
2013

Abstract

A cyber physical system (CPS) is an intelligent integration of computation and communication infrastructure for monitoring and/or control of an underlying physical system. In this dissertation, we consider a specific class of CPS architectures where state of the system is spatially distributed in physical space. Examples that fit this category of CPS include, smart distribution gird, smart highway/transportation network etc. We study state estimation and control process in such systems where, (1) multiple sensors and actuators are arbitrarily deployed to jointly sense and control the system; (2) sensors directly communicate their observations to a central estimation and control unit (ECU) over communication links; and, (3) the ECU, on computing the control action, communicates control actions to actuators over communication links. Since communication links are susceptible to random failures, the overall estimation and control process is subjected to: (1) partial observation updates in estimation process; and (2) partial actuator actions in control process. We analyze stochastic stability of estimation and control process, in this scenario by establishing the conditions under which estimation accuracy and deviation from desired state trajectory is bounded. Our key contribution is the derivation of a new fundamental result on bounds for critical probabilities of individual communication link failure to maintain stability of overall system. The overall analysis illustrates that there is trade-off between stability of estimation and control process and quality of underlying communication network.

In order to demonstrate practical implication of our work, we also present a case study in smart distribution grid as a system example of spatially distributed CPSs. Voltage/VAR support via distributed generators is studied in a stochastic nonlinear control framework.

ESTIMATION & CONTROL IN SPATIALLY DISTRIBUTED CYBER PHYSICAL SYSTEMS

by

SIDDHARTH DESHMUKH

B.E., National Institute of Technology, Raipur, India, 2004
M.Tech., Indian Institute of Technology, Delhi, India, 2006

A DISSERTATION

submitted in partial fulfillment of the
requirements for the degree

DOCTOR OF PHILOSOPHY

Department of Electrical and Computer Engineering
College of Engineering

KANSAS STATE UNIVERSITY
Manhattan, Kansas
2013

Approved by:

Major Professor
Dr. Balasubramaniam Natarajan

Abstract

A cyber physical system (CPS) is an intelligent integration of computation and communication infrastructure for monitoring and/or control of an underlying physical system. In this dissertation, we consider a specific class of CPS architectures where state of the system is spatially distributed in physical space. Examples that fit this category of CPS include, smart distribution gird, smart highway/transportation network etc. We study state estimation and control process in such systems where, (1) multiple sensors and actuators are arbitrarily deployed to jointly sense and control the system; (2) sensors directly communicate their observations to a central estimation and control unit (ECU) over communication links; and, (3) the ECU, on computing the control action, communicates control actions to actuators over communication links. Since communication links are susceptible to random failures, the overall estimation and control process is subjected to: (1) partial observation updates in estimation process; and (2) partial actuator actions in control process. We analyze stochastic stability of estimation and control process, in this scenario by establishing the conditions under which estimation accuracy and deviation from desired state trajectory is bounded. Our key contribution is the derivation of a new fundamental result on bounds for critical probabilities of individual communication link failure to maintain stability of overall system. The overall analysis illustrates that there is trade-off between stability of estimation and control process and quality of underlying communication network.

In order to demonstrate practical implication of our work, we also present a case study in smart distribution grid as a system example of spatially distributed CPSs. Voltage/VAR support via distributed generators is studied in a stochastic nonlinear control framework.

Table of Contents

List of Figures

List of Tables

Notations

- $\mathbb{R}$: denotes real scalar space
- $\mathbb{R}^n$: denotes real vector space of dimension n
- $\mathbb{R}^{m \times n}$: denotes real matrix space of dimension $m \times n$
- x: denotes a scalar
- $\mathbf{x}$: denotes a vector
- $\mathbf{X}$: denotes a matrix
- $\mathbf{x}_t$: denotes true state vector
- $\mathbf{x}_{t|t}$: denotes estimated state vector
- $\mathbf{x}_{t+1|t}$: denotes predicted state vector
- $\succ$: denotes greater than inequality for positive definite matrix
- $\succeq$: denotes greater than equal-to inequality for positive definite matrix
- $\prec$: denotes less than inequality for positive definite matrix
- $\preceq$: denotes less than equal-to inequality for positive definite matrix
- $[\mathbf{A}]'$ denotes transpose / Hermitian of matrix $\mathbf{A}$
- $[\mathbf{A}]^{-1}$ denotes inverse of matrix of matrix $\mathbf{A}$
- $diag(\mathbf{A})$ denotes vector of diagonal elements of matrix $\mathbf{A}$
- $\mathbf{I}_n$ denotes an identity matrix of dimension $n \times n$

- $\mathbf{0}_n$ denotes zero matrix of dimension $n \times n$
- $\mathbb{E}[\mathbf{X}]$: denotes expectation of random matrix $\mathbf{X}$
- $Pr(x)$: denotes probability of random variable x.
- γ: denotes Binomial random variable taking value 0 and 1
- λ: denotes probability of γ taking value 1, $Pr(\gamma = 1)$
- λ_c: denotes critical probability of taking value 1
- $||\mathbf{A}||$: denotes spectral norm of matrix $\mathbf{A}$
- $||.||_2$: denotes $\mathbf{L}^2$-norm of matrix/vector
- $\mathbf{X} \odot \mathbf{Y}$: denotes element wise product of two vectors/matrices $\mathbf{X}$, $\mathbf{Y}$

Acknowledgments

I would like to express my gratitude to my academic advisor **Dr. Bala Natarajan**, whose research enthusiasm is eternal. His ability to instruct, guide, and inspire is truly remarkable and is only surpassed by his knowledge and passion for work. In addition to academic supervision, I have also received useful friendly support and unrelenting encouragement from him which I hope to carry as guiding principle for my future academic career.

I also owe a debt of gratitude to other members of my committee **Dr. Anil Pahwa**, **Dr. Nathan Albin**, **Dr. Todd Easton**, and **Dr. Daniel Andresen** for their valuable suggestions and advice. I am especially grateful to **Dr. Anil Pahwa** for guiding me in analyzing Smart distribution grid as an examplary case study for spatially distributed cyber-physical systems.

I would like to pay my special thanks to all member of WICOM group for thorough discussions and feedbacks on several key topics presented in dissertation. I specially owe much gratitude to **Nicholas Roseveare**, **Avik Sengupta** and **Mohammad Reza Sanatkar** for their friendship, support and encouragement. Special thanks goes to my friends **Prashant Wani**, and **Arka Chattopadhyay** for being best roommates one can have.

Last but not least, I would like to thank my family: grandmother **Kesar Deshmukh**, father **V. B. Deshmukh**, mother **Preeti Deshmukh**, brother **Vikrant Deshmukh**, and sister-in-law **Kanak Deshmukh** for their patience, encouragement and unquestioned support.

Dedication

I would like to dedicate my doctoral work to late **I. B. Bopche**. His blessings and benevolent support for my family will always motivate me to succeed in this life.

Chapter 1

Introduction

Cyber-Physical Systems (CPS) are intelligent systems where computation and networking infrastructure is integrated with physical system. Typically, CPS involves the cooperation of embedded computers, performing coordinated monitoring and control of the underlying physical system. The coordination is supported via network infrastructure which results in flexible, low cost, and easy to install / maintain system architecture. Thanks to advancement in embedded systems, CPS can play a transformative role in diverse areas such as, aerospace, automation, chemical processes, energy, health care, manufacturing, transportation, entertainment and consumer appliances. In this dissertation, we specifically consider CPS architectures, where states of the underlying system are spatially distributed in physical space. Examples of such systems include, smart distribution grids, smart highway / city traffic networks, smart irrigation networks, etc. Since these are large dynamical systems, multiple sensors and actuators arbitrarily deployed over the physical space are more appealing and practical for monitoring and control. This dissertation discusses estimation and control solutions in this scenario, and analyzes the impact of communication network on stability of the estimation and control process.

In this chapter, we provide a brief discussion on estimation and control in spatially distributed CPS - the primary topic of interest in this dissertation. In section 1.1, we first discuss CPS in general, and then specifically layout the challenges in estimation and control of spatially dispersed CPS 1.2. Section 1.3 presents a review of prior efforts related to estimation and control of physical system over a network. We briefly discuss the limitations and open research questions in this area. In section 1.3, we present an overview of our analysis and contributions of this dissertation. Finally, 1.4 outlines the organization of this dissertation.

1.1 Background

The recent confluence of computation and communication capabilities in embedded systems has created applications of enormous societal impact and economic benefits [1]. Such system architecture, integrating the cyber-space of computation and communications with physical systems, are known as cyber physical systems (CPS). CPS are designed architectures which monitor, control, coordinate, and integrate physical systems by computation and communication cores called embedded computers. This integration of cyber-space with the physical world ranges from the nano-world to large-scale, wide-area systems. If Internet is considered as revolution in information exchange between the computation cores, CPS is expected to revolutionize how embedded cores interact and control physical world around us.

The diverse application areas of CPS include, medical devices and systems, aerospace systems, transportation vehicles and intelligent highways, defense systems, robotics systems, process control, factory automation, building and environments control, and smart spaces. In the past, the system and control engineers in these areas have successfully developed the analysis and design tools, such as time and frequency domain methods, state space analysis, filtering/prediction, optimized control, etc. At the same time, advances in computer science has developed new programming languages, real time computing techniques, visualization methods, compiler designs, embedded systems architecture etc. Similarly, communication engineering has advanced in networking protocols, bandwidth utilization, energy minimization etc. CPS research aims to exploit knowledge and advancements in all such engineering disciplines to develop new interdisciplinary science and supporting technology.

As stated earlier, the CPS application area extends to large scale complex dynamical systems. A subset of such systems are spatially distributed systems such as smart distribution networks, smart highways / city traffic transportation network, smart irrigation networks, etc. Broadly speaking according to modalities of operation and behavior analysis, such CPS architectures can be differentiated into four major groups:

- A large physical system with state associated nodes distributed over the physical space.
- Multiple sensors arbitrarily deployed over the area to jointly observe the complete system.
- Multiple actuators arbitrarily deployed over the area to jointly control the complete system.
- A network infrastructure assisting in information exchange from sensors to a centralized estimation and control unit (ECU), and from the ECU to the actuators.

A symbolic view of such a CPS architecture is shown in Figure 1.1.

In Figure 1.1, we also show spatially located dynamical agents which collectively define the dynamics of the underlying physical system. We are using agents as the generic term in this work denoting, for example (1) local load fluctuations and randomly distributed generation in power distribution networks; (2) streams coming from rivers for irrigation hydro power network; (3) vehicles entering the city from highways or from residential/office campus for city traffic networks etc. The state vector in such physical systems is the collection of states of arbitrary nodes spatially distributed over physical place. For example, the state vector in a power distribution network comprises voltage phasors at arbitrary locations; similarly, the state of a city traffic network is the congestion at signal posts located across the city; and, the state of an irrigation network is the water level at various distribution points. Additionally, these state elements are nonlinear function of the system dynamics defined by coupling of agents (for example, voltage state is nonlinearly related to the power flow equations defined by load and distributed generation). Thus, if behavior of agents are

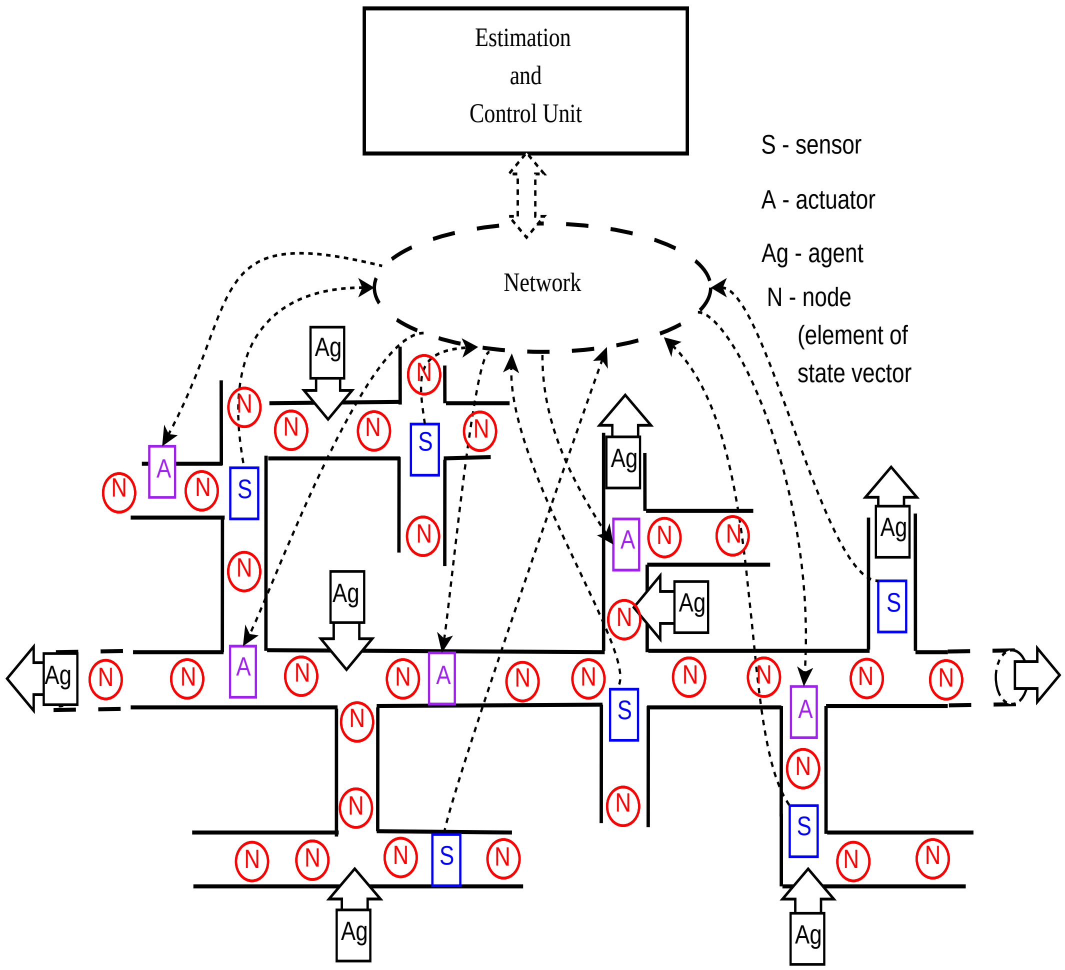

Figure 1.1: *Spatially distributed Cyber-Physical Systems - Estimation and Control over Network*

modeled statistically, then the complete physical system model is a nonlinear stochastic system model. Now, inclusion of network infrastructure for estimation and control in such systems presents new challenges in signal processing, which in effect determines the safe and efficient operation of considered physical system. This dissertation aims to address these challenges by proposing appropriate estimation and control solutions and analyzing the impact of communication network on stability of overall control process.

1.2 Challenges

As mentioned in previous section, CPS demands an interdisciplinary perspective, and solutions to challenges in CPS require expertise from several engineering disciplines [2],[3]. In this section, we present some research challenges related to signal processing for estimation and control in CPS architecture. A diagrammatic view of these challenges is shown in Figure 1.2.

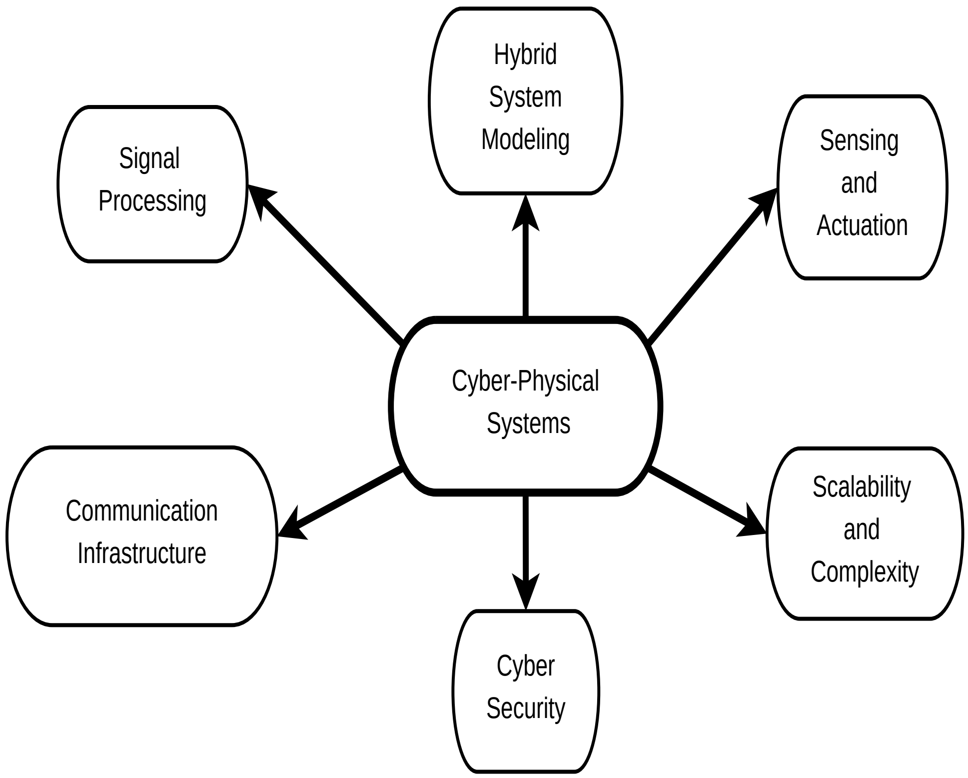

Figure 1.2: *Cyber-Physical Systems - Estimation and Control Challenges*

Hybrid System Modeling: One of the challenges in CPS is the integration of hybrid system models of physical systems and digital signal processing units. By hybrid system models we mean: (1) Coexistence of continuous and discrete time process: Physical systems in CPS operate in time continuum, where as other CPS subsystems are composed of discrete time operations [4]; (2) Quantized system models: Physical models have continuous states, while signal processing is performed on quantized states [5]; (3) Stochastic systems: Physical systems can not be completely defined by deterministic models, and dynamical CPS models may include a combination of stochastic and deterministic processes [6]; (4) Nonlinear system models: Physical system models are mostly nonlinear systems, and controller design gets very complicated for large dynamical systems [7],[8]. Thus, the goal of CPS research is co-designing and analyzing integration physical system model with computation models.

Controller Design: After system modeling, the next step in CPS architecture is controller design. The controller design for a hybrid system model includes: (1) State estimation: This is an important design consideration for stochastic system models as one essentially desires to minimize the estimation error; (2) Control computation: Next important design consideration is control solution computation based on minimization of a certain cost function of state and control vectors. Both these designs must be adaptive and predictive as the CPS needs to be responsive to changing system conditions and must anticipate and track the changes in physical process [9],[10].

Scalability and Complexity: Considering large dynamical systems, the controller deigns need to be computationally efficient and easy to implement [11],[12]. One way of addressing the computational complexity is by approximating the nonlinear system models by Taylor series expansion, or by finite dimensional orthogonal functions. However, the impact of approximation error on stability and accuracy of controller design needs to be considered in such cases. Another approach is to have distributed or decentralized implementation of controller design, in which small subproblems of much lower complexity are cooperatively solved at several computational cores. However in this case, one needs to take care of convergence and degree of cooperation and its effect on the stability of the overall system [13],[14].

Sensing and Actuation: Sensing and actuation is another challenging research area, especially considering low-power wireless sensors and actuators [15]. The objective is to enable much richer measurement and control of physical processes than what is affordable with wired systems. To achieve better and more reliable performance, issues like, low power transceiver design, sensor/actuator localization, distributed data modeling, timing synchronization etc. needs to be addressed carefully.

Communication Infrastructure: The emergence of communication network infrastructure for estimation and control in CPS has brought new challenges in signal processing [16]. One of the biggest challenge is to accommodate stochastic nature of communication network in controller design and analysis. By stochastic nature of communication network we mean: (1) random packet drops; (2) random packet delays; (3) random reordering of packets, etc. The network challenges can be addressed by: (1) analyzing the impact of network infrastructure on stability of controller design; (2) establishing the critical network conditions for ensuring stability of control process; (3) robust controller design; (4) communication protocol design etc.

Cyber Security: Designing a secure CPS architecture is an important consideration in practice [17]. It includes: (1) Resilience: ability of CPS to continue operating satisfactorily when stressed by unexpected inputs, subsystem failures, or environmental conditions or inputs that are outside the specified operating range; (2) privacy: protecting information from unauthorized access; (3) malicious attacks: protection from hackers, viruses etc.

In the next section, we present some relevant prior research work in estimation and control of physical systems.

1.3 Prior Work & Motivation

In this section, we first present estimation and control in general for linear and nonlinear physical system models, followed by estimation and control over network.

1.3.1 Controller Design - Stochastic Nonlinear System Models

The estimation and control process in most physical system models is subjected to some degree of uncertainty. Even when the fundamental system dynamics are mathematically modeled, the existence of some probabilistic parameters or unknown random disturbance can not be ignored. Additionally, nonlinear mathematical models aggravates the complexity incurred in solving the problem. Thus, the traditional deterministic linear control theory becomes inadequate when the process uncertainties and nonlinearity becomes significant. Research interest in nonlinear stochastic systems is not new, since it applies to most practical systems. In 1970, [18] formulated a scheme for continuous time stirred reactor, by which the corresponding nonlinear system dynamics with noise corrupted observations can be controlled. The scheme was based on a nonlinear Kalman filter in the feedback loop, and a controller designed to minimize an instantaneous cost criterion based on estimated states.

A different approach was used in [19] for controlling a statistical mechanics problem, where emphasis was on the applicability of linear control theory concepts for a class of nonlinear stochastic systems. The research showed that under certain conditions on process noise, the Hamilton-Jacobi-Bellman (HJB) equation can be written in form of partial differential equations. Thus, the solution was obtained from path integral of modified HJB equation. Similarly, [20] analyzes nonlinear stochastic dynamics for three typical model: (1) bilinear models; (2) Hammerstein models, and (3) model with output nonlinearity. The analysis finds that it is impossible to have a global stability results for a high-order polynomial nonlinear systems.

The traditional Lyapunov based framework is deployed in [21], designing an adaptive control methods for a multi variable discrete time nonlinear system with exogenous bounded amplitude disturbance. Similarly, [22] designs a sliding mode control to deal with nonlinearities in actuator.

It can be noticed that, most of above research [18]-[20] exploits the certain nonlinear behavior which is specific to the considered system model. Additionally, above efforts on control solutions for nonlinear system models are very computationally complex to exploit it for large scale spatially distributed systems. Thus, exploration of new estimation and control solutions specifically suited to spatially distributed systems is necessary.

Another thrust in control systems literature is to state optimality of the solution, along with global stability of the system. The optimality and stability of a control solution depends on present and future state of the observed physical system [23]. Thus, it is necessary to first investigate the design of an accurate dynamic state observer. However, the separation principle of breaking down the control problem into: (1) accurate observer design, and (2) optimal and stable feedback controller design, is not valid for nonlinear stochastic systems [24]. Considering complexity in nonlinear control solutions, several researches have shown applicability of separation principle locally around a known state equilibrium point; especially when exponential feedback stabilizers and exponential observers are used [25].

Thus, with the objective of reducing computational cost along with ensuring almost optimal solution, it is worthy to investigate local stability and optimality for estimation and control solution in nonlinear spatially distributed CPS.

1.3.2 Estimator Design - Nonlinear Discrete-time Stochastic System

An accurate state estimator design is one of the challenging problems in the broader area of nonlinear stochastic control. Since control input is constructed based on state estimates, an exponentially stable state estimator design needs to be investigated for assuring stability of overall controller synthesis. Considering single input/output nonlinear uncertain system, a sliding mode observer is proposed in [26] for state estimation. The adopted strategy is shown to guarantee convergence of estimation error to some bounded region. A new concept of change of co-ordinates is presented in [27], which transforms the nonlinear discrete time system with inputs into a linear system with output injection. This leads to linearized error dynamics, which results in exponential convergence of estimated state to the actual state in new co-ordinates.

An information theoretic framework is presented in [28] for nonlinear estimation problem using Renyi entropy as a measure of state uncertainty of the system. The observer design problem is formulated as a finite horizon stochastic optimal control problem with an objective to minimize the estimated state uncertainty. The problem is solved based on a neural network approach. Similarly, [29], [30] assumes that an additional physical insight of the problem is known in form of constraints on state and disturbances. The observer problem is solved using finite horizon optimization problem with an objective to reduce the estimation error. An unscented Kalman filter based state estimation approach is used in [31] for system where both state and measurement process are modeled as stochastic nonlinear difference equation. Under some assumptions on model parameters, an asymptotic convergence of state estimates is established. Similarly, [32] assumes that process model is affine with respect to the unmeasured disturbance and any measured state variable. The disturbances are considered as an additional state variables, and a nonlinear observer is designed for the augmented state space system. Considering computational efficiency and hence practical applicability for large scale nonlinear system, several research work [33]-[29] have analyze the robustness and stability of extended Kalman filter for nonlinear stochastic process and measurement model. Extended Kalman filter is a linear extension of Kalman filter (optimal state estimator for linear systems) for nonlinear systems.

Now, considering computational cost incurred in nonlinear state estimator design, it is worthy to investigate applicability of extended Kalman filter for spatially distributed CPS. A stability analysis establishing conditions on system parameters which in effect limits the linearization error will be a suitable approach in investigating use of extended Kalman filter for state estimation process.

1.3.3 Control Solution - Nonlinear Discrete-time Stochastic System

Next, considering optimality of control solution, model predictive control (MPC) has emerged as a powerful tool for feedback control design of constrained linear and nonlinear system. The underlying idea for MPC is stated as: At every sampling instant t, MPC computes and minimizes, a cost function of control and state over a short time horizon T. While corresponding optimal control inputs for the entire time horizon is calculated, only the first step control is implemented as control action for the system. Due to the wide acceptability of MPC for controller synthesis of practical dynamic systems, there has been extensive research results available in analyzing its performance in terms of robustness, optimality and stability [35].

However, for nonlinear stochastic systems there are still some unanswered questions. Considering stability as major performance criterion, [36],[37] establishes stability in terms of region of attraction properties for nonlinear MPC. The formulation is an unconstrained finite horizon optimization problem; and with proper terminal cost settings, stability of candidate Lyapunov function is ensured. [38] emphasizes on practical difficulties in implementing nonlinear MPC, when the optimization problem is non convex and computation time is limited. The research proposes a sub-optimal controller design, and establishes conditions under control solution is stable.

Similarly, [39] considers nonlinear problems which can be modeled as a set of piecewise linear, or affine systems. Stability and robustness conditions are then established for piecewise affine systems. Considering perturbation of discrete time nonlinear model, [40] establishes exponential stability theorems that allows to retain asymptotic stability in face of decaying perturbations. [41] investigates robust MPC for constrained discrete time nonlinear systems with additive uncertainties. The controller uses a terminal region constraint, which are computed to get robust feasibility of closed loop system for a given bound on admissible uncertainties. [35], focuses on the robust stability of nonlinear MPC when it is integrated with extended Kalman filter as state estimator. The analysis establishes that the EKF error is not influenced by control action of nonlinear MPC.

Now, control solution in most spatially distributed physical systems is subjected to some system constraints. Further, most system models being nonlinear and stochastic and of large dimension, conventional nonlinear control strategies like sliding mode control, manifold / passive control theory, etc. are impractical. Thus, it is important to investigate applicability of MPC solution for spatially distributed CPS. Additionally, some simplification in non convex optimization formulation for nonlinear system model can be investigated to reduce the computation cost with consideration of limiting approximation error.

1.3.4 Estimation Solution Over Network

For state estimation in cyber physical systems, the measurements are packetized and are communicated to central estimation unit over a network. These measurement packets are susceptible to abnormalities in communication links resulting in measurements getting delayed or lost due to packet drops. Addressing the impact of intermittent observation on performance of stability of Kalman filter based state estimation, [42] models the arrival rate of observations though the lossy network as Bernoulli random process. The analysis investigates the statistical convergence properties of the estimation error covariance, and further shows the existence of a critical value for arrival rate of the observations, beyond which state error covariance is unbounded. A similar analysis is done for extended Kalman filter in [43],[44], where sufficient system conditions are derived for bounded EKF error covariance. The analysis is valid if noise covariance, and initial estimation error are small.

In another approach, [45] models packet loss effect on Kalman filtering as a two state Markovian chain. The normal operating condition state when packet arrives, and no measurement case when there is transmission failure. Based on sojourn time of each visit to failure or packet reception state, behavior of estimation error is analyzed, and a notion of peak covariance is introduced. Further, sufficient conditions for stability of peak covariance is established. Addressing the delay and reordering of packets, variants on modeling the packet arrival are discussed in [46]-[50], with corresponding design modification in the recursive least square estimator for linear system.

It needs to be noticed that spatially distributed CPS are large dynamical systems, and is prudent to arbitrarily deploy multiple sensors over the physical space to completely observe the system. In such scenario, there will be multiple communication links relaying local sensor measurements, resulting in reception of partial measurements at centralized estimation unit. Thus, for spatially distributed CPS architecture, the estimation process stability is still as open question that we seek to address in this work.

1.3.5 Control Solution Over Network

: Similar to state observer stability, the feedback control stability over a lossy network has received considerable attention in past few years. In [51], a model based stabilization of a nonlinear system is investigated, with the assumption that both feed forward and feedback paths are subjected to network induced constraints. To overcome network effects like transfer interval, time varying communication delay, and possibly packet loss, a communication protocol is proposed to synchronizes the packet transfer between controller and actuator.

Considering network impact in form of quantization and packet drops, [52] investigates the stability of nonlinear control problem using global Lipschitz arguments. Modeling the packet drops as independent Bernoulli sequence, an observer based controller is designed to exponentially stabilize the networked system in mean square sense. Similarly, [53] considers network impact in form of packet reordering and random delay, and establishes a new closed loop model based on Markovian jump process. The authors further use Lyapunov function and LMI arguments to establish sufficient stability conditions and an upper bound on closed loop performance index. [54] considers networked control systems with arbitrarily large constant delays, and proposes novel stability conditions based on input output models of the subsystems and scattering transforms.

Exploiting nonlinear characteristics of a class of nonlinear systems, [55] presents sufficient conditions for robust asymptotic stability in presence of uncertain network delays. Further, an upper bound on network induced delay is derived to ensure system stability. Similar to above research, [56] develops a framework for stabilizing controller design of discrete time nonlinear models, with time varying sampling intervals, potentially large time varying delays and packet drop outs. Subsequently, sufficient conditions for the global exponential stability and semi-global practical asymptotic stability are provided.

Once again, considering large scale dynamics of spatially distributed CPS, it is realistic to deploy multiple actuators over the physical space to have complete control of underlying physical system. Also, similar to network facilitated estimation process, there will be multiple communication links relaying control inputs to individual actuators from central estimation and control unit. The, control process stability in such distributed CPS architecture is still unexplored and needs to be investigated.

In next section, we present an overview of our analysis and approach that attempts to address the

1.4 Contribution

In this dissertation, we analyze the impact of communication network on stability of estimation and control in spatially distributed CPS. As discussed in section 1.1, these systems generally exhibit nonlinear stochastic dynamical system model. Considering optimality and analytical tractability, we consider the first order Taylor series approximation of the underlying system model in estimation and control solution computation. This essentially results in computing estimation and control solution for linear system model valid locally around the computation time step. Thus, we first consider state estimation and control solution stability in linear system models.

1.4.1 State Estimation over Network in Spatially Distributed Physical System

Considering Kalman filter based state estimation, our work presented in chapter 3 is the first attempt in analyzing estimation stability in spatially distributed CPS. We consider state estimation process in practical spatially distributed system shown in Figure 1.3, with sensor measurements communicated to centralized state estimation unit over individual communication links. Figure 1.3 presents a conceptual view of the considered spatially distributed CPS, where nodes (with a state associated) are distributed all over a physical area. Arbitrarily located sensors jointly observe the complete system. Each sensor makes

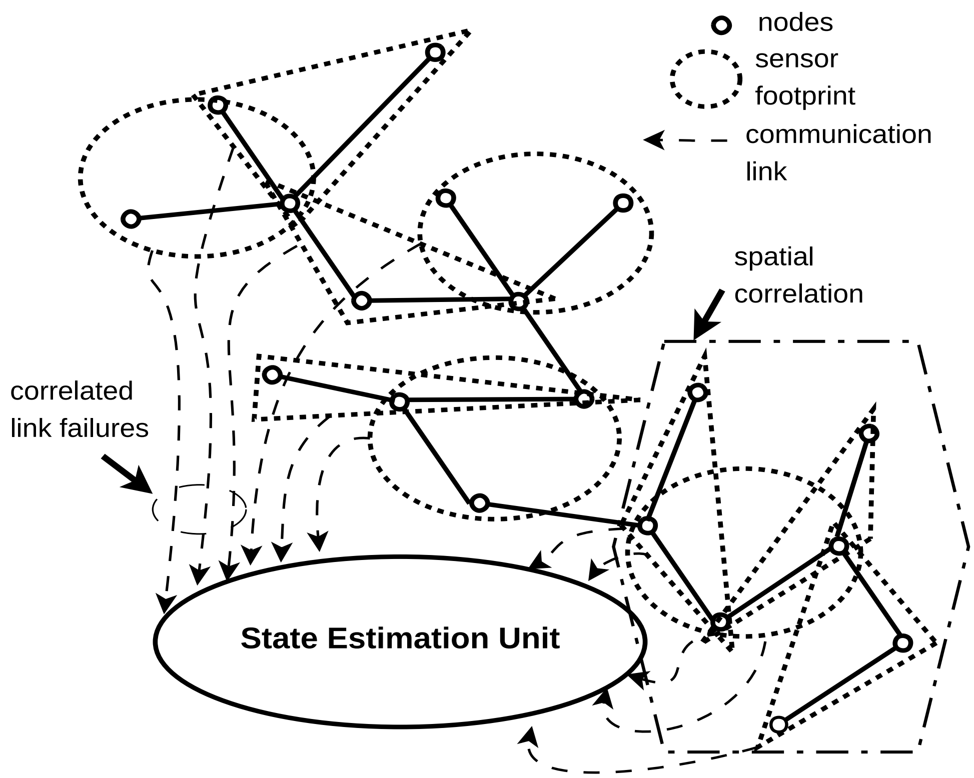

Figure 1.3: *State estimation of spatially distributed physical system over a network*

a measurement which is related to the nodes/states in its neighborhood. The observation space of neighboring sensors typically overlaps, resulting in redundancy in state information. These sensor measurements are sent to a central estimation unit over lossy networks resulting in measurements getting delayed or lost due to packet drops. Thus, at any state estimation step, received measurements may not be enough for observing all states of the system. We denote this system configuration as dispersed measurement scenario, which is completely different from well studied gathered measurement scenario [57]-[62] where measurements are collected and then sent to estimation unit over a communication link. We assume delayed measurements can not be used for state estimation and are considered equivalent to lost measurements. As discussed [57], the error covariance matrix iteration and the Kalman filter updates are stochastic and depend on randomness of measurement losses. Thus, we study the statistical properties of error covariance matrix iteration, and establish necessary and sufficient conditions for boundedness of error covariance matrix in steady state. The key contributions of this research are:

- We first study statistical convergence properties of error covariance matrix under dispersed measurement scenario. Based on information theoretic concepts, we establish a connection between gathered and dispersed measurement scenario: we then exploit this connection to obtain bounds on error covariance at steady state.

- After computing the error covariance bounds, we distribute the observation loss of gathered measurement scenario to dispersed measurement scenario. We accomplish this by formulating an linear equality constrained feasibility problem with probabilities of all possible measurement loss scenarios as its variables. Since this is a convex formulation, after obtaining the lower and upper bound on critical probabilities for all loss combination scenarios, the lower and upper bound on individual critical sensor link probability is computed.

- We exploit spatial correlation (a conceptual spatial correlation footprint is shown in Figure 1.3) in determining its impact on critical packet drop rates. We use a Wiener filter [63] to estimate the lost measurements from received measurements, with the assumption of known spatial correlation between the states. This analysis finally results in redefining the received measurement vector comprising of actual received measurements, and reconstructed measurements, followed by computing new measurement loss rates.

- We consider the scenario of correlated communication link failures (also shown in Figure 1.3) with the assumption of joint probability mass function of random link failures being stationary and known. Thus, new constraints resulting from joint probability mass function are then incorporated into the formulation for computing lower and upper bound on critical measurement rates.

- Finally we can state, our theoretical analysis quantifies the performance trade-off between state estimation accuracy and quality of the underlying communication network.

Details of our analysis and simulations are presented in chapter 3, and in publications,

[64]: S.Deshmukh, B.Natarajan and A.Pahwa, “State estimation in Spatially Distributed Cyber-Physical systems: Bounds on Critical Measurement Drop Rates”, (accepted in) *IEEE* 9^{th} *International Conference on Distributed computing in Sensor Systems, IEEE DCOSS 2013, 20-23 May 2013, Cambridge, Massachusetts.*

[65]: S.Deshmukh, B.Natarajan and A.Pahwa, “State Estimation over a Lossy Network in Spatially Distributed Cyber-Physical Systems”, (under review in)*IEEE Transactions on Systems, Man, and Cybernetics: Systems.*

1.4.2 LQR Controller over Network in Spatially Distributed Physical Systems

Considering linear quadratic regulator (LQR) based control solution, our work presented in chapter 4 is the first attempt in analyzing control stability in spatially distributed CPS. In this work, we consider an extension of scenario in Figure 1.3, with control solution communicated to actuators over individual communication links. Figure 1.4 presents a conceptual view of the considered system. In order to separate the analysis of estimation process, we assume that the underlying state estimation process in stable and the error in state estimates is accommodated as process noise in controller design. Thus, we are primarily concerned about the communication of computed control actions to actuators over individual communication links. Compared to conventional system models where there is one communication link between actuator and controller (denoted as unified actuator case), we denote the scenario in Figure 1.4 as dispersed actuator case. The control space of neighboring actuators typically overlaps, resulting in redundancy in control implementation. Further, due to network characteristics, actuator inputs are susceptible to delay, reordering and drops. At any control step, control implementation may not be enough for controlling all states of the system. Thus, use of communication network (while providing operational flexibility), can eventually adversely effect the stability of control process. The key contributions of this work are,

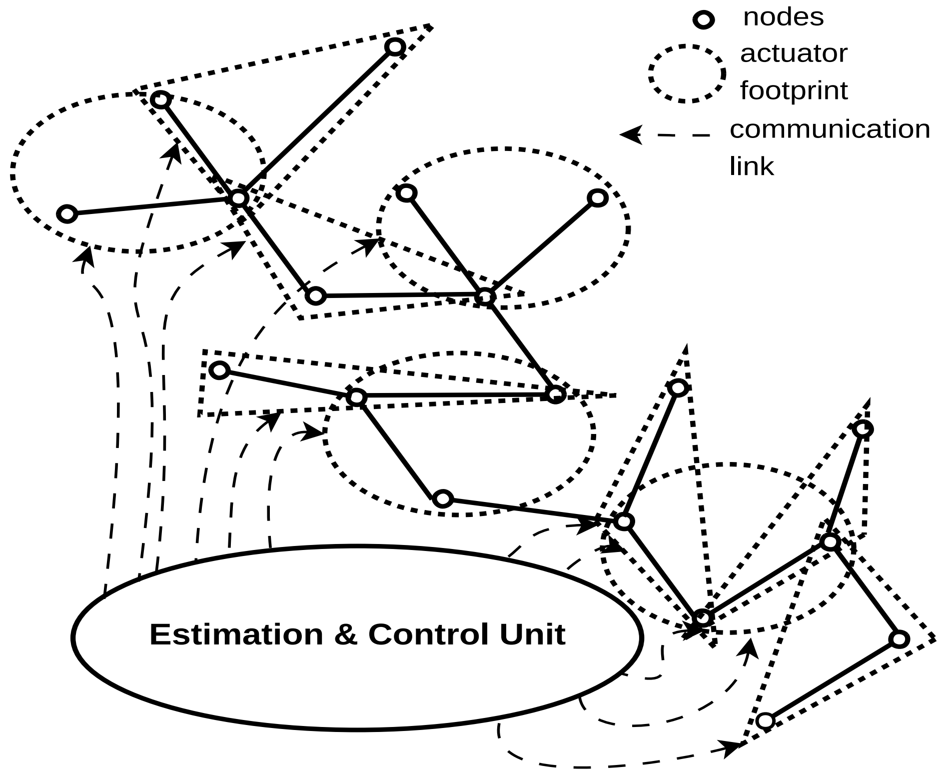

Figure 1.4: *Control implementation of spatially distributed physical system over a network*

- Due to process noise in system model and random packet loss in multiple communication links, we consider stochastic Lyapunov function for analyzing stability of a given linear quadratic control. We study statistical properties of Lyapunov function iterations and establish the existence of critical probability of successful packet transmission ensuring boundedness of Lyapunov function in steady state.

- Since, stochastic analysis and computation of critical probability require on-line information, we study convergence in mean of Lyapunov function and establish upper and lower bound on critical probability.

- Next based on analogy between Kalman filter based state estimation and linear quadratic control, we establish similarity in converges properties of Lyapunov function and error covariance matrix in state estimation; this helps in effectively using the stability results of unified actuator scenario in dispersed actuator scenario, thereby getting the same bounds on convergence of Lyapunov function iteration in steady state.

- Next based on converging solution of Lyapunov function iteration, we distribute the critical control loss in unified actuator scenario to dispersed actuator scenario. We accomplish this by formulating a linear feasibility problem, establishing same bound on Lyapunov function convergence for dispersed actuator scenario.

- We provide an upper and lower bound on convergence of Lyapunov function in steady state along with corresponding upper and lower bound on critical probabilities. This analysis quantifies the performance tradeoff between stability and quality of underlying communication network.

Details of our analysis and simulations are presented in chapter 4, and in publications,
[66]: S.Deshmukh, B.Natarajan and A.Pahwa, "LQG Control with Intermittent Actuator Inputs", (submitted in) *IEEE Multi-conference on Systems and Control, IEEE MSC 2013, 28-30 Aug. 2013, Hyderabad, India*,
[67]: S.Deshmukh, B.Natarajan and A.Pahwa, "LQR Controller over a Lossy Network in Spatially Distributed Cyber-Physical Systems", (under review in)*IEEE Transactions on Automatic Control*.

1.4.3 Case Study: Voltage/VAR Control In Smart Distribution Network

As discussed in section 1.1, most spatially distributed CPS have nonlinear stochastic system model. In our work in chapter 5, we consider a practical spatial distributed CPS architecture and present case study on voltage/VAR support in smart distribution network. The presented study essentially integrate the three aspects of voltage/VAR support: (1) nonlinear stochastic system modeling; (2) nonlinear state estimation; and (3) nonlinear control solution computation in single framework. A diagrammatic presentation of such a framework, with measurement and control information communication over network is presented in Figure 1.5. The key contributions of this work are,

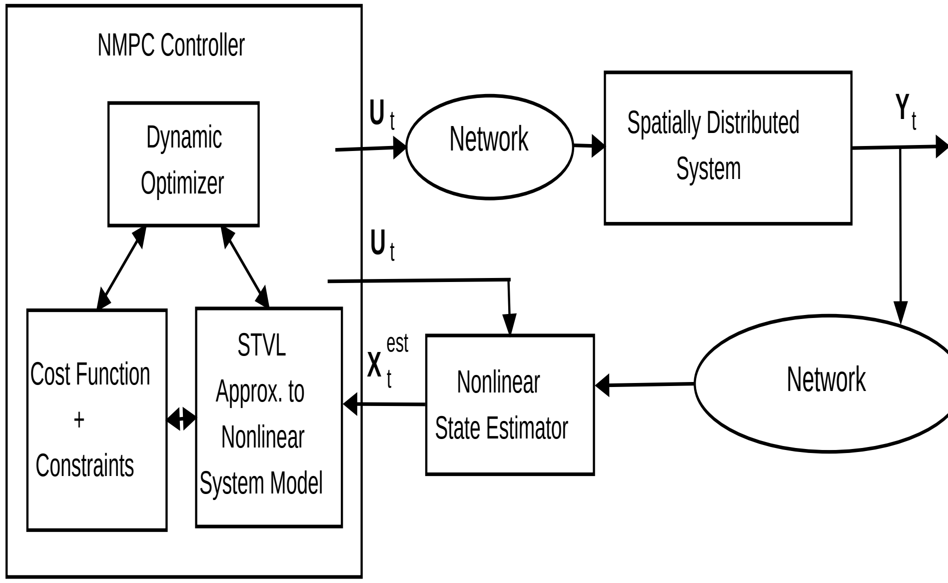

Figure 1.5: *Nonlinear Control framework for DG integrated at Distribution network level*

- First, as part of modeling efforts, we capture load fluctuations and DG power variability as a first order auto-regressive (AR(1)) time series with time varying coefficients. Since, relationship between voltage phasor and power is nonlinear, the resulting dynamic model is a stochastic discrete-time nonlinear time varying model.

- Next, we intend to design an accurate state estimator and controller which efficiently injects reactive power through DGs, for maintaining the voltage/VAR support at distribution network level. Now for nonlinear stochastic systems, we can not globally separate the problem into (1) accurate observer design, and (2) optimal feedback controller design [68]. However, separate designs can be done locally if we linearize the nonlinear state model around a state equilibrium point [69]. Thus, a locally optimal state estimator and feedback controller design is investigated in this work. Further, it should be noted that local applicability of separation principle does not ensures global optimality and stability [70]. Thus, we separate design local observer and control process for the underlying power distribution system.

- Considering nonlinear, time varying and stochastic properties of our system model, we propose an EKF based state estimation approach for distribution networks. Further we quantify conditions on system parameters and communication network for stability of state estimate error covariance matrix.

- As reactive power injection has a natural trade-off relative to real power injection by DGs, it is crucial to optimally use the reactive power of DGs. Additionally, the control design needs to be predictive, based on dynamics of the system. Thus, a quasi-infinite nonlinear model predictive control (NMPC) problem is formulated, with an objective of computing minimum distributed reactive power required for voltage/VAR support. Our formulation also places constraints on minimum and maximum reactive power a DG can inject based on economic viability and limitations of power electronics interface. To address the computational complexity incurred in searching optimal solution for large scale nonlinear control problems, we further propose a successive time varying linear (STVL) approximation to our voltage/VAR control problem.

More detailed discussion our case study in smart power distribution networks is presented in chapter 5, and in publications,

[71]: S.Deshmukh, B.Natarajan and A.Pahwa, "Voltage/VAR control in distribution networks via reactive power injection through distributed generators", *IEEE Transactions on Smart Grid*, March 2012,

[72]: S.Deshmukh, B.Natarajan and A.Pahwa, "Stochastic State Estimation for Smart Grids in the Presence of Intermittent Measurements", 4^{th} *IEEE Latin-American Conference on Communications, LATINCOM 2012, 7-9 Nov. 2012, Cuenca - Equador.*

[73]: S.Deshmukh, B.Natarajan and A.Pahwa, "State estimation and voltage/VAR control in distribution networks with intermittent measurements", (under review in)*IEEE Transactions on Smart Grid*.

1.5 Dissertation Organization

Following is the the chapter wise organization of this dissertation. In chapter 2, we discuss the existing control and estimation solutions for discrete time system models. The chapter first considers linear models in both deterministic and stochastic scenario, and later extends it to nonlinear system models.

Chapter 3, presents the stochastic stability of Kalman filter based state estimation process in spatially distributed cyber physical systems. The analysis establishes necessary and sufficient network conditions for ensuring boundedness of state estimation error, followed by computation of upper and lower bound on critical packet drop rates of individual sensor communication link.

In chapter 4 we consider stability of control operation for cyber physicals systems in both unified and dispersed actuator scenario. The analysis considers boundedness of Lyapunov function as stability criterion, and establishes necessary and sufficient network conditions along with computation of upper and lower bound on critical probabilities of packet drop in individual actuator communication links.

A case study on estimation and control in smart distribution network is presented in chapter 5, where a extensive discussion on nonlinear stochastic system modeling and extended Kalman filter based estimation and nonlinear model predictive control based voltage/VAR support is presented. The chapter later presents a discussion through simulations on network impact on estimation and control process to support the theory presented in previous chapters.

Finally, in chapter 6 we summarize our major contribution and discuss ideas for future work.

Chapter 2

Estimation and Control of Discrete-time System Models

The description of physical systems by a mathematical model was discussed in Chapter 1. It was also pointed out that discrete time models are an approximation of continuous time system models; and, study of such descriptive models are necessary because of sampling sensors and digital controllers. Further, discrete time system models are appealing for analysis of cyber physical systems. The estimation and control in these systems is subjected to delays between the instant measurements are sampled to the instant actuator implements the control action. However, dynamics of most cyber physical systems are slow, and along with advancement in signal processing / communication strategies, the delay is usually ignored. Thus, practical continuous time models of cyber physical systems are approximated by discrete time system models.

This chapter is devoted to the discussion of existing control and state estimation solutions for discrete time system models. We start our discussion by first considering linear models in both deterministic and stochastic scenario. In later sections, we consider nonlinear discrete time models and discuss the applicable state estimation and control strategies.

2.1 Deterministic Linear System Model

Consider a deterministic, discrete time linear dynamical system model,

$$\mathbf{x}_{t+1} = \mathbf{A}_t \mathbf{x}_t + \mathbf{B}_t \mathbf{u}_t \tag{2.1}$$

where, $\mathbf{x}_t \in \mathbb{R}^n$ represents the state vector of the underlying system; $\mathbf{A}_t \in \mathbb{R}^{n \times n}$ is the state transition matrix; $\mathbf{u}_t \in \mathbf{R}^m$ represents the input control vector for driving the underlying system towards desired trajectory; and $\mathbf{B}_t \in \mathbf{R}^{n \times m}$ is the control input matrix. Since this is deterministic model, the estimation of next state $\mathbf{x}_{t+1}$ is directly obtained by equation (2.1). In other words, due to absence of randomness in the system model, we do not consider measurements, and thus state estimation algorithms are also not required. So, in following subsections we directly consider the two popular control strategies for linear system model.

2.1.1 Linear Quadratic Regulator

In this subsection we first considers homogeneous or constant coefficient linear system models, i.e. the model matrices $\mathbf{A}_t$, and $\mathbf{B}_t$ are independent of time. In later discussion we show, how the presented analysis can be directly applied to more general time varying linear system models. Thus, consider a homogeneous linear system model,

$$\mathbf{x}_{t+1} = \mathbf{A}\mathbf{x}_t + \mathbf{B}\mathbf{u}_t. \tag{2.2}$$

Next, let the system be at some initial condition $\mathbf{x}_0 = \mathbf{x}_{init}$; and in this setup, we aim to compute small control inputs $\mathbf{u}_0, \mathbf{u}_1, \cdots$ such that state trajectory move towards desired trajectory. It should be noted that these two objectives: (1) minimizing different between current and desired state trajectory; (2) minimizing control input, are complementary to each other, i.e., a large control input can be computed which will rapidly drive the state trajectory $\mathbf{x}_t$ to desired state trajectory faster. In general, the desired state trajectory is considered as $\mathbf{0}$ (else, $\mathbf{x}_t$ can be modified to denote the difference between desired and current state trajectory); then, the linear quadratic theory is used to addresses this problem by defining a linear quadratic cost function,

$$J(\mathbf{U}) = \sum_{\tau=0}^{T-1} \mathbf{x}'_\tau \mathcal{Q} \mathbf{x}_\tau + \mathbf{u}'_\tau \mathcal{R} \mathbf{u}_\tau + \mathbf{x}_T \mathcal{Q}_f \mathbf{x}_T \tag{2.3}$$

where, $\mathbf{U} := \{\mathbf{u}_0, \mathbf{u}_1, \cdots \mathbf{u}_{T-1}\}$; $\mathcal{Q} = \mathcal{Q}' \in \mathbb{R}^{n \times n}, \succeq \mathbf{0}$ is the state weight matrix; $\mathcal{Q}_f = \mathcal{Q}'_f \in \mathbb{R}^{n \times n}, \succeq \mathcal{Q}$ is the final state weight matrix; and $\mathcal{R} = \mathcal{R}' \in \mathbb{R}^{m \times m}, \succ \mathbf{0}$ is the control input weight matrix. Variable $\tau \in t$, and T represents the duration of finite control horizon. The infinite horizon scenario is discussed in later in this section. So the problem is to compute optimal control input sequence $\mathbf{U}^*$ that minimizes the cost function (2.3), which essentially will satisfy our control objectives.

Least Square Solution

The solution of linear quadratic cost function (2.3) can be obtained by formulating a least square problem. In this approach, we first expand the system model for horizon period T in matrix form,

$$\begin{bmatrix} \mathbf{x}_0 \\ \mathbf{x}_1 \vdots \mathbf{x}_T \end{bmatrix} = \begin{bmatrix} \mathbf{0} & \cdots & \cdots & \cdots \\ \mathbf{B} & \mathbf{0} & \cdots & \cdots \\ \mathbf{AB} & \mathbf{B} & \cdots & \cdots \\ \vdots & \vdots & \vdots & \vdots \\ \mathbf{A}^{T-1}\mathbf{B} & \mathbf{A}^{T-2}\mathbf{B} & \cdots & \mathbf{B} \end{bmatrix} \begin{bmatrix} \mathbf{u}_0 \\ \mathbf{u}_1 \vdots \mathbf{u}_{T-1} \end{bmatrix} + \begin{bmatrix} \mathbf{I} \\ \mathbf{A} \\ \vdots \\ \mathbf{A}^T \end{bmatrix} \mathbf{x}_0, \tag{2.4}$$

where, $\mathbf{x}_0 = \mathbf{x}_{init}$ is the starting state of horizon period T. It is easy to notice that, equation (2.4) represents the state trajectory $\mathbf{X} := \{\mathbf{x}_0, \mathbf{x}_1, \cdots \mathbf{x}_T\}$ as linear function of the control input sequence $\mathbf{U} := \{\mathbf{u}_0, \mathbf{u}_1, \cdots \mathbf{u}_{T-1}\}$ and the initial state vector $\mathbf{x}_0$. Expressing $\mathbf{X} = \mathbf{GU} + \mathbf{Hx}_0$, the linear quadratic cost (2.3) can be expressed as,

$$\mathbf{J}(\mathbf{U}) = \left[diag\left(\mathcal{Q}^{1/2}, \cdots \mathcal{Q}^{1/2}\right)(\mathbf{GU} + \mathbf{Hx}_0)\right]^2 + \left[diag\left(\mathcal{R}^{1/2}, \cdots \mathcal{R}^{1/2}\right)\mathbf{U}\right]^2. \tag{2.5}$$

The optimal control action is now easily computed by setting the derivative of (2.5) with respect to $\mathbf{U}$ to zero. It is easy to notice that, this computation strategy will require formulating a least square problem with size $N(n+m) \times Nm$ at every time step. For a large physical system with thousands of state elements, this will be highly computationally expensive, specifically an order of $\mathcal{O}(N^3nm^2)$ if the naive methods like QR factorization are used. More details of least squares solution in linear quadratic regulators can be followed in [74],[75]. In next subsection we discuss a more practical recursive control solution based on dynamic programming.

Dynamic Programming Solution

Dynamic programming is an efficient and practical viable recursive method to solve the linear quadratic problem. In this approach, we first define a value function $V_t(\mathbf{x}_0) := \mathbb{R}^n \rightarrow \mathbb{R}$ representing linear quadratic cost to go, starting from initial state $\mathbf{x}_{init}$ at time t to $T-1$,

$$\begin{array}{rl} V_t(\mathbf{x}_{init}) = & \min_{\mathbf{u}_t,\cdots\mathbf{u}_{T-1}} \sum_{\tau=0}^{T-1} \mathbf{x}_\tau' \mathcal{Q} \mathbf{x}_\tau + \mathbf{u}_\tau' \mathcal{R} \mathbf{u}_\tau + \mathbf{x}_T \mathcal{Q}_f \mathbf{x}_T \\ & s.t.\ \mathbf{x}_0 = \mathbf{x}_{init}\ \&\ \mathbf{x}_{\tau+1} = \mathbf{A}\mathbf{x}_\tau + \mathbf{B}\mathbf{u}_\tau \end{array} \tag{2.6}$$

It can be noted that value function (2.6) at first step $t = 0$ is essentially a quadratic function of initial state $\mathbf{x}_{init}$, i.e., $V_0(\mathbf{x}_{init} = \mathbf{x}_{init}'\mathbf{P}_t\mathbf{x}_{init}$, whre $\mathbf{P}_t \succeq \mathbf{0}$. Thus, the recursion of quadratic function of state trajectory can be expressed as,

$$V_t(\mathbf{x}_{init}) = \mathbf{x}_0' \mathcal{Q} \mathbf{x}_0 + \min_{\mathbf{u}} \left(\mathbf{u}' \mathcal{R} \mathbf{u} + V_{t+1}\left(\mathbf{A}\mathbf{x}_0 + \mathbf{B}\mathbf{u} \right) \right). \tag{2.7}$$

Above value function recursion (2.7) is also called DP, Bellman or Hamilton-Jacobi equation. Once again, value function at step $t+1$ is essentially $\mathbf{V}_{t+1}(\mathbf{x}_{init}) = \mathbf{x}_{init}'\mathbf{P}_{t+1}\mathbf{x}_{init}$, with $\mathbf{P}_{t+1} \succeq \mathbf{0}$. Substituting $\mathbf{x}_{t+1}$ from system model in (2.7) we obtain,

$$V_t(\mathbf{x}_{init}) = \mathbf{x}_{init}' \mathcal{Q} \mathbf{x}^{init} + \min_{\mathbf{u}} \left(\mathbf{u}' \mathcal{R} \mathbf{u} + \left(\mathbf{A}\mathbf{x}_{init} + \mathbf{B}\mathbf{u} \right)' \mathbf{P}_{t+1} \left(\mathbf{A}\mathbf{x}_{init} + \mathbf{B}\mathbf{u} \right) \right) \tag{2.8}$$

Equation (2.8) can be solved by setting derivative with respect to $\mathbf{u}$ to zero. Thus, the optimal control input is computed as,

$$\mathbf{u}^* = -\left(\mathcal{R} + \mathbf{B}'\mathbf{P}_{t+1}\mathbf{B} \right)^{-1} \mathbf{B}'\mathbf{P}_{t+1}\mathbf{A}\mathbf{x}_{init} \tag{2.9}$$

Substituting the optimal control solution in value function (2.8) and with algebraic simplification we get,

$$\begin{array}{l} V_t(\mathbf{x}_{init}) \\ = \mathbf{x}_{init}' \left(\mathcal{Q} + \mathbf{A}'\mathbf{P}_{t+1}\mathbf{A} - \mathbf{A}'\mathbf{P}_{t+1}\mathbf{B} \left(\mathcal{R} + \mathbf{B}'\mathbf{P}_{t+1}\mathbf{B} \right)^{-1} \mathbf{B}'\mathbf{P}_{t+1}\mathbf{A} \right) \mathbf{x}_{init} \\ = \mathbf{x}_{init}'\mathbf{P}_t\mathbf{x}_{init} \end{array} \tag{2.10}$$

Thus, the backward recursive equation for $\mathbf{P}_t$ is expressed as,

$$\mathbf{P}_t = \mathbf{Q} + \mathbf{A}'\mathbf{P}_{t+1}\mathbf{A} - \mathbf{A}'\mathbf{P}_{t+1}\mathbf{B}\left(\mathbf{R} + \mathbf{B}'\mathbf{P}_{t+1}\mathbf{B}\right)^{-1}\mathbf{B}'\mathbf{P}_{t+1}\mathbf{A} \tag{2.11}$$

Finally, the linear quadratic regulator solution via dynamic programming can now be summarized as,

1). Initialize the final $\mathbf{P}_T = \mathbf{Q}_f$

2). Recursive compute in backward direction, i.e., $t = T-1, \cdots 1$, $\mathbf{P}_{t-1} = \mathcal{Q} + \mathbf{A}'\mathbf{P}_t\mathbf{A} - \mathbf{A}'\mathbf{P}_t\mathbf{B}\left(\mathcal{R} + \mathbf{B}'\mathbf{P}_t\mathbf{B}\right)^{-1}\mathbf{B}'\mathbf{P}_t\mathbf{A}$

3). Recursively compute in forward direction i.e., $t = 0, \cdots T-1$, control gain $\mathbf{K}_t := -\left(\mathcal{R} + \mathbf{B}'\mathbf{P}_{t+1}\mathbf{B}\right)^{-1}\mathbf{B}'\mathbf{P}_{t+1}\mathbf{A}$

4). Finally, compute the optimal control for horizon period T, $\mathbf{u}_t^* = \mathbf{K}_t\mathbf{x}_t$ for $t = 0, \cdots T-1$.

The dynamic programming solution can also be extended for infinite horizon scenario, also known as steady state solution. The corresponding recursive equation (2.11) is called discrete time algebraic Riccati equation and is expressed as,

$$\mathbf{P}_{ss} = \mathbf{Q} + \mathbf{A}'\mathbf{P}_{ss}\mathbf{A} - \mathbf{A}'\mathbf{P}_{ss}\mathbf{B}\left(\mathbf{R} + \mathbf{B}'\mathbf{P}_{ss}\mathbf{B}\right)^{-1}\mathbf{B}'\mathbf{P}_{ss}\mathbf{A} \tag{2.12}$$

where, $\mathbf{P}_{ss}$ is the converging solution of iteration (2.11). The solution for (2.12) can be obtained by either iterating the Riccati recursion or by direct methods. Once, the conversing solution $\mathbf{P}_{ss}$ is computed, the infinte horizon linear quadratic solution os essentially a constant linear feedback solution, $\mathbf{u}_t = \mathbf{K}_{ss}\mathbf{x}_t$, where $\mathbf{K}_{ss} = -\left(\mathbf{R} + \mathbf{B}'\mathbf{P}_{ss}\mathbf{B}\right)^{-1}\mathbf{B}'\mathbf{P}_{ss}\mathbf{A}$.

More details of dynamic programming solution in linear quadratic regulators can be followed in [74],[75]. There a several other strategies of computing the linear quadratic control solution. One ways is to directly formulate an optimization problem with: (1) minimization of quadratic cost function as the objective function; (2) initial state and the system model as the constraints; (3) and solving the problem via Lagrange analysis or other convex optimization methods. We show this setup as model predictive solution in next subsection.

2.1.2 Model Predictive Control Solution

One way of designing a control strategy is greedy approach in which immediate future state $\mathbf{x}_{t+1}$ is only considered in computing the solution, and impact of computed control action on future state trajectory is ignored. This is essentially a greedy approach and typically preforms very poorly in long run. Model predictive control (MPC) solution, address this problem in linear system models, by formulating a convex optimization problem. At each time step t

$$\begin{array}{ll} min. & \sum_{\tau=t}^{\infty} l\left(\mathbf{x}_t, \mathbf{u}_t\right) \\ s.t. & \mathbf{u}_t \in \mathcal{U}, \mathbf{x}_t \in \mathcal{X},\ \tau = t, \cdots \infty \\ & \mathbf{x}_{t+1} = \mathbf{A}\mathbf{x}_t + \mathbf{B}\mathbf{u}_t,\ \tau = t, \cdots \infty \end{array} \tag{2.13}$$

where, $l(.)$ is a cost function of state trajectory and control input; and $\mathcal{X}$ and $\mathcal{U}$ are polyhedral constraining the state trajectory and feasibility of control action. MPC is also known by many other names (with some variants in general formulation), e.g. dynamic matrix control, infinite horizon control dynamic linear programming, rolling horizon planing, etc. One simple variant of MPC is with quadratic cost function, similar to cost function in linear quadratic regulator solution,

$$\begin{array}{ll} min. & \sum_{\tau=t}^{\infty} \mathbf{x}_t' \mathcal{Q} \mathbf{x}_t + \mathbf{u}_t' \mathcal{R} \mathbf{u}_t \\ s.t. & \mathbf{u}_t \in \mathcal{U}, \mathbf{x}_t \in \mathcal{X},\ \tau = t, \cdots \infty \\ & \mathbf{x}_{t+1} = \mathbf{A}\mathbf{x}_t + \mathbf{B}\mathbf{u}_t,\ \tau = t, \cdots \infty \end{array} \tag{2.14}$$

Notice that without state space and control space constraints quadratic cost MPC problem (2.15) is simply a steady state LQR problem with solution expressed by equation (2.12). However, due to these constraints it difficult to express an analytical solution. Instead, the MPC problem is transformed to finite horizon MPC problem,

$$\begin{array}{ll} minimize & \sum_{\tau=t}^{t+T} l\left(\mathbf{x}_t' \mathcal{Q} \mathbf{x}_t + \mathbf{u}_t' \mathcal{R} \mathbf{u}_t\right) \\ subject\ to & \mathbf{u}_t \in \mathcal{U}, \mathbf{x}_t \in \mathcal{X},\ \tau = t, \cdots t+T \\ & \mathbf{x}_{t+1} = \mathbf{A}\mathbf{x}_t + \mathbf{B}\mathbf{u}_t,\ \tau = t, \cdots t+T-1 \end{array} \tag{2.15}$$

At this point we define the model predictive control solution computation steps as,

1). Compute optimal control solution $\mathbf{u}_t$ $t = 0, \cdots T-1$by solving optimization problem (2.15)

2). Implement $\mathbf{u}_0$ as the control input solution for current sampling instant

3). Update the time step $t := t + 1$ and repeat the control process for for time step $t + 1$

Finite horizon MPC is also called receding horizon or rolling horizon MPC. More details about MPC solution can be found in [76]. There are several other variants of MPC and can be followed in [77]. In next section, we consider disturbance or noise in our system model; and discuss corresponding state estimation and control strategies.

2.2 Stochastic Linear System Models

In this section, we consider system models influenced by process noise, which eventually result in state trajectory as a random process. Since, there is randomness involved in computing the future states, a measurement based feedback mechanism is essential to better estimate the future state trajectory. Further, the control algorithms also have to consider the stochastic nature of system model in order to maintain stability of underling physical system. In following discussion, we discuss the state estimation and optimal control computation strategies dealing with stochastic linear system models.

2.2.1 Kalman Filter

Kalman filter is most popular state estimation algorithm for linear dynamical systems. It is also known as linear quadratic estimator, as it minimizes means square state estimation error. So, first consider a stochastic linear dynamical system observed by a series of measurements,

$$\begin{aligned} \mathbf{x}_{t+1} &= \mathbf{A}\mathbf{x}_t + \mathbf{w}_t \\ \mathbf{y}_t &= \mathbf{C}\mathbf{x}_t + \mathbf{v}_t \end{aligned} \tag{2.16}$$

where, vector $\mathbf{y}_t \in \mathbb{R}^m$ represents observed measurements; $\mathbf{C} \in \mathbb{R}^{n\times m}$ represents measurement matrix; and, vector $\mathbf{w}_t \in \mathbb{R}^n$, $\mathbf{v}_t \in \mathbb{R}^m$ represent process and measurement noise, respectively. We assume that the initial state $\mathbf{x}_{init} = \mathbf{x}_0$ and noise sequences $\mathbf{w}_0, \mathbf{w}_1, \cdots, \mathbf{v}_0, \mathbf{v}_1, \cdots$ are independent of each other; All random processes are assumed to be second order stationary processes, with Gaussian distribution and mean $\mathbb{E}[\mathbf{w}_t] = \mathbb{E}[\mathbf{v}_t] = \mathbf{0}$ and varince

$\mathbb{E}[\mathbf{w}_t\mathbf{w}'] = \mathbf{Q}, \mathbb{E}[\mathbf{v}_t\mathbf{v}'] = \mathbf{R}$. Further, the mean initial state is denoted as $\mathbb{E}[\mathbf{x}_0] = \bar{\mathbf{x}}_0$ with variance $\mathbb{E}[(\mathbf{x}_0 - \bar{\mathbf{x}}_0)(\mathbf{x}_0 - \bar{\mathbf{x}}_0)'] = \Sigma_0$. Now, it is easy to notice that the state sequence $\{\mathbf{x}_1, \cdots\}$ and observation sequence $\{\mathbf{y}_1, \cdots\}$ are linear function of $\mathbf{x}_0$, $\mathbf{Q}$ and $\mathbf{R}$, and thus we can conclude that they are all jointly Gaussian. Based on the assumption that process and measurement noise are independent of state sequence $\{\mathbf{x}_1, \cdots\}$, we can further conclude that $\mathbf{x}_t$ is Markov process, i.e.,

$$\mathbf{x}_t|\mathbf{x}_0, \mathbf{x}_1, \cdots \mathbf{x}_{t-1} = \mathbf{x}_t|\mathbf{x}_{t-1}$$

Thus, our dynamical model (2.16) is linear Gauss Markov process, with mean $\bar{\mathbf{x}}_{t+1} = \mathbf{A}\bar{\mathbf{x}}_t = \mathbf{A}^t\bar{\mathbf{x}}_0$, and covariance $\Sigma_{\mathbf{x}}(t+1) = \mathbf{A}\Sigma_{\mathbf{x}}(t)\mathbf{A}' + \mathbf{Q}$. Next, based on observed measurements $\{\mathbf{y}_1, \cdots \mathbf{y}_{t-1}\}$ we want to improves our estimate of state $\mathbf{x}_t$. Thus, we specifically focus on two step estimation problem,

- Estimating the current state of the system $\mathbf{x}_{t|t}$ based on the current and past observed measurements
- Predicting the next state of the system $\mathbf{x}_{t+1|t}$, based on current and past observed measurements

The standard formula of minimum mean square estimate (Wiener filter) to compute $\mathbf{x}_{t|t}$ is,

$$\mathbf{x}_{t|t} = \bar{\mathbf{x}}_t + \Sigma_{\mathbf{x}_t,\mathbf{Y}_t}\Sigma_{\mathbf{Y}_t}^{-1}\left(\mathbf{Y}_t - \bar{\mathbf{Y}}_t\right) \tag{2.17}$$

where, $\Sigma_{\mathbf{x}_t,\mathbf{Y}_t}$ is cross covariance between $\mathbf{x}_t$ and $\mathbf{Y}_t$; $\Sigma_{\mathbf{Y}_t}$ is covariance of $\mathbf{Y}_t$; and $\mathbf{Y}_t$ denotes set of observed measurements $\{\mathbf{y}_1, \cdots \mathbf{y}_t\}$. It is easy to notice that the computation of state estimate $\mathbf{x}_{t|t}$ grows with iteration t. Kalman filter based state estimation is an intelligent method of recursively computing $\mathbf{x}_{t|t}$ and $\mathbf{x}_{t|t+1}$, and thus avoiding the growth in computational complexity. Let us first express $\mathbf{x}_{t|t}$ and $\Sigma t|t$ in terms of $\mathbf{x}_{t|t-1}$ and $\Sigma_{t|t-1}$. The measurement $\mathbf{y}_t$ conditioned on past measurements $\mathbf{Y}_{t-1}$ is given by,

$$\mathbf{y}_t|\mathbf{Y}_{t-1} = \mathbf{C}\mathbf{x}_t|\mathbf{Y}_{t-1} + \mathbf{v}_t|\mathbf{Y}_{t-1} = \mathbf{C}\mathbf{x}_t|\mathbf{Y}_{t-1} + \mathbf{v}_t$$

as $\mathbf{v}_t$ and $\mathbf{Y}_{t-1}$ are independent. $\mathbf{x}_t|\mathbf{Y}_{t-1}$ and $\mathbf{y}_t|\mathbf{Y}_{t-1}$ are jointly Gaussian with mean and covariance given by,

$$\begin{bmatrix} \mathbf{x}_t|\mathbf{x}_{t-1} \\ \mathbf{C}\mathbf{x}_t|\mathbf{x}_{t-1} \end{bmatrix}, \begin{bmatrix} \Sigma_{t|t-1} & \Sigma_{t|t-1}\mathbf{C}' \\ \mathbf{C}\Sigma_{t|t-1} & \mathbf{C}\Sigma_{t|t-1}\mathbf{C}' + \mathbf{R} \end{bmatrix}$$

Next using the standard formula (2.17), we can state

$$\begin{aligned} \mathbf{x}_{t|t} &= \mathbf{x}_{t|t-1} + \Sigma_{t|t-1}\mathbf{C}'\left(\mathbf{C}\Sigma_{t|t-1}\mathbf{C}' + \mathbf{R}\right)^{-1}(\mathbf{y}_t - \mathbf{C}\mathbf{x}_{t|t-1}) \\ \Sigma_{t|t} &= \Sigma_{t|t-1} - \Sigma_{t|t-1}\mathbf{C}'\left(\mathbf{C}\Sigma_{t|t-1}\mathbf{C}' + \mathbf{R}\right)^{-1}\mathbf{C}\Sigma_{t|t-1} \end{aligned} \tag{2.18}$$

Equation (2.18) is called measurement update, since it gives updated estimate of $\mathbf{x}_t$ based on the measurement $\mathbf{y}_t$ becoming available. After applying the measurement update, we can preform time update as,

$$\begin{aligned} \mathbf{x}_{t+1|t} = \mathbf{x}_{t+1}|\mathbf{Y}_t &= \mathbf{A}\mathbf{x}_t|\mathbf{Y}_t + \mathbf{w}_t|\mathbf{Y}_t \\ &= \mathbf{A}\mathbf{x}_t|\mathbf{Y}_t + \mathbf{w}_t \\ &= \mathbf{A}\mathbf{x}_{t|t} \end{aligned} \tag{2.19}$$

as $\mathbf{w}_t$ and $\mathbf{Y}_t$ are independent of each other. The error covariance time update is computed as,

$$\begin{aligned} \Sigma_{t+1|t} &= \mathbb{E}\left[(\mathbf{x}_{t+1|t} - \mathbf{x}_{t+1})(\mathbf{x}_{t+1|t} - \mathbf{x}_{t+1})'\right] \\ &= \mathbb{E}\left[(\mathbf{A}\mathbf{x}_{t|t} - \mathbf{A}\mathbf{x}_t - \mathbf{w}_t)(\mathbf{A}\mathbf{x}_{t|t} - \mathbf{A}\mathbf{x}_t - \mathbf{w}_t)'\right] \\ &= \mathbf{A}\Sigma_{t|t}\mathbf{A}' + \mathbf{Q} \end{aligned} \tag{2.20}$$

A more detailed discussion about Kalman filter based state estimation can be found in [78]. Some variants of Kalman filter for linear dynamical system can be followed in [79],[80]. In next subsection, we discuss control strategies considering randomness in system model.

2.2.2 Linear Quadratic Stochastic Control

In this subsection we extend our analysis on deterministic linear quadratic control to stochastic linear system models. Continuing after state estimation, we assume that the estimated state is the true state with some finite error covariance. The state estimation error is accommodated in process noise for underlying dynamical system model. So, once again consider a stochastic linear dynamical system,

$$\mathbf{x}_{t+1} = \mathbf{A}\mathbf{x}_t + \mathbf{B}\mathbf{u}_t + \mathbf{w}_t \tag{2.21}$$

where, $\mathbf{w}_t \in \mathbb{R}^n$ is stationary Gaussian process noise with $\mathbb{E}[\mathbf{w}_t] = \mathbf{0}$ and $\mathbb{E}[\mathbf{w}_t\mathbf{w}_t'] = \mathbf{Q}$. Further we assume initial state $\mathbf{x}_0$ is is also Gaussian random process independent of noise $\mathbf{w}_t$ with mean and variance $\mathbb{E}[\mathbf{x}_0] = \mathbf{0}$, $\mathbb{E}[\mathbf{x}_0\mathbf{x}_0'] = \mathbf{X}$. We aim to compute the optimal control input $\mathbf{u}_t^*$ such that the following objective function is minimized,

$$J_t = \mathbb{E}\left[\sum_{t=0}^{T-1}(\mathbf{x}_t'\mathcal{Q}\mathbf{x}_t + \mathbf{u}_t'\mathcal{R}\mathbf{u}_t) + \mathbf{x}_T'\mathbf{Q}_f\mathbf{x}_T\right] \tag{2.22}$$

Notice that because of stochastic system model, we are minimizing expected cost function, else cost function itself is stochastic. Further, due to stochastic system model, we do do not consider least square approach for control solution. Instead, we directly discuss dynamic programming solution for stochastic linear systems.

Dynamic Programming Solution

The value function or cost to go function for (2.22) is defined as,

$$\begin{aligned} V_t(\mathbf{x}_{init}) = \quad & \min_{\mathbf{u}_t,\cdots\mathbf{u}_{T-1}} \mathbb{E}\left[\sum_{\tau=0}^{T-1}\mathbf{x}_\tau'\mathcal{Q}\mathbf{x}_\tau + \mathbf{u}_\tau'\mathcal{R}\mathbf{u}_\tau + \mathbf{x}_T\mathcal{Q}_f\mathbf{x}_T\right] \\ & s.t.\ \mathbf{x}_0 = \mathbf{x}_{init},\ \ \mathbf{x}_{\tau+1} = \mathbf{A}\mathbf{x}_\tau + \mathbf{B}\mathbf{u}_\tau + \mathbf{w}_\tau \end{aligned} \tag{2.23}$$

Similar to deterministic Linear quadratic regulator problem, the final value function at time step t is given by $V_T(\mathbf{x}) = \mathbf{x}_T'\mathcal{Q}_f\mathbf{x}_T$. Value function at other time steps can be computed by backward recursion,

$$V_t(\mathbf{x}_t) = \mathbf{x}_t'\mathcal{Q}\mathbf{x}_t + min_{\mathbf{u}}\left[\mathbf{u}'\mathcal{R}\mathbf{u} + \mathbb{E}[V_{t+1}(\mathbf{A}\mathbf{x}_t + \mathbf{B}\mathbf{u} + \mathbf{w}_t)]\right] \tag{2.24}$$

for $t = T-1, \cdots, 0$. Thus, the optimal control action has the form,

$$\mathbf{u}_t^* = argmin_{\mathbf{u}}\left[\mathbf{u}'\mathcal{R}\mathbf{u} + \mathbb{E}[V_{t+1}(\mathbf{A}\mathbf{x}_t + \mathbf{B}\mathbf{u} + \mathbf{w}_t)]\right] \tag{2.25}$$

Since, this is analytically intractable, let value function is a quadratic function, with form

$$V_t(\mathbf{x}_t) = \mathbf{x}_t'\mathbf{P}_t\mathbf{x}_t + q_t,$$

for $t = 0, \cdots T$ with $\mathbf{P}_t \succeq \mathbf{0}$. Assuming $\mathbf{P}_T = \mathcal{Q}_f$, $q_T = 0$ and value function iteration as $V_{t+1}(\mathbf{x}) = \mathbf{x}'\mathbf{P}_{t+1}\mathbf{x} + q_{t+1}$, the Bellman recursion is given by,

$$\begin{aligned} & V_t(\mathbf{x}_t) = \\ & \mathbf{x}_t'\mathcal{Q}\mathbf{x}_t + min_{\mathbf{u}}\left\{\mathbf{u}'\mathcal{R}\mathbf{u} + \mathbb{E}\left[(\mathbf{A}\mathbf{x}_t + \mathbf{B}\mathbf{u} + \mathbf{w}_t)'\mathbf{P}_t(\mathbf{A}\mathbf{x}_t + \mathbf{B}\mathbf{u} + \mathbf{w}_t)\right] + q_{t+1}\right\} \\ & = \mathbf{x}_t'\mathcal{Q}\mathbf{x}_t + tr(\mathcal{Q}\mathbf{P}_{t+1}) + q_{t+1} + min_{\mathbf{u}}\left\{\mathbf{u}'\mathcal{R}\mathbf{u} + (\mathbf{A}\mathbf{x}_t + \mathbf{B}\mathbf{u})'\mathbf{P}_{t+1}(\mathbf{A}\mathbf{x}_t + \mathbf{B}\mathbf{u})\right\} \end{aligned} \tag{2.26}$$

where we represent $\mathbb{E}[\mathbf{w}_t'\mathbf{P}_{t+1}\mathbf{w}_t] = tr(\mathcal{Q}\mathbf{P}_{t+1})$. It can be easily noted that, recursion in equation (2.26) is same as recursion for deterministic LQR with added constant. Thus the optimal control is linear state feedback given by $\mathbf{u}_t^* = \mathbf{K}_t\mathbf{x}_t$ where, $\mathbf{K}_t = -(\mathbf{B}'\mathbf{P}_{t+1}\mathbf{B}+\mathcal{R})^{-1}\mathbf{B}'\mathbf{P}_{t+1}\mathbf{A}$ (same as deterministic LQR). Substituting the optimal control in value function iteration, we get,

$$\begin{aligned} \mathbf{P}_t &= \mathbf{A}'\mathbf{P}_{t+1}\mathbf{A} - \mathbf{A}'\mathbf{P}_{t+1}\mathbf{B}\left(\mathbf{B}'\mathbf{P}_{t+1}\mathbf{B} + \mathcal{R}\right)^{-1}\mathbf{B}'\mathbf{P}_{t+1}\mathbf{A} + \mathcal{Q} \\ q_t &= q_{t+1} + tr(\mathbf{Q}\mathbf{P}_{t+1}) \end{aligned} \tag{2.27}$$

Thus, stochastic LQR is same as deterministic LQR with another running term contributed by process noise. Further the steady state control solution is also constant linear feedback solution. More details about stochastic dynamic programming can be found in [75]. In following subsection, we discuss model predictive control extension for stochastic linear dynamical system.

2.2.3 Model Predictive Stochastic Control

In this subsection, we extend the discussion of model predictive control solution for linear deterministic systems to stochastic systems. Similar to deterministic MPC, at each time step t

$$\begin{array}{ll} min. & \sum_{\tau=t}^{\infty} l\left(\mathbf{x}_t, \mathbf{u}_t\right) \\ s.t. & \mathbf{u}_t \in \mathcal{U}, \mathbf{x}_t \in \mathcal{X},\ \tau = t, \cdots \infty \\ & \mathbf{x}_{t+1} = \mathbf{A}\mathbf{x}_t + \mathbf{B}\mathbf{u}_t + \mathbf{w}_t,\ \tau = t, \cdots \infty \end{array} \tag{2.28}$$

Now, as we assume the process noise to of zero mean, the expected state trajectory evolution is same as of deterministic system model. Thus, considering the quadratic cost function, and optimizing control solution for horizon t, the general model problem (2.28) transforms as,

$$\begin{array}{ll} min. & \sum_{\tau=t}^{t+T} l\left(\mathbf{x}_{t+1}'\mathcal{Q}\mathbf{x}_{t+1} + \mathbf{u}_{t+1}'\mathcal{R}\mathbf{u}_{t+1}\right) \\ s.t. & \mathbf{u}_t \in \mathcal{U}, \mathbf{x}_t \in \mathcal{X},\ \tau = t, \cdots t+T \\ & \mathbf{x}_{t+1} = \mathbf{A}\mathbf{x}_t + \mathbf{B}\mathbf{u}_t,\ \tau = t, \cdots t+T-1 \end{array} \tag{2.29}$$

Thus, the model predictive control solution for stochastic system is same as control solution for deterministic system model. For more dentals about model predictive control solution, interested readers can follow [77]. In next section, we discuss the estimation and control strategies for nonlinear system models.

2.3 Deterministic Nonlinear System Model

In this section, we consider nonlinear discrete time system models and discuss control strategies for this scenario. Similar to deterministic linear model case, deterministic nonlinear state trajectory is computed directly from the system model. So, we directly discuss the control strategies for nonlinear system model.

2.3.1 Nonlinear Model Predictive Control

Consider the following nonlinear discrete time nonlinear system model,

$$\mathbf{x}_{t+1} = f_t\left(\mathbf{x}_t, \mathbf{u}_t\right) \tag{2.30}$$

where, $f_t()$ and $h_t()$ are the nonlinear functions. Similar to model predictive control for linear system models, the nonlinear model predictive control problem is solved by formulating an optimization problem. At each time step t,

$$\begin{array}{ll} min. & \sum_{\tau=t}^{\infty} l\left(\mathbf{x}_t, \mathbf{u}_t\right) \\ s.t. & \mathbf{u}_t \in \mathcal{U}, \mathbf{x}_t \in \mathcal{X},\ \tau = t, \cdots \infty \\ & \mathbf{x}_{t+1} = f_t\left(\mathbf{x}_t, \mathbf{u}_t\right),\ \tau = t, \cdots \infty \end{array} \tag{2.31}$$

The nonlinear model predictive control problem can reformulated for quadratic cost function; however due to nonlinearity in system model, (2.31) is in general a non convex problem; and is generally solved by nonlinear optimization solver. The computational complexity of solution generally depends on: (1) order of nonlinearity; (2) the horizon length T; and, (3) optimization algorithm to solve. In next subsection we formulate an alternate MPC problem; a suboptimal control solution with a lower computational complexity compared to generalized nonlinear MPC (2.31).

Linear Time Varying MPC Approximation

Consider the state $\mathbf{x}_0 \in \mathcal{X}$ and the input $\mathbf{u}_0 \in \mathcal{U}$; and $\hat{\mathbf{x}}_0$ be the state trajectory obtained after applying control sequence $\mathbf{u}_t = \mathbf{0}$, then the LTV approximation of nonlinear system model is given by,

$$\mathbf{x}_{t+1} = \mathbf{A}_{t,0}\mathbf{x}_t + \mathbf{B}_{t,0}\mathbf{u}_t + \mathbf{d}_{t,0} \tag{2.32}$$

where, $\mathbf{A}_{t,0} = \frac{\partial f}{\partial \mathbf{x}}\Big|_{\hat{\mathbf{x}}_t,\mathbf{u}_0}$; $\mathbf{B}_{t,0} = \frac{\partial f}{\partial \mathbf{u}}\Big|_{\hat{\mathbf{x}}_t,\mathbf{u}_0}$; and $\mathbf{d}_{t,0} = \hat{\mathbf{x}}_{t+1} - \mathbf{A}_{t,0}\hat{\mathbf{x}}_t - \mathbf{B}_{t,0}\mathbf{u}_0$. Equation (2.32) is first order approximation of system around a nominal state trajectory $\hat{\mathbf{x}}_t,\ t > 0$. Substituting linear approximation in our nonlinear model predictive control formulation, the finite horizon linear time varying MPC formulation with quadratic cost function is expressed as,

$$\begin{array}{ll} min. & \sum_{\tau=t}^{t+T} \mathbf{x}_t' \mathcal{Q} \mathbf{x}_t + \mathbf{u}_t' \mathcal{R} \mathbf{u}_t \\ s.t. & \mathbf{u}_t \in \mathcal{U}, \mathbf{x}_t \in \mathcal{X},\ \tau = t, \cdots T \\ & \mathbf{x}_{t+1} = \mathbf{A}_{t,0}\mathbf{x}_t + \mathbf{B}_{t,0}\mathbf{u}_t + \mathbf{d}_{t,0},\ \tau = t, \cdots T \end{array} \tag{2.33}$$

Since, (2.33) is linear optimization problem to solve, the dynamic approach taken in deterministic linear system model can now be easily applied. It must be noted that this is suboptimal approach, one needs to be careful about considering linearization error. In next section we finally discuss the estimation and control strategies in presence of process noise.

2.4 Stochastic Nonlinear System Model

Similar, to linear system model influenced by process noise, in this section we consider nonlinear system model in presence of process and measurement noise. We first discuss state estimation strategies followed by nonlinear control strategies for nonlinear stochastic system models.

2.4.1 Extended Kalman Filter

Extended Kalman Filter (EKF) is an extension of Kalman filter to a form linearization about the current state estimates. Over the past several years, EKF has undoubtedly been the most widely used nonlinear estimation technique. When it does not works, the underlying system model is severely nonlinear system or noise variances are relatively large; for such system models higher order EKFs can be exploited by including the higher order Taylors series terms. This improves the performance of EKF at the price of much higher mathematical and computational complexity. First consider the nonlinear system and measurement model,

$$\begin{array}{ll} \mathbf{x}_{t+1} & = f_t\left(\mathbf{x}_t, \mathbf{u}_t, \mathbf{w}_t\right) \\ \mathbf{y}_t & = \mathbf{h}_t\left(\mathbf{x}_t, \mathbf{v}_t\right) \end{array} \tag{2.34}$$

where, $f_t()$ and $h_t()$ are the nonlinear functions; and other variables have notion similar to subsection (). First computing the Jacobian matrices for the nonlinear system model,

$$\mathbf{A}_t = \frac{\partial f_t}{\mathbf{x}}\Big|_{\mathbf{x}_{t|t}} \quad \mathbf{W}_t = \frac{\partial f_t}{\mathbf{w}}\Big|_{\mathbf{x}_{t|t}} \tag{2.35}$$

The time update of state estimate and error covariance are expressed as,

$$\begin{aligned} \mathbf{x}_{t+1|t} &= f_t\left(\mathbf{x}_{t|t}, \mathbf{u}_t, \mathbf{0}\right) \\ \mathbf{P}_{t+1|t} &= \mathbf{A}_t \mathbf{P}_{t|t} \mathbf{A}' + \mathbf{W}_t \mathbf{Q} \mathbf{W}_t'. \end{aligned} \tag{2.36}$$

Once again, computing the Jacobian matrices for nonlinear measurement model,

$$\mathbf{C}_t = \frac{\partial h_t}{\mathbf{x}}\Big|_{\mathbf{x}_{t+1|t}} \quad \mathbf{V}_t = \frac{\partial h_t}{\mathbf{v}}\Big|_{\mathbf{x}_{t+1|t}} \tag{2.37}$$

The measurement update of state estimate and error covariance is expressed as,

$$\begin{aligned} \mathbf{x}_{t+1|t+1} &= \mathbf{x}_{t+1|t} + \mathbf{K}_{t+1}\left(\mathbf{y}_{t+1} = h_t(\mathbf{x}_{t+1|t}, \mathbf{0})\right) \\ \mathbf{P}_{t+1|t+1} &= \left(\mathbf{I} - \mathbf{K}_{t+1}\mathbf{C}_{t+1}\right)\mathbf{P}_{t+1|t} \end{aligned} \tag{2.38}$$

where, $\mathbf{K}_{t+1} = \mathbf{P}_{t+1|t}\mathbf{C}_{t+1}'\left(\mathbf{C}_{t+1}\mathbf{P}_{t+1|t}\mathbf{C}_{t+1}' + \mathbf{V}\mathbf{R}\mathbf{V}'\right)^{-1}$ is called the Kalman gain.

EKF extends the capability of Kalman filter for nonlinear system models, but EKF has following drawbacks: (1) Linearization can produce unstable filter performance if the time sampling step is not sufficiently small (the local linearity is not valid); (2) The composition of Jacobian matrix is non trivial and in some applications leads to unstable performance; (3) Sufficiently small time step intervals require high sampling rate and high computational complexity; (4) Hardware implementation is difficult and and tuning is not possible; (5) EKF using higher order approximations can be very computationally complicated. Other variants of EKF can be followed in [81],[82]. In next subsection, we discuss an alternate state estimation technique for nonlinear systems, which aims in reducing estimation error.

2.4.2 Unscented Kalman Filter

Nonlinear filtering requires a complete description of the conditional probability density function; and to define it requires an unbounded number of sample points to approximate the density function. As mentioned earlier, EKF is based on approximating the nonlinear function or transformation (up to first order terms of Taylor series) instead of probability density function; therefore if higher order terms in Taylor series are dominant, EKF will result in poor filter performance. One approach in nonlinear filtering is particle filter, essentially an extension of Monte Carlo method; as it uses thousands of sample points to fulfill this process, particle filter is rarely used due to its computational burden.

Unscented Kalman filter (UKF) is recent approach in nonlinear filtering with reduced computational complexity, and exhibits less estimation error in many application. It is essentially based on two important principles: (1) perform a nonlinear transformation on to a single point; (2) select a set of points in state space (called sigma points) whose sample probability density function can represent the true density function of state vectors. Therefore, based on the information from these sigma points, we can approximate the statistical properties of the true nonlinear transformation.

Consider the same model represented in equation (2.34); denoting κ as a tuning factor, the time update of state estimates and error covariance is computed by first approximating the n dimensional state vector $\mathbf{x}_t$ (with mean $\mathbf{x}_{t|t}$ and covariance $\mathbf{P}_{t|t}$) in terms of $(2n+1)$ weighted samples or sigma points,

$$\begin{aligned} \mathbf{x}_{t,0} &= \mathbf{x}_{t|t} \\ \mathbf{x}_{t,i} &= \mathbf{x}_{t|t} + \tilde{\mathbf{x}}_i,\ i = 1, \cdots 2n \\ \tilde{\mathbf{x}}_i &= \left(\sqrt{(n+\kappa)\mathbf{P}_{t|t}}\right)_i',\ i = 1, \cdots n \\ \tilde{\mathbf{x}}_{n+i} &= -\left(\sqrt{(n+\kappa)\mathbf{P}_{t|t}}\right)_i',\ i = 1, \cdots n \end{aligned} \tag{2.39}$$

where, $\left(\sqrt{(n+\kappa)\mathbf{P}_{t|t}}\right)_i'$ is the i^{th} row or column of the matrix square root of $(n+\kappa)\mathbf{P}_{t|t}$. Next, $(2n+1)$ weight coefficients are computed,

$$\begin{aligned} W_0 &= \tfrac{\kappa}{n+\kappa} \\ W_i &= \tfrac{1}{2(n+\kappa)},\ i = 1, \cdots 2n. \end{aligned} \tag{2.40}$$

Initiating each sigma point through the process model, $\mathbf{x}_{t+1,i} = f(\mathbf{x}_{t,i}, \mathbf{u}_t, \mathbf{0})$, the apriori mean and covariance are computed as,

$$\begin{aligned} \mathbf{x}_{t+1|t} &= \textstyle\sum_{i=0}^{2n} W_i x_{t+1,i} \\ \mathbf{P}_{t+1|t} &= \mathbf{Q} + \textstyle\sum_{i=1}^{2n} W_i \left(\mathbf{x}_{t+1,i} - \mathbf{x}_{t+1|t}\right)\left(\mathbf{x}_{t+1,i} - \mathbf{x}_{t+1|t}\right)'. \end{aligned} \tag{2.41}$$

The measurement update of state estimate and error covariance is computed by first initializing the observation sample points, i.e., $\mathbf{y}_{t,i} = h_t(\mathbf{x}_{t+1,i}, \mathbf{0})$. Then, predicted observation is calculated as $\tilde{\mathbf{y}}_{t+1} = \sum_{i=0}^{2n} W_i \mathbf{y}_{t+1,i}$. Since, measurement noise is AWGN with covariance $\mathbf{R}$, the covariance of predicted measurement is given by,

$$\mathbf{P}_y = \mathbf{R} + \sum_{i=1}^{2n} W_i \left(\mathbf{y}_{t+1,i} - \mathbf{y}_{t\tilde{+}1|t}\right) \left(\mathbf{x}_{t+1,i} - \mathbf{t+1|t}\right)' \tag{2.42}$$

Similarly, the cross correlation is computed as,

$$\mathbf{P}_{xy} = \sum_{i=1}^{2n} W_i \left(\mathbf{x}_{t+1,i} - \mathbf{x}_{t+1|t}\right) \left(\mathbf{x}_{t+1,i} - \mathbf{t+1|t}\right)' \tag{2.43}$$

Finally, the posterior state estimates and error covariance is computed using Kalman filter equations as,

$$\begin{aligned} \mathbf{K}_{t+1} &= \mathbf{P}_{xy}\mathbf{P}_y^{-1} \\ \mathbf{x}_{t+1|t+1} &= \mathbf{x}_{t+1|t} + \mathbf{K}_{t+1}\left(\mathbf{y}_{t+1} - \tilde{\mathbf{y}}_{t+1}\right) \\ \mathbf{P}_{t+1|t+1} &= \mathbf{P}_{t+1|t} - \mathbf{K}_{t+1}\mathbf{P}_y\mathbf{K}'_{t+1} \end{aligned} \tag{2.44}$$

In following section we discuss control strategy for nonlinear stochastic system models.

2.4.3 Stochastic Nonlinear Model Predictive Control

Consider the following nonlinear discrete time nonlinear system model,

$$\mathbf{x}_{t+1} = f_t\left(\mathbf{x}_t, \mathbf{u}_t, \mathbf{w}_t\right) \tag{2.45}$$

where, $\mathbf{w}_t$ is the process noise influencing the nonlinear system model. Similar to nonlinear model predictive control for deterministic models, the nonlinear model predictive control problem is solved by formulating an optimization problem. At each time step t,

$$\begin{aligned} min. \quad & \textstyle\sum_{\tau=t}^{\infty} l\left(\mathbf{x}_t, \mathbf{u}_t\right) \\ s.t. \quad & \mathbf{u}_t \in \mathcal{U}, \mathbf{x}_t \in \mathcal{X}, \ \tau = t, \cdots \infty \\ & \mathbf{x}_{t+1} = f_t\left(\mathbf{x}_t, \mathbf{u}_t, \mathbf{w}_t\right), \ \tau = t, \cdots \infty \end{aligned} \tag{2.46}$$

Similar, to non convexity problem of deterministic nonlinear model predictive control, in next subsection we formulate an alternate stochastic linear time varying model predictive control; with a quadratic cost function and propose a suboptimal control solution with a lower computational complexity compared to generalized nonlinear MPC (2.46).

Stochastic Linear Time Varying MPC Approximation

Consider the state $\mathbf{x}_0 \in \mathcal{X}$ and the input $\mathbf{u}_0 \in \mathcal{U}$; and $\hat{\mathbf{x}}_0$ be the state trajectory obtained after applying control sequence $\mathbf{u}_t = \mathbf{0}$, then the stochastic linear time varying approximation of nonlinear system model is given by,

$$\mathbf{x}_{t+1} = \mathbf{A}_{t,0}\mathbf{x}_t + \mathbf{B}_{t,0}\mathbf{u}_t + \mathbf{W}_{t,0}\mathbf{w}_t + \mathbf{d}_{t,0} \tag{2.47}$$

where, $\mathbf{A}_{t,0} = \frac{\partial f}{\partial \mathbf{x}}\big|_{\hat{\mathbf{x}_t},\mathbf{u}_0}$; $\mathbf{B}_{t,0} = \frac{\partial f}{\partial \mathbf{u}}\big|_{\hat{\mathbf{x}}_t,\mathbf{u}_0}$; $\mathbf{W}_{t,0} = \frac{\partial f}{\partial \mathbf{w}}\big|_{\hat{\mathbf{x}}_t,\mathbf{u}_0}$; and $\mathbf{d}_{t,0} = \hat{\mathbf{x}}_{t+1} - \mathbf{A}_{t,0}\hat{\mathbf{x}}_t - \mathbf{B}_{t,0}\mathbf{u}_0 - \mathbf{W}_{t,0}\mathbf{w}_t$. Equation (2.47) is first order approximation of system around a nominal state trajectory $\hat{\mathbf{x}}_t,\ t > 0$. Substituting linear approximation in our nonlinear model predictive control formulation, the finite horizon linear time varying MPC formulation with quadratic cost function is expressed as,

$$\begin{array}{ll} min. & \sum_{\tau=t}^{t+T} \mathbf{x}_t'\mathcal{Q}\mathbf{x}_t + \mathbf{u}_t'\mathcal{R}\mathbf{u}_t \\ s.t. & \mathbf{u}_t \in \mathcal{U}, \mathbf{x}_t \in \mathcal{X},\ \tau = t, \cdots T \\ & \mathbf{x}_{t+1} = \mathbf{A}_{t,0}\mathbf{x}_t + \mathbf{B}_{t,0}\mathbf{u}_t + \mathbf{W}_{t,0}\mathbf{w}_t\mathbf{d}_{t,0},\ \tau = t, \cdots T \end{array} \tag{2.48}$$

Now, if we consider that process noise is a zero mean process, then the nonlinear stochastic control reduces similar to control solution for nonlinear deterministic system. More discussion and variants in nonlinear model predictive control solution can be found in [83].

2.5 Summary

In this chapter we discussed estimation and control strategies for various discrete time system models. Firstly, linear system model in both deterministic and stochastic scenario are considered, and respective control strategies like linear quadratic control, model predictive control are presented. For state estimation in stochastic linear system model, Kalman filter is presented. In later sections, nonlinear discrete system models in deterministic and stochastic scenario is considered; and control strategy based on nonlinear model predictive control is presented. State estimation based on extended Kalman filter and unscented Kalman filter is presented for nonlinear stochastic system models.

Chapter 3

Estimation with Intermittent Sensor Measurements

In this chapter, we analyze the stochastic stability of state estimation process in spatially distributed cyber physical systems. We first present the system framework where, Kalman filter is considered for state estimation of stochastic linear dynamical system. The states of underlying dynamical system are spatially distributed over physical space; and sensors are arbitrarily deployed over the area to jointly observe the complete system. In this system setup, there are two possible measurement communication strategies: (1) gathered measurements: sensor measurements are collected first and then sent to estimation over a communication link; (2) Dispersed measurements: sensors directly communicate their measurements to central estimation unit over individual communication links. Since, we are considering large dynamical systems with states distributed over the physical space, dispersed measurements is more appealing feasible implementation strategy. However, the communication links in both these strategies are susceptible to random failures, results in: (1) random measurement losses; and (2) partial observation updates in Kalman filter.

We analyze the stability of the state estimation process in this stochastic scenario by: (1) characterizing the statistical properties of error covariance iteration; (2) and then establishing the necessary and sufficient network conditions under which the steady state error covariance matrix is bounded. In later sections of this chapter, we exploit the possible existence of spatial correlation among states in filtering process; and characterize its impact on critical measurement loss probability. We further extend our analysis by considering correlated loss in communication links. The overall analysis presented in this chapter quantifies the trade-off between state estimation accuracy and the quality of underlying communication network. Further, analysis demonstrates that by exploiting spatial correlation among states, a higher degree of information loss (or lower network quality) can be tolerated to achieve a certain estimation accuracy. Since estimation accuracy directly impacts the stability of control operation, this analysis is critical in ensuring safe and efficient operation of a cyber-physical system.

3.1 Estimation Process Framework

In this section we discuss the state estimation framework for spatially distributed cyber physical system, where measurements are communicated over a lossy network. More specifically, we consider the systems where: (1) system states are distributed in physical space; (2) sensors are arbitrarily deployed such that they jointly sense the complete system; (3) a network infrastructure is used for communicating measurements to a central estimation unit; (4) states may be spatially correlated, and (5) communication links connecting sensors to estimation unit are susceptible to possibly correlated failures. These characteristics (1)-(5) listed above can impact the accuracy of estimated states and can result in an unstable estimation process.

Figure 3.1 presents a conceptual view of the considered system, where nodes (with a state associated) are distributed all over a physical area. Arbitrarily located sensors jointly observe the complete system. Each sensor makes a measurement which is related to the nodes/states in its neighborhood. The observation space of neighboring sensors typically overlaps, resulting in redundancy in state information. These sensor measurements are sent to a central estimation unit over lossy networks resulting in measurements getting delayed or lost due to packet drops. Thus, at any state estimation step, received measurements may

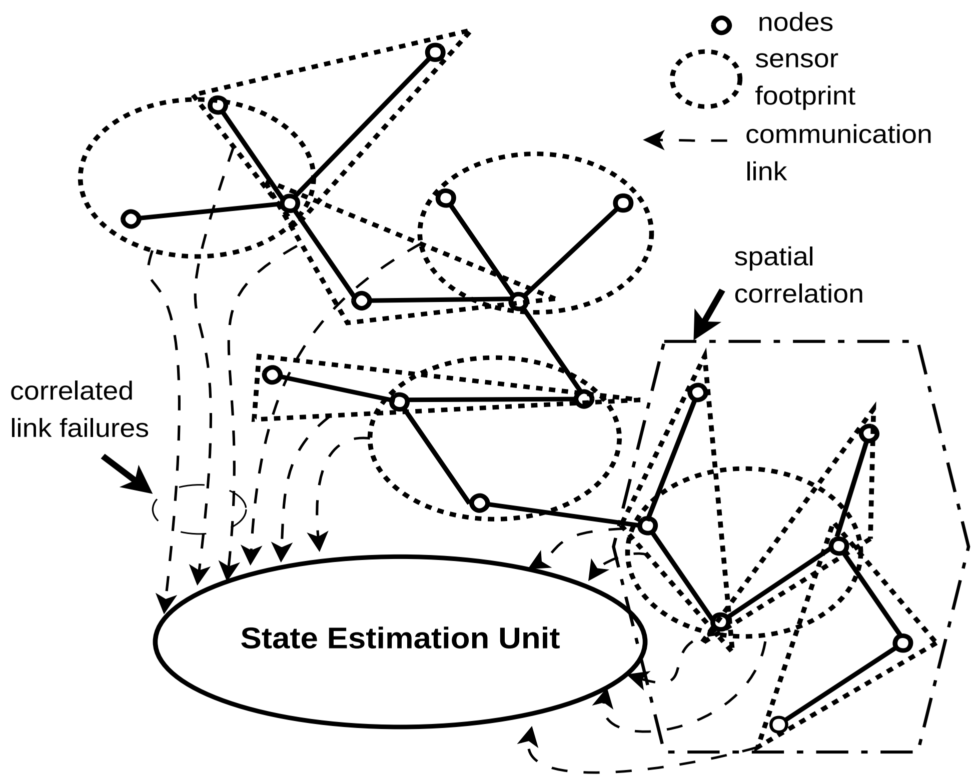

Figure 3.1: *State estimation of spatially distributed physical system over a network*

not be enough for observing all states of the system. We denote this system configuration as dispersed measurement scenario, which is completely different from gathered measurement scenario where measurements are collected and then sent to estimation unit over a communication link. In the analysis shown in later sections, we assume delayed measurements can not be used for state estimation and are considered equivalent to lost measurements.

Figure 3.1 also shows an example footprint of physical area where states exhibit spatial correlation. In addition to temporal correlation, many practical physical systems exhibit spatial correlation between the nodes/states. For example, distributed solar/wind generation in a power distribution systems typically are correlated across space. This results in correlated voltages in neighboring nodes, which are essentially the state elements of power distribution system. Similarly, because of flood/drought in rivers in irrigation networks; localized traffic congestion in city traffic networks, the states of these physical systems may also be spatially correlated. In later sections of this chapter, we show how spatial correlation can be exploited to estimate lost measurements from received measurements. This results in redefining the received measurement vector comprising of actual received measurements, and reconstructed measurements; essentially modifying measurement updates in estimation process. Thus, we present how we can achieve better estimation stability by exploiting spatial correlation among states.

Additionally, considering the arbitrary general nature of communication link between the sensor and central state estimation unit, the communication link failure can be either independent or correlated to each other. However, in practice the communication links are susceptible to correlated failure as illustrated in the Figure 3.1. This occurs mostly in cases where there is local network congestion resulting in high probability of loosing measurements from an area. Additionally, if measurements are routed through a common router that is heavily loaded, measurements in the corresponding communication links will experience similar quality of service. Thus, it is important to consider correlated measurement loss in practice. There is still a need to understand how spatial correlation between states and correlated packet drops in communication links affect estimation accuracy under a dispersed measurement scenario.

Kalman filter based state estimation and its variations have found wide acceptance in many application areas including networked control systems. In following sections we present Kalman filter for state estimation of system framework presented in this section. Later, we discuss the stability of the process by characterizing the statistical properties of error covariance iteration, followed by establishing the necessary and sufficient network conditions for ensuring boundedness of state estimation error at steady state.

3.2 Kalman filter over Intermittent Observations

Minimum mean square error (MMSE) based Kalman filter (KF) is a popular state estimation approach for practical dynamical systems. In this section we present the system model and the problem setup for Kalman filter based state estimation when measurements are communicated over a lossy network. We essentially present, the instability attributed in estimation process under packets drops, with the assumption that underlying system is completely observable under lossless network.

3.2.1 System Model

Consider a discrete time linear dynamical system model,

$$\mathbf{x}_{t+1} = \mathbf{A}\mathbf{x}_t + \mathbf{w}_t$$
$$\mathbf{y}_t = \mathbf{C}\mathbf{x}_t + \mathbf{v}_t \quad (3.1)$$

where, $\mathbf{x}_t \in \mathbb{R}^n$ is the state vector; $\mathbf{A} \in \mathbb{R}^{n\times n}$ is state transition matrix; $\mathbf{y}_t \in \mathbb{R}^m$ is the measurement vector; $\mathbf{C} \in \mathbb{R}^{m\times n}$ is the measurement matrix; and, $\mathbf{w}_t \in \mathbb{R}^n$ and $\mathbf{v}_t \in \mathbb{R}^m$ are the corresponding process and measurement noise. We first consider the scenario without spatial correlation among states i.e., $\mathbb{E}[\mathbf{x}_t\mathbf{x}_t'] = \mathbf{I}_n$. In later sections, we extend our analysis by including spatial correlation among states and using it to estimate lost measurements. We assume both $\mathbf{w}_t$ and $\mathbf{v}_t$ are Gaussian vectors with zero mean and covariances $\mathbf{Q} \succeq \mathbf{0}$ and $\mathbf{R} \succ \mathbf{0}$, respectively. Additionally, we assume $\mathbf{w}_t$ and $\mathbf{v}_t$ are independent of each other.

The elements of measurement vector $\mathbf{y}_t \in \{\mathbf{y}_{t,1}, \mathbf{y}_{t,2}, \cdots \mathbf{y}_{t,k}\}$ consists of measurements from multiple sensors received over a communication network. Thus, there are k measurement sensors, sensing the complete state information. Further, the sensor measurement $\mathbf{y}_{t,j}$ is local in nature, capturing information about state elements located in its observation space j. The observation space of neighboring sensors normally overlap, resulting in state information being captured by more than one sensor. These measurements received over the network, may be lost or delayed. In our system model, we consider network impact in form of packet drops, and assume that the delayed packets are similar to lost packets. Further we assume that measurements are packetized in single packet, i.e., lost packets are equivalent to lost measurements. The measurement model of (3.1) can now be restated as,

$$\begin{bmatrix} \mathbf{y}_{t,1} \\ \mathbf{y}_{t,2} \\ \vdots \\ \mathbf{y}_{t,k} \end{bmatrix} = \begin{bmatrix} \gamma_{t,1}\left(\mathbf{C}_{t,1}\mathbf{x}_t + \mathbf{v}_{t,1}\right) \\ \gamma_{t,2}\left(\mathbf{C}_{t,2}\mathbf{x}_t + \mathbf{v}_{t,2}\right) \\ \vdots\ \vdots\ \vdots \\ \gamma_{t,k}\left(\mathbf{C}_{t,k}\mathbf{x}_t + \mathbf{v}_{t,k}\right) \end{bmatrix} \tag{3.2}$$

where, $\mathbf{y}_{t,j} \in \mathbb{R}^{m_j}$ is the measurement received from sensor j; $\mathbf{C}_{t,j} \in \mathbb{R}^{m_j \times n}$ and $\mathbf{v}_{t,j} \in \mathbb{R}^{m_j}$ are the corresponding measurement matrix and measurement noise, respectively; and $\gamma_{t,j}$ represents the binary random variable taking values 1 for successfully received packet and 0 for dropped packet. For practical physical systems, the random variables indicating measurement loss $\gamma_{t,1}, \cdots, \gamma_{t,k}$ can be either correlated or independent of each other. In either case, we assume that the joint probability mass function $Pr\left(\gamma_{t,1}, \cdots, \gamma_{t,k}\right)$is known. In our initial analysis, we consider independent $\gamma_{t,1}, \cdots, \gamma_{t,k}$, i.e. $Pr\left(\gamma_{t,1}, \cdots, \gamma_{t,k}\right) = Pr\left(\gamma_{t,1}\right) \cdots Pr\left(\gamma_{t,k}\right)$, followed by extending the analysis for general correlated loss scenario.

3.2.2 Problem Formulation

Let $\gamma_t = [\gamma_{t,1}, \gamma_{t,2}, \cdots, \gamma_{t,k}]'$, $\gamma_0^t = \{\gamma_0, \gamma_1, \cdots, \gamma_t\}$, and $\mathbf{y}_0^t = [\mathbf{y}_0, \mathbf{y}_1, \cdots, \mathbf{y}_t]'$. Then following KF approach, we define

$$\begin{aligned} \hat{\mathbf{x}}_{t|t} &= \mathbb{E}[\mathbf{x}_t | \mathbf{y}_0^t, \gamma_0^t], \\ \mathbf{P}_{t|t} &= \mathbb{E}[(\mathbf{x}_t - \hat{\mathbf{x}}_{t|t})(\mathbf{x}_t - \hat{\mathbf{x}}_{t|t})' | \mathbf{y}_0^t, \gamma_0^t], \\ \hat{\mathbf{x}}_{t+1|t} &= \mathbb{E}[\mathbf{x}_{t+1} | \mathbf{y}_0^t, \gamma_0^t], \\ \mathbf{P}_{t+1|t} &= \mathbb{E}[(\mathbf{x}_{t+1} - \hat{\mathbf{x}}_{t+1|t})(\mathbf{x}_{t+1} - \hat{\mathbf{x}}_{t+1|t})' | \mathbf{y}_0^t, \gamma_0^t], \end{aligned} \tag{3.3}$$

where, $\mathbf{x}_t$, $\hat{\mathbf{x}}_{t|t}$ and $\hat{\mathbf{x}}_{t+1|t}$ denotes true, estimated and predicted state vector; and $\mathbf{P}_{t|t}$ and $\mathbf{P}_{t+1|t}$ are the corresponding posterior and a priori error covariance matrix. The prediction stage of KF is independent of the observation process, and is expressed as,

$$\begin{aligned} \mathbf{x}_{t+1|t} &= \mathbf{A}\hat{\mathbf{x}}_{t|t}, \\ \mathbf{P}_{t+1|t} &= \mathbf{A}\mathbf{P}_{t|t}\mathbf{A}' + \mathbf{Q}. \end{aligned} \tag{3.4}$$

The measurement update stage depends on random variable $\gamma_{t,1}, \gamma_{t,2}, \cdots, \gamma_{t,k}$ and is thus stochastic in nature. When $\gamma_{t,1} = \gamma_{t,2} = \cdots = \gamma_{t,k} = 1$ then the system is completely

$\{\gamma_{t,1}, \gamma_{t,2}, \gamma_{t,3}, \gamma_{t,4}\}$	$\alpha_{\lambda_1,\lambda_2,\lambda_3,\lambda_4}$
$0,0,0,0$	$(1-\lambda_1)(1-\lambda_2)(1-\lambda_3)(1-\lambda_4)$
$0,0,0,1$	$(1-\lambda_1)(1-\lambda_2)(1-\lambda_3)\lambda_4$
$0,0,1,0$	$(1-\lambda_1)(1-\lambda_2)\lambda_3(1-\lambda_4)$
$\vdots$	$\vdots$
$0,0,1,1$	$(1-\lambda_1)(1-\lambda_2)\lambda_3\lambda_4$
$0,1,1,0$	$(1-\lambda_1)\lambda_2\lambda_3(1-\lambda_4)$
$\vdots$	$\vdots$
$1,1,1,1$	$\lambda_1\lambda_2\lambda_3\lambda_4$

Table 3.1: *Possible measurement sets for 4 sensor network*

observable and the measurement update can be expressed as,

$$\begin{aligned}\hat{\mathbf{x}}_{t+1/t+1} &= \hat{\mathbf{x}}_{t+1/t} + \mathbf{P}_{t+1/t}\mathbf{C}'[\mathbf{C}\mathbf{P}_{t+1/t}\mathbf{C}' + \mathbf{R}]^{-1}(\mathbf{y}_{t+1} - \mathbf{C}\hat{\mathbf{x}}_{t+1,t}),\\ \mathbf{P}_{t+1/t+1} &= \mathbf{P}_{t+1/} - \mathbf{P}_{t+1/t}\mathbf{C}'[\mathbf{C}\mathbf{P}_{t+1/t}\mathbf{C}' + \mathbf{R}]^{-1}\mathbf{C}\mathbf{P}_{t+1/t+1} \qquad (3.5)\end{aligned}$$

When $\gamma_{t,1} = \gamma_{t,2} = \cdots = \gamma_{t,m} = 0$, then the system is completely unobservable and the measurement update is same as prediction stage (3.4), i.e. $\mathbf{x}_{t+1|t+1} = \mathbf{x}_{t+1|t}$; and $\mathbf{P}_{t+1|t+1} = \mathbf{P}_{t+1|t}$. Apart from being completely observable and unobservable, there are other possible scenarios. Specifically, depending on received set of measurements, the system may be observable or unobservable. In these scenarios, the sensor measurements with packet drops are assumed to have infinite noise variance, and the measurement update is only based on successfully received sensor measurements. Let $\mathbf{H}_t$ and $\mathcal{R}_t$ denote the measurement matrix and the measurement noise vector for the received measurement set, then the measurement update for stochastic packet drops can be expressed as,

$$\begin{aligned}\hat{\mathbf{x}}_{t+1|t+1} &= \hat{\mathbf{x}}_{t+1|t} + \mathbf{P}_{t+1|t}\mathbf{H}_t'[\mathbf{H}_t\mathbf{P}_{t+1|t}\mathbf{H}_t' + \mathcal{R}_t]^{-1}(\mathbf{y}_{t+1} = \mathbf{H}_t\hat{\mathbf{x}}_{t+1,t}),\\ \mathbf{P}_{t+1/t+1} &= \mathbf{P}_{t+1/} - \mathbf{P}_{t+1/t}\mathbf{H}_t'[\mathbf{H}_t\mathbf{P}_{t+1/t}\mathbf{H}_t' + \mathcal{R}_t]^{-1}\mathbf{H}_t\mathbf{P}_{t+1/t+1} \qquad (3.6)\end{aligned}$$

Substituting $\mathbf{P}_{t|t}$ from (3.6) in expression of $\mathbf{P}_{t+1|t}$ (3.4), and denoting $\mathbf{P}_t = \mathbf{P}_{t+1|t}$, the recursive state error covariance prediction can be expressed as,

$$\mathbf{P}_{t+1} = \mathbf{A}\mathbf{P}_t\mathbf{A}' + \mathbf{Q} - \mathbf{A}\mathbf{P}_t\mathbf{H}_t'[\mathbf{H}_t\mathbf{P}_t\mathbf{H}_t' + \mathcal{R}_t]^{-1}\mathbf{H}_t\mathbf{P}_t\mathbf{A}_t' \qquad (3.7)$$

The stability of Kalman filter depends on convergence of error covariance matrix $\mathbf{P}_t$ to some finite matrix. In case of ideal communication network with no packet drops, the hypothesis of stabilizability of pair $(\mathbf{A}, \mathbf{Q})$, and detectability of the pair $(\mathbf{A}, \mathbf{C})$ ensures convergence of $\mathbf{P}_t$ to unique value from any initial conditions [84]. However, because of random packet drops, we no longer have unique deterministic error covariance matrix in the steady state. Further it can be noticed that the received measurement set is random and there are 2^k possible measurement sets. In our analysis we consider packet drops as Bernoulli random variable with $Pr(\gamma_{t,j} = 1) = \lambda_j$ as probability of successfully receiving a packet from sensor j. Thus, we can compute probabilities for all 2^k possible measurement sets. For example, if total number of sensors is 4, then possible set of received measurements with their respective probabilities α_λ is shown in table (3.2.2). Our goal is to determine the critical rates for packet drops from individual sensors, sufficient to bound the estimation error to a desired value. In next section, we focus on the statistical properties of the Kalman filter in presence of these partial observation losses.

3.3 Stability Analysis: Statistical Properties

It was observed in section 3.2.2 that the error covariance update equation (3.7) is function of measurement matrix $\mathbf{H}_t$ which depends on random packet drops. Thus, the error covariance matrix propagation along the time $\{\mathbf{P}_t\}_{t=0}^{\infty}$ is a random process for any given starting point $\mathbf{P}_0$. This section focuses on statistical convergence properties of $\{\mathbf{P}_t\}_{t=0}^{\infty}$, yielding to stability analysis of state estimation error. Since $\mathbf{P}_t$ is random process, we are considering convergence in mean i.e. $\mathbb{E}[\mathbf{P}_{t+1}] = \mathbb{E}[\mathbb{E}[\mathbf{P}_{t+1} \,|\mathbf{P}_t]] \leq \infty$ as $t \to \infty$. Further, it can be noted that we consider two expectation operations: (1) as error covariance is itself stochastic the outer expectation taken over $\mathbf{P}_t$; (2) and inner expectation over random packet drops at given iteration t, i.e. over $\gamma_{t,1}, \gamma_{t,2}, \cdots, \gamma_{t,k}$. We define $\mathbb{E}[\mathbf{P}_{t+1}|\mathbf{P}_t]$, as modified algebraic Riccati equation with a short hand notation $\mathbb{E}[\mathbf{P}_{t+1}|\mathbf{P}_t] = \mathbf{g}_\alpha(\mathbf{X})$ expressed as,

$$\mathbf{g}_\alpha(\mathbf{X}) = \quad \mathbf{AXA}' + \mathbf{Q} - \textstyle\sum_{i=1}^{2^k-1} \alpha_i \mathbf{AXH}_i'[\mathbf{H}_i\mathbf{XH}_i' + \mathcal{R}_i]^{-1}\mathbf{H}_i\mathbf{XA}_t' \tag{3.8}$$

where, $\alpha_i = \alpha_{\lambda_1,\cdots,\lambda_k}$ is the probability of receiving i^{th} set of measurements. Next, we define an auxiliary function whose properties are closely related to $\mathbf{g}_\alpha(\mathbf{X})$. Let

$$\phi(\mathcal{K}_1, \mathcal{K}_2, \cdots, \mathcal{K}_{2^k-1}, \mathbf{X}) = \alpha_0(\mathbf{AXA'} + \mathbf{Q}) + \textstyle\sum_{i=1}^{2^k-1} \alpha_i \left(\mathbf{F}_i\mathbf{XF}_i' + \mathbf{V}_i\right) \tag{3.9}$$

where, $\alpha_0 = (1-\sum_{i=1}^{2^k-1} \alpha_i)$; $\mathbf{F}_i = \mathbf{A}+\mathcal{K}_i\mathbf{H}_i$; $\mathbf{V}_i = \mathbf{Q}+\mathcal{K}_i\mathcal{R}_i\mathcal{K}_i'$; and $\mathbf{X} \succeq 0$. This equation intuitively is a balance between various measurement update scenarios $(\mathbf{F}_i\mathbf{XF}_i' + \mathbf{V}_i)$ and not receiving any measurement $(\mathbf{AXA'} + \mathbf{Q})$; with the balancing weights $\alpha_0, \cdots, \alpha 2^k - 1$. Observe that, $\mathbf{F}_i\mathbf{XF}_i'+\mathbf{V}_i$ is quadratic function of $\mathcal{K}_i$; further one can verify $(\mathbf{A} + \mathcal{K}_i^x\mathbf{C}_i)\,\mathbf{XC}_i'+\mathcal{K}_i^x\mathbf{R}_i = 0$; thus, $argmin_{\mathcal{K}_i}\ \mathbf{F}_i\mathbf{XF}_i' + \mathbf{V}_i$ is $\mathcal{K}_i^X = -\mathbf{AXH}_i'\left(\mathbf{H}_i\mathbf{XH}_i' + \mathcal{R}_i\right)^{-1}$. These observations further quantify our observations as,

$$\mathbf{g}_\alpha(\mathbf{X}) = \phi(\mathcal{K}_1^X, \mathcal{K}_2^X, \cdots, \mathcal{K}_{2^k-1}^X, \mathbf{X}) \preceq \min{}_{\mathcal{K}_1,\cdots,\mathcal{K}_{2^k-1}} \phi(\mathcal{K}_1, \cdots, \mathcal{K}_{2^k-1}, \mathbf{X}) \tag{3.10}$$

Thus from (3.10), the auxiliary function $\phi(\cdots)$ acts as an upper bound to $\mathbf{g}_\alpha(\mathbf{X})$. Next, we present some useful properties of $\mathbf{g}_\alpha(\mathbf{X})$, which will allow us to bound the steady state error covariance matrix $lim_{t\to\infty}\mathbb{E}[\mathbf{P}_t]$. The proofs of the following lemmas appear in appendix A.

Lemma 3.1. $\mathbf{g}_\alpha(\mathbf{X})$ *is concave function in* $\mathbf{X}$*, for* $\mathbf{X} \succeq 0$*. Thus, by Jensen's inequality* $\mathbb{E}[\mathbf{g}_\alpha(\mathbf{X})] \preceq \mathbf{g}_\alpha(\mathbb{E}[\mathbf{X}])$*.*

The concave nature of function $\mathbf{g}_\alpha(\mathbf{X})$ helps us in establishing an upper bound on $\mathbb{E}[\mathbf{P}_{t+1}]$ as a function of $\mathbb{E}[\mathbf{P}_t]$.

Lemma 3.2. $\mathbf{g}_\alpha(\mathbf{X})$ *is monotonously nondecreasing function of* $\mathbf{X}$*. Thus if, if* $0 \preceq \mathbf{X} \preceq \mathbf{Y}$*, then* $\mathbf{g}_\alpha(\mathbf{X}) \preceq \mathbf{g}_\alpha(\mathbf{Y})$*.*

This monotonous nondecreasing property helps us in proving the convergence of recursion $\mathbf{P}_{t+1} = \mathbf{g}_\alpha(\mathbf{P}_t)$. Thus, if $\mathbf{X}_{t+1} = \mathbf{g}_\alpha(\mathbf{X}_t)$ and $\mathbf{Y}_{t+1} = \mathbf{g}_\alpha(\mathbf{Y}_t)$, then initial conditions $\mathbf{X}_0 \succeq \mathbf{Y}_0 \succeq \mathbf{0} \ \Rightarrow\ \mathbf{X}_t \succeq \mathbf{Y}_t$ for all iterations t.

Lemma 3.3. *Fixing packet drop rate for all sensor measurements except for one sensor* j*, such that* $\lambda_j^1 \leq \lambda_j^2$*, then for corresponding* α^1 *and* α^2*,* $\mathbf{g}_{\alpha^1}(\mathbf{X}) \preceq \mathbf{g}_{\alpha^2}(\mathbf{X})$

This property intuitively explains that regular sensor measurements will better stabilize the estimation process. Thus, if arrival probabilities of sensor measurements increases, the underlying system is better estimated. In other words, the convergence of $\mathbf{P}_t$ is faster as the measurement receiving rate increased. This lemma eventually helps us in determining instability region for the recursion $\mathbb{E}[\mathbf{P}_t] = \mathbf{g}_\lambda(\mathbf{P}_t)$.

Before, discussing other properties, we define another auxiliary function that captures the linear part of $\phi(\mathcal{K}_1, \cdots, \mathcal{K}_{2^k-1}, \mathbf{X})$. Let

$$\mathcal{L}(\mathbf{X}) = \alpha_0 \mathbf{A}\mathbf{X}\mathbf{A}' + \sum_{i=1}^{2^k-1} \alpha_i \mathbf{F}_i \mathbf{X} \mathbf{F}_i' \tag{3.11}$$

It can be easily observed that $\mathcal{L}(\mathbf{X})$ is linear function of $\mathbf{X}$ and due to $\mathbf{X} \succeq \mathbf{0}$, $\mathcal{L}(\mathbf{X}) \succeq \mathbf{0}$. Furthermore, we can identify auxiliary function $\phi(\mathcal{K}_1, \cdots, \mathcal{K}_{2^k-1}, \mathbf{X})$ as an affine function of $\mathbf{X}$, with $\phi(\mathcal{K}_1, \cdots, \mathcal{K}_{2^k-1}, \mathbf{X}) = \mathcal{L}(\mathbf{X}) + \mathcal{V}$, where $\mathcal{V} = \alpha_0 \mathbf{Q} + \sum_{i=1}^{2k-1} \alpha_i \mathbf{V}_i$. Notice, since $\mathbf{Q} \succeq 0$ and $\mathbf{V}_i \succeq 0$, $\mathcal{V} \succeq 0$.

Lemma 3.4. *Let there exists a bounded solution of $\mathcal{L}(\mathbf{X})$, such that $\mathcal{Y} \succeq \mathcal{L}(\mathcal{Y})$, then, (1) $\forall\ \mathcal{W} \succeq \mathbf{0}$, $lim_{t\to\infty}\mathcal{L}(\mathcal{W}) = \mathbf{0}$; (2) For $\mathcal{V} \geq 0$, $\mathcal{Y}_{t+1} = \mathcal{L}(\mathcal{Y}_t) + \mathcal{V}$. Thus, for any arbitrary initial condition $\mathcal{Y}_0$, $\mathcal{Y}_t$ is bounded.*

This property gives a condition that the recursion of linear auxiliary function $\mathcal{L}(\mathbf{X})$ converges to $\mathbf{0}$, which in turn leads to convergence of recursion of affine auxiliary function $\mathbf{Y}_{t+1} = \mathcal{L}(\mathbf{Y}_t) + \mathcal{T}$ for bounded initial condition $\mathbf{Y}_0$.

Lemma 3.5. *If there exists some $\bar{\mathcal{K}}_1, \cdots, \bar{\mathcal{K}}_{2^k-1}$, and $\bar{\mathbf{P}} \succ 0$, such that $\bar{\mathbf{P}} \succ \phi(\bar{\mathcal{K}}_1, \cdots, \bar{\mathcal{K}}_{2^k-1}, \bar{\mathbf{P}})$, then for any arbitrary initial condition $\bar{\mathbf{P}}_0 \succeq 0$, $\bar{\mathbf{P}} = g_\alpha^t(\bar{\mathbf{P}}_0)$ is bounded.*

This lemma establishes the condition for the recursion of $\bar{\mathbf{P}}_{t+1} = \mathbf{g}_\lambda(\bar{\mathbf{P}}_t)$ to be bounded for any arbitrary initial condition $\bar{\mathbf{P}}_0$. In the following section, we use above properties to establish the conditions for convergence of recursion $\mathbf{g}_\lambda(\mathbf{X})$.

In following subsection we use above properties of $\mathbf{g}_\alpha(\mathbf{X})$, to analyze the conditions for convergence of error covariance matrix.

3.3.1 Convergence conditions

It can be observed that, Lemma 3.5 establishes conditions for boundedness of auxiliary function, which further ensures boundedness of error covariance matrix. We formally put these conditions in form of following theorem, (proof follow in appendix A)

Theorem 3.1. *Let there exists a bound* $\mathbf{X} \succ \phi(\mathcal{K}_1, \cdots, \mathcal{K}_{2^k-1}, \mathbf{P})$ *for* $\mathbf{X} \succeq \mathbf{0}$*, then (1)* $lim_{t\to\infty}\mathbf{X}_t = lim_{t\to\infty}\mathbf{g}_\alpha\ (\mathbf{X_0}) = \mathbf{X}$*, for any starting* $\mathbf{X}_0 \succeq \mathbf{0}$*; (2) converging solution* $\mathbf{X}$ *is unique.*

This theorem proves the convergence of $\mathbf{P}_{t+1} = \mathbf{g}_\alpha(\mathbf{P}_t)$ under some given conditions. It also shows the uniqueness of solution when it converges. Next theorem establishes existence of stability region boundary such that the expected error covariance becomes unbounded if packet drop rates are beyond the specified critical values. Next theorem establishes existence of stability region boundary such that the expected error covariance becomes unbounded if packet drop rates are beyond the specified critical values.

Theorem 3.2. *Given a stable system i.e. matrix pair* $(\mathbf{A}, \mathbf{Q})$ *and* $(\mathbf{A}, \mathbf{C})$ *are controllable and observable, then* $\exists\ 0 \leq \{\lambda_1^c, \cdots, \lambda_k^c\} \leq 1$ *such that* $lim_{t\to\infty}\mathbb{E}[\mathbf{X}_t] = \infty$ *if all sensor packet drop probabilities are at critical rate except one sensor* j*, i.e.* $0 \leq \lambda_j \leq \lambda_j^c$*.*

In general, we can not explicitly compute the critical probabilities of successful transmission, but we can compute both and upper and lower bounds on $\{\lambda_{c,1}, \cdots, \lambda_{c,k}\}$. Now, as we have established conditions for existence of converging solution, in following section we analyze the lower and upper bound on converging solution, along with corresponding lower and upper bound on critical measurement drop rates.

3.4 Bounds on Critical Measurement Loss

The stability of state estimation error depends on convergence of (3.7),(3.8), which in turn depended on probability of measurement drop rates. Further due to randomness of packet drops in received measurement set, solving for bounded error covariance at steady state is extremely difficult. In the following analysis, we compute upper and lower bounds on converging solution followed by computation of corresponding upper and lower bound on critical measurement drop rates. This results in a concatenated k-dimensional regions (assuming k independent sensors) where: (1) inside inner region, the system is definitely unstable; (2) outside outer region, the system is definitely stable; (3) the in between region system is indeterminate. To proceed further in our analysis, we first compare the considered system model with the measurement scenario studied in [57].

3.4.1 Gathered / Dispersed Measurements Analogy

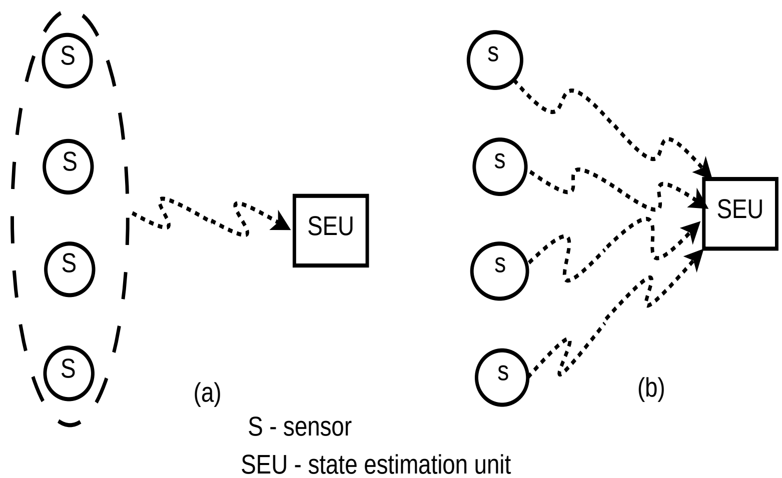

Figure 3.2: *Measurement transmission strategies: (a) gathered information (b) dispersed information*

Consider two strategies of communicating measurements to state estimation unit: (1) measurements from multiple sensors are first gathered and then sent over the communication network, as shown in Figure 3.2(a); (2) dispersed measurements are individually sent over the communication network as in Figure 3.2(b). For ideal loss free communication network, the observed information is same in both the scenarios as received set of measurements is identical. Thus, the Fisher information matrix (FIM) of state vector $\mathbf{x}$ in observed measurements $\mathbf{y}_1, \cdots, \mathbf{y}_k$ is the same and corresponds to,

$$\mathcal{J}(\mathbf{x}) = -\mathbb{E}\left[\frac{\partial}{\partial \mathbf{x}} log\left(f(\mathbf{y}_1, \cdots, \mathbf{y}_k|\mathbf{x})\right)\right]^2,$$

where, $f(.|.)$ is conditional density. Following the discussion in [85], the recursive equation for FIM can be expressed as,

$$\mathcal{J}_{t+1} = \mathbf{Q}^{-1} - \mathbf{Q}^{-1}\mathbf{A}\left(\mathcal{J}_t + \mathbf{A}'\mathbf{Q}^{-1}\mathbf{A} + \mathbf{C}'\mathbf{R}^{-1}\mathbf{C}\right)^{-1}\mathbf{A}\mathbf{Q}^{-1} \tag{3.12}$$

Further, Kalman filter being optimal for linear dynamic system under known Gaussian noise covariance, the error covariance recursive equation (3.5) and FIM recursive equation (3.12) converge to same matrix, i.e., $lim_{t\to\infty}\mathbf{P}_t = \mathcal{J}_t^{-1}$ Cramer-Rao lower bound (CRLB). In the case of lossy communication network, information for state estimation unit is reduced. However, as effective information required to observe the states depends on dynamics of the underlying system, the Kalman filter can still be stable. Thus, every system can afford a critical amount of information loss before becoming unobservable. This critical information loss can be accommodated in both the communication strategies shown in Figure 3.2. Since, the Riccati equation for error covariance in these two strategies are different, the corresponding recursive equations for FIM in gathered and dispersed measurement scenario can be re-derived as,

$$\begin{aligned} (Gathered) \quad \mathcal{J}^s_{t+1} &= \mathbf{Q}^{-1} - \mathbf{Q}^{-1}\mathbf{A}\left(\mathcal{J}^s_t + \mathbf{A}'\mathbf{Q}^{-1}\mathbf{A} + \lambda_s\mathbf{C}'\mathbf{R}^{-1}\mathbf{C}\right)^{-1}\mathbf{A}\mathbf{Q}^{-1} \\ (Dispersed) \quad \mathcal{J}^{ms}_{t+1} &= \mathbf{Q}^{-1} - \mathbf{Q}^{-1}\mathbf{A}\left(\mathcal{J}^{ms}_t + \mathbf{A}'\mathbf{Q}^{-1}\mathbf{A} + \sum_{i=1}^{2k-1}\alpha_i\mathbf{H}'_i\mathcal{R}_i^{-1}\mathbf{H}_i\right)^{-1}\mathbf{A}\mathbf{Q}^{-1} \end{aligned} \tag{3.13}$$

With the underlying system dynamics being same, the trajectories of recursive equations in (3.13) will converges to same FIM in both communication strategies for the same amount of loss of critical information loss. Additionally, Kalman filter being optimal in both these communication strategies, the corresponding Riccati equations for error covariance will also converge to same matrix, $lim_{t\to\infty}\mathbf{P}^s_t = \mathbf{P}^{ms}_t = (\mathcal{J}^t_s)^{-1} = (\mathcal{J}^{ms}_t)^{-1}$. In the following analysis we use the above intuition to compute bounds on critical measurement drop rates.

3.4.2 Lower bound on packet drop probabilities

The error covariance iteration for gathered measurement exchange is expressed as,

$$\mathbf{P}_{t+1} = \mathbf{A}\mathbf{P}_t\mathbf{A}' + \mathbf{Q} - \lambda\mathbf{A}\mathbf{P}_t\mathbf{C}\left(\mathbf{C}\mathbf{P}_t\mathbf{C}' + \mathbf{R}\right)^{-1}\mathbf{C}\mathbf{P}_t\mathbf{A}' \tag{3.14}$$

At every iteration, the error covariance can be in either converging or diverging state with λ

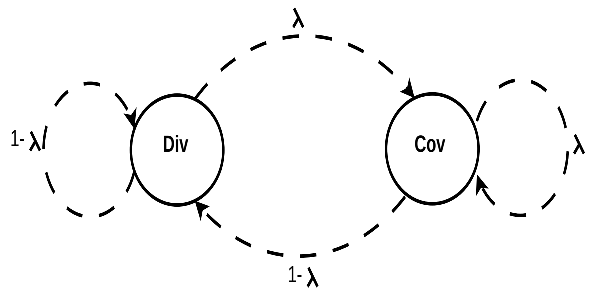

Figure 3.3: *Error covariance convergence and divergence for gathered measurements*

being the transition probability, as shown in Figure 3.3. The lower bound on critical packet drop rate (or transition probability) is determined by computing the minimum arrival rate which will keep the diverging state bounded. Thus, the lower bound on probability of packet drop in gathered measurement scenario is given by, $1 - \lambda^c_{s,lb} = max[1, \frac{1}{\rho_A^2}]$, where ρ_A is the maximum eigen value of $\mathbf{A}$ [57]. Further, lower bound on error covariance at convergence can be obtained by solving,

$$\mathbf{P}_s = (1 - \hat{\lambda}^c_{s,lb})\mathbf{A}\mathbf{P}_s\mathbf{A}' + \mathbf{Q} \tag{3.15}$$

where, $\hat{\lambda}^c_{s,lb} > \lambda^c_{s,lb}$. It should be noted that $\lambda^c_{s,lb}$ is the probability of $\mathbf{P}_s$ getting unbounded. So we need to solve (3.15), at probability slightly higher then $\lambda^c_{s,lb}$.

Now at steady state, the error covariance iteration for the considered spatially distributed system is expressed as,

$$\mathbf{P} = \mathbf{A}\mathbf{P}\mathbf{A}' + \mathbf{Q} - \sum_{i=1}^{2^k-1}\alpha_i\mathbf{A}\mathbf{P}\mathbf{H}_i'\left(\mathbf{H}_i\mathbf{P}\mathbf{H}_i' + \mathcal{R}_i\right)^{-1}\mathbf{H}_i\mathbf{P}\mathbf{A}' \tag{3.16}$$

Let $\mathbf{C} = \begin{bmatrix}\mathbf{H}\\ \mathbf{G}\end{bmatrix}$ where, $\mathbf{H}$ is the received set of sensor measurement matrix, and $\mathbf{G}$ is the corresponding set of lost measurements. Figure 3.4, represents an equivalence to gathered

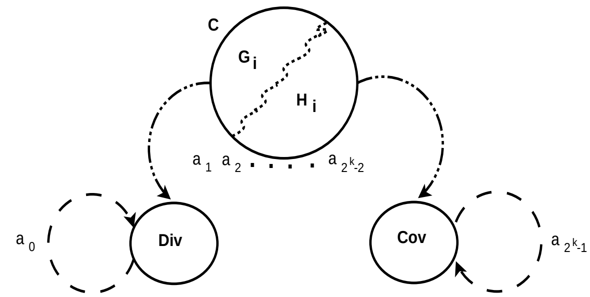

Figure 3.4: *Error covariance convergence and divergence for dispersed measurements*

measurement case, with $\mathbf{H}_i$ contributing to convergence and $\mathbf{G}_i$ contributing to divergence for i^{th} measurement set. Now expanding $\mathbf{C}' \left[\mathbf{CPC}' + \mathbf{R}\right]^{-1} \mathbf{C}$ we get,

$$\begin{aligned} & \mathbf{C}' \left[\mathbf{CPC}' + \mathbf{R}\right]^{-1} \mathbf{C} = \\ & \begin{bmatrix} \mathbf{H}' & \mathbf{G}' \end{bmatrix} \left[\begin{bmatrix} \mathbf{H} \\ \mathbf{G} \end{bmatrix} \mathbf{P} \begin{bmatrix} \mathbf{H}' & \mathbf{G}' \end{bmatrix} + \begin{bmatrix} \mathbf{R}_H & \mathbf{R}_{HG} \\ \mathbf{R}_{GH} & \mathbf{R}_G \end{bmatrix} \right]^{-1} \begin{bmatrix} \mathbf{H} \\ \mathbf{G} \end{bmatrix} \\ & \begin{bmatrix} \mathbf{H}' & \mathbf{G}' \end{bmatrix} \begin{bmatrix} \mathbf{HPH}' + \mathbf{R}_H & \mathbf{HPG}' + \mathbf{R}_{HG} \\ \mathbf{GPH}' + \mathbf{R}_{GH} & \mathbf{GPG}' + \mathbf{R}_G \end{bmatrix}^{-1} \begin{bmatrix} \mathbf{H} \\ \mathbf{G} \end{bmatrix} \\ & = \begin{bmatrix} \mathbf{H}' & \mathbf{G}' \end{bmatrix} \begin{bmatrix} A & B \\ C & D \end{bmatrix} \begin{bmatrix} \mathbf{H} \\ \mathbf{G} \end{bmatrix} \\ & = \mathbf{H}'A\mathbf{H} + \mathbf{G}'C\mathbf{H} + \mathbf{H}'B\mathbf{G} + \mathbf{G}'D\mathbf{G} \end{aligned} \tag{3.17}$$

Further, representing $\mathbf{HPH}' + \mathbf{R}_H = K$, $\mathbf{HPG}' + \mathbf{R}_{HG} = L$, $\mathbf{GPH}' + \mathbf{R}_{GH} = M$, and $\mathbf{GPG}' + \mathbf{R}_G = N$, the expressions for block matrix inverses can be stated as,

$$\begin{aligned} A = & \quad K^{-1} + K^{-1}L\left(N - MK^{-1}L\right)^{-1} MK^{-1} \\ B = & \quad -K^{-1}L\left(N - MK^{-1}L\right)^{-1} \\ C = & \quad -N^{-1}M\left(K - LN^{-1}M\right)^{-1} \\ D = & \quad N^{-1} + N^{-1}M\left(K - LN^{-1}M\right)^{-1} LN^{-1} \end{aligned}$$

Rearranging the terms in (3.17) we get,

$$\mathbf{H}'\left(\mathbf{HPH}' + \mathbf{R}_H\right)^{-1}\mathbf{H} = \quad \mathbf{C}'\left(\mathbf{CPC}' + \mathbf{R}\right)^{-1}\mathbf{C} - \mathcal{F}\left(\mathbf{H}, \mathbf{G}, \mathbf{P}\right) \tag{3.18}$$

where,

$$\begin{aligned} \mathcal{F}\left(\mathbf{H}, \mathbf{G}, \mathbf{P}\right) = & \quad \mathbf{H}'K^{-1}L\left(N - MK^{-1}L\right)^{-1}\left(MK^{-1}\mathbf{H} - \mathbf{G}\right) \\ & +\mathbf{G}'N^{-1}M\left(K - LN^{-1}M\right)^{-1}\left(LN^{-1}\mathbf{G} - \mathbf{H}\right) + \mathbf{G}'N^{-1}\mathbf{G} \end{aligned}$$

Finally, substituting $\mathbf{H}'\left(\mathbf{HXH}' + \mathbf{R}_H\right)^{-1}\mathbf{H}$ in (3.16), the error covariance iteration for multi sensor case in steady state can be expressed as,

$$\begin{aligned} \mathbf{P} = & \quad \mathbf{APA}' + \mathbf{Q} - \left[\textstyle\sum_{i=1}^{2^k-1} \alpha_i\right] \mathbf{APC}'\left(\mathbf{CPC}' + \mathbf{R}\right)^{-1}\mathbf{CPA}' \\ & + \textstyle\sum_{i=1}^{2^k-2} \alpha_i \mathbf{AP}\mathcal{F}\left(\mathbf{H}_i, \mathbf{G}_i, \mathbf{P}\right)\mathbf{PA}' \end{aligned} \tag{3.19}$$

The corresponding auxiliary function similar to (3.9) can be expressed as,

$$\begin{aligned}\phi(\mathcal{K}, \mathbf{X}) = \;& \alpha_0 \left(\mathbf{AXA}' + \mathbf{Q}\right) + (1-\alpha_0)\left(\mathbf{FXF}' + \mathbf{V}\right) \\ & + \textstyle\sum_{i=1}^{2^k-2} \alpha_i \mathbf{AX}\mathcal{F}\left(\mathbf{H}_i, \mathbf{G}_i, \mathbf{X}\right)\mathbf{XA}'\end{aligned} \tag{3.20}$$

where, $\mathbf{F} = \mathbf{A} + \mathcal{K}\mathbf{C}$; and $\mathbf{V} = \mathbf{Q} + \mathcal{K}\mathbf{R}\mathcal{K}'$. Next, we present a lemma providing a universal lower bound on steady state error covariance $\mathbf{P}$ (proof follows in appendix A). Note that we are interchanging terms $\mathbf{g}_\alpha(\mathbf{X})$ with $\mathbf{P}$.

Lemma 3.6. *For any* $\mathbf{X} \succeq \mathbf{0}$*, and* $\mathbf{R} \succeq \mathbf{0}$*,*

$$\mathbf{g}_\alpha(\mathbf{X}) \succeq \;\; \alpha_0 \mathbf{AXA}^T + \mathbf{Q} + \textstyle\sum_{i=1}^{2^k-2} \alpha_i \mathbf{AX}\mathcal{F}\left(\mathbf{H}_i, \mathbf{G}_i, \mathbf{X}\right)\mathbf{XA}' \tag{3.21}$$

Consider the two recursive sequences $\mathbf{X}_{t+1} = \mathbf{g}_\alpha(\mathbf{X}_t)$, and $\hat{\mathbf{X}}_{t+1} = \alpha_0 \mathbf{AXA}^T$ $+\mathbf{Q} + \sum_{i=1}^{2^k-2} \alpha_i \mathbf{AX}\mathcal{F}\left(\mathbf{H}_i, \mathbf{G}_i, \mathbf{X}\right)\mathbf{XA}'$ with same initial condition, then at time step t, $\mathbf{X}_t \succ \hat{\mathbf{X}}_t$. Thus, if $\hat{\mathbf{X}}_{t+1}$ diverges, then $\mathbf{X}_{t+1} = \mathbf{g}_\alpha(\mathbf{X}_t)$ also diverges. This allows us to find the lower bounds on critical sensor probabilities $\{\lambda_1^c, \cdots, \lambda_k^c\}$ that lead to convergence of $\mathbf{X}_t$.

Lemma 3.7. *Since,* $\mathbf{X} \succeq 0$ *is a random matrix,*

$$\begin{aligned}&\alpha_0 \mathbf{A}\mathbb{E}[\mathbf{X}]\mathbf{A}' + \mathbf{Q} + \textstyle\sum_{i=1}^{2^k-2} \alpha_i \mathbf{A}\mathbb{E}\left[\mathbf{X}\mathcal{F}\left(\mathbf{H}_i, \mathbf{G}_i, \mathbf{X}\right)\mathbf{X}\right]\mathbf{A}' \\ &\preceq \mathbb{E}[\mathbf{g}_\alpha(\mathbf{X})] \preceq \mathbf{g}_\alpha(\mathbb{E}[\mathbf{X}])\end{aligned} \tag{3.22}$$

(proof follows in appendix A). This property combines concavity property of lemma 3.1 and bounded condition of lemma 3.6 and lead to both an upper and lower bound on $\mathbb{E}[\mathbf{g}_\alpha(\mathbf{X})]$.

Using Lemma 3.7, we are now able to compute both upper and lower bound on expected error covariance matrix. The lower bound can be obtained by solving,

$$\mathbf{P} = \alpha_0 \mathbf{APA}' + \sum_{i=1}^{2^k-2} \alpha_i \mathbf{AP}\mathcal{F}\left(\mathbf{H}_i, \mathbf{G}_i, \mathbf{P}\right)\mathbf{PA}' + \mathbf{Q} \tag{3.23}$$

Comparing to gathered measurement case solution (3.15), let $\mathbf{P}_s = \mathcal{Q}_s\mathcal{D}_s\mathcal{Q}_s'$ be the eigen decomposition of converging solution, then

$$\begin{aligned}\mathbf{P}_s = & \quad \mathbf{A}(1-\lambda)\mathbf{P}_s\mathbf{A}' + \mathbf{Q} \\ & = \mathbf{A}\mathcal{Q}_s\left((1-\lambda)\,\mathcal{D}_s\right)\mathcal{Q}_s'\mathbf{A}' + \mathbf{Q}\end{aligned} \tag{3.24}$$

As established in section 3.2.1, both gathered measurement scenario and dispersed measurement scenario will converge to same solution. Then comparing (3.23) and (3.24) we get,

$$\begin{aligned}&\mathbf{A}\mathcal{Q}_s(1-\lambda)\mathcal{D}_s\mathcal{Q}_s'\mathbf{A}' = \\ &\mathbf{A}\mathcal{Q}_s\left[\alpha_0\mathcal{D}_s + \textstyle\sum_{i=1}^{2^k-2}\alpha_i\mathcal{D}_s\mathcal{Q}_s'\mathcal{F}\left(\mathbf{H}_i,\mathbf{G}_i,\mathbf{P}_s\right)\mathcal{Q}_s\mathcal{D}_s\right]\mathcal{Q}_s'\mathbf{A}'\end{aligned} \tag{3.25}$$

To compute $\alpha_0, \cdots, \alpha_{2^k-2}$ (thus, $\lambda^c_{1,lb}, \cdots, \lambda^c_{lb,k}$) satisfying equation (3.25), we propose solution by formulating an optimization problem,

$$\begin{aligned}&\min. && trace(\mathbf{S}) \\ &\text{st.} && \begin{cases}(1-\lambda) & = \alpha_0 + d_s(1)\sum_{i=1}^{2^k-2}\alpha_i\mathbf{q}_s'(1)\mathcal{F}\left(\mathbf{H}_i,\mathbf{G}_i,\mathbf{P}_s\right)\mathbf{q}_s(1) + s_1 \\ (1-\lambda) & = \alpha_0 + d_s(2)\sum_{i=1}^{2^k-2}\alpha_i\mathbf{q}_s'(2)\mathcal{F}\left(\mathbf{H}_i,\mathbf{G}_i,\mathbf{P}_s\right)\mathbf{q}_s(2) + s_2 \\ \vdots & \quad \vdots \cdots \vdots \\ (1-\lambda) & = \alpha_0 + d_s(n)\sum_{i=1}^{2^k-2}\alpha_i\mathbf{q}_s'(n)\mathcal{F}\left(\mathbf{H}_i,\mathbf{G}_i,\mathbf{P}_s\right)\mathbf{q}_s(n) + s_n\end{cases}\end{aligned} \tag{3.26}$$

where, $\lambda > \lambda^c_{s,lb}$; $d_s(i)$ is the i^{th} diagonal element of $\mathcal{D}_s$; $\mathbf{q}_s'(i)$ is the i^{th} eigen vector; and $\mathbf{S} = diag(s_1, \cdots, s_n)$ is the slack matrix. Further, adding constraint $\mathbf{S} \preceq \mathbf{0}$, assures that the converging solution of dispersed measurement scenario is always bounded below the converging solution of gathered measurement scenario. It is easy to notice that, the formulation (3.26) is a minimization problem with linear constraints in probability variables $\alpha_0, \cdots, \alpha_{2^m-2}$ and slack variables $s_1, \cdots, s_n$. Since, $\sum_{i=0}^{2^k-1}\alpha_i = 1$ and $\alpha_{2^k-1} \neq 0$ (probability of receiving all measurements), placing an additional linear inequality constraint $\sum_{i=0}^{2^k-2}\alpha_i < 1$, will optimally solve for variables $\alpha_0, \cdots, \alpha_{2^k-2}$. Thereafter, the lower bound on individual critical sensor probabilities $\lambda^c_{1,lb}, \cdots, \lambda^c_{k,lb}$ can be computed, as probabilities of all possible loss scenarios is now known.

3.4.3 Upper bound on packet drop probabilities

The upper bound on critical packet $\lambda^c_{s,ub}$ drop rate in gathered information case is obtained by solving following optimization problem [57],

$$\begin{aligned} &\lambda^c_{s,ub} = argmin._{\lambda}\mathbf{\Psi}_{\lambda}\left(\mathbf{Y},\mathbf{Z}\right) \succ \mathbf{0}, \\ &st.\ \mathbf{0} \preceq \mathbf{Y} \preceq \mathbf{I} \end{aligned} \tag{3.27}$$

where, $\mathbf{\Psi}_{\lambda}\left(\mathbf{Y},\mathbf{Z}\right) = \begin{bmatrix} \mathbf{Y} & \sqrt{\lambda}\left(\mathbf{YA}+\mathbf{ZC}\right) & \sqrt{1-\lambda}\mathbf{YA} \\ \sqrt{\lambda}\left(\mathbf{A}'\mathbf{Y}+\mathbf{C}'\mathbf{Z}'\right) & \mathbf{Y} & \mathbf{0} \\ \sqrt{1-\lambda}\mathbf{A}'\mathbf{Y} & \mathbf{0} & \mathbf{Y} \end{bmatrix}$.
This a quasi-convex optimization problem in variables $(\lambda, \mathbf{Y}, \mathbf{Z})$ and solution can be obtained by iterating LMI feasibility problems and using bisection of variable λ.The upper bound on error covariance $\mathbf{P}_{ub}$ is obtained by solving following semidefinite problem,

$$\begin{aligned} &argmax._{\mathbf{P}}\ trace(\mathbf{P}) \\ &st. \begin{cases} \begin{bmatrix} \mathbf{APA}'+\mathbf{Q}-\mathbf{P} & \sqrt{\lambda}\mathbf{APC}' \\ \sqrt{\lambda}\mathbf{CA}' & \mathbf{CPC}'+\mathbf{R} \end{bmatrix} \succeq \mathbf{0} \\ \mathbf{P} \succeq \mathbf{0} \end{cases} \end{aligned} \tag{3.28}$$

with $\lambda = \lambda^c_{s,ub}$. Above optimization problem is essentially a Schur compliment of following expression,

$$\mathbf{P} \succeq \mathbf{APA}' + \mathbf{Q} - \lambda^c_{s,ub}\mathbf{AXC}\left(\mathbf{CXC}'+\mathbf{R}\right)^{-1}\mathbf{CXA}' \tag{3.29}$$

Again following our discussion in section 3.2.1, if $\mathbf{P}_{ub}$ is the solution of optimization problem (3.29), then the corresponding equation for our considered problem can be expressed as,

$$\mathbf{P}_{ub} \succeq \mathbf{AP}_{ub}\mathbf{A}' + \mathbf{Q} - \textstyle\sum_{i=1}^{2^k-1}\alpha_i\mathbf{AP}_{ub}\mathbf{H}_i'[\mathbf{H}_i\mathbf{P}_{ub}\mathbf{H}_i' + \mathcal{R}_i]^{-1}\mathbf{H}_i\mathbf{P}_{ub}\mathbf{A}' \tag{3.30}$$

Thus, for (3.29) and (3.30) to converge to same solution following condition must be satisfied.

$$\lambda^c_{s,ub}\mathcal{Q}_s'\mathbf{C}'\left(\mathbf{CXC}'+\mathbf{R}\right)^{-1}\mathbf{C}\mathcal{Q}_s = \textstyle\sum_{i=1}^{2^k-1}\alpha_i\mathcal{Q}_s'\mathbf{H}_i'[\mathbf{H}_i\mathbf{P}_{ub}\mathbf{H}_i' + \mathcal{R}_i]^{-1}\mathbf{H}_i\mathcal{Q}_s \tag{3.31}$$

where, $\mathcal{Q}_s$ is the unitary matrix corresponding to eigen decomposition of $\mathbf{P}_{ub}$. To compute $\alpha_1, \cdots, \alpha_{2^m-1}$ (thus, $\lambda^c_{1,ub}, \cdots, \lambda^c_{ub,k}$) satisfying equation (3.31), we propose solution by formulating an optimization problem,

$$\begin{aligned} &\min. \quad trace(\mathbf{S}) \\ &st. \quad \begin{cases} \lambda^c_{s,ub}\mathbf{q}'_s(1)\mathcal{G}(\mathbf{C},\mathbf{P}_{ub})\mathbf{q}_s(1) = \sum_{i=1}^{2^k-1}\alpha_i\mathbf{q}'_s(1)\mathcal{G}(\mathbf{H}_i,\mathbf{P}_{ub})\mathbf{q}_s(1) + s(1) \\ \lambda^c_{s,ub}\mathbf{q}'_s(2)\mathcal{G}(\mathbf{C},\mathbf{P}_{ub})\mathbf{q}_s(2) = \sum_{i=1}^{2^k-1}\alpha_i\mathbf{q}'_s(2)\mathcal{G}(\mathbf{H}_i,\mathbf{P}_{ub})\mathbf{q}_s(2) + s(2) \\ \vdots \cdots \cdots \vdots \\ \lambda^c_{s,ub}\mathbf{q}'_s(n)\mathcal{G}(\mathbf{C},\mathbf{P}_{ub})\mathbf{q}_s(n) = \sum_{i=1}^{2^k-1}\alpha_i\mathbf{q}'_s(n)\mathcal{G}(\mathbf{H}_i,\mathbf{P}_{ub})\mathbf{q}_s(n) + s(n) \end{cases} \end{aligned} \tag{3.32}$$

where, $\mathcal{G}(\mathbf{C},\mathbf{X}) = \mathbf{C}'\left(\mathbf{CXC}'+\mathbf{R}\right)^{-1}\mathbf{C}$ and $\mathcal{G}(\mathbf{H}_i,\mathbf{X}) = \mathbf{H}'_i[\mathbf{H}_i\mathbf{X}\mathbf{H}'_i + \mathcal{R}_i]^{-1}\mathbf{H}_i$; $\mathbf{q}_s()$ is the eigen vector; and $\mathbf{S} - diag(s(1),\cdots,s(n))$ is slack matrix. Again, adding additional constraint $\mathbf{S} \succeq \mathbf{0}$ ensures that the converging solution of dispersed measurements is bounded below the converging solution of gathered measurement case. Also, we notice that the formulation (3.32) is a minimization problem with linear constraints in probability variables $\alpha_1,\cdots,\alpha_{2^k-1}$ and slack variables $s_1,\cdots,s_n$. Further placing a linear inequality constraint $\sum_{i=1}^{2^m-1}\alpha_i < 1$ (as $\sum_{i=0}^{2^k-2}\alpha_i < 1$ and $\alpha_0 \neq 0$), $\alpha_1,\cdots,\alpha_{2^k-1}$ can be optimally computed. Thereafter, the upper bound on individual critical sensor probabilities $\lambda^c_{1,ub},\cdots,\lambda^c_{k,ub}$ can be computed, as probabilities of all possible loss scenarios is now known. In next section, we analyze the impact of exploiting spatial correlation in state estimation process on critical measurement loss rate of individual dispersed sensors.

3.5 Estimation of Spatial Correlation States

Let the states of spatially distributed system be spatially correlated with a stationary covariance matrix, given by $\mathbb{E}\left[(\mathbf{x}-\mathbb{E}[\mathbf{x}])(\mathbf{x}-\mathbb{E}[\mathbf{x}])'\right] = \mathbf{\Sigma_{xx}}$. Further, let $\mathbf{y}_H$ and $\mathbf{y}_G$ be the vectors of received and lost measurements at any filtering instant t, such that the original sensed measurement vector $\mathbf{y} = [\mathbf{y}_H;\mathbf{y}_G]$. Based on spatial correlation of states $\mathbf{\Sigma_{xx}}$, we aim to estimate the lost measurement vector from the received measurement vector. Since, we are considering linear dynamic system, the best linear minimum mean square estimate (Wiener filter) of lost measurements is given by, $\hat{\mathbf{y}}_G = \mathbf{\Sigma}_{GH}\mathbf{\Sigma}_{HH}^{-1}\mathbf{y}_H$, where $\mathbf{\Sigma}_{GH}$ is cross covariance between lost and received measurements and $\mathbf{\Sigma}_{HH}$ is covariance of received measurement vector [63]. The cross covariance between received and lost measurement vector can be computed as,

$$
\begin{aligned}
\boldsymbol{\Sigma}_{GH} &= \mathbb{E}\left[\left(\mathbf{y}_G - \mathbb{E}[\mathbf{y}_G]\right)\left(\mathbf{y}_H - \mathbb{E}[\mathbf{y}_H]\right)'\right] \\
&= \mathbb{E}\left[\left(\mathbf{G}\mathbf{x} + \mathbf{v}_G - \mathbf{G}\mathbb{E}[\mathbf{x}]\right)\left(\mathbf{H}\mathbf{x} + \mathbf{v}_H - \mathbf{H}\mathbb{E}[\mathbf{x}]\right)'\right] \\
&= \mathbb{E}\left[\mathbf{G}\left(\mathbf{x} - \mathbb{E}[\mathbf{x}]\right)\left(\mathbf{x} - \mathbb{E}[\mathbf{x}]\right)'\mathbf{H}'\right] + \mathbb{E}\left[\mathbf{v}_G\mathbf{v}_H'\right] \\
&= \mathbf{G}\boldsymbol{\Sigma}_{\mathbf{xx}}\mathbf{H}' + \mathbf{R}_{GH}
\end{aligned}
\tag{3.33}
$$

The final expression comes from assumption that the state $\mathbf{x}$ and measurement noise $\mathbf{v}$ are independent of each other. Additionally, as we assume measurement noise as zero mean random process, the mean of lost and received measurement vector is given by, $\mathbb{E}[\mathbf{y}_H] = \mathbf{H}\mathbb{E}[\mathbf{x}]$, and $\mathbb{E}[\mathbf{y}_G] = \mathbf{G}\mathbb{E}[\mathbf{x}]$. Similarly, the covariance of received measurements is expressed as, $\boldsymbol{\Sigma}_{HH} = \mathbf{H}\boldsymbol{\Sigma}_{\mathbf{xx}}\mathbf{H}' + \mathbf{R}_H$. Next, the estimate of lost measurement vector $\hat{\mathbf{y}}_G$ can be introduced in our packet drop analysis as the actual lost measurement vector with different measurement noise $\bar{\mathbf{v}}_G$, i.e.,

$$
\begin{aligned}
\hat{\mathbf{y}}_G &= \boldsymbol{\Sigma}_{GH}\boldsymbol{\Sigma}_{HH}^{-1}\left(\mathbf{H}\mathbf{x} + \mathbf{v}_H\right) \\
&= \bar{\mathbf{G}}\mathbf{x} + \bar{\mathbf{v}}_G
\end{aligned}
\tag{3.34}
$$

where, $\bar{\mathbf{G}}$ represents only those rows of $\mathbf{G}$ which combine states having spatial correlation with states in $\mathbf{H}$ of received measurement vector. Thus, even if one state in the row is spatially uncorrelated and can't be estimated from received measurement vector, then we consider the entire measurement corresponding to that row being lost. The new noise $\bar{\mathbf{v}}_G$ can be effectively expressed as,

$$
\bar{\mathbf{v}}_G = \left(\boldsymbol{\Sigma}_{GH}\boldsymbol{\Sigma}_{HH}^{-1}\mathbf{H} - \bar{\mathbf{G}}\right)\mathbf{x} + \boldsymbol{\Sigma}_{GH}\boldsymbol{\Sigma}_{HH}^{-1}\mathbf{v}_H \tag{3.35}
$$

Further, the covariance of $\bar{\mathbf{v}}_G$ can be computed as,

$$
\begin{aligned}
&\mathbb{E}\left[\left(\bar{\mathbf{v}}_G - \mathbb{E}[\bar{\mathbf{v}}_G]\right)\left(\bar{\mathbf{v}}_G - \mathbb{E}[\bar{\mathbf{v}}_G]\right)'\right] = \\
&\left(\boldsymbol{\Sigma}_{GH}\boldsymbol{\Sigma}_{HH}^{-1}\mathbf{H} - \bar{\mathbf{G}}\right)\boldsymbol{\Sigma}_{\mathbf{xx}}\left(\boldsymbol{\Sigma}_{GH}\boldsymbol{\Sigma}_{HH}^{-1}\mathbf{H} - \bar{\mathbf{G}}\right)' \\
&+ \left(\boldsymbol{\Sigma}_{GH}\boldsymbol{\Sigma}_{HH}^{-1}\right)\mathbf{R}_H\left(\boldsymbol{\Sigma}_{GH}\boldsymbol{\Sigma}_{HH}^{-1}\right)'
\end{aligned}
\tag{3.36}
$$

Next, let $\bar{\mathbf{y}}_H$ be the final vector of measurements which are actually received and the ones which can be estimated because of spatial correlation i.e., $\bar{\mathbf{y}}_H = [\mathbf{y}_H; \hat{\mathbf{y}}_G]$; let $\bar{\mathbf{y}}_G$ be the final vector of lost measurements i.e., those which are lost and can not be estimated. The new upper and lower bound on critical probability of receiving measurements is computed by redefining $\bar{\mathbf{y}}_H$ and $\bar{\mathbf{y}}_G$ for all $2^k - 1$ possible scenarios of loosing measurements, and then following the analysis of section III.B.2 and section III.B.3. It should be further noted that if the physical system is spatially correlated over most of the physical area, then most of the lost measurements can be estimated from the received measurements; In other words, $\hat{\mathbf{G}}$ is empty for most of the measurement receiving scenarios. This adversely affects the computation of lower bound on individual sensor critical measurement loss rates based on (3.26), as most of corresponding loss scenario probabilities α_i can not be computed. One way of circumventing this problem is by understanding that this scenario of either loosing all the measurements or recovering and receiving all measurements is equivalent to the gathered measurement scenario. Thus, it is expected that in such scenarios, the upper and lower bound on individual sensor critical loss probability will get closer to upper and lower bound on critical loss probability of gathered measurement case.

3.6 Estimation over Correlated Communication Link Failures

In this subsection, we relax our assumption of independence of binary random variables $\{\gamma_{t,1}, \gamma_{t,2}, \cdots, \gamma_{t,k}\}$; where $\gamma_{t,j}$ takes value 1 for successfully receiving and 0 for loosing the measurement from sensor j at any time t (in equation (3.2)). Let $\mathcal{Z} := \{\gamma^z_{t,1}, \gamma^z_{t,2}, \cdots, \gamma^z_{t,k_z}\}$ represents the set of communication links effected by local congestion resulting in correlated measurement loss. For a large cyber physical system, there can be several such sets of communication links exhibiting correlated statistics, with communication link in one set being independent of communication link in other sets. In the following analysis, we assume that the joint probability mass function $Pr(\gamma^z_{t,1}, \gamma^z_{t,2}, \cdots, \gamma^z_{t,k_z})$ for a given set $\mathcal{Z}$ is known and is stationary. Now, the probability of successfully receiving a measurement from any sensor i, $\lambda_i = Pr(\gamma^z_i = 1)$ is function of probability of successfully receiving the measurement from the sensor j. Thus,

$$\begin{array}{ll}\lambda_1 & = Pr(\gamma_1 = 1)\\ \lambda_2 & = Pr\left(\gamma_2^z = 1|\gamma_1^z = 1\right)\lambda_1 + Pr\left(\gamma_2^z = 1|\gamma_1^z = 0\right)(1-\lambda_1)\\ \lambda_3 & = Pr\left(\gamma_3^z = 1|\gamma_1^z = 1\right)\lambda_1 + Pr\left(\gamma_3^z = 1|\gamma_1^z = 0\right)(1-\lambda_1)\\ \cdots & \cdots\\ \lambda_{k_z} & = Pr\left(\gamma_{k_z}^z = 1|\gamma_1^z = 1\right)\lambda_1 + Pr\left(\gamma_{k_z}^z = 1|\gamma_1^z = 0\right)(1-\lambda_1)\end{array} \tag{3.37}$$

where, $Pr\left((\gamma_j = 1)|(\gamma_1 = 1)\right)$ is the conditional probability of successfully receiving the measurement from sensor j, given measurement from sensor 1 is successfully received. Above relationship between probabilities (3.37) for every correlated set $\mathcal{Z}$ can be added as constraints in the formulations (3.26) and (3.32). Once again, the solution to the optimization problems will yield in computing the lower and upper bound on critical measurement receiving probabilities of individual sensors. In following section, we present some system examples illustrating theory developed in this paper.

3.7 System Examples

This section validates the analytical results from previous sections by finding stability regions (defined by lower and upper bound on measurement loss rates) for several example systems. The upper and lower bound on expected error covariance matrix is computed first from the gathered measurement scenario, and then measurement loss is distributed to dispersed measurement scenario by solving the optimization problems (3.26) and (3.32). In the numerical examples of generalized system, we also present performance trade-off in estimation accuracy and quality of underlying network defined by measurement loss rate.

3.7.1 Decoupled system with no overlap in observation space

Consider a simple system of two nodes with: state transition matrix $\mathbf{A} = \begin{bmatrix} 1.25 & 0 \\ 0 & 1.5 \end{bmatrix}$; and two dispersed sensors with $\mathbf{C}_1 = [1\ 0]$ and $\mathbf{C}_2 = [0\ 1]$ as their measurement matrix. We assume noise covariance matrix $\mathbf{Q} = 20\mathbf{I}_2$ and $\mathbf{R} = 2.5\mathbf{I}_2$.

First, considering gathered measurement scenario, the critical measurement loss probability $1 - \lambda_s^c$ has lower bound as $\lambda_s^c \geq \lambda_{s,lb}^c = (1 - 1/1.5^2) \approx 0.56$, and upper bound

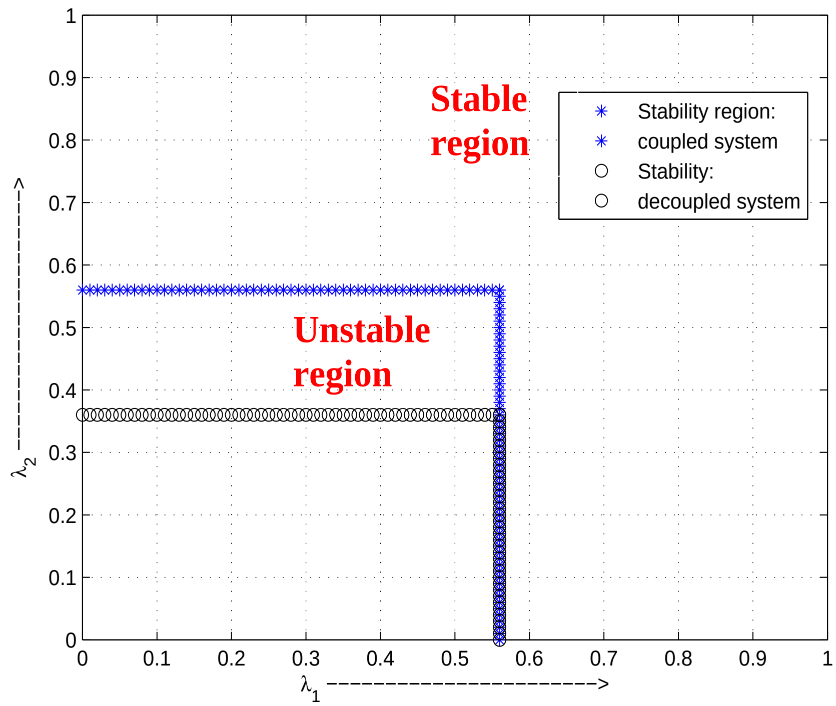

Figure 3.5: *Stability region - Decoupled System*

as $\lambda_s^c \leq \lambda_{s,ub}^c \approx 0.56$. Both upper and lower bounds coincide as $\mathbf{C} = [\mathbf{C}_1; \mathbf{C}_2]$ is invertible [58]. Now, considering dispersed measurement scenario, the stability region defined by critical measurement loss rates $1 - \lambda_1^c$ and $1 - \lambda_2^c$ is shown in Figure 4.3 (shown. by $*$). Both upper and lower bounds coincide, with $\lambda_1^c = \lambda_2^c = 0.56$. However, it is easy to notice that this system is completely decoupled and each sensor directly measures the states. The estimation process is essentially of two independent scalar system with critical rates $\lambda_1^c > 1 - 1/1.25^2 \approx 0.36$ and $\lambda_1^c > 1 - 1/1.25^2 \approx 0.55$ (shown, by o in Figure 4.3). Thus, bounds computed using (3.26) and (3.32) are relaxed; so it is prudent to first decouple the system and then compute the bounds.

3.7.2 Coupled system with completely redundant measurements

Consider another simple system of two nodes with: state transition matrix $\mathbf{A} = \begin{bmatrix} 1.25 & 0 \\ 1 & 1.1 \end{bmatrix}$; and two dispersed sensors with $\mathbf{C}_1 = \begin{bmatrix} 1 & 0 \\ 0 & 1 \end{bmatrix}$ and $\mathbf{C}_2 = \begin{bmatrix} 1 & 0 \\ 1 & 1 \end{bmatrix}$ as their measurement matrix. We assume noise covariance matrix $\mathbf{Q} = 20\mathbf{I}_2$ and $\mathbf{R} = 2.5\mathbf{I}_2$. It is easy to notice that both sensor measurements are self-sufficient in sensing the system, and their critical measurement receiving probability can be individually computed as $\lambda_1^c = \lambda_2^c = 1 - 1/1.25^2 \approx 0.36$. Now, if the measurements are jointly received for state estimation, we expect a reduction in the individual critical rate.

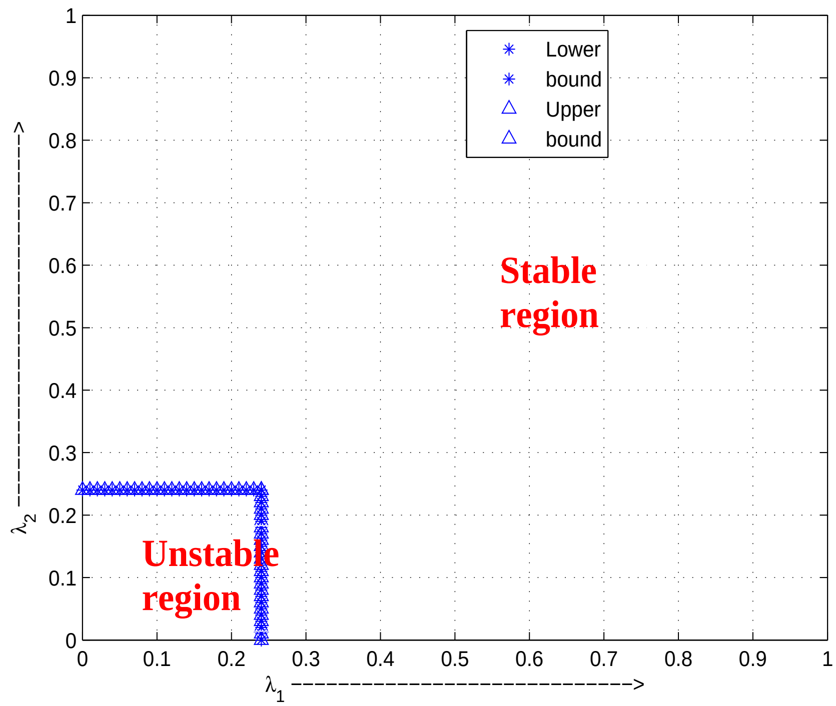

Figure 3.6: *Stability region - Completely redundant measurements*

Figure 4.4 shows stability region when state estimation is performed when both the sensor measurements are communicated for state estimation. It can be observed that both lower and upper bound solutions coincide and critical probability of receiving the measurements is reduces to $\lambda_1^c = \lambda_2^c \approx 0.24$. thus, at the cost of deploying two sensors for overlapping measurements, we can afford lower quality of underlying communication network.

3.7.3 Generalized system

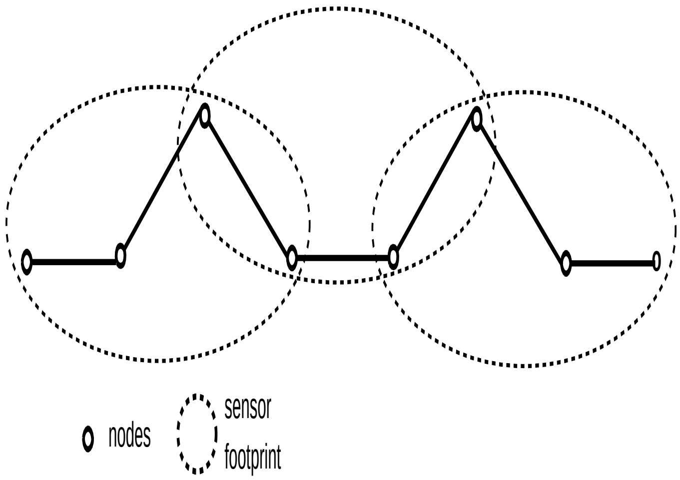

Figure 3.7: *Radial system with overlap in sensor observation space*

Next consider a radial cyber physical system system sensed along overlapping sensor measurements as shown in Figure 4.5. There are 8 nodes sensed by 3 overlapping sensor measurements. We assume noise covariance matrix $\mathbf{Q} = 20\mathbf{I}_8$ and $\mathbf{R} = 2.5\mathbf{I}_2$ for each sensor measurement. Following are the considered state transition and measurement matrices.

$$\mathbf{A} = \begin{bmatrix} 1.1 & 0.2 & 0 & 0 & 0 & 0 & 0 & 0 \\ 0.2 & 0.3 & 0.3 & 0 & 0 & 0 & 0 & 0 \\ 0 & 0.3 & 0.5 & 0.2 & 0 & 0 & 0 & 0 \\ 0 & 0 & 0.2 & 1.1 & 0.3 & 0 & 0 & 0 \\ 0 & 0 & 0 & 0.3 & 0.2 & 0.4 & 0 & 0 \\ 0 & 0 & 0 & 0 & 0.4 & 0.4 & 0.3 & 0 \\ 0 & 0 & 0 & 0 & 0 & 0.3 & 0.5 & 0.3 \\ 0 & 0 & 0 & 0 & 0 & 0 & 0.3 & 1.1 \end{bmatrix}$$

$$\mathbf{C}_1 = \begin{bmatrix} 1 & 1 & 1 & 0 & 0 & 0 & 0 & 0 \\ 0 & 0 & 1 & 1 & 0 & 0 & 0 & 0 \end{bmatrix}$$
$$\mathbf{C}_2 = \begin{bmatrix} 0 & 0 & 1 & 1 & 0 & 0 & 0 & 0 \\ 0 & 0 & 0 & 0 & 1 & 1 & 0 & 0 \end{bmatrix}$$
$$\mathbf{C}_3 = \begin{bmatrix} 0 & 0 & 0 & 0 & 1 & 1 & 0 & 0 \\ 0 & 0 & 0 & 0 & 0 & 1 & 1 & 1 \end{bmatrix}$$

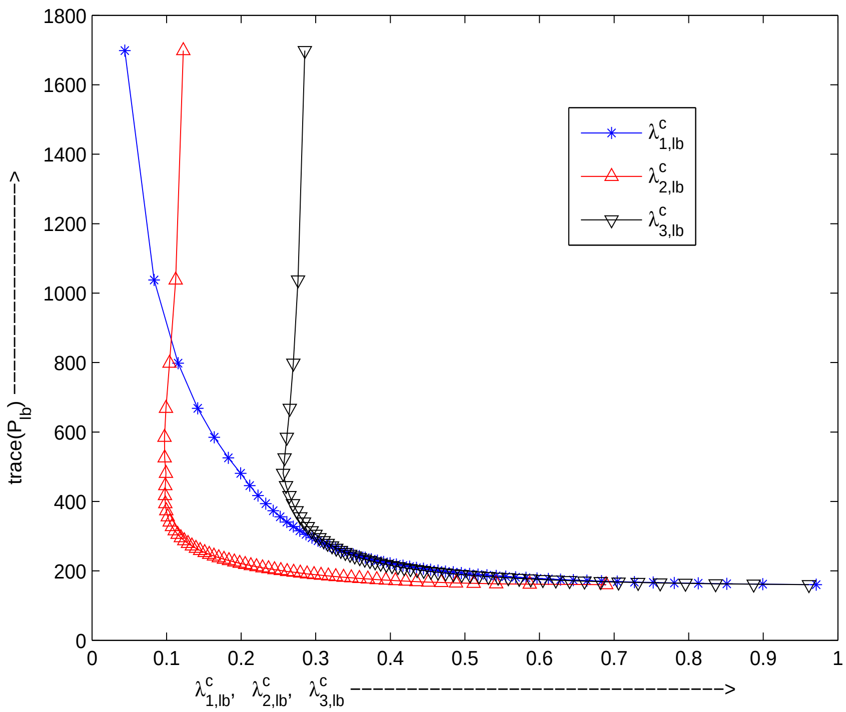

Figure 3.8: *Critical measurement receiving probability - lower bound*

First considering gathered measurement scenario, the lower bound on critical probability of successfully receiving the measurements is given by $\lambda^c_{s,lb} = (1 - 1/\rho^2) \approx 0.39$, where maximum eigen value of state transition matrix $\rho = 1.28$. Similarly, the upper bound on λ^c_s can be obtained by solving (3.27), and is computed as $\lambda^c_{s,ub} = 0.42$. The corresponding lower and upper bound on converging error covariance can be computed by solving (3.15) and (3.29); and bounds on critical probabilities of each sensor can be computed by solving (3.26) and (3.32). Repeating above steps for $\lambda^c_{s,lb} > 0.39 \rightarrow 1$, and $\lambda^c_{s,ub} > 0.42 \rightarrow 1$ we can compute the trade off in state estimation accuracy with quality of underlying communication network. Figure 4.6 and 4.7, shows the lower and upper bound on critical probabilities of each sensor vs trace of converging error covariance matrix. Now, depending on the required accuracy in estimated states for stability of control operation, the corresponding requirement in quality of network infrastructure can be easily inferred from Figures 4.6 and 4.7. For example, if the demanded $trace(\mathbf{P})$ at steady state is 300, then for $\lambda_1 < 0.27$, $\lambda_2 < 0.12$, $\lambda_3 < 0.31$ system

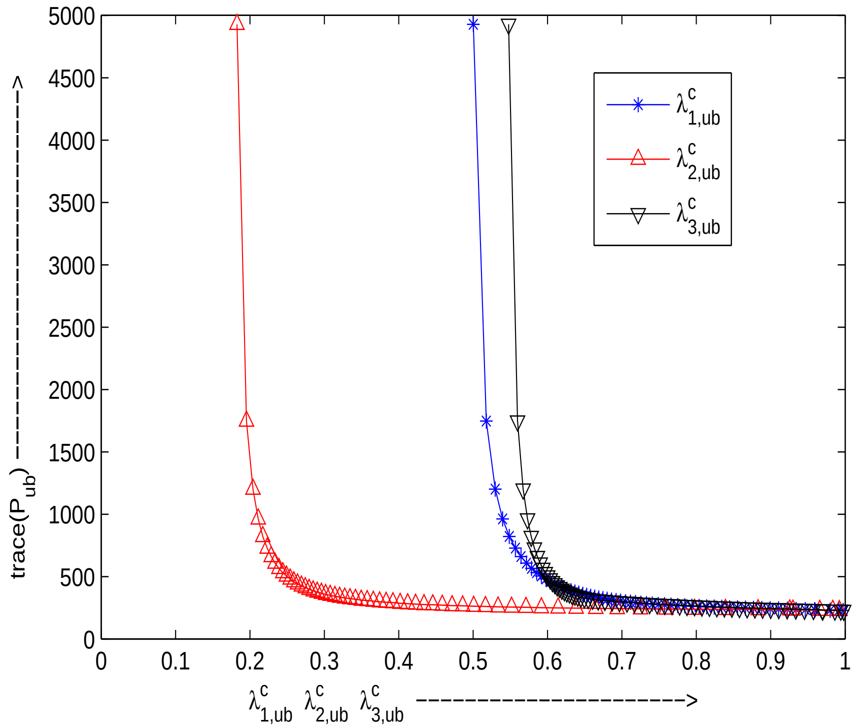

Figure 3.9: *Critical measurement receiving probability - upper bound*

is definitely unstable, while for $\lambda_1 > 0.70$, $\lambda_2 > 0.37$, $\lambda_3 > 0.69$ is definitely stable. Thus, this analysis plays a crucial role in safe and efficient operation of cyber physical systems.

3.7.4 Generalized system exploiting spatial correlation

Let us assume that because of physical effects there is spatial correlation among the states of the system (defined in section V.C), with the following covariance matrix,

$$\Sigma_{\mathbf{xx}} = \begin{bmatrix} 1.0 & 0.5 & 0.1 & 0 & 0 & 0 & 0 & 0 \\ 0.5 & 1.0 & 0.5 & 0.1 & 0 & 0 & 0 & 0 \\ 0.1 & 0.5 & 1.0 & 0.5 & 0 & 0 & 0 & 0 \\ 0 & 0.1 & 0.5 & 1.0 & 0 & 0 & 0 & 0 \\ 0 & 0 & 0 & 0 & 1.0 & 0.5 & 0.1 & 0 \\ 0 & 0 & 0 & 0 & 0.5 & 1.0 & 0.5 & 0.1 \\ 0 & 0 & 0 & 0 & 0.1 & 0.5 & 1.0 & 0.5 \\ 0 & 0 & 0 & 0 & 0 & 0.1 & 0.5 & 1.0 \end{bmatrix}$$

It can be noticed from structure of $\Sigma_{\mathbf{xx}}$, that spatial correlation is separated in two regions $\{x_1, x_2.x_3, x_4\}$ and $\{x_5, x_6.x_7, x_8\}$. Thus, if measurement from sensor 1 is only received, then only first row of measurement from sensor 2 can be estimated by exploiting spatial correlation. However, if measurement from sensor 2 is only received, then measurements from both sensor 1 and 3 can be estimated. Thus, considering all such scenarios we redefine the received measurement vector for all measurement loss combinations. Further, system being spatially correlated for most of the physical space we only compute the upper bound on critical critical probabilities of receiving measurements (3.32).

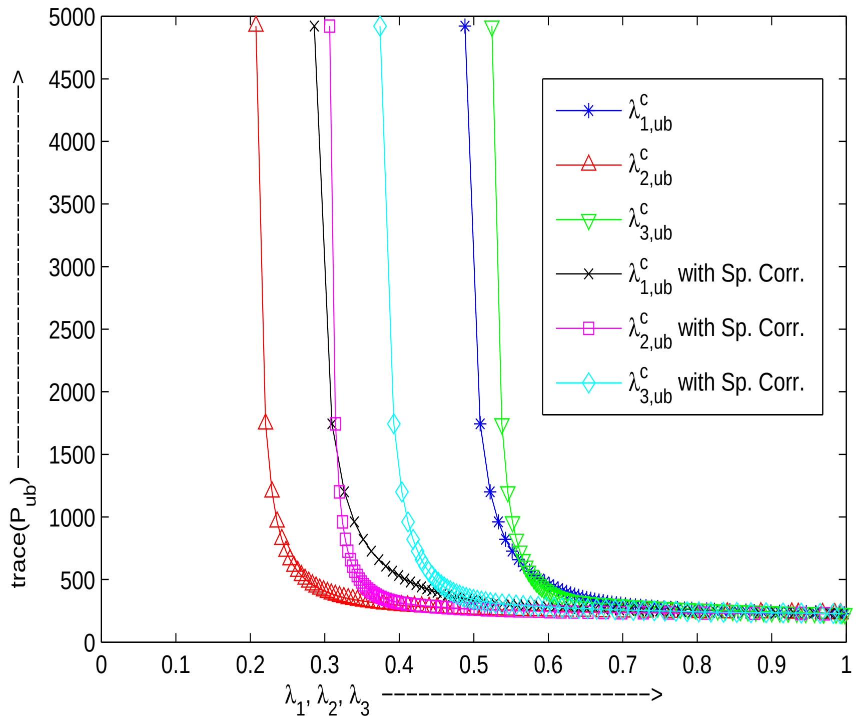

Figure 3.10: *Exploiting spatial correlation in critical measurement receiving probability - upper bound*

Figure 3.10 shows the upper bound on critical probabilities of receiving sensor measurements vs trace of converging error covariance matrix. It can be observed that because of spatial correlation critical probability of receiving measurement decreases for sensor 1 and 3, with slight increase for sensor 2. The reason for this behavior is due to the critical probabilities varying as a group, i.e., if there is a change in critical probability of one sensor, then there is an appropriate change in critical probabilities of other sensors such that the overall system states are observable. In the system without spatial correlation, more value is placed on sensor 1 and 3 which are able to completely observe the system, while less value is given to sensor 2 which acts as redundant measurement. However, after considering spatial correlation sensor 2 itself is capable of observing the whole system; resulting in an increase in its value in terms of critical probability, and corresponding decrease in the probabilities for sensors 1 and 3. Also, because of spatial correlation over most of the physical area, the system is equivalent to either loosing all the measurements or receiving all the measurements. This behavior is almost equivalent to gathered measurement scenario, as critical probabilities of all the sensors are getting closer to 0.42 (upper bound for gathered measurement case). Thus, we can further conclude that the lower bound on individual sensor measurement receiving probability will be closer to 0.39 (lower bound for gathered measurement case).

3.7.5 Generalized system with correlated packet drops

Let us again consider the system defined in section V.C, with correlated measurement loss from sensor 1 and 2, and measurement loss from sensor 3 being independent of loss from sensor 1 and 2. Further, let random variables indicating successful arrival of measurements from sensor 1 and 2 have a joint probability mass function given by,

$\Pr(\gamma_1, \gamma_2) =$

$\gamma_1 \backslash \gamma_2$	0	1
0	0.4	0.1
1	0.1	0.4

The equivalent functional dependence on probability of successful reception of measurements between sensors 1 and 2 can be expressed as,

$$\lambda_2^c = \lambda_1^c Pr(\gamma_2 = 1|\gamma_1 = 1) + (1 - \lambda_1^c) Pr(\gamma_2 = 1|\gamma_1 = 0)$$

where, conditional probabilities can be computed from joint probability mass function ($Pr((\gamma_2 = 1)|(\gamma_1 = 1)) = 0.8$, and $Pr(\gamma_2 = 1|\gamma_1 = 0 = 0.2)$. The above functional dependence is placed as an equality constraint in our optimization formulation for computing upper and lower bound on critical probabilities of packet drop rates (3.26) and (3.32).

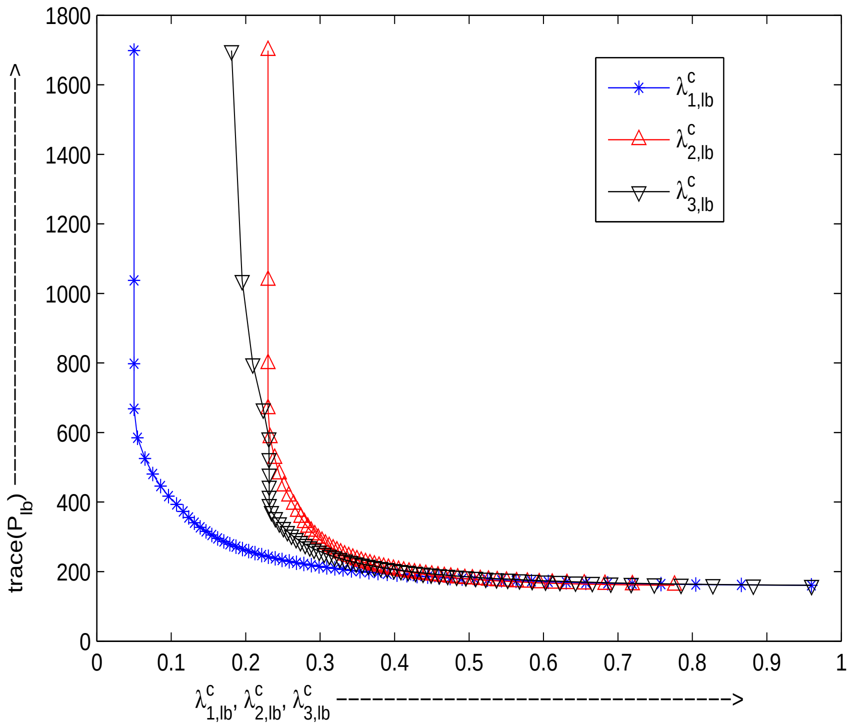

Figure 3.11: *Critical measurement receiving probability with correlated λ_1 and λ_2 - lower bound*

The lower and upper bound on critical packet drop rate vs trace of converging error covariance matrix, under this scenario is shown in Figure 3.11 and 3.12 respectively. It can be observed from both the Figures that correlated measurement loss increases critical probability of receiving measurement of sensor 2. This eventually reduces critical probability of receiving measurement from sensor 3, as critical probabilities varying with each other in a group. Thus, correlation among measurement loss can be substituted as a constraint in our formulation, and new bounds can be computed.

3.8 Summary

In this chapter, we address the Kalman filter (KF) based state estimation for spatially distributed cyber physical system in presence of random measurement loss. The measurements are taken by dispersed sensors, and are encoded in packets to be sent over a lossy

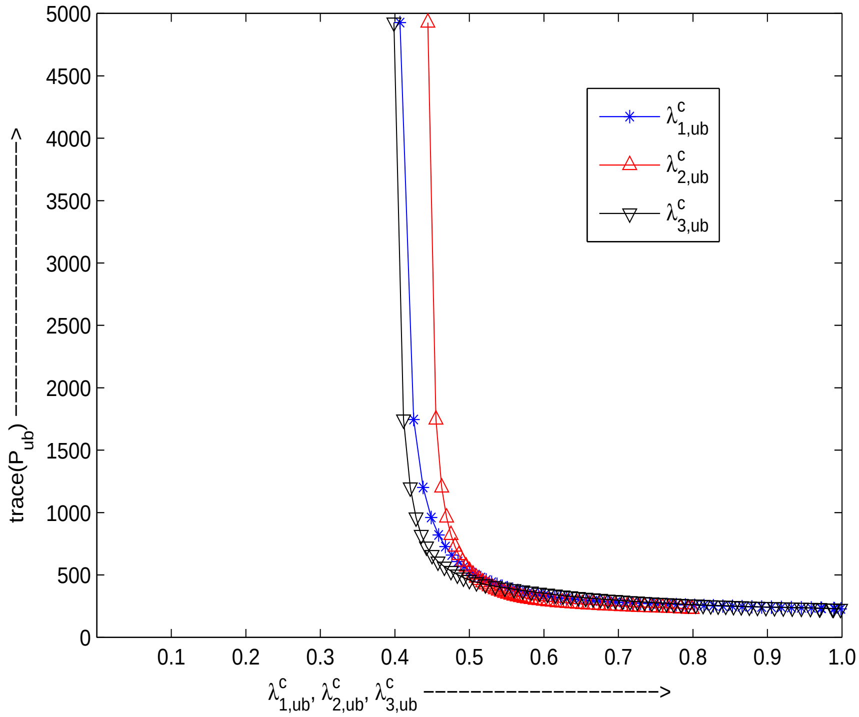

Figure 3.12: *Critical measurement receiving probability with correlated λ_1 and λ_2 - upper bound*

network. Since, random measurement loss results in stochastic error covariance iteration, we establish the lower and upper bounds on expected steady state error covariance as function of probability of receiving measurement from individual sensors. We use information theoretic concepts to establish the analogy in convergence with gathered measurement scenario. Using this analogy, we compute upper and lower bounds on critical loss probability of individual sensors, by formulating a optimization problem. The feasibility solution distributes the measurement loss of gathered measurement scenario to loss in dispersed sensor measurements. The analysis is further enhanced by exploiting spatially correlation between states in estimating lost measurements from received measurements. This eventually results in redefining new set of measurements for all possible measurement loss configurations, followed by conclusive analysis that a higher degree of information loss or poor network quality can be tolerated to archive a certain estimation accuracy. The analysis also accommodates correlated link failure scenario by placing constraints of joint probability mass function in computation of lower and upper bound on critical measurement loss rates.

Chapter 4

Control with Intermittent Actuator Inputs

In this chapter, we analyze the Lyapunov stability of stochastic linear quadratic controller over a network in spatially distributed cyber-physical systems. We first present the system framework where, linear quadratic controller is considered for computing control solution of stochastic linear dynamical system. Similar to chapter 3, the states of underlying dynamical system are spatially distributed over the physical area; and actuators are arbitrarily deployed over the physical space to jointly control the complete system. In this system setup, there are two possible strategies of communicating control actions to actuators: (1) Unified control: control actions are collectively communicated to actuators over a single communication link; (2) dispersed control: control actions are communicated to actuators over individual communication links. Since, we are considering control solution for large dynamical solution, dispersed actuators is more appealing feasible implementation strategy. However, the communication links in both these strategies are susceptible to random failures, resulting in: (1) random actuator loss; (2) partial control action implementation.

We analyze the stability of the linear quadratic regulator in this stochastic scenario by: (1) characterizing the statistical properties of stochastic Lyapunov function iteration; (2) and, then establishing the necessary and sufficient network conditions under which the steady state Lyapunov function is bounded. These conditions essentially establish existence of critical probabilities of successful control input transmission from control unit to individual actuators; followed by computation of upper and lower bound on corresponding critical probabilities. The overall analysis quantifies the trade-off between stability and the quality of underlying communication network. Thus, our analysis on impact of communication network on stability of control operation is critical in ensuring safe and efficient operation of underlying cyber-physical system.

4.1 Control System Framework

In this section, we discuss the control system framework for spatially distributed cyber physical system, where control actions are communicated to actuators over lossy network. More specifically, we consider the system where: (1) system state are spatially distributed in physical space; (2) actuators are arbitrarily deployed such that they jointly control the complete system; (3) and, a network infrastructure is used for communicating control action to actuators. These characteristics (2)-(3) can impact the stability of control process.

Figure 4.1 presents a conceptual view of the considered system, where nodes (with a state element associated) are distributed all over a physical area. The sensors for measurements are not shown as we assume that underlying state estimation process is stable and the error in state estimates is accommodated as process noise in the controller design. Therefore, we are specifically consider the communication of computed control action to actuators over individual communication links. Compared to conventional system models where there is one communication link between actuator and controller (denoted as unified actuator case), we denote the scenario in Figure 4.1 as dispersed actuator case. The control space of neighboring actuators typically overlaps, resulting in redundancy in control implementation. Further, due to network characteristics, actuator inputs are susceptible to delays, reordering and drops. At any control step, control implementation may not be enough for controlling all states of the system. Thus, use of communication network with its attractive advantages, can eventually adversely effect the stability of control process. In this analysis, we assume

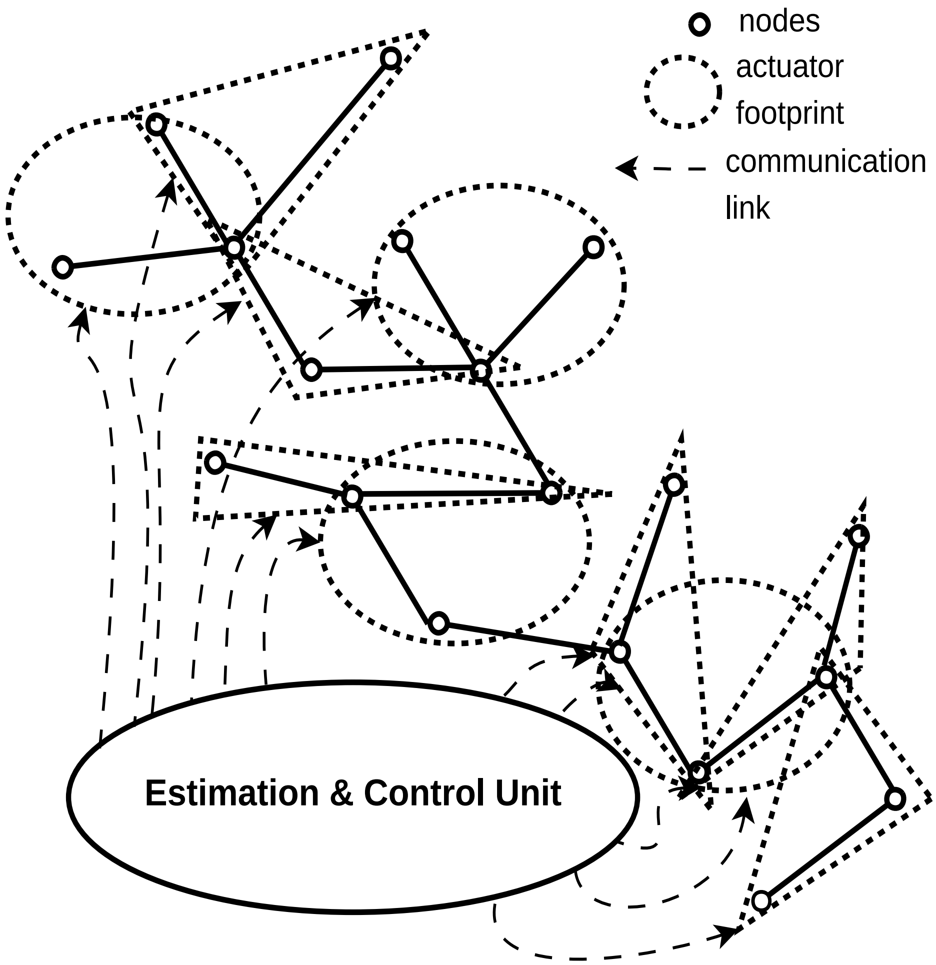

Figure 4.1: *Control of spatially distributed physical system over a network*

delayed actuator actions are not applicable for control and are considered equivalent to lost actions.

Linear quadratic regulator (LQR) based control solution and its variations have found wide acceptance in many application areas including networked control systems. In the following sections we present LQR based control for controlling the system framework presented in this section. Later, we will discuss the stability of the process by characterizing the statistical properties of stochastic Lyapunov function iteration, followed by establishing necessary and sufficient network conditions for ensuring boundedness of Lyapunov function at steady state.

4.2 Linear Quadratic Controller over Intermittent Actuator Inputs

Linear quadratic controller (LQR) is a popular control computation strategy for practical dynamical systems. In this section, we consider stability of a discrete time linear system model under packet dropping in multiple controller to actuator communication links (Figure 4.1),

$$\mathbf{x}_{t+1} \quad = \mathbf{A}\mathbf{x}_t + \gamma_{t,a_1}\mathbf{B}_1\mathbf{u}_{t,1} + \gamma_{t,a_2}\mathbf{B}_2\mathbf{u}_{t,2}\cdots\gamma_{t,a_k}\mathbf{B}_k\mathbf{u}_{t,k} + \mathbf{w}_t$$

where, $\gamma_{t,a_1}\cdots\gamma_{t,a_k}$ are the random variables denoting packet drops in the corresponding communication links. We assume that the state estimation process is stable and the error in state estimates can be accommodated as process noise in controller design. Thus, controller stability under random packet drops in forward direction is analyzed independently of the state estimation process. In this section we essentially present, the instability attributed in control process under packet drops, with the assumption that underlying system is completely controllable in loss less network scenario.

4.2.1 System Model

Consider a discrete time linear dynamic system model,

$$\mathbf{x}_{t+1} = \mathbf{A}\mathbf{x}_t + \mathbf{B}\mathbf{u}_t + \mathbf{w}_t \tag{4.1}$$

where, $\mathbf{x}_t \in \mathbb{R}^n$ is the state vector; $\mathbf{A} \in \mathbb{R}^{n\times n}$ is state transition matrix; $\mathbf{u}_t \in \mathbb{R}^m$ is the control vector; $\mathbf{B} \in \mathbb{R}^{n\times m}$ is the control matrix; and, $\mathbf{w}_t \in \mathbb{R}^n$ is the process noise. We assume $\mathbf{w}_t$ is a Gaussian random process with zero mean and covariance $\mathbf{W} \succeq \mathbf{0}$.

We consider control action $\mathbf{u}_t$ is implemented by k dispersed actuators. Thus, the elements of control vector $\mathbf{u}_t \in \{\mathbf{u}_{t,1}, \mathbf{u}_{t,2}, \cdots \mathbf{u}_{t,k}\}$ consists of control actions for multiple actuators communicated over a communication network. These control inputs transmitted over the network, may be lost or delayed. In our system model, we consider network impact in form of packet drops, and assume that the delayed packets are similar to lost packets.

Further we assume that control action for a actuator at time step t is packetized in single packet, i.e., lost packets are equivalent to lost control action for corresponding actuator. The system model of (4.1) can now be restated as,

$$\mathbf{x}_{t+1} = \mathbf{A}\mathbf{x}_t + [\mathbf{B}_1, \mathbf{B}_2, \cdots, \mathbf{B}_k] \begin{bmatrix} \gamma_{t,1}\mathbf{u}_{t,1} \\ \gamma_{t,2}\mathbf{u}_{t,2} \\ \vdots \\ \gamma_{t,k}\mathbf{y}_{t,k} \end{bmatrix} + \mathbf{w}_t \tag{4.2}$$

where, $\mathbf{u}_{t,j} \in \mathbb{R}^{m_j}$ is the control action for actuator j; $\mathbf{B}_{t,j} \in \mathbb{R}^{n \times m_j}$ is the corresponding control matrix for actuator j; and $\gamma_{t,j}$ represents the binary random variable taking values 1 for successfully transmitted packet and 0 for dropped packet.

4.2.2 Problem Formulation

Since, the underlying dynamic system is stochastic, consider an expected linear quadratic cost function,

$$J = \mathbb{E}\left[lim_{N\to\infty}\frac{1}{N}\sum_{t=0}^{N-1}(\mathbf{x}_t'\mathbf{Q}\mathbf{x}_t + \mathbf{u}_t'\mathbf{R}\mathbf{u}_t)\right] \tag{4.3}$$

where, $\mathbf{Q} \in \mathbb{R}^{n\times n}$ and $\mathbf{R} \in \mathbb{R}^{m\times m}$ are the positive definite weight matrices. Similarly, for stability analysis we consider stochastic Lyapunov function V_t, the expected value of which is defined as,

$$\mathbb{E}[V_t] = \mathbf{x}_t'\mathbf{P}_t\mathbf{x}_t + q_t \tag{4.4}$$

where, $\mathbf{P}_t$ is a symmetric positive definite matrix; and q_t is the contribution of process noise. At a discrete time instant $t+1$, the evolution of equation (4.4) can be expressed as,

$$\begin{aligned} \mathbb{E}[V_{t+1}] &= \mathbf{x}_{t+1}'\mathbf{P}_t\mathbf{x}_{t+1} + q_t \\ &= \mathbf{x}_t'\mathbf{P}_{t+1}\mathbf{x}_t + q_{t+1} \end{aligned} \tag{4.5}$$

where, $\mathbf{P}_{t+1}$ and q_{t+1} denotes the respective recursion of $\mathbf{P}_t$ and q_t over time. For dynamic system defined in (4.1) to be Lyapunov stable, the iterations of $\mathbb{E}[V_t]$ must converge, implying the sequence of $\{\mathbf{P}_t\}$ and q_t must also converge. In the following analysis, we develop recursive equations for $\mathbf{P}_t$ and q_t considering the system model defined in (4.1) and stochastic linear quadratic regulator (SLQR) control strategy. We define mean of Lyapunov function (4.5) as the cost to go function and the optimal control input can then be expressed as,

$$\begin{aligned}\mathbf{u}_t^* &= \min_{\mathbf{u}_t} \left[\mathbf{u}_t'\mathbf{R}\mathbf{u}_t + \mathbb{E}[V_{t+1}]\right] \\ &= \min_{\mathbf{u}_t} \left[\mathbf{u}_t'\mathbf{R}\mathbf{u}_t + (\mathbf{A}\mathbf{x}_t + \mathbf{B}\mathbf{u}_t)' \mathbf{P}_t (\mathbf{A}\mathbf{x}_t + \mathbf{B}\mathbf{u}_t) + q_t\right].\end{aligned} \tag{4.6}$$

$\mathbf{u}_t^*$ can be computed by setting the derivative of (4.6) with respect to $\mathbf{u}_t$ to zero,

$$\mathbf{u}_t^* = (\mathbf{R} + \mathbf{B}'\mathbf{P}_t\mathbf{B})^{-1} \mathbf{B}'\mathbf{P}_t\mathbf{A}\mathbf{x}_t.$$

Note that expression for $\mathbf{u}_t^*$ is similar to optimal control input obtained from solving Hamilton-Jacobi Bellman equation, with $\mathbf{P}_t$ being the matrices computed from backward recursion [86]. Next consider, the implication of this control input being applied over a lossy network, such that system follows dynamic model presented in equation (4.2). Notice, that matrix $\mathbf{R}$ is the weight over control input, and for multiple actuators the quadratic control cost can be expressed,

$$\begin{bmatrix}\mathbf{u}_{t,1}, \mathbf{u}_{t,2}, \cdots \mathbf{u}_{t,k}\end{bmatrix} \begin{bmatrix}\mathbf{R}_{11} & . & \cdots & . \\ . & \mathbf{R}_{22} & \cdots & . \\ \vdots & \vdots & \vdots \cdots \vdots & \vdots \\ . & . & \cdots & \mathbf{R}_{kk}\end{bmatrix} \begin{bmatrix}\mathbf{u}_{t,1} \\ \mathbf{u}_{t,2} \\ \vdots \\ \mathbf{u}_{t,k}\end{bmatrix}$$

where, $\mathbf{R}_{ii}$ is the weight matrix corresponding to control actuator i. Now, if control input for actuator i is lost (i.e., $\gamma_{t,i} = 0$), the apriori effect on quadratic control cost can be accommodated by considering corresponding weight matrix to be infinity, such that $\mathbf{R}_{ii} \to \infty, \Rightarrow \mathbf{u}_{t,i} \to \mathbf{0}$. Let for simplicity of discussion, consider $\mathbf{u}_t$ to be implemented by two actuators i.e. $\mathbf{u}_t = [\mathbf{u}_{t,1}, \mathbf{u}_{t,2}]'$. Further, let $\gamma_{t,1} = 1$ and $\gamma_{t,2} = 0$, i.e., only first actuator control action is successfully transmitted while second actuator action is lost. The corresponding weight matrix is defined as,

$$\tilde{\mathbf{R}} = \begin{bmatrix}\mathbf{R}_{11} & \mathbf{R}_{12} \\ \mathbf{R}_{21} & \sigma_2^2\mathbf{I}\end{bmatrix} = \mathbf{R} + \begin{bmatrix}\mathbf{0} & \mathbf{0} \\ \mathbf{0} & \sigma_2^2\mathbf{I} - \mathbf{R}_{22}\end{bmatrix}$$

where, σ_2^2 is weight for second actuator action. The corresponding optimal control input is stated as,

$$\tilde{\mathbf{u}}_t^* = \left(\tilde{\mathbf{R}} + \mathbf{B}'\mathbf{P}_t\mathbf{B}\right)^{-1} \mathbf{B}'\mathbf{P}_t\mathbf{A}\mathbf{x}_t.$$

and effect on state $\mathbf{x}_t$ at time $t+1$ is $\mathbf{B}\tilde{\mathbf{u}}_t^* = \mathbf{B}\left(\tilde{\mathbf{R}} + \mathbf{B}'\mathbf{P}_t\mathbf{B}\right)^{-1}\mathbf{B}'\mathbf{P}_t\mathbf{A}\mathbf{x}_t$. Notice that the factor $\mathbf{B}\left(\tilde{\mathbf{R}} + \mathbf{B}'\mathbf{P}_t\mathbf{B}\right)^{-1}\mathbf{B}'$ can be simplified as,

$$\begin{aligned}
\mathbf{B}\left(\tilde{\mathbf{R}} + \mathbf{B}'\mathbf{P}_t\mathbf{B}\right)^{-1}\mathbf{B}' &= \mathbf{B}\left(\mathbf{R} + \begin{bmatrix}\mathbf{0} & \mathbf{0}\\ \mathbf{0} & \sigma_2^2\mathbf{I} - \mathbf{R}_{22}\end{bmatrix} + \mathbf{B}'\mathbf{P}_t\mathbf{B}\right)^{-1}\mathbf{B}' \\
&=^{(a)} \mathbf{B}\left(\mathbf{R} + \begin{bmatrix}\mathbf{0} & \mathbf{0}\\ \mathbf{0} & \sigma_2^2\mathbf{I}\end{bmatrix} + \mathbf{B}'\mathbf{P}_t\mathbf{B}\right)^{-1}\mathbf{B}' \\
&=^{(b)} \mathbf{B}\begin{bmatrix}\mathcal{M}_{11} - \mathcal{M}_{12}\mathcal{M}_{22}^{-1}\mathcal{M}_{21} & \mathbf{0}\\ \mathbf{0} & \mathbf{0}\end{bmatrix}\mathbf{B}' \\
&=^{(c)} \mathbf{B}\begin{bmatrix}(\mathbf{R}_{11} + \mathbf{B}'\mathbf{P}_t\mathbf{B})^{-1} & \mathbf{0}\\ \mathbf{0} & \mathbf{0}\end{bmatrix}\mathbf{B}' \\
&=^{(d)} \mathbf{B}\left(\mathbf{R}_{11} + \mathbf{B}'\mathbf{P}_t\mathbf{B}\right)^{-1}\mathbf{B}' \\
&\text{where, } \left(\mathbf{R} + \mathbf{B}'\mathbf{P}_t\mathbf{B}\right)^{-1} = \begin{bmatrix}\mathcal{M}_{11} & \mathcal{M}_{12}\\ \mathcal{M}_{21} & \mathcal{M}_{22}\end{bmatrix}
\end{aligned} \tag{4.7}$$

and (a) follows since $\sigma_2^2 \to \infty$, (b) is outcome of low rank adjustment of matrix inversion [87] and $\sigma_2^2 \to \infty$, (c) is due to the alternate formula of inversion of a partitioned matrix [87], and (d) is outcome of multiplication of partitioned matrices. So, effectively the state is controlled as, $\mathbf{B}_1\left(\mathbf{R}_1 + \mathbf{B}_1'\mathbf{P}_t\mathbf{B}_1\right)^{-1}\mathbf{B}_1'\mathbf{P}_t\mathbf{A}\mathbf{x}_t$.

Thus, for general k actuator implementation the control matrix $\mathbf{B}$ is random with its realization depending on which actuators successfully receive the control actions; thus there are 2^k possible control matrices. Representing control matrix at time t by $\mathbf{H}_{t,i}$, such that i^{th} combination of actuator successfully receive the control actions, the dynamical state model can be expressed as

$$\mathbf{x}_{t+1} = \mathbf{A}\mathbf{x}_t - \sum_{i=1}^{2^k-1}\delta_{t,i}\mathbf{H}_{t,i}\left(\mathbf{R}_{t,i} + \mathbf{H}_{t,i}'\mathbf{P}_t\mathbf{H}_{t,i}\right)^{-1}\mathbf{H}_{t,i}'\mathbf{P}_t\mathbf{A}\mathbf{x}_t + \mathbf{w}_t \tag{4.8}$$

where, $\delta_{t,i}$ is binary random variable taking variable taking 1 if i^{th} combination of control inputs get applied, and 0 if that combination is not applied; and $\mathbf{R}_{t,i}$ is corresponding weight matrix. Substituting (4.8) in Lyapunov function (4.5) we get,

$$\begin{aligned}
V_{t+1} &= \left(\mathbf{A}\mathbf{x}_t - \textstyle\sum_{i=1}^{2^k-1}\delta_{t,i}\mathbf{H}_{t,i}\left(\mathbf{R}_{t,i} + \mathbf{H}_{t,i}'\mathbf{P}_t\mathbf{H}_{t,i}\right)^{-1}\mathbf{H}_{t,i}'\mathbf{P}_t\mathbf{A}\mathbf{x}_t + \mathbf{w}_t\right)' \\
&\quad \mathbf{P}_t\left(\mathbf{A}\mathbf{x}_t - \textstyle\sum_{i=1}^{2^k-1}\delta_{t,i}\mathbf{H}_{t,i}\left(\mathbf{R}_{t,i} + \mathbf{H}_{t,i}'\mathbf{P}_t\mathbf{H}_{t,i}\right)^{-1}\mathbf{H}_{t,i}'\mathbf{P}_t\mathbf{A}\mathbf{x}_t + \mathbf{w}_t\right) + q_t
\end{aligned} \tag{4.9}$$

The Lyapunov function in (4.9) is stochastic in terms of two random process: (1) process noise, and (2) packet drops. We first take the expectation with respect to process noise $\mathbf{w}_t$,

$$\begin{aligned}\mathbb{E}[V_{t+1}] \;&= \mathbf{x}_t' \Big(\mathbf{A}'\mathbf{P}_t\mathbf{A} - \textstyle\sum_{i=1}^{2^k-1} \delta_{t,1}\mathbf{A}'\mathbf{P}_t\mathbf{H}_{t,i}\left(\mathbf{R}_{t,i} + \mathbf{H}_{t,i}'\mathbf{P}_t\mathbf{H}_{t,i}\right)^{-1} \\ &\Big(2\mathbf{I} - \mathbf{H}_{t,i}'\mathbf{P}_t\mathbf{H}_{t,i}\left(\mathbf{R}_{t,i} + \mathbf{H}_{t,i}'\mathbf{P}_t\mathbf{H}_{t,i}\right)^{-1}\Big)\mathbf{H}_{t,i}'\mathbf{P}_t\mathbf{A}\Big)\mathbf{x}_t \\ &+\mathbb{E}\left[\mathbf{w}_t'\mathbf{P}_t\mathbf{w}_t\right] + q_t\end{aligned} \tag{4.10}$$

where, the cross product terms are set to zero as $\delta_{t,i}\delta_{t,j} = 1$ only if $i = j$ at any iteration t. Comparing, equation (4.10) with (4.5), we express the recursive equations for $\mathbf{P}_t$ and q_t as,

$$\begin{aligned}\mathbf{P}_{t+1} \;&= \mathbf{A}'\mathbf{P}_t\mathbf{A} - \textstyle\sum_{i=1}^{2^k-1} \delta_{t,i}\mathbf{A}'\mathbf{P}_t\mathbf{H}_{t,i}\left(\mathbf{R}_{t,i} + \mathbf{H}_{t,i}'\mathbf{P}_t\mathbf{H}_{t,i}\right)^{-1} \\ &\mathcal{F}(\mathbf{H}_{t,i},\mathbf{P}_t)\mathbf{H}_{t,i}'\mathbf{P}_t\mathbf{A} \\ q_{t+1} \;&= q_t + tr\left(\mathbf{W}\mathbf{P}_t\right)\end{aligned} \tag{4.11}$$

where, $\mathcal{F}(\mathbf{H}_{t,i},\mathbf{P}_t) := 2\mathbf{I} - \mathbf{H}_{t,1}'\mathbf{P}_t\mathbf{H}_{t,1}\left(\mathbf{R}_{t,i} + \mathbf{H}_{t,i}'\mathbf{P}_t\mathbf{H}_{t,i}\right)^{-1}$, and $tr\left(\mathbf{W}\mathbf{P}_t\right) = \mathbb{E}\left[\mathbf{w}_t'\mathbf{P}_t\mathbf{w}_t\right]$. It can be observed that the recursion of $\mathbf{P}_t$ is also stochastic, and its convergence properties depends on the random variables $\delta_{t,i}$ which are effectively determined by $\gamma_{t,1}, \gamma_{t,2}, \cdots, \gamma_{t,k}$. If $\gamma_{t,1} = \gamma_{t,2} = \cdots = \gamma_{t,k} = 0 \;\forall\; t$, i.e., there is no control input, then $\mathbf{P}_t$ diverges as $\mathbf{A}$ is unstable, $lim_{t\to\infty}\mathbf{P}_t \to \infty$. Additionally, as $\mathcal{F}_{t,i} \succeq \mathbf{0} \;\forall\; \mathbf{P}_t \succeq \mathbf{0}$, if $\gamma_{t,1} = \gamma_{t,2} = \cdots = \gamma_{t,k} = 1 \;\forall\; t$, i.e., there is no control input loss over the network then the recursion of $\mathbf{P}_t$ converges. Now, if $\mathbf{P}_t$ converges then q_t also converges and the system is interpreted as Lyapunov stable. In our analysis we consider packet drops as Bernoulli random variable with $Pr(\gamma_{t,j} = 1) = \lambda_j$ as probability of successfully transmitting a packet to actuator j. Thus, we can compute probabilities for all 2^k possible control action sets. For example, if total number of actuators is 4, then possible set of control actions getting successfully transmitted with their respective probabilities α_λ is shown in table (4.2.2). Our goal is to determine the critical rates for packet drops to individual actuators, sufficient to bound expectation of Lyapunov function to a desired value. In the following analysis we characterize the statistical properties of recursion of $\mathbf{P}_t$ in order to establish the conditions for its convergence.

$\{\gamma_{t,1},\gamma_{t,2},\gamma_{t,3},\gamma_{t,4}\}$	$\alpha_{\lambda_1,\lambda_2,\lambda_3,\lambda_4}$
$0,0,0,0$	$(1-\lambda_1)(1-\lambda_2)(1-\lambda_3)(1-\lambda_4)$
$0,0,0,1$	$(1-\lambda_1)(1-\lambda_2)(1-\lambda_3)\lambda_4$
$\vdots$	$\vdots$
$1,1,1,1$	$\lambda_1\lambda_2\lambda_3\lambda_4$

Table 4.1: *Possible control input sets for 4 actuator network*

4.3 Stochastic Lyapunov Function: Stability Properties

It was observed in section 2 that the $\mathbf{P}_t$ update equation (4.11) is function of control matrix $\mathbf{H}_{t,i}$ which depends on random packet drops. Thus, the error $\mathbf{P}_t$ iteration along the time $\{\mathbf{P}_t\}_{t=0}^{\infty}$ is a random process for any given starting point $\mathbf{P}_0$. This section focuses on statistical convergence properties of $\{\mathbf{P}_t\}_{t=0}^{\infty}$, yielding to Lyapunov stability analysis of underlying system. Since $\mathbf{P}_t$ is random process, we consider convergence in mean i.e. $\mathbb{E}[\mathbf{P}_{t+1}] = \mathbb{E}[\mathbb{E}[\mathbf{P}_{t+1}\ |\mathbf{P}_t]] \leq \infty$ as $t \to \infty$. Further, it can be noted that we consider two expectation operations: (1) the outer expectation over stochastic nature of $\mathbf{P}_{t-1}$; (2) and inner expectation over random packet drops at given iteration t, i.e. over $\gamma_{t,1}, \gamma_{t,2}, \cdots, \gamma_{t,k}$. We define $\mathbb{E}[\mathbf{P}_{t+1}|\mathbf{P}_t]$, as modified algebraic Riccati equation (MARE) with a short hand notation $\mathbb{E}[\mathbf{P}_{t+1}|\mathbf{P}_t] = \mathbf{g}_\alpha(\mathbf{X})$ expressed as,

$$\mathbf{g}_\alpha(\mathbf{X}) = \mathbf{A}'\mathbf{X}\mathbf{A} - \textstyle\sum_{i=1}^{2^k-1} \alpha_i \mathbf{A}'\mathbf{X}\mathbf{H}_i(\mathbf{H}_i\mathbf{X}\mathbf{H}_i' + \mathbf{R}_i)^{-1}\mathcal{F}(\mathbf{H}_i, \mathbf{R}_i, \mathbf{X})\mathbf{H}_i'\mathbf{X}\mathbf{A} \qquad (4.12)$$

where, $\alpha_i = \alpha_{\lambda_1,\cdots,\lambda_k}$ is the probability of receiving i^{th} set of measurements. Next, we define an auxiliary function $\phi(\mathcal{K}_1, \mathcal{K}_2, \cdots, \mathcal{K}_{2^k-1}, \mathbf{X})$ whose properties are closely related to $\mathbf{g}_\lambda(\mathbf{X})$.

$$\phi(\mathcal{K}_1, \cdots, \mathcal{K}_{2^k-1}, \mathbf{X}) = \alpha_0\mathbf{A}'\mathbf{X}\mathbf{A} + \textstyle\sum_{i=1}^{2^k-1} \alpha_i \left(\mathbf{F}_i'\mathbf{X}\mathbf{F}_i + \mathbf{T}_i\right) \qquad (4.13)$$

where, $\alpha_0 = (1 - \sum_{i=1}^{2^k-1} \alpha_i)$; $\mathbf{F}_i = \mathbf{A} + \mathbf{H}_i\mathcal{K}_i'$; $\mathbf{V}_i = \mathcal{K}_i\mathcal{R}_i\mathcal{K}_i'$; and $\mathbf{X} \succeq 0$. By differentiating the quadratic form of $\mathbf{F}_i'\mathbf{X}\mathbf{F}_i + \mathbf{T}_i$ with respect to $\mathcal{K}_i$ and setting it to zero, the $\mathcal{K}_i^{\mathbf{X}}$ which minimizes the quadratic form is given by $\mathcal{K}_i = \mathcal{K}_i^{\mathbf{X}} = -\mathbf{A}'\mathbf{X}\mathbf{H}_i\left(\mathbf{R}_i + \mathbf{H}_i'\mathbf{X}\mathbf{H}_i\right)^{-1}$. Further, substituting $\mathcal{K}_i^{\mathbf{X}}$ in auxiliary function (4.13) results in MARE equation (4.12). These observations further quantify our observations as,

$$\mathbf{g}_\alpha(\mathbf{X}) = \phi(\mathcal{K}_1^X, \cdots, \mathcal{K}_{2^k-1}^X, \mathbf{X}) \preceq \min{}_{\mathcal{K}_1,\cdots,\mathcal{K}_{2^k-1}} \phi(\mathcal{K}_1, \cdots, \mathcal{K}_{2^k-1}, \mathbf{X}) \tag{4.14}$$

Thus from (4.14), the auxiliary function $\phi(\cdots)$ acts as an upper bound to $\mathbf{g}_\alpha(\mathbf{X})$. Now, we present some useful lemmas as properties of the function $\mathbf{g}_\lambda(\mathbf{X})$, where $\mathbf{X} \succeq \mathbf{0}$ for establishing the convergence conditions of equation (4.12). The proofs of the lemmas appear in Appendix B.

Lemma 4.1. *The MARE equation (4.12) is concave function in* $\mathbf{X}$*, for* $\mathbf{X} \succeq \mathbf{0}$*. Thus, by Jensen's inequality* $\mathbb{E}[\mathbf{g}_\lambda(\mathbf{X})] \preceq \mathbf{g}_\lambda(\mathbb{E}[\mathbf{X}])$*.*

The concave nature of function $\mathbf{g}_\lambda(\mathbf{X})$ helps us in establishing an upper bound on $\mathbb{E}[\mathbf{P}_{t+1}]$ as a function of $\mathbb{E}[\mathbf{P}_t]$.

Lemma 4.2. $\mathbf{g}_\lambda(\mathbf{X})$ *is monotonously nondecreasing function of* $\mathbf{X}$*. Thus, if* $0 \preceq \mathbf{X} \preceq \mathbf{Y}$*, then* $\mathbf{g}_\lambda(\mathbf{X}) \preceq \mathbf{g}_\lambda(\mathbf{Y})$*.*

This monotonous nondecreasing property helps us in proving the convergence of recursion $\mathbf{P}_{t+1} = \mathbf{g}_\lambda(\mathbf{P}_t)$. Thus, if $\mathbf{X}_{t+1} = \mathbf{g}_\lambda(\mathbf{X}_t)$ and $\mathbf{Y}_{t+1} = \mathbf{g}_\lambda(\mathbf{Y}_t)$, then initial conditions $\mathbf{X}_0 \succeq \mathbf{Y}_0 \succeq \mathbf{0} \;\Rightarrow\; \mathbf{X}_t \succeq \mathbf{Y}_t$ for all iterations t.

Lemma 4.3. *Fixing packet drop rate for all actuator communication links except for one actuator* j*, such that* $\lambda_j^1 \leq \lambda_j^2$*, then for corresponding* α^1 *and* α^2*,* $\mathbf{g}_{\alpha^1}(\mathbf{X}) \preceq \mathbf{g}_{\alpha^2}(\mathbf{X})$

This property intuitively explains that regular control inputs will better stabilize the system. Thus, if arrival probabilities of control input increases, the underlying system is better controlled. In other words, the convergence of $\mathbf{P}_t$ is faster as the control input rate is increased. This lemma eventually helps us in determining instability region for the recursion $\mathbb{E}[\mathbf{P}_t] = \mathbf{g}_\lambda(\mathbf{P}_t)$.

Let $\mathbf{B} = \begin{bmatrix}\mathbf{H} & \mathbf{G}\end{bmatrix}$ where, $\mathbf{H}$ is the portion of control matrix denoting successfully transmitted control inputs, and $\mathbf{G}$ is the corresponding portion of lost control inputs. Now expanding $\mathbf{B}\left(\mathbf{R}+\mathbf{B}'\mathbf{X}\mathbf{B}\right)^{-1}\mathcal{F}(\mathbf{B},\mathbf{R},\mathbf{X})\mathbf{B}'$ we get,

$$\begin{array}{c}\mathbf{B}\left(\mathbf{R}+\mathbf{B}'\mathbf{X}\mathbf{B}\right)^{-1}\mathcal{F}(\mathbf{B},\mathbf{R},\mathbf{X})\mathbf{B}' = \\ \mathbf{H}_i\left(\mathbf{R}_{Hi}+\mathbf{H}_i'\mathbf{X}\mathbf{H}_i\right)^{-1}\mathcal{F}(\mathbf{H}_i,\mathbf{R}_{Hi},\mathbf{X})\mathbf{H}_i' + \mathcal{Z}\left(\mathbf{H}_i,\mathbf{R}_{Hi},\mathbf{G}_i,\mathbf{R}_{Gi},\mathbf{X}\right)\end{array} \tag{4.15}$$

where, expression for $\mathcal{Z}\left(\mathbf{H}_i,\mathbf{R}_{Hi},\mathbf{G}_i,\mathbf{R}_{Gi},\mathbf{X}\right)$ is derived in appendix B. Finally, substituting (4.15) in (4.12), the $\mathbf{g}_\alpha(\mathbf{X})$ iteration is expressed as,

$$\begin{array}{rl}\mathbf{g}_\alpha(\mathbf{X}) = & \mathbf{A}'\mathbf{X}\mathbf{A} - \left[\sum_{i=1}^{2^k-1}\alpha_i\right]\mathbf{A}'\mathbf{X}\mathbf{B}\left(\mathbf{R}+\mathbf{B}'\mathbf{X}\mathbf{B}'\right)^{-1}\mathcal{F}(\mathbf{H}_i,\mathbf{R}_i,\mathbf{X})\mathbf{B}'\mathbf{X}\mathbf{A} \\ & +\sum_{i=1}^{2^k-2}\alpha_i\mathbf{A}'\mathbf{X}\mathcal{Z}\left(\mathbf{H}_i,\mathbf{R}_{Hi},\mathbf{G}_i,\mathbf{R}_{Gi},\mathbf{X}\right)\mathbf{X}\mathbf{A}\end{array} \tag{4.16}$$

The corresponding auxiliary function similar to (4.13) can be expressed as,

$$\begin{array}{rl}\phi(\mathcal{K},\mathbf{X}) = & \alpha_0\left(\mathbf{A}'\mathbf{X}\mathbf{A}\right) + (1-\alpha_0)\left(\mathbf{F}'\mathbf{X}\mathbf{F}+\mathbf{T}\right) \\ & +\sum_{i=1}^{2^k-2}\alpha_i\mathbf{A}'\mathbf{X}\mathcal{Z}\left(\mathbf{H}_i,\mathbf{R}_{Hi},\mathbf{G}_i,\mathbf{R}_{Gi},\mathbf{X}\right)\mathbf{X}\mathbf{A}\end{array} \tag{4.17}$$

Next, we present a lemmas where we exploit above discussion for establishing convergence condition on recursion of $\mathbf{g}_\alpha(\mathbf{X})$.

Lemma 4.4. *For any* $\mathbf{X}\succeq\mathbf{0}$*, and* $\mathbf{R}\succeq\mathbf{0}$*,*

$$\mathbf{g}_\alpha(\mathbf{X}) \succeq \alpha_0\mathbf{A}'\mathbf{X}\mathbf{A} + \sum_{i=1}^{2^k-2}\alpha_i\mathbf{A}'\mathbf{X}\mathcal{Z}\left(\mathbf{H}_i,\mathbf{R}_{Hi},\mathbf{G}_i,\mathbf{R}_{Gi},\mathbf{X}\right)\mathbf{X}\mathbf{A} \tag{4.18}$$

Consider the two recursive sequences $\mathbf{X}_{t+1} = \mathbf{g}_\alpha(\mathbf{X}_t)$, and $\hat{\mathbf{X}}_{t+1} = \alpha_0\mathbf{A}'\hat{\mathbf{X}}\mathbf{A} + \sum_{i=1}^{2^k-2}\alpha_i\mathbf{A}'\hat{\mathbf{X}}\mathcal{Z}\Big(\mathbf{H}_i,\mathbf{R}_{Hi},$ with same initial condition, then at time step t, $\mathbf{X}_t \succ \hat{\mathbf{X}}_t$. Thus, if $\hat{\mathbf{X}}_{t+1}$ diverges, then $\mathbf{X}_{t+1} = \mathbf{g}_\alpha(\mathbf{X}_t)$ also diverges. This allows us to find the lower bounds on critical actuator probabilities $\{\lambda_1^c,\cdots,\lambda_k^c\}$ that lead to convergence of $\mathbf{X}_t$.

Lemma 4.5. *Since,* $\mathbf{X}\succeq 0$ *is a random matrix,*

$$\begin{array}{l}\alpha_0\mathbf{A}'\mathbb{E}[\mathbf{X}]\mathbf{A} + \sum_{i=1}^{2^k-2}\alpha_i\mathbf{A}'\mathbb{E}\left[\mathbf{X}\mathcal{Z}\left(\mathbf{H}_i,\mathbf{R}_{Hi},\mathbf{G}_i,\mathbf{Gi},\mathbf{X}\right)\mathbf{X}\right]\mathbf{A} \\ \preceq \mathbb{E}[\mathbf{g}_\alpha(\mathbf{X})] \preceq \mathbf{g}_\alpha(\mathbb{E}[\mathbf{X}])\end{array} \tag{4.19}$$

This property combines concavity property of lemma 4.1 and bounded condition of lemma 4.4 and lead to both an upper and lower bound on $\mathbb{E}[\mathbf{g}_\alpha(\mathbf{X})]$. Before, discussing other properties, we define another auxiliary function that captures the linear part of $\phi(\mathcal{K}_1, \cdots, \mathcal{K}_{2^k-1}, \mathbf{X})$. Let

$$\mathcal{L}(\mathbf{X}) = \alpha_0 \mathbf{A}'\mathbf{X}\mathbf{A} + \sum_{i=1}^{2^k-1} \alpha_i \mathbf{F}_i' \mathbf{X} \mathbf{F}_i \tag{4.20}$$

It can be easily observed that $\mathcal{L}(\mathbf{X})$ is linear function of $\mathbf{X}$ and due to $\mathbf{X} \succeq \mathbf{0}$, $\mathcal{L}(\mathbf{X}) \succeq \mathbf{0}$. Furthermore, we can identify auxiliary function $\phi(\mathcal{K}_1, \cdots, \mathcal{K}_{2^k-1}, \mathbf{X})$ as an affine function of $\mathbf{X}$, with $\phi(\mathcal{K}_1, \cdots, \mathcal{K}_{2^k-1}, \mathbf{X}) = \mathcal{L}(\mathbf{X}) + \mathcal{T}$, where $\mathcal{T} = \sum_{i=1}^{2^k-1} \alpha_i \mathbf{T}_i$. Notice, since $\mathbf{T}_i \succeq 0$, $\mathcal{T} \succeq 0$.

Lemma 4.6. *Let there exists a bounded solution of $\mathcal{L}(\mathbf{X})$, such that $\mathcal{Y} \succeq \mathcal{L}(\mathcal{Y})$, then, (1) $\forall\ \mathcal{W} \succeq \mathbf{0}$, $lim_{t\to\infty}\mathcal{L}(\mathcal{W}) = \mathbf{0}$; (2) For $\mathcal{T} \geq 0$, $\mathcal{Y}_{t+1} = \mathcal{L}(\mathcal{Y}_t) + \mathcal{T}$. Thus, for any arbitrary initial condition $\mathcal{Y}_0$, $\mathcal{Y}_t$ is bounded.*

This property gives a condition that the recursion of linear auxiliary function $\mathcal{L}(\mathbf{X})$ converges to $\mathbf{0}$, which in turn leads to convergence of recursion of affine auxiliary function $\mathbf{Y}_{t+1} = \mathcal{L}(\mathbf{Y}_t) + \mathcal{T}$ for bounded initial condition $\mathbf{Y}_0$.

Lemma 4.7. *If there exists some $\bar{\mathcal{K}}_1, \cdots, \bar{\mathcal{K}}_{2^k-1}$, and $\bar{\mathbf{P}} \succ 0$, such that $\bar{\mathbf{P}} \succ \phi(\bar{\mathcal{K}}_1, \cdots, \bar{\mathcal{K}}_{2^k-1}, \bar{\mathbf{P}})$, then for any arbitrary initial condition $\bar{\mathbf{P}}_0 \succeq 0$, $\bar{\mathbf{P}} = g_\alpha^t(\bar{\mathbf{P}}_0)$ is bounded.*

This lemma establishes the condition for the recursion of $\bar{\mathbf{P}}_{t+1} = \mathbf{g}_\lambda(\bar{\mathbf{P}}_t)$ to be bounded for any arbitrary initial condition $\bar{\mathbf{P}}_0$. In following subsection we use above properties of $\mathbf{g}_\alpha(\mathbf{X})$, to analyze the conditions for convergence of $\mathbf{P}_t$ matrix.

4.3.1 Convergence Conditions

It can be observed that, lemma 4.5-4.7 establishes conditions for boundedness of auxiliary function, which further ensures boundedness of matrix $\mathbf{P}_t$. We formally put these conditions in form of following theorem (proofs follow in appendix B).

Theorem 4.1. *Let there exists a bound $\mathbf{X} \succ \phi(\mathcal{K}_1, \cdots, \mathcal{K}_{2^k-1}, \mathbf{X})$ for $\mathbf{X} \succeq \mathbf{0}$, then (1) $lim_{t\to\infty}\mathbf{X}_t = lim_{t\to\infty}\mathbf{g}_\alpha\ (\mathbf{X}_\mathbf{0}) = \mathbf{X}$, for any starting $\mathbf{X}_0 \succeq \mathbf{0}$; (2) converging solution $\mathbf{X}$ is unique.*

This theorem proves the convergence of $\mathbf{P}_{t+1} = \mathbf{g}_\alpha(\mathbf{P}_t)$ under some given conditions. It also shows the uniqueness of solution when it converges. Next theorem establishes existence of stability region boundary such that the expected Lyapunov function becomes unbounded if packet drop rates are beyond the specified critical values.

Theorem 4.2. *Given a stable system i.e. matrix pair* $(\mathbf{A}, \mathbf{W})$ *is controllable, then there exists critical control input successful transmission probabilities* $0 \leq \{\lambda_{c,1}, \cdots, \lambda_{c,k}\} \leq 1$ *such that* $lim_{t\to\infty}\mathbb{E}[\mathbf{X}_t] = \infty$ *if all actutor packet drop probabilities are at critical rate except one actuator* j*, i.e.* $0 \leq \lambda_j \leq \lambda_{c,j}$*. Further,* $\mathbb{E}[\mathbf{P}_t] \preceq \mathbf{P}_{max}\ \forall\ t$*, if* $\lambda_{c,j} < \lambda_j \leq 1\ \forall\ j = 1, \cdots, k$ *and initial condition* $\mathbf{P}_0 \succeq \mathbf{0}$.

In general, we can not explicitly compute the critical probabilities of successful transmission, but we can compute both and upper and lower bounds on $\{\lambda_{c,1}, \cdots, \lambda_{c,k}\}$. In following section we first analyze the lower and upper bound on converging solution, and then we compute the corresponding lower and upper bound on critical control loss rates.

4.4 Bounds on Critical Actuator Loss

In the following analysis, we compute upper and lower bounds on converging solution of $\mathbf{P}_t$ iteration by exploiting the analogy between dispersed and unified control. This understanding enables us to effectively use the stability results of unified actuator scenario for the dispersed actuator scenario, followed by computation of corresponding upper and lower bound on control action critical probabilities. The analysis finally results in a concatenated k-dimensional regions (assuming k independent communication links) where: (1) inside inner region, the system is definitely unstable; (2) outside outer region, the system is definitely stable; (3) the in between region system is indeterminate. So, we first discuss and establish stability conditions for $unified$ actuator scenario, followed by developing the the analogy between dispersed and unified control.

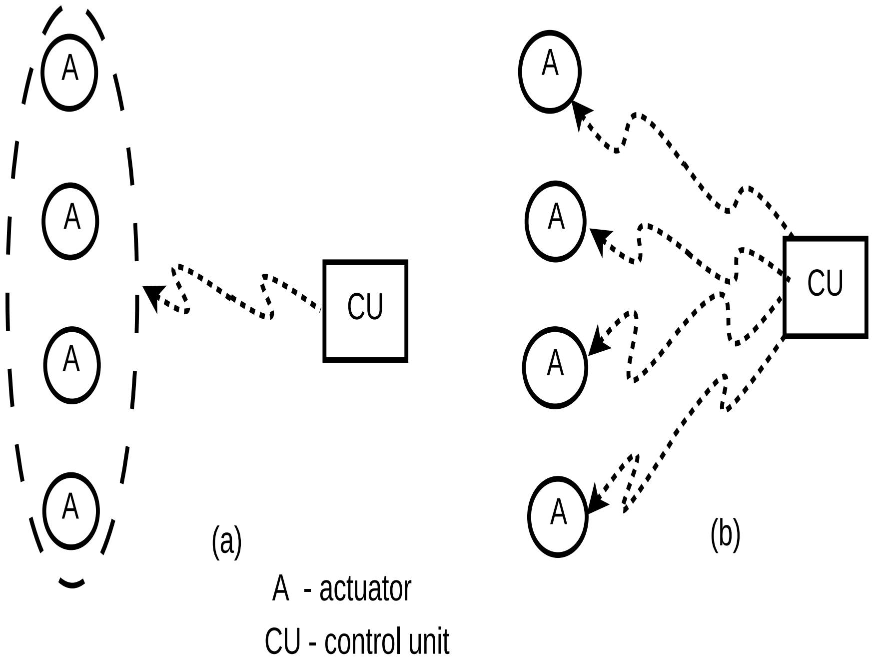

Figure 4.2: *Measurement transmission strategies: (a) gathered information (b) dispersed information*

4.4.1 Unified Control Over a Network

Consider the two strategies of communicating the control actions to actuators: (1) control input is transmitted over a single communication link (unified control) as shown in Figure 4.2(a); (2) control action for actuators is transmitted over individual communication links (dispersed control) as shown in Figure 4.2(b). It is easy to deduce that if λ is the probability for successful transmission of control input in 4.2(a), the corresponding iteration for $\mathbf{P}_t$ in form of MARE is given by,

$$\mathbf{g}_\lambda(\mathbf{X}) = \mathbf{A}'\mathbf{X}\mathbf{A} - \lambda\mathbf{A}'\mathbf{X}\mathbf{B}\left(\mathbf{R} + \mathbf{B}'\mathbf{X}\mathbf{B}\right)^{-1}\mathcal{F}(\mathbf{B},\mathbf{X})\mathbf{B}'\mathbf{X}\mathbf{A}. \tag{4.21}$$

Equation (4.21) satisfies all statistical properties and convergence condition discussed in section 4.3 (more details are discussed in our publication [66]). The lower bound $\lambda_{c,lb}$ on critical value λ_c satisfies the following proposition,

$$\exists\mathbf{P}_{lb}\ s.t.\ \lambda_{c,lb} = \ argmin\ f_\lambda\left(\mathbf{P}_{lb}\ =\ (1-\lambda)\mathbf{A}'\mathbf{P}_{lb}\mathbf{A}\right)\ =\ 1 - \frac{1}{\rho_A^2} \tag{4.22}$$

where, $\rho_A = max_i\{|\sigma_i|\}$; and σ_i are the eigen values of $\mathbf{A}$. Similarly, upper bound $\lambda_{c,ub}$ on critical value λ_c satisfies the following proposition,

$$\exists \left(\hat{\mathbf{K}}, \hat{\mathbf{X}}\right) \; s.t. \; \lambda_{c,ub} \; = \; argmin \; f_\lambda \left(\hat{\mathbf{X}} \succ \phi(\mathbf{P}_{ub}, \hat{\mathbf{K}})\right) \tag{4.23}$$

Using Schur compliment decomposition and matrix analysis on proposition (4.23), $\lambda_{c,ub}$ is obtained by solving following optimization problem,

$$\lambda_{c,ub} = argmin_\lambda \Psi_\lambda(\mathbf{Y}, \mathbf{Z}) \succ \mathbf{0}, \; st. \; \mathbf{0} \preceq \mathbf{Y} \preceq \mathbf{I} \tag{4.24}$$

where, $\Psi_\lambda(\mathbf{Y}, \mathbf{Z}) \; = \begin{bmatrix} \mathbf{Y} & \sqrt{\lambda}\,(\mathbf{YA}' + \mathbf{ZB}') & \sqrt{1-\lambda}\mathbf{YA}' \\ \sqrt{\lambda}\,(\mathbf{AY} + \mathbf{BZ}') & \mathbf{Y} & \mathbf{0} \\ \sqrt{1-\lambda}\mathbf{AY} & \mathbf{0} & \mathbf{Y} \end{bmatrix}$

This is quasi-convex optimization problem in variables $(\lambda, \mathbf{Y}, \mathbf{Z})$ and solution can be obtained by iterating LMI feasibility problems and using bisection of variable λ.

The lower bound $\mathbf{P}_{lb}$ for $\mathbb{E}[\mathbf{P}_t]$ is easily obtained by iterating $\mathbf{X}_{t+1} = (1 - \lambda_{c,lb})\mathbf{A}'\mathbf{X}_t\mathbf{A}$ starting with some initial condition $\mathbf{X}_0$. Similarly, the upper bound $\mathbf{P}_{ub}$ can be computed by iterating MARE for $\lambda_{c,ub}$ starting with some initial condition $\mathbf{X}_0$. In both these iteration we can put the convergence of Lyapunov function as converging condition.

4.4.2 Unified / Dispersed Actuator Analogy

Once again, consider the two strategies of communicating the control actions: (1) unified control, as shown in Figure 4.2(a); (2) dispersed control Figure 4.2(b). For ideal loss free communication network, the control action implementation is same in both these strategies as computed optimal control action is same for both the cases. Thus, at steady state the $\mathbf{P}_t$ iteration will converge to same $\mathbf{P}_{ss}$, i.e., $lim_{t\to\infty}\mathbf{P}_t \to \mathbf{P}_{ss}$ for both these strategies. This statement can be further verified if we reverse the analysis of equation (4.7) and reconstruct the unified control from dispersed control for lossless network scenario. Now, considering unified control strategy under lossy network, the $\mathbf{P}_t$ iteration can still converge, depending on the probability of successful actuator input transmission λ [66]. At critical value λ_c, the systems at the verge of getting uncontrollable; the iteration $\mathbf{P}_t$ converges to $\mathbf{P}_{c,ss}$, i.e.,

$lim_{t\to\infty}\mathbf{P}_t \to \mathbf{P}_{c,ss} \succ \mathbf{P}_{ss}$. Thus, at steady state, MARE for unified control strategy at λ_c is,

$$\mathbf{P}_{c,ss} = \mathbf{A}'\mathbf{P}_{c,ss}\mathbf{A} - \lambda_c\mathbf{A}'\mathbf{P}_{c,ss}\mathbf{B}\left(\mathbf{R}+\mathbf{B}'\mathbf{P}_{c,ss}\mathbf{B}\right)^{-1}\mathcal{F}(\mathbf{B},\mathbf{P}_{c,ss})\mathbf{B}'\mathbf{P}_{c,ss}\mathbf{A}. \tag{4.25}$$

It can be noticed from equation (4.25), that $(1-\lambda_c)\mathbf{A}'\mathbf{P}_{c,ss}\mathbf{B}\left(\mathbf{R}+\mathbf{B}'\mathbf{P}_{c,ss}\mathbf{B}\right)^{-1}\mathcal{F}(\mathbf{B},\mathbf{P}_{c,ss})$ $\mathbf{B}'\mathbf{P}_{c,ss}\mathbf{A}$ is the critical loss beyond which the $\mathbf{P}_t$ iteration diverges. Now, as underlying dynamical system is same for both unified and *disperse* control strategy, the affordable critical loss must be same for both the cases independent of the strategies of communicating actuator actions. Thus, in dispersed actuator scenario, we expect to distribute this critical control input loss among the individual actuator communication links. With the argument that affordable critical control input loss is same in both the strategies, we can further argue that the $\mathbf{P}_t$ iteration will converge to same $\mathbf{P}_{c,ss}$ for both these cases. In the following analysis we use the above intuition to compute bounds on critical measurement drop rates.

4.4.3 Lower Bound on Packet Drop Probabilities

Comparing to unified control action scenario, let the lower bound solution to $\mathbf{P}_t$ iteration be $\mathbf{P}_{lb} = \mathcal{Q}_{lb}\mathcal{D}_{lb}\mathcal{Q}'_{lb}$ where, $\mathcal{Q}_{lb},\mathcal{D}_{lb}$ is the eigen decomposition of converging solution, then at steady state

$$\begin{aligned}\mathbf{P}_{lb} &= (1-\lambda)\mathbf{A}'\mathbf{P}_{lb}\mathbf{A}\\ &= \mathbf{A}'\mathcal{Q}_{lb}\left((1-\lambda)\,\mathcal{D}_{lb}\right)\mathcal{Q}'_{lb}\mathbf{A}\end{aligned} \tag{4.26}$$

Then following argument that both dispersed and unified control strategy will converge to same value at steady state, we can utilize the computed lower bound $\mathbf{P}_{lb}$ of unified actuator case for dispersed actuator case. Comparing (4.26) and (4.11) we get,

$$\begin{aligned}&\mathbf{A}'\mathcal{Q}_{lb}(1-\lambda)\mathcal{D}_{lb}\mathcal{Q}'_{lb}\mathbf{A} =\\ &\mathbf{A}'\mathcal{Q}_{lb}\left[\alpha_0\mathcal{D}_{lb} + \textstyle\sum_{i=1}^{2^k-2}\alpha_i\mathcal{D}_{lb}\mathcal{Q}'_{lb}\mathcal{Z}\left(\mathbf{H}_i,\mathbf{G}_i,\mathbf{P}_{lb}\right)\mathcal{Q}_{lb}\mathcal{D}_{lb}\right]\mathcal{Q}'_{lb}\mathbf{A}\end{aligned} \tag{4.27}$$

To compute $\alpha_0,\cdots,\alpha_{2^k-2}$ (thus, $\lambda_{1,lb},\cdots,\lambda_{k,lb}$) satisfying equation (4.27), we propose solution by formulating an optimization problem,

$$
\begin{array}{ll}
\min . & trace(\mathbf{S}) \\
\text{st.} & \begin{cases} (1-\lambda) & = \alpha_0 + d_{lb}(1)\sum_{i=1}^{2^k-2}\alpha_i \mathbf{q}'_{lb}(1)\mathcal{Z}\left(\mathbf{H}_i, \mathbf{G}_i, \mathbf{P}_{lb}\right)\mathbf{q}_{lb}(1) + s_1 \\ (1-\lambda) & = \alpha_0 + d_{lb}(2)\sum_{i=1}^{2^k-2}\alpha_i \mathbf{q}'_{lb}(2)\mathcal{Z}\left(\mathbf{H}_i, \mathbf{G}_i, \mathbf{P}_{lb}\right)\mathbf{q}_{lb}(2) + s_2 \\ \vdots & \vdots \cdots \vdots \\ (1-\lambda) & = \alpha_0 + d_{lb}(n)\sum_{i=1}^{2^k-2}\alpha_i \mathbf{q}'_{lb}(n)\mathcal{Z}\left(\mathbf{H}_i, \mathbf{G}_i, \mathbf{P}_{lb}\right)\mathbf{q}_{lb}(n) + s_n \end{cases}
\end{array} \tag{4.28}
$$

where, $\lambda > \lambda_{c,lb}$; $d_{lb}(i)$ is the i^{th} diagonal element of $\mathcal{D}_{lb}$; $\mathbf{q}_{lb}(i)$ is the i^{th} eigen vector; and $\mathbf{S} = diag(s_1, \cdots, s_n)$ is the slack matrix. Further, adding constraint $\mathbf{S} \preceq \mathbf{0}$, assures that the converging solution of dispersed actuator scenario is always bounded below the converging solution of unified actuator scenario. It is easy to notice that, the formulation (4.28) is a minimization problem with linear constraints in probability variables $\alpha_0, \cdots, \alpha_{2^k-2}$ and slack variables $s_1, \cdots, s_n$. Since, $\sum_{i=0}^{2^k-1}\alpha_i = 1$ and $\alpha_{2^k-1} \neq 0$ (probability of successfully transmitting all actuator inputs), placing an additional linear inequality constraint $\sum_{i=0}^{2^k-2}\alpha_i < 1$, will optimally solve for variables $\alpha_0, \cdots, \alpha_{2^k-2}$. Thereafter, the lower bound on individual critical link probabilities $\lambda_{c,1,lb}, \cdots, \lambda_{c,k,lb}$ can be computed, as probabilities of all possible loss scenario is now known.

4.4.4 Upper Bound on Packet Drop Probabilities

Again following our discussion on analogy between dispersed and unified actuator case, if $\mathbf{P}_{ub}$ is the upper bound on $\mathbf{P}_{c,ss}$ (obtained form unified actuator case), then

$$
\mathbf{P}_{ub} \succeq \mathbf{A}'\mathbf{P}_{ub}\mathbf{A} - \lambda_{c,ub}\mathbf{A}'\mathbf{P}_{ub}\mathbf{B}\left(\mathbf{R} + \mathbf{B}'\mathbf{P}_{ub}\mathbf{B}\right)^{-1}\mathcal{F}(\mathbf{B}, \mathbf{R}, \mathbf{P}_{ub})\mathbf{B}'\mathbf{P}_{ub}\mathbf{A}. \tag{4.29}
$$

Next utilizing the upper bound $\mathbf{P}_{ub}$ computed from unified actuator case in dispersed actuator case, the corresponding equation for dispersed actuator scenario can be expressed as,

$$
\begin{array}{ll} \mathbf{P}_{ub} & \succeq \mathbf{A}'\mathbf{P}_{ub}\mathbf{A} - \sum_{i=1}^{2^k-1}\alpha_i \mathbf{A}'\mathbf{P}_{ub}\mathbf{H}_i\left(\mathbf{R}_{Hi} + \mathbf{H}'_i\mathbf{P}_{ub}\mathbf{H}_i\right)^{-1} \\ & \mathcal{F}(\mathbf{H}_i, \mathbf{P}_{ub})\mathbf{H}'_i\mathbf{P}_{ub}\mathbf{A}. \end{array} \tag{4.30}
$$

Thus, for (4.29) and (4.30) to converge to same solution following condition must be satisfied,

$$
\begin{array}{l} \lambda_{c,ub}\mathcal{Q}'_{ub}\mathbf{B}\left(\mathbf{R} + \mathbf{B}'\mathbf{P}_{ub}\mathbf{B}\right)^{-1}\mathcal{F}(\mathbf{B}, \mathbf{R}, \mathbf{P}_{ub})\mathbf{B}'\mathcal{Q}_{ub} = \\ \sum_{i=1}^{2^k-1}\alpha_i\mathcal{Q}'_{ub}\mathbf{H}_i\left(\mathbf{R}_{Hi} + \mathbf{H}'_i\mathbf{P}_{ub}\mathbf{H}_i\right)^{-1}\mathcal{F}(\mathbf{H}_i, \mathbf{R}_{Hi}, \mathbf{P}_{ub})\mathbf{H}'_i\mathcal{Q}_{ub} \end{array} \tag{4.31}
$$

where, $\mathcal{Q}_{ub}$ is the unitary matrix corresponding to eigen decomposition of $\mathbf{P}_{ub}$. To compute $\alpha_1, \cdots, \alpha_{2^k-1}$ (thus, $\lambda_{c,1,ub}, \cdots, \lambda_{c,ub,k}$) satisfying equation (4.31), we propose solution by formulating an optimization problem,

$$\begin{aligned} \min. \quad & trace(\mathbf{S}) \\ st. \quad & \begin{cases} \lambda_{c,ub}\mathbf{q}'_{ub}(1)\mathcal{G}(\mathbf{B},\mathbf{P}_{ub})\mathbf{q}_{ub}(1) = \\ \sum_{i=1}^{2^k-1} \alpha_i \mathbf{q}'_{ub}(1)\mathcal{G}(\mathbf{H}_i,\mathbf{P}_{ub})\mathbf{q}_{ub}(1) + s(1) \\ \lambda_{c,ub}\mathbf{q}'_{ub}(2)\mathcal{G}(\mathbf{B},\mathbf{P}_{ub})\mathbf{q}_{ub}(2) = \\ \sum_{i=1}^{2^k-1} \alpha_i \mathbf{q}'_{ub}(2)\mathcal{G}(\mathbf{H}_i,\mathbf{P}_{ub})\mathbf{q}_{ub}(2) + s(2) \\ \vdots \cdots \cdots \vdots \\ \lambda_{c,ub}\mathbf{q}'_{ub}(n)\mathcal{G}(\mathbf{B},\mathbf{P}_{ub})\mathbf{q}_{ub}(n) = \\ \sum_{i=1}^{2^k-1} \alpha_i \mathbf{q}'_{ub}(n)\mathcal{G}(\mathbf{H}_i,\mathbf{P}_{ub})\mathbf{q}_{ub}(n) + s(n) \end{cases} \end{aligned} \tag{4.32}$$

where, $\mathcal{G}(\mathbf{B},\mathbf{X}) = \mathbf{B}\left(\mathbf{R}+\mathbf{B}'\mathbf{X}\mathbf{B}\right)^{-1}\mathcal{F}(\mathbf{B},\mathbf{R},\mathbf{X})\mathbf{B}'$; $\mathbf{q}_{ub}()$ is the eigen vector; and $\mathbf{S} = diag(s(1), \cdots, s(n))$ is slack matrix. Again, adding additional constraint $\mathbf{S} \succeq \mathbf{0}$ ensures that the converging solution of dispersed actuators is bounded below the converging solution of unified actuator case. Also, we can again notice that the formulation (4.32) is a minimization problem with linear constraints in probability variables $\alpha_1, \cdots, \alpha_{2^k-1}$ and slack variables $s_1, \cdots, s_n$. Further placing a linear inequality constraint $\sum_{i=1}^{2^k-1} \alpha_i < 1$ (as $\sum_{i=0}^{2^k-2} \alpha_i < 1$ and $\alpha_0 \neq 0$), $\alpha_1, \cdots, \alpha_{2^k-1}$ can be optimally computed. Thereafter, the upper bound on individual critical actuator probabilities $\lambda_{c,1,ub}, \cdots, \lambda_{c,k,ub}$ can be computed, as probabilities of all possible loss scenario is now known.

4.5 System Examples

This section validates the analytical results of previous sections by finding stability regions defined by lower and upper bound on critical probability of successful actuator input transmission for several system examples. The upper and lower bound on convergence of $\mathbf{P}_t$ iteration is computed first from the unified control scenario, and then actuator input loss is distributed to dispersed actuators scenario by solving the optimization problems (4.28) and (4.32). In the numerical examples of generalized system, we also present performance trade-off in stability and quality of underlying network defined by actuator input loss rate.

4.5.1 Decoupled system with no overlap in control space

Consider a simple system of two nodes with: state transition matrix $\mathbf{A} = \begin{bmatrix} 1.25 & 0 \\ 0 & 1.5 \end{bmatrix}$; and two dispersed actuators with $\mathbf{B}'_1 = [1\ 0]$ and $\mathbf{B}'_2 = [0\ 1]$ as their control matrix. We assume process noise covariance matrix $\mathbf{W} = 20\mathbf{I}_2$ and control weight $\mathbf{R} = 5\mathbf{I}_2$.

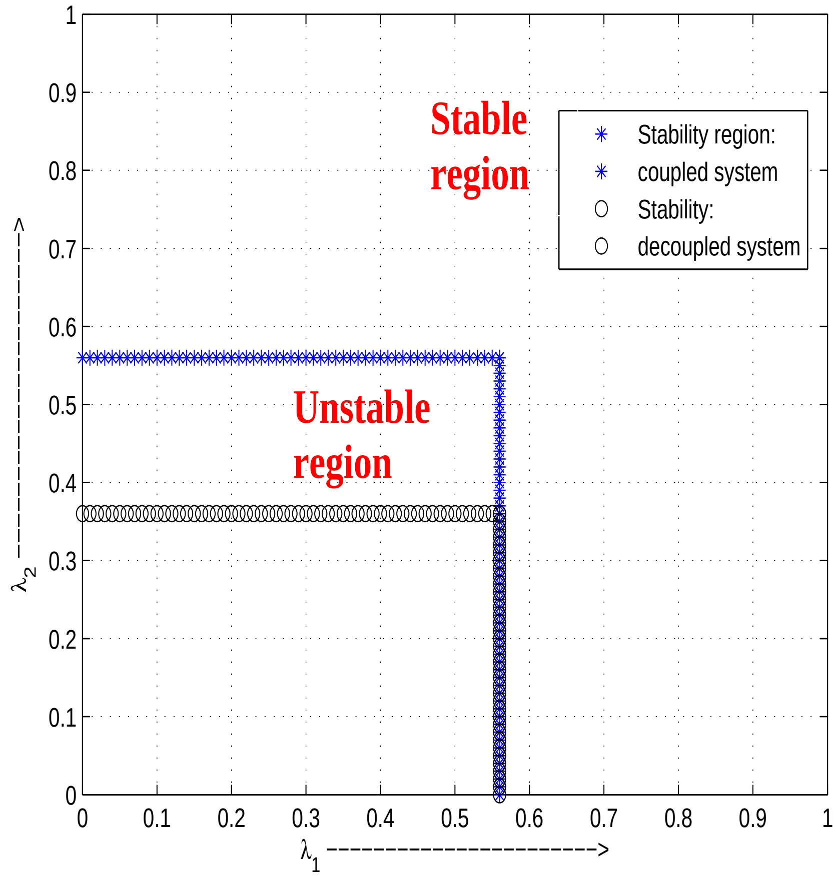

Figure 4.3: *Stability region - Decoupled System*

First, considering unified actuator scenario, the critical probability of successful actuator input transmission λ_c has lower bound as $\lambda_c \geq \lambda_{c,lb} = (1 - 1/1.5^2) \approx 0.56$, and upper bound as $\lambda_c \leq \lambda_{c,ub} \approx 0.56$. Both upper and lower bounds coincide as $\mathbf{B} = [\mathbf{B}_1\ \mathbf{B}_2]$ is invertible (It is easy to notice that by setting $\mathcal{K}' = -\mathbf{B}^{-1}\mathbf{A}$ results in $\mathbf{F} = 0$). Now, considering dispersed actuators scenario, the stability region defined by critical probabilities of individual links

$\lambda_{c,1}$ and $\lambda_{c,2}$ is shown in Figure 4.3 (shown. by $*$). Both upper and lower bounds coincide, with $\lambda_{c,1} = \lambda_{c,2} = 0.56$. However, it is easy to notice that this system is completely decoupled and each actuators directly control the states. The control process is essentially of two independent scalar system with critical probabilities $\lambda_{c,1} > 1 - 1/1.25^2 \approx 0.36$ and $\lambda_{c,2} > 1 - 1/1.25^2 \approx 0.55$ (shown, by o in Figure 4.3). Thus, bounds computed using (4.28) and (4.32) are relaxed; so it is prudent to first decouple the system if the system can be decoupled and then compute the bounds.

4.5.2 Coupled system with completely redundant actuator inputs

Once again consider system model of subsection (4.5.1) with: state transition matrix $\mathbf{A} = \begin{bmatrix} 1.25 & 0 \\ 1 & 1.1 \end{bmatrix}$; and two dispersed actuators with $\mathbf{B}'_1 = \begin{bmatrix} 1 & 0 \\ 0 & 1 \end{bmatrix}$ and $\mathbf{B}'_2 = \begin{bmatrix} 1 & 0 \\ 1 & 1 \end{bmatrix}$ as their control matrix. It is easy to notice that both actuators are self-sufficient in controlling the system, and their critical reception probability can be individually computed as $\lambda_{c,1} = \lambda_{c,2} = 1 - 1/1.25^2 \approx 0.36$. Now, if the two actuators are jointly deployed to control the system, we expect a reduction in the individual critical probability.

Figure 4.4 shows stability region when control is performed when corresponding control actions are communicated to both the actuators. It can be observed that both lower and upper bound solutions coincide and critical probability of successful actuator input transmission is reduces to $\lambda_{c,1} = \lambda_{c,2} \approx 0.255$. Thus, at the cost of deploying two actuators for overlapping control actions, we can afford lower quality of underlying communication network.

4.5.3 Generalized system

Next consider a radial cyber physical system system controlled along overlapping actuators as shown in Figure 4.5. There are 8 nodes controlled by 3 overlapping actuator actions. We assume similar system model of subsection (4.5.1) with following state transition and control matrices.

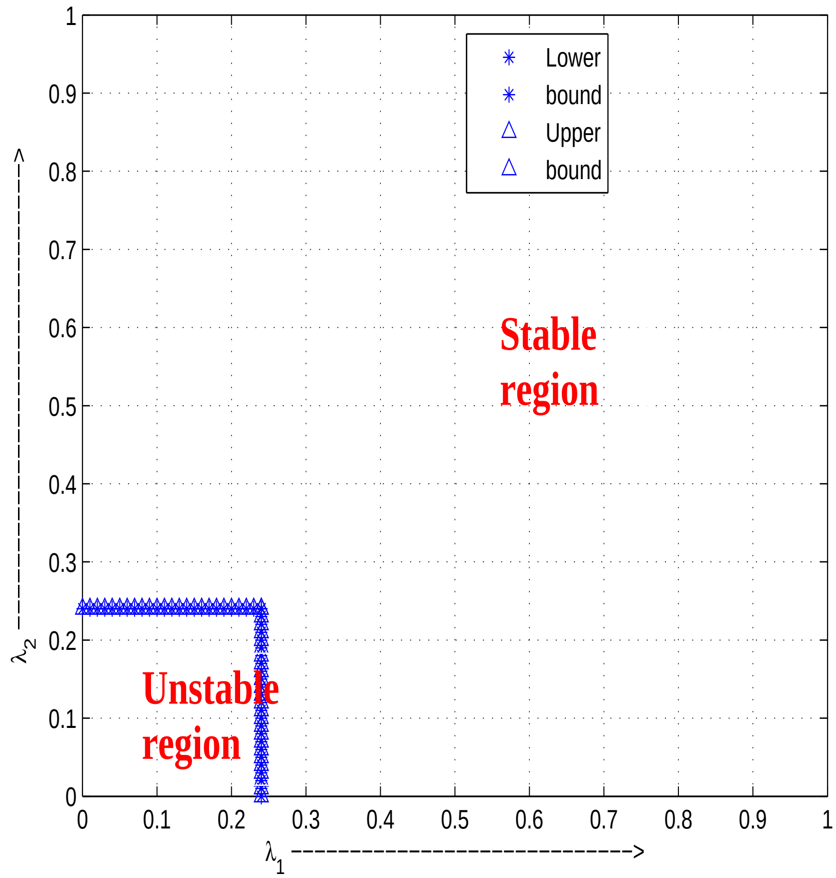

Figure 4.4: *Stability region - Completely redundant actuator inputs*

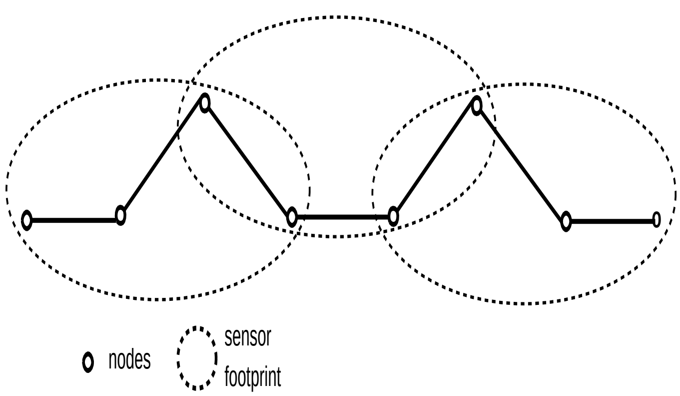

Figure 4.5: *Radial system with overlap in actuator control space*

$$\mathbf{A} = \begin{bmatrix} 1.15 & 0.2 & 0 & 0 & 0 & 0 & 0 & 0 \\ 0.2 & 0.3 & 0.3 & 0 & 0 & 0 & 0 & 0 \\ 0 & 0.3 & 0.5 & 0.2 & 0 & 0 & 0 & 0 \\ 0 & 0 & 0.2 & 1.1 & 0.3 & 0 & 0 & 0 \\ 0 & 0 & 0 & 0.3 & 0.2 & 0.4 & 0 & 0 \\ 0 & 0 & 0 & 0 & 0.4 & 0.4 & 0.3 & 0 \\ 0 & 0 & 0 & 0 & 0 & 0.3 & 0.5 & 0.3 \\ 0 & 0 & 0 & 0 & 0 & 0 & 0.3 & 1.11 \end{bmatrix}$$

$$\mathbf{B}_1' = \begin{bmatrix} 1 & 1 & 1 & 0 & 0 & 0 & 0 & 0 \\ 0 & 0 & 1 & 1 & 0 & 0 & 0 & 0 \end{bmatrix}$$
$$\mathbf{B}_2' = \begin{bmatrix} 0 & 0 & 1 & 1 & 0 & 0 & 0 & 0 \\ 0 & 0 & 0 & 0 & 1 & 1 & 0 & 0 \end{bmatrix}$$
$$\mathbf{B}_3' = \begin{bmatrix} 0 & 0 & 0 & 0 & 1 & 1 & 0 & 0 \\ 0 & 0 & 0 & 0 & 0 & 1 & 1 & 1 \end{bmatrix}$$

First considering unified control scenario, the lower bound on critical probability of successfully transmitting the control action is given by $\lambda_{s,lb}^c = (1 - 1/\rho^2) \approx 0.39$, where maximum eigen value of state transition matrix $\rho = 1.28$. Similarly, the upper bound on λ_s^c can be obtained by solving (4.24), and is computed as $\lambda_{s,ub}^c = 0.42$. The corresponding lower bound $\mathbf{P}_{lb}$ on converging $\mathbf{P}_t$ can be computed by iterating $\mathbf{P}_{t+1} = (1 - \lambda_{c,lb})\mathbf{A}'\mathbf{P}_t\mathbf{A}$ starting with some initial condition $\mathbf{P}_0$. Similarly, the upper bound $\mathbf{P}_{ub}$ for unified case can be computed by iterating the corresponding MARE for $\lambda_{c,ub}$ starting with some initial condition $\mathbf{X}_0$. Then, the bounds on critical probabilities for each actuator can be computed by iterating (4.28) and (4.32). Repeating above steps for $\lambda_{s,lb}^c > 0.39 \rightarrow 1$, and $\lambda_{s,ub}^c > 0.42 \rightarrow 1$ we can compute the trade off in stability with quality of underlying communication network. Figure 4.6 and 4.7, shows the lower and upper bound on critical probabilities for individual actuators vs converging Lyapunov function at steady state. Now, depending on the required stability of control operation, the corresponding requirement in quality of network infrastructure can be easily inferred from Figures 4.6 and 4.7. For example, if the demanded V_{ss} at steady state is 250, then for $\lambda_1 < 0.37$, $\lambda_2 < 0.37$, $\lambda_3 < 0.65$ system is definitely unstable, while for $\lambda_1 > 0.80$, $\lambda_2 > 0.75$, $\lambda_3 > 0.75$ is definitely stable. Thus, this analysis plays a crucial role in safe and efficient operation of cyber physical systems.

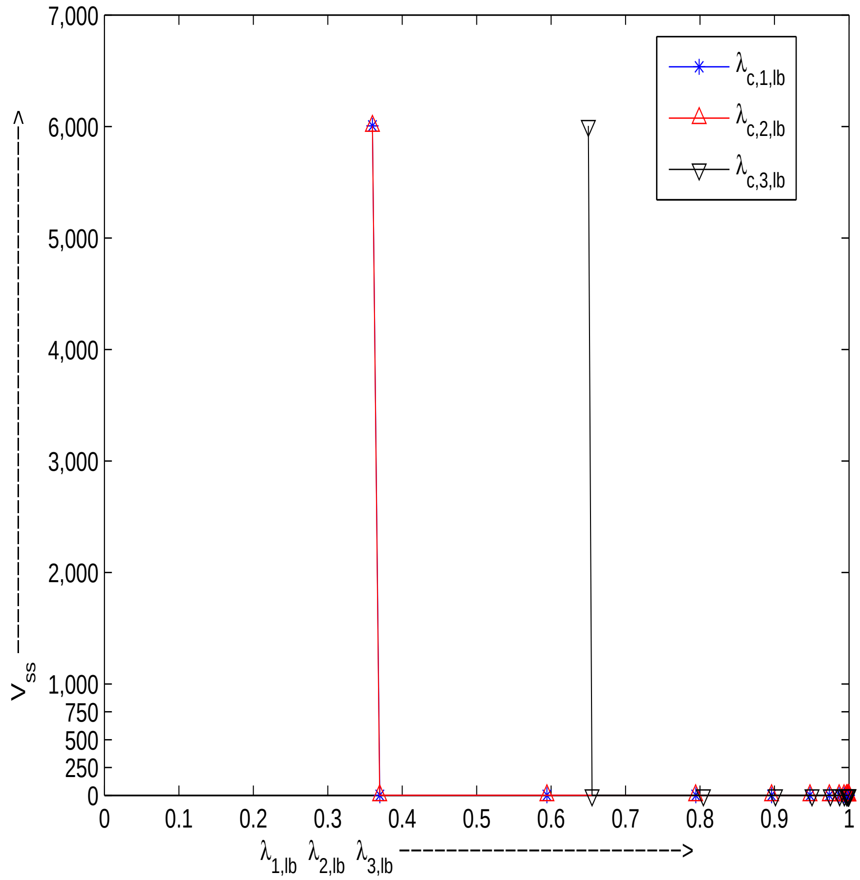

Figure 4.6: *Critical actuators receiving probability - lower bound*

4.6 Summary

In this chapter, we address the stochastic Lyapunov function based linear quadratic controller stability for spatially distributed cyber physical system in presence of random actuator action loss. The control action is computed at centralized control unit, encoded in packets and communicated to dispersed actuators over a lossy network. Since, random actuator action loss results in stochastic Lyapunov function iteration, we establish the lower and upper bounds on expected steady state Lyapunov function. We utilize the stability results of unified actuator scenario and compute upper and lower bounds on critical loss probability for individual actuators, by formulating optimization/feasibility problem. The

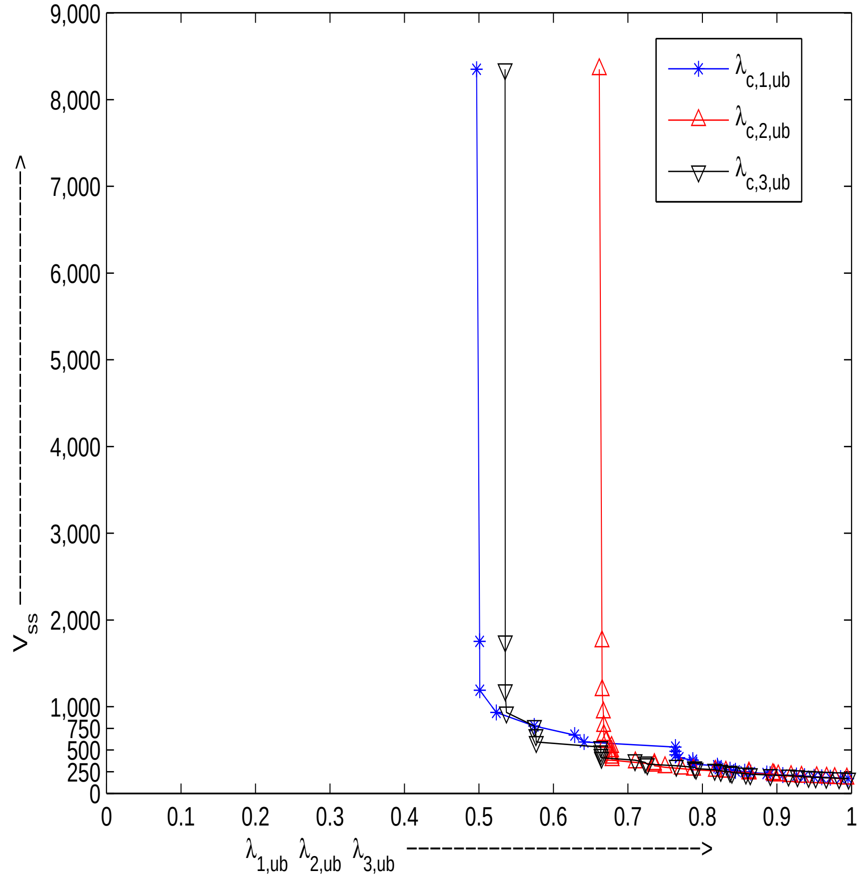

Figure 4.7: *Critical actuators receiving probability - upper bound*

feasibility solution distributes the control action loss of unified actuator scenario to loss in individual communication links of dispersed actuators.

Chapter 5

Case Study: Voltage/VAR Support Over Network In Smart Distribution Grid

In this chapter we present voltage/VAR support via distributed generation in smart distribution network as an example of spatially distributed CPS architecture. Reactive power injection in smart grid distribution networks via distributed generators is envisioned to play a vital role in voltage/VAR support. In this case study, we integrate the three aspects of voltage/VAR support: modeling, state estimation and network control in a single framework.

Firstly, we develop an input to state nonlinear dynamic model that incorporates power flow equations along with load and distributed generation (DG) forecasts. Then, considering an extended Kalman filter (EKF) approach for nonlinear state estimation, we analyze the impact of dropped packets on stability of estimation process. Finally, we apply separation principle locally around some known state estimates, to design a nonlinear model predictive control (NMPC) based voltage/VAR support strategy. The control problem aims to minimize the aggregate reactive power injected by DG with the following constraints: (1) voltage regulation; (2) phase imbalance correction, and (3) maximum and minimum reactive power injection by individual generators. Considering computational complexity incurred in search for the optimal solution for large scale nonlinear control problems, we propose a successive time varying linear (STVL) approximation to our voltage/VAR control problem. The control framework approach and the analytical results presented in this paper are validated by simulating a radial distribution network as an example.

5.1 Distributed Generation In Smart Distribution Grid: An Overview

Distributed generation (DG) is expected to play a vital role in future smart grid based power networks [88]. Integrating DG at the distribution network level is expected to increase power supply capacity within the existing infrastructure [88], [89]. However, inclusion of DG in distribution network negates the traditional approach of considering distribution network as passive. Addition of dynamic active components (DG) at distribution network level can destabilize the system in terms of: (1) power quality; (2) voltage regulation; (3) protection; (4) reliability, and safety issues [88]. Although, DG poses challenges for smart grid stability, some researchers [90], [91] have shown that reactive power contributed by DG can support voltage/VAR at distribution network level. Thus, a well controlled integrated operation of DGs with the grid is required for maintaining distribution network stability.

The first step in designing an efficient control for DG is to effectively model the impact of DG on dynamics of distribution network. Authors in [92] propose a zero point analysis method for analyzing the DG-feeder interaction. This approach focuses on discovering and mitigating the points at which DG unit output render zero power flow. Considering model based approach, statistical and deterministic models of of load and DG are respectively used in [93],[94] to analyze the impact of DG penetration on voltage regulation. Similarly, probabilistic approach in characterizing the impact of stochastic behavior of DG in voltage profiles is used in [95]. Addressing the huge dimensionality of distribution network, authors in [96] have used special techniques based on: (1) linearization; (2) state space representation; (3) coherency identification; (4) load and generator aggregation, for order reduction and aggregation of distribution network with DG. In spite of the plethora of efforts in DG integrated distribution network modeling, a comprehensive dynamic model relating voltage vector as states and DG as control inputs is currently lacking. A proper input to state dynamic model is an essential ingredient in designing a control problem.

The state of a power network is defined by phasor voltages observed at different nodes. These state estimates play a crucial role in computing optimal control actions which affects the overall grid performance [97],[98]. Traditionally, distribution networks were considered as static with marginal load variations.Hence, most of the state estimation techniques available in the literature are static, such as those based on weighted least squares [99]. However, with increase in underlying load fluctuations and the stochastic nature of DG, there is an increase in uncertainty of phasor voltage profile with time. Also, with the addition of communication and smart metering technologies as part of smart grid's infrastructure, state estimation is now feasible at all levels of the distribution network. Therefore, for real time efficient control of grid and DG, several dynamic state estimators like Kalman filter in [100] and unscented Kalman filter in [101] have been proposed. Further, considering complexity associated with large scale estimation problem, approaches like network reduction and domain decomposition have been respectively proposed in [102], [103] for distribution network. Unfortunately, most of these prior efforts do not analyze stochastic stability of their state estimate considering uncertainty associated with both load and generation. Additionally, estimation is dependent on measurements that are typically transmitted through a communication network. Therefore, it is critical to quantify the effect of packet delay, packet drops etc. on the quality and stability of state estimate. This paper aims to bridge this gap.

Finally, many research work [91]-[104] have demonstrated that, reactive power injected by DG can be used for voltage/VAR support of distribution networks. The primary focus is on two aspects of DG's contribution to voltage control: (1) effective interfacing of DG at point of coupling (PCC) [105],[106], and (2) managing and optimizing multiple DG reactive power contribution [107],[108]. [109] investigates, both coordinated and uncoordinated voltage control with DG involvement. In uncoordinated control reactive power interface operates locally; while in the coordinated control, reactive power interface is controlled considering its effect on whole distribution network. The results indicates superiority of coordinated control over uncoordinated control in reducing voltage fluctuations and system losses. Authors in [110],[104] have presented a real time control framework for controlling the end-user reactive power devices to mitigate low voltage problems. However, most of the prior efforts related to voltage/VAR control are typically single shot strategies that ignore some basic economic assurances/policies regarding DG reactive power injection. DG at distribution network are owned by customers who are only paid for real power. Additionally, distributed generators have limits on maximum and minimum reactive power injection based on power electronic interface used. In our publication [111], we have illustrated the feasibility of reactive power injection from DGs for voltage/VAR support. That is, at each time instant t, using the approach in [111], we can identify the most appropriate injected real power Pg and reactive power Qg for each DG.

Thus encouraged by importance of integrating DG and optimally utilizing the reactive power injection, we present an voltage/VAR support via DG in CPS architecture setup.

5.2 Cybyer Physical Framework: Voltage/VAR support via Distributed Generation

In this section we present voltage/VAR support via DG in CPS framework. A conceptual description of framework is presented in figure 5.1. Following are the key features of this framework:

- Voltage/VAR support via DG is related by a nonlinear power flow equations. Also load fluctuations are time varying and distributed generation is stochastic process. Thus, input (reactive power injection) to state (voltage phasors) system model in smart distribution network is a nonlinear stochastic system model.

- Considering nonlinear, time varying and stochastic system model, a nonlinear state estimation approach is required for smart distribution network. Next considering esti-

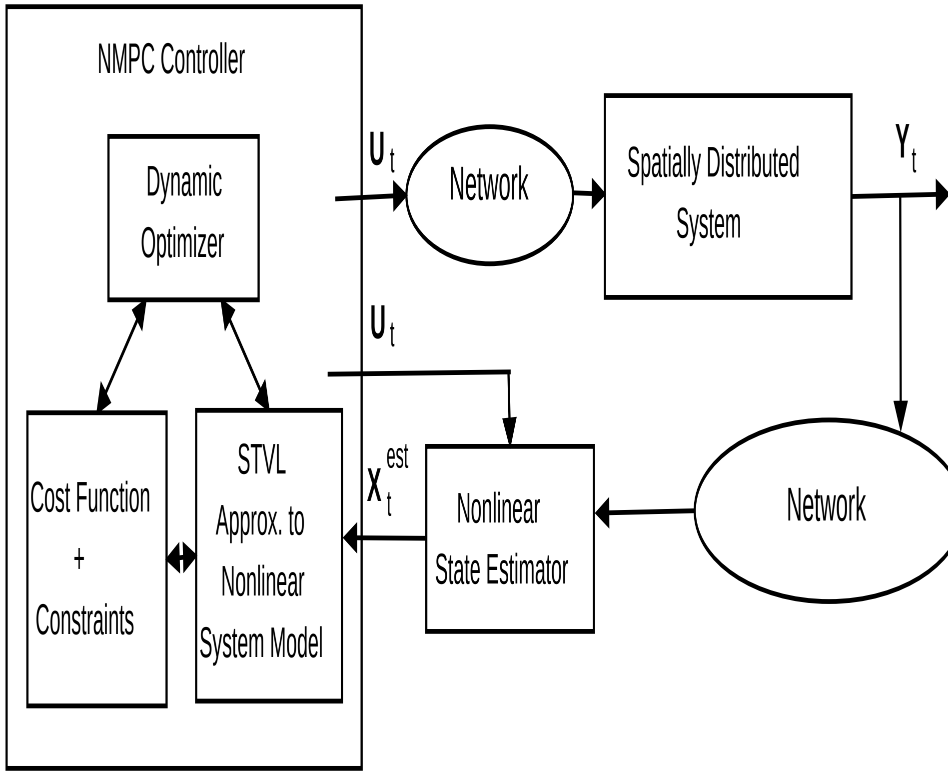

Figure 5.1: *Nonlinear Control framework for DG integrated at Distribution network level*

mation stability, conditions on system parameters and communication infrastructure (for communicating measurements) needs to be quantified.

- Finally, as reactive power injection has a natural trade-off relative to real power injection by DGs, it is crucial to optimally use the reactive power of DGs. Furthermore, the reactive power injection computation needs to be predictive, based on dynamics of the system.

In next section, we preset the system model followed by estimation and control solution for considered smart distribution network scenario.

5.3 Smart Distribution Grid: Dynamic System Model

For simplicity in modeling and analysis in this case study, we only consider randomness caused by load and distributed generation in the power dynamics. In [112],[113], it is shown that the load and DG can be modeled via statistical models. Following this, we assume that real and reactive load, and power generated by DGs are modeled by first order auto-regressive process. To extend the generality of the AR(1) model, we allow for coefficients to vary with time. The time series representation for real load (Pl), reactive load (Ql) and apparent power of DG (Sg) can be expressed as

$$Z_{t+1} - D^Z_{t+1} = \alpha^Z_t (Z_t - D^Z_t) + W^Z_t, \tag{5.1}$$

where, $Z \in \{Pl, Ql, Sg\}$, i.e., Z is common notation for Pl, Ql and Sg; $\alpha^{(\cdot)}_{(\cdot)}$ is the corresponding AR(1) coefficient; $D^{(\cdot)}_{(\cdot)}$ is the corresponding deterministic component; $W^{(\cdot)}_{(\cdot)}$ is the corresponding noise component of the time series model; and t is time index. Furthermore, a time series model similar to (5.1) can be developed to capture the DG contribution. In following analysis, we use above statistical models to derive time dependent dynamic of power distribution system.

The power flowing at every observed node in the network is a linear combination of real and reactive component of load and generated power. Hence, the net real and reactive power entering or leaving can be expressed via an AR(1) model. Let Pg_t and Pl_t represent net real power generation and load on the node. Then, the net real power P_t injected at $t+1$ can be expressed as

$$\begin{aligned} P_{t+1} &= Pg_{t+1} - Pl_{t+1} \\ &= \alpha^{Pl}_t P_t + \beta^P_t Pg_t + L^P_t + W^P_t. \end{aligned} \tag{5.2}$$

where, $\beta^P_t = \alpha^{Pg}_t - \alpha^{Pl}_t$; $L^P_t = \alpha^{Pl}_t (D^{Pg}_t - D^{Pl}_t) + (\alpha^{Pg}_t - \alpha^{Pl}_t) D^{Pg}_t + D^{Pg}_{t+1} - D^{Pl}_{t+1}$; and $W^P_t = W^{Pg}_t - W^{Pl}_t$. Similarly, net reactive power flowing through a node can be expressed as

$$Q_{t+1} = \alpha^{Ql}_t Q_t + \beta^Q_t Qg_t + L^Q_t + W^Q_t. \tag{5.3}$$

It can be noticed that in our modeling we are assuming generation capability at every node. However, in practice generation capability may be limited to very few nodes. For those nodes our model is still applicable with $Sg_t = 0$. Consider now a three phase distribution network, with state defined by a vector of phasor voltages at observable nodes. Let $V_t^{abc} := [V_t^a(i), V_t^b(i), V_t^c(i)]^T$, $\theta_t^{abc} := [\theta_t^a(i), \theta_t^b(i), \theta_t^c(i)]^T$ denote the three phase voltage vector magnitude and phase at node i, with a, b, c representing the corresponding phases; then the three phase power flow equations for real and reactive power defined by , $P_t^{abc} := [P_t^a(i), P_t^b(i), P_t^c(i)]^T$ and $Q_t^{abc} := [Q_t^a(i), Q_t^b(i), Q_t^c(i)]^T$, at node i can be expressed as

$$\begin{aligned} P_t^{abc}(i) &= V_t^{abc}(i) \odot \textstyle\sum_{k=0}^{n} V_t^{abc}(k) \odot \big(G^{abc}(i,k) cos(\theta_t^{abc}(i,k)) \\ &\quad + B^{abc}(i,k) sin(\theta_t^{abc}(i,k))\big) \\ Q_t^{abc}(i) &= V_t^{abc}(i) \odot \textstyle\sum_{k=0}^{n} V_t^{abc}(k) \odot \big(G^{abc}(i,k) sin(\theta_t^{abc}(i,k)) \\ &\quad - B^{abc}(i,k) cos(\theta_t^{abc}(i,k))\big)\,, \end{aligned} \tag{5.4}$$

where, $\theta_t^{abc}(i,k) := \theta_t^{abc}(i) - \theta_t^{abc}(k)$; $G^{abc}(i,k)$ and $B^{abc}(i,k)$ are three phase conductance and susceptance matrices between node i and k, respectively; The detailed analysis and derivation of (5.4) is investigated in our publication [111]. Defining state vector $\mathbf{X}_t := [V_t^{abc}(1), \theta_t^{abc}(1) \cdots V_t^{abc}(n), \theta_t^{abc}(n)]^T$, and $\mathbf{F}(\mathbf{X}_t) := [P_t^{abc}(1), \cdots, P_t^{abc}(n), Q_t^{abc}(1), \cdots, Q_t^{abc}(n)]^T$, the nonlinear dynamic state model can be stated as

$$\mathbf{F}(\mathbf{X}_{t+1}) = \mathbf{A}_t^F \mathbf{F}(\mathbf{X}_t) + \mathbf{B}_t^F \mathbf{U}_t + \mathbf{L}_t^F + \mathbf{W}_t^F, \tag{5.5}$$

where,

$$\mathbf{A}_t^F := diag(\alpha_t^{Pl}(1), \cdots, \alpha_t^{Pl}(n), \alpha_t^{Ql}(1), \cdots, \alpha_t^{Ql}(n)),$$

$$\begin{aligned} \mathbf{B}_t^F &:= diag(\beta_t^P(1), \cdots, \beta_t^P(n), \beta_t^Q(1), \cdots, \beta_t^Q(n)), \\ \mathbf{U}_t &:= [Pg_t(1), \cdots, Pg_t(n), Qg_t(1), \cdots, Qg_t(n)]^T, \\ \mathbf{L}_t^F &:= [L_t^P(1), \cdots, L_t^P(n), L_t^Q(1), \cdots, L_t^Q(n)]^T, \\ \mathbf{W}_t^F &:= [W_t^P(1), \cdots, W_t^P(n), W_t^Q(1), \cdots, W_t^Q(n)]^T, \end{aligned}$$

and n represents the total number of observed nodes. We assume that $\mathbf{W}_t^F$ is i.i.d. noise with $\mathbf{Q}$ as covariance matrix. It can be observed that the dynamic model (5.5) can be controlled by control input $\mathbf{U}_t$, the real and reactive power injected by DG. However, the design of the control input $\mathbf{U}_t$ is dependent on the knowledge of the state $\mathbf{X}_t$ of the system.

5.4 Nonlinear State Estimation

State estimation in nonlinear dynamical system has been well studied and many methods have been proposed over last two decades. For our system, we propose the use of Extended Kalman filter (EKF) for state estimation for the following reasons: (1) Estimators based on Monte Carlo approaches like Unscented Kalman filter and Particle filter are computationally inefficient for large networks; (2) The nonlinear state model expressed in (5.5) is not one-to-one mapped, i.e., it is possible to have more than one voltage distribution corresponding to a give power distribution. Therefore, propagating the sigma points of $\mathbf{X}_t$ may result in more than one distribution of $\mathbf{X}_{t+1}$.

5.4.1 EKF based estimation

EKF is a minimum mean square error (MMSE) estimator based on first order Taylors series expansion of the nonlinear state evolution model. Linearizing (5.5) results in

$$\bar{\mathbf{F}}_{t+1} + \mathbf{J}^{\mathbf{F}}_{t+1}(\mathbf{X}_{t+1} - \bar{\mathbf{X}}_{t+1}) = \mathbf{A}^{\mathbf{F}}_t(\bar{\mathbf{F}}_t + \mathbf{J}^{\mathbf{F}}_t(\mathbf{X}_t - \bar{\mathbf{X}}_t)) + \mathbf{B}^{F}_t\mathbf{U}_t + \mathbf{L}^{\mathbf{F}}_t + \mathbf{W}^{\mathbf{F}}_t \tag{5.6}$$

where, $\bar{\mathbf{X}}_t$ is a linearization point at some t; $\bar{\mathbf{F}}_t$ is real and reactive power at time t evaluated by $\bar{\mathbf{F}}_t = \mathbf{F}(\bar{\mathbf{X}}_t)$; $\mathbf{J}^{\mathbf{F}}_{t+1}$ is the Jacobian of $\mathbf{F}(\mathbf{X}_t)$ evaluated at $\bar{\mathbf{X}}_t$. It can be observed that equation (5.6) requires knowledge of linearization points $\bar{\mathbf{X}}$ at t and $t+1$. Since power distribution at these observable nodes are known at t and can be obtained for $t+1$ by time series forecasts, the linearization points can be obtained by solving power flow equation. Linearization represents a local characterization of the nonlinear function. Selection of linearization points close to true state values is expected to reduce linearization error. In our analysis, we use Newton's algorithm to search linearization points $\bar{\mathbf{X}}_t$ and $\bar{\mathbf{X}}_{t+1}$ in the neighborhood of known state $\mathbf{X}_t$ at time t. After obtaining the linearization points, the linearized time varying state model can be expressed as

$$\mathbf{X}_{t+1} = \mathbf{A}_t\mathbf{X}_t + \mathbf{L}_t + \mathbf{W}_t, \tag{5.7}$$

where,

$$\begin{aligned} \mathbf{A}_t &= \mathbb{J}^{\mathbf{F}}{}_{t+1}\mathbf{A}_t^{\mathbf{F}}\mathbf{J}_t^{\mathbf{F}} \\ \mathbf{L}_t &= \bar{\mathbf{X}}_{\mathbf{t+1}} - \mathbb{J}^{\mathbf{F}}{}_{t+1}\mathbf{A}_t^{\mathbf{F}}\mathbf{J}_t^{\mathbf{F}}\bar{\mathbf{X}}_{\mathbf{t}} - \mathbb{J}^{\mathbf{F}}{}_{t+1}(\bar{\mathbf{F}}_{t+1} - \mathbf{A}_t^{\mathbf{F}}\bar{\mathbf{F}}_t) + \mathbb{J}^{\mathbf{F}}{}_{t+1}(\mathbf{L}_t^{\mathbf{F}} + \mathbf{B}_t^{F}\mathbf{U}_t) \\ \mathbf{W}_t &= \mathbb{J}^{\mathbf{F}}{}_{t+1}\mathbf{W}_t^{\mathbf{F}} \ \& \ \mathbb{J}^{\mathbf{F}} := (\mathbf{J}^{\mathbf{F}})^{-1} \end{aligned} \tag{5.8}$$

Typically, state is estimated based on measurements across the power network. The measurements in the power network are either direct measurements like voltage at the node or current flowing between adjacent nodes, or indirect measurements like real and reactive power flowing through the network. A general measurement model corresponds to $\mathbf{Y}_t := \mathbf{G}(\mathbf{X}_t) + \mathbf{W}_t^Y$, where, $\mathbf{Y}_t$ is the measurement vector; $\mathbf{G}(\mathbf{X}_t) = [g_1(\mathbf{X}_t), \cdots, g_m(\mathbf{X}_t)]^T$, with $g_j(\cdot)$ representing the local measurement at node j which can be a linear or nonlinear function of some elements of $\mathbf{X}$; $\mathbf{W}_t^Y := [W_t^Y(1), \cdots, W_t^Y(m)]^T$ is the process noise.

5.4.2 Intermittent measurement model

The measurements in a smart grid network are typically transmitted over a communication network to a local fusion center or a back office controller where state estimation is performed. In this process of communication, it is possible that the measurement data packets may get delayed, reordered or even dropped. In this subsection, we accommodate the impact of dropped packets on EKF based state estimate. Towards this end we assume that the dropped packets are modeled as independent and identically distributed, i.i.d. Bernoulli random process. The measurement vector $\mathbf{Y}_t$ for intermittent measurements, is expressed as

$$\mathbf{Y}_t = \mathbf{\Gamma}_t(\mathbf{G}(\mathbf{X}_t) + \mathbf{W}_t^Y) \tag{5.9}$$

where, $\mathbf{\Gamma}_t := diag(\gamma_t(1), \cdots, \gamma_t(m))$, γ_t is a binary matrix; $\gamma_t(j)$ is a Bernoulli random variable with $Pr(\gamma_t(j) = 1) = \lambda_t(j)$. The measurement noise in our analysis is assumed to be i.i.d. with $\mathbf{R}$ as covariance matrix. Denoting, $\hat{\mathbf{Y}}(t) = \boldsymbol{\Gamma}_t\mathbf{G}(\mathbf{X}_{t/t-1})$ where, $\hat{\mathbf{Y}}$ is the predicted measurement; $\mathbf{X}_{t/t-1}$ is the predicted state at time t; $\mathbf{H}_t := [\frac{\partial \mathbf{G}}{\partial \mathbf{X}}_t]$, and $\mathbb{H}_t := \boldsymbol{\Gamma}_t\mathbf{H}_t$, Kalman filter equations for localized linear state estimation are stated as

Prediction Cycle

$$\mathbf{X}_{t+1/t} = \mathbf{A}_t\mathbf{X}_{t/t} + \mathbf{L}_t; \quad \mathbf{P}_{t+1/t} = \mathbf{A}_t\mathbf{P}_{t/t}\mathbf{A}_t^T + \mathbb{Q}_t \tag{5.10}$$

where, $\mathbf{X}_{t/t-1}$ and $\mathbf{X}_{t/t}$ are the predicted and estimated state vectors; similarly $\mathbf{P}_{t/t-1}$ and $\mathbf{P}_{t/t}$ are the predicted and estimated error covariance matrix for linearized model; and $\mathbb{Q}_t = (\mathbb{J}^{\mathbf{F}}{}_{t+1})^T\mathbf{Q}\mathbb{J}^{\mathbf{F}}{}_{t+1}$ is the covariance of process noise.

Filtering Cycle

$$\begin{aligned}
\mathbf{K}_{t+1} &= \mathbf{P}_{t+1/t}\mathbb{H}_{t+1}^T[\mathbb{H}_{t+1}\mathbf{P}_{t+1/t}\mathbb{H}_{t+1}^T + \mathbf{R}]^{-1} \\
\mathbf{P}_{t+1} &= [\mathbf{I}_n - \mathbf{K}_{t+1}\mathbb{H}_{t+1}]\mathbf{P}_{t+1/t} \\
\mathbf{X}_{t+1}^{est} &= \mathbf{X}_{t+1/t} + \mathbf{K}_{t+1}[\mathbf{Y}_{t+1} - \hat{\mathbf{Y}}_{t+1}]
\end{aligned} \tag{5.11}$$

where, $\mathbf{K}_t$ is Kalman gain and $\mathbf{I}_n$ is nxn identity matrix. In following section, we analyze the stochastic stability of our state estimate considering randomness due to model mismatch, linearization error and intermittent measurements.

5.5 Stochastic Stability Analysis of State Estimate

The nonlinear state estimate defined in (5.10),(5.11) can be considered as stable, if the estimation error covariance matrix remain bounded over time. The conditions for stochastic stability of discrete time EKF has been investigated in [114],[115]. It is shown that under small noise covariance and initial estimation error, and with certain system regulation, stochastic stability of EKF with intermittent measurements can be achieved. In our analysis, we follow similar arguments and establish conditions for stochastic boundedness of the estimation error and error covariance matrix for our system.

Firstly, it should be noted that matrices $\mathbf{P}_{t+1/t}$ and $\mathbf{P}_{t/t}$ (5.10,5.11) represents the error covariance matrices for the linearized model, and hence are not equal to error covariance matrices for true nonlinear state evolution model represented by (5.5). So, we first quantify deviation between the estimated state $\mathbf{X}_{t/t}$ obtained from the linearized model and the true state $\mathbf{X}_t$ of the nonlinear system. For this, consider a hypothetical function $\mathbb{F}(\cdot)$, which performs inverse mapping from $\mathbf{F}(\mathbf{X}_t)$ to $\mathbf{X}_t$, i.e. $\mathbb{F}(\mathbf{F}(\mathbf{X}_t)) := \mathbf{X}_t$. Using the Taylors expansion, we establish

$$\begin{aligned}
\mathbf{X}_{t+1} &= \mathbb{F}(\mathbf{A}_t^F \mathbf{F}(\mathbf{X}_{t/t}) + \mathbf{D}_{t+1}^F - \mathbf{A}_t^F \mathbf{D}_t^F) + \mathbf{A}_t(\mathbf{X}_t - \mathbf{X}_{t/t}) + \mathbb{J}^{\mathbf{F}}{}_{t+1}\mathbf{W}_t^{\mathbf{F}} \\
&\quad + \phi(\mathbf{X}_t, \mathbf{X}_{t/t}, \mathbf{W}_t^{\mathbf{F}}) \\
\mathbf{X}_{t+1/t} &= \mathbb{F}(\mathbf{A}_t^F \mathbf{F}(\mathbf{X}_{t/t}) + \mathbf{D}_{t+1}^F - \mathbf{A}_t^F \mathbf{D}_t^F) - \psi(\mathbf{X}_t, \mathbf{X}_{t/t}, \mathbf{W}_t^{\mathbf{F}}) \\
\mathbf{Y}_t &= \mathbf{G}(\mathbf{X}_t) + \mathbf{W}_t^Y \\
&= \mathbf{G}(\mathbf{X}_{t/t-1}) + \mathbf{W}_t^Y + \mathbf{H}_t(\mathbf{X}_t - \mathbf{X}_{t/t}) + \chi(\mathbf{X}_t, \mathbf{X}_{t/t-1})
\end{aligned} \tag{5.12}$$

where, $\mathbf{X}_t$ is the true state vector, and functions $\phi(\cdot), \psi(\cdot), \chi(\cdot)$ represent the remainder terms corresponding to linearization error. Defining the estimation errors as $e_{t+1/t} = \mathbf{X}_{t+1} - \mathbf{X}_{t+1/t}$, $e_{t+1/t+1} = \mathbf{X}_{t+1} - \mathbf{X}_{t+1/t+1}$, and using (5.12) we derive

$$\begin{aligned}
e_{t/t} &= (\mathbf{I}_n - \mathbf{K}_t \mathbb{H}_t) e_{t/t-1} - \mathbf{K}_t \left(\mathbf{W}_t^Y + \chi(\mathbf{X}_t, \mathbf{X}_{t/t-1}) \right) \\
e_{t+1/t} &= \mathbf{A}_t (\mathbf{I}_n - \mathbf{K}_t \mathbb{H}_t) e_{t/t-1} + \mathbf{r}_t + \mathbf{s}_t
\end{aligned} \tag{5.13}$$

where,

$$\begin{aligned}
\mathbf{r}_t &= \phi(\mathbf{X}_t, \mathbf{X}_{t/t}, \mathbf{W}_t^{\mathbf{F}}) + \psi(\mathbf{X}_t, \mathbf{X}_{t/t}, \mathbf{W}_t^{\mathbf{F}}) - \mathbf{A}_t \mathbf{K}_t \chi(\mathbf{X}_t, \mathbf{X}_{t/t-1}) \\
\mathbf{s}_t &= \mathbb{J}^{\mathbf{F}}{}_{t+1} \mathbf{W}_t^{\mathbf{F}} - \mathbf{A}_t \mathbf{K}_t \mathbf{W}_t^Y
\end{aligned} \tag{5.14}$$

For our state estimate to be stable, the estimation error $e_{t/t-1} \leq e_{t/t}$ and $e_{t/t}$ must be bounded.

5.5.1 Boundedness of estimation error

Theorem 5.1. *The estimation error $e_{t+1/t}$ is exponentially bounded in mean square, (i.e. $\mathbb{E}[||e_{t+1/t}||_2^2] \leq \kappa$, where $\mathbb{E}[\cdot]$ is expectation operation, $||\cdot||$ is euclidean norm of vector, and κ is a positive constant) under following system regulations:*

1. *$||\mathbf{A}_t|| \leq \bar{a}$: bounded state transition matrix.*

2. *$||\mathbf{H}_t|| \leq \bar{h}$: bounded Jacobian of measurement matrix.*

3. *$||\mathbb{J}^{\mathbf{F}}{}_{t+1}|| \leq \bar{j}$: bounded Jacobian of dynamic model.*

4. $\underline{p}\mathbf{I}_n \le \mathbf{P}_{t+1/t+1} \le \mathbf{P}_{t+1/t} \le \bar{p}\mathbf{I}_n$: *bounded error covariance.*

5. $\underline{q}\mathbf{I}_n \le \mathbf{Q} \le \bar{q}\mathbf{I}_n$: *bounded model mismatch.*

6. $\underline{r}\mathbf{I}_n \le \mathbf{R} \le \bar{r}\mathbf{I}_n$: *bounded measurement noise.*

7. $||\phi(\mathbf{X}_t, \mathbf{X}_{t/t}, \mathbf{W}_t^{\mathbf{F}})||_2 \le \epsilon_\phi ||\mathbf{X}_t - \mathbf{X}_{t/t}||_2^2$: *bounded model linearization error.*

8. $||\psi(\mathbf{X}_t, \mathbf{X}_{t/t}, \mathbf{W}_t^{\mathbf{F}})||_2 \le \epsilon_\psi ||\mathbf{X}_t - \mathbf{X}_{t/t}||_2^2$: *bounded linearization error for prediction.*

9. $||\chi(\mathbf{X}_t, \mathbf{X}_{t/t-1})||_2 \le \epsilon_\chi ||\mathbf{X}_t - \mathbf{X}_{t/t-1}||_2^2$: *bounded linearization error for measurements.*

where, $\bar{a}, \bar{h}, \bar{j}, \underline{p}, \bar{p}, \underline{q}, \bar{q}, \underline{r}, \bar{r}, \epsilon_\phi, \epsilon_\psi, \epsilon_\chi > 0$;

Proof. The proof follows similar to [115] section III. □

Condition (1) and (3) can be established for our power network if: (1) $\underline{j} \le ||\mathbf{J^F}_t|| \le \bar{j}$, i.e. Jacobian must be nonsingular and bounded for all t. Since Jacobian for our system is rate at which power flow changes with change in voltage, the only instants it can be unbounded is under some abnormalities like short circuit. So in normal operating conditions Jacobian is always bounded; (2) $\underline{a}_l \le ||\mathbf{A}_t^F|| \le \bar{a}_l$, since $\mathbf{A}_t^F$ is matrix of load AR(1) coefficients so it is always bounded. Thus regulations of Theorem 1 can be satisfied for our system under normal operating conditions.

However, our measurement model is probabilistic and if $Pr(\gamma_t(i) \ne 1), i \in \{1, \cdots m\}$ for some large number of t or i, the system may become unobservable. Thus, we need to establish network conditions on packet drop rate for boundedness of $\mathbf{P}_{t+1/t+1}$ and $\mathbf{P}_{t+1/t}$.

5.5.2 Boundedness of the error covariance matrix

The algebraic Riccati update equation for error covariance matrix of linearized model $\mathbf{P}_{t+1/t}$ is given by

$$\mathbf{P}_{t+1/t} = \mathbf{A}_t\mathbf{P}_{t/t-1}\mathbf{A}_t + \mathbf{Q}_t - \mathbf{A}_t\mathbf{P}_{t/t-1}\mathbb{H}_t^T(\mathbb{H}_t\mathbf{P}_{t/t-1}\mathbb{H}_t^T + \mathbf{R}_t)^{-1}\mathbb{H}_t\mathbf{P}_{t/t-1}\mathbf{A}_t \tag{5.15}$$

Since $\mathbf{A}_t$, $\mathbf{H}_t$ are time varying, it is difficult to give general conditions on uniform boundedness of error covariance $\mathbf{P}_{t+1/t}$. Authors in [114] have studied this problem, with the condition that all measurements are received from single source. The analysis shows existence of critical packet drop rate for boundedness of error covariance matrix $\mathbf{P}_{t+1/t}$. For our system, we simplify the analysis by making following assumptions,

Assumption 5.1. *Packet drop rate for all sensors are assumed to be i.i.d. with parameter λ. Thus $Pr(\gamma_t(1) = 1) = \cdots = Pr(\gamma_t(m) = 1) = \lambda$. So the number of received measurements denoted by $\mathbb{M}_t$ at time t is a Binomial distribution. Further we assume for satisfying the observability condition, we require at least k measurements at every sampling instant t. This requirement puts condition that $\mathbb{M}_t \geq k$, or over time $\mathbb{E}[\mathbb{M}_t] = \lambda m \geq k$.*

Assumption 5.2. *The final assumption we make is that if we have less than k measurements at any sampling instant then the effect of measurement on Riccati update equation (5.15) is negligible. Thus error covariance matrix update with less then k measurements is approximated as, $\mathbf{P}_{t+1/t} = \mathbf{A}_t \mathbf{P}_{t/t-1} \mathbf{A}_t + \mathbf{Q}_t$.*

It can be observed that, with *Assumptions*(5.1,5.2), we are approximating our measurement model behavior with model in [114]. The probability Λ that error covariance matrix will get updated with measurements is given by

$$\Lambda = \sum_{j=\lceil \lambda m \rceil}^{m} \binom{m}{j} \lambda^j (1-\lambda)^{m-j} \tag{5.16}$$

The analysis in [114] has found analytical expressions for lower and upper bound on critical packet drop rate. In our analysis, we only concentrate on lower bound expressed as, $\Lambda_c \geq 1 - 1/\rho(\mathbf{A}_t)^2, \forall t$, where $\rho(\mathbf{A}_t)$ is the spectral radius of the linearized state evolution matrix $(\mathbf{A}_t)$.

Thus, if λ_c is the critical packet drop rate then

$$\sum_{j=\lceil \lambda_c m \rceil}^{m} \binom{m}{j} \lambda_c^j (1-\lambda_c)^{m-j} \geq 1 - 1/\rho(\mathbf{A}_t)^2 \tag{5.17}$$

Lemma 5.1. *Under the condition that Jacobian $\mathbf{J}_t^{\mathbf{F}}$ is perturbed minimally at every time step, the packet drop rate can be bounded as*

$$\sum_{j=\lceil \lambda_c m \rceil}^{m} \binom{m}{j} \lambda_c^j (1-\lambda_c)^{m-j} \geq 1 - 1/\bar{\alpha}^{Pl} \tag{5.18}$$

where, $\bar{\alpha}^{Pl}$ is largest AR(1) load coefficient.

Proof. Let ϵ_j be the maximum perturbation for the Jacobian $\mathbf{J}_t^{\mathbf{F}}$ as the system evolves in time, then $\mathbf{J}_t^{\mathbf{F}} = \mathbf{J}_{t+1}^{\mathbf{F}} + \epsilon_j \mathbf{I}_n$. Spectral radius of the linearized state evolution matrix is expressed as

$$\begin{aligned}
\rho(\mathbf{A}_t) &= \rho(\mathbb{J}^{\mathbf{F}}{}_{t+1} \mathbf{A}_t^{\mathbf{F}} \mathbf{J}_t^{\mathbf{F}}) \\
&\leq \rho(\mathbb{J}^{\mathbf{F}}{}_{t+1} \mathbf{A}_t^{\mathbf{F}} \mathbf{J}_{t+1}^{\mathbf{F}}) + \rho(\mathbb{J}^{\mathbf{F}}{}_{t+1} \mathbf{A}_t^{\mathbf{F}} \epsilon_j \mathbf{I}_n))) \\
&\leq \rho(\mathbf{A}_t^{\mathbf{F}}) + \epsilon_j \rho(\mathbb{J}^{\mathbf{F}}{}_{t+1} \mathbf{A}_t^{\mathbf{F}})
\end{aligned}$$

For $\epsilon_j \approx 0$, $\rho(\mathbf{A}_t) \approx \rho(\mathbf{A}_t^{\mathbf{F}})$. Since $\mathbf{A}_t^{\mathbf{F}}$ is a diagonal matrix of load AR(1) coefficients, $\rho(\mathbf{A}_t) \approx \bar{\alpha}^{Pl}$. □

In next section, we formulate a nonlinear control problem to determine the injected DG reactive power for voltage/VAR support at distribution network level.

5.6 Nonlinear Voltage/VAR control

In this section, we formulate a nonlinear control problem to determine the optimal reactive power injection by DG in order to satisfy the following requirements: (1) voltage is maintained within safety limits; (2) phase imbalance is mitigated, and (3) individual distributed generator minimum/maximum reactive power constraints are met. For simplicity in this work, we assume a quadratic penalty function, i.e., $\phi(Qg_t^x(i)) = (Qg_t^x(i))^2$ as the objective to minimize. Further, for phase imbalance correction, we limit the phase difference between any two phases to $\frac{2\pi\epsilon}{3}$radians, where $0 < \epsilon < 1$ is the tolerance of phase imbalance. From a control perspective, the first two constraints are the state constraints and the final constraint is on the control input. The nonlinear control optimization problem can be expressed as

$$\begin{aligned} \min. \quad & \sum_i^n \sum_{x \in \{a,b,c\}} \alpha_t^x(i)(Qg_t^x(i))^2 \ \forall i = 1...n, \\ \text{subject to} \quad & \begin{cases} C_1: \ \mathbf{F}(\mathbf{X}_{t+1}) = \mathbf{A}_t^F \mathbf{F}(\mathbf{X}_t) + \mathbf{B}_t^F \mathbf{U}_t + \mathbf{L}_t^F, \\ C_2: \ (Sg_t^x(i))^2 = (Pg_t^x(i))^2 + (Qg_t^x(i))^2, \\ C_3: \ (Qg^x(i))_{min} \leq Qg_t^x(i) \leq (Qg^x(i))_{max}, \\ C_4: \ 0.95 \leq V_t^x(i) \leq 1.05, \\ C_5: \ |\theta_t^x(i) - \theta_t^y(i)| > 2\pi/3 * \epsilon, \\ \ \forall i = 0...n, \ x, y \in \{a,b,c\}, \ \& \ 0 < \epsilon < 1. \end{cases} \end{aligned} \tag{5.19}$$

In (5.19), the objective function $\alpha_t^x(i)$ are the regressors indicating preference of generators in reactive power contribution; equality constraints, C_1 represent the dynamics of distribution network (5.5); C_2 is the limit on net power generation capacity of individual generators obtained from the time series; C_3 captures the limits on maximum and minimum reactive power injected by individual distributed generators; C_4 represents 5% voltage regulation, and C_5 represents tolerance on phase imbalance. It needs to be noticed that (5.19) is a one step optimization problem. The obtained solution does not consider impact of reactive power injection on future dynamics of distribution network. In the following subsection, we extend the control problem formulation in (5.19) to a finite horizon nonlinear model predicitive problem.

5.6.1 Quasi-Infinite Horizon NMPC

The nonlinear model predictive control (NMPC) approach formulates a finite horizon open loop control problem subject to nonlinear system dynamics and constraints involved in state and control input. At every sampling instant t, NMPC computes and minimizes a cost function of control and state over a short time horizon $\mathbf{T}$. While corresponding optimal control inputs for the entire time horizon are calculated, only the first step control is implemented as control action for the system. Also the ideal state for every node is to have 1.00 pu, with phase angle separation of $\frac{2\pi}{3}$. Further, because of very small phase deviation between adjacent nodes, the observed phase angles at the nodes is very close to the phase angle of grid. Thus, grid phase angle can be considered as the ideal phase for every node. The cost function considering deviation from the ideal state and control input at every instance t can be stated as

$$J(\mathbf{X}_t, \mathbf{Qg}_t) = \mathbf{Qg}_t^T \mathbb{R}_t \mathbf{Qg}_t + (\mathbf{X}_t - \mathbf{X_o})^T \mathbb{S}_t (\mathbf{X}_t - \mathbf{X_o}) \tag{5.20}$$

where, $\mathbf{Qg}_t := [Qg_t^a(1), Qg_t^b(1), Qg_t^c(1), \cdots, Qg_t^c(n)]$; $\mathbb{R}_t := diag(\alpha_t^a(1), \cdots, \alpha_t^a(n))$; $\mathbf{X}_o$ is ideal state of system comprising 1.00 pu as voltage magnitude and grid phase as ideal phasor; and $\mathbb{S}_t$ is a diagonal matrix that allows us to place weights on achievable ideal state at a node (which depends on structure of distribution network). In order to enforce stability within finite prediction horizon, we apply methods of quasi-infinite horizon NMPC. For our problem, we achieve this by placing heavier weights for state deviation in the final cost function. Thus quasi-infinite horizon NMPC for distribution system with T as horizon period can be formulated as

$$\begin{array}{lll} \min. & J(\mathbf{X}_t, \mathbf{Qg}_t) = & \sum_t^{t+T-1} (\mathbf{Qg}_t^T \mathbb{R}_t \mathbf{Qg}_t + (\mathbf{X}_t - \mathbf{X_o})^T \mathbb{S}_t (\mathbf{X}_t - \mathbf{X_o})) \\ & & +(\mathbf{X}_{t+\mathbf{T}} - \mathbf{X_o})^T \mathbb{S}_f (\mathbf{X}_{t+\mathbf{T}} - \mathbf{X_o}) \\ \text{subject to} & & \text{Constraints } C_1\text{-}C_5 \ (5.19), \end{array} \tag{5.21}$$

where, $\mathbb{S}_f$ is final cost on state deviation, and for stability $\mathbb{S}_f \geq \mathbb{S}_t \ \forall t = 1 \cdots T-1$. To obtain an optimal solution for (5.21), the inequality and the equality constraints, must be convex functions and affine, respectively. However, the equality constraints in our formulation, especially the dynamic system model constraint C_1 is highly nonlinear. Also, the inequality constraints C_1, C_5 are non convex. Therefore, in next subsection we propose to apply a heuristic approach based on successive time varying linear (STVL) approximation to obtain an approximately feasible sub-optimal solution.

5.6.2 STVL approximation to Quasi-Infinite horizon NMPC

Linear time varying approximation of (5.21) requires T step linearization of the dynamic state model (5.5) around known linearization points. The linearization points for $t, t+$

$1, \cdots t+T$ can be obtained by: (1) predicting the power flow for for $t, t+1, \cdots t+T$ time steps; (2) obtain the linearization points by solving power flow equations. The linearization error can be reduced if the linearization points are very close to true predicted states. However, directly solving power flow equations does not ensure this condition.

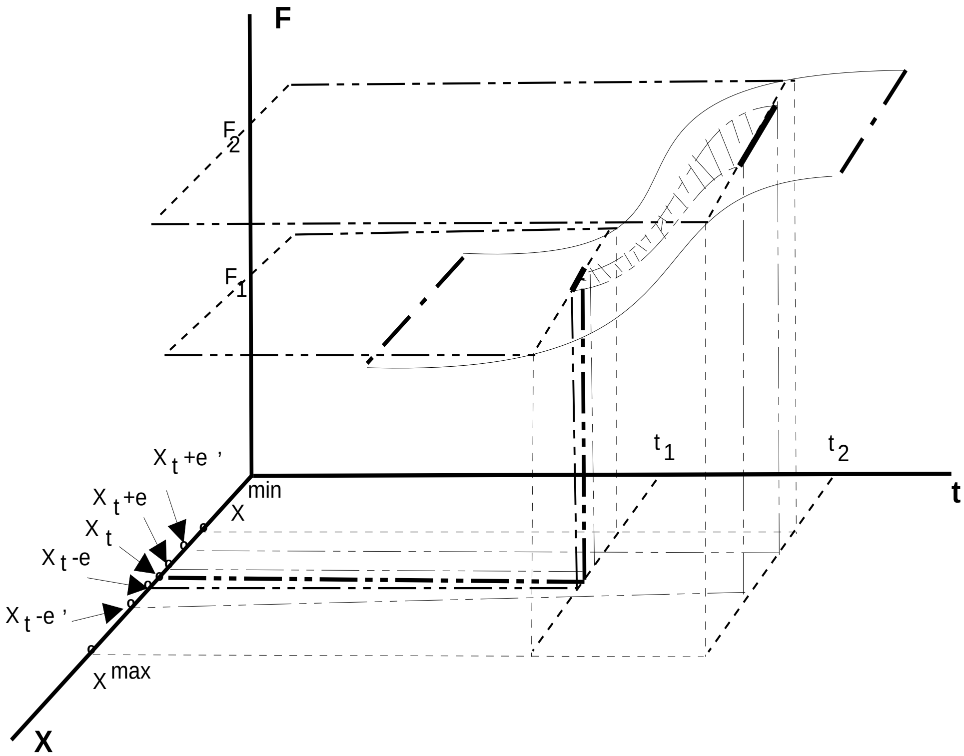

Figure 5.2: *Linearization of nonlinear state model*

Figure 5.2 shows a three dimensional view of the nonlinear state evolution model where, $\mathbf{X}_t$ is the known true state at time t. To get a linearization point at t, using Newtons method we search for a solution of $\mathbf{F}(\mathbf{X}_t)$ in neighborhood of $\mathbf{X}_t$. The neighborhood is denoted by e, a very small n dimensional space around $\mathbf{X}_t$. Similarly, linearization point at $t+1$ can be obtained by searching the solution space of $\mathbf{F}(\mathbf{X}_{t+1})$ in neighborhood of $\mathbf{X}_t$. However, this neighborhood denoted by e' will be greater that e. Since linearization error depends on this neighborhood, linearization error will increase at every step. Linearization error can be reduced, if we restrict the search space of Newtons method around true predicted state at every step. To bring linearization points closer to the predicted states, we propose a novel method in which linearization is done iteratively. At every iteration a linear optimization problem is solved and the model is predicted one step further by obtaining solution using the Newtons method. The open loop control optimization algorithm starting at the estimated state $\mathbf{X}_t$, and using SLTV model approximation can be stated in a flowchart shown in figure 5.3. The linearized control problem to be solved at every iteration is stated as

$$
\begin{array}{ll}
\min. & \sum_t^{t+T-1}(\mathbf{Qg}_t^T \mathbb{R}_t \mathbf{Qg}_t + (\mathbf{X}_t - \mathbf{X_o})^T \mathbb{S}_t (\mathbf{X}_t - \mathbf{X_o})) \\
& +(\mathbf{X}_{t+\mathbf{T}} - \mathbf{X_o})^T \mathbb{S}_f (\mathbf{X}_{t+\mathbf{T}} - \mathbf{X_o}) \\
\text{subject to,} & \begin{cases}
C_1: & \bar{\mathbf{F}}_{t+1} + \mathbf{J}_{t+1}^{\mathbf{F}}(\mathbf{X}_{t+1} - \bar{\mathbf{X}}_{t+1}) \\
& \quad = \mathbf{A}_t^{\mathbf{F}}(\bar{\mathbf{F}}_t + \mathbf{J}_t^{\mathbf{F}}(\mathbf{X}_t - \bar{\mathbf{X}}_t)) + \mathbf{B}_t^F \mathbf{U}_t + \mathbf{L}_t^{\mathbf{F}} \\
C_2: & (Sg_t^x(i))^2 = Pg_t^x(i)\hat{Pg}_t^x(i) + Qg_t^x(i)\hat{Qg}_t^x(i) \\
C_3: & (Qg^x(i))_{min} \leq Qg_t^x(i) \leq (Qg^x(i))_{max}, \\
C_4: & 0.95 \leq V_t^x(i) \leq 1.05, \\
C_5: & \theta_t^b(i) - \theta_t^a(i) \geq \epsilon\frac{2\pi}{3}, \theta_t^c(i) - \theta_t^b(i) \geq \epsilon\frac{2\pi}{3}, \\
& \theta_t^c(i) - (\theta_t^a(i) + \frac{2\pi}{3}) \geq \epsilon\frac{2\pi}{3} \\
& \forall i = 0...n,\ 0 < \epsilon < 1\epsilon \ \&\ t \in \{t, t+1 \cdots t+T-1\}
\end{cases}
\end{array}
\tag{5.22}
$$

where, C_1 is obtained by linearizing dynamic system model (5.6); C_2 is the linearized form of $(Sg_t^x(i))^2 = (Pg_t^x(i))^2 + (Qg_t^x(i))^2$, with $\hat{Pg}_t^x(i)$ and $\hat{Qg}_t^x(i)$ as expected real and reactive injected power following real to reactive power ratio of step $t-1$; C_5 assumes that if phasor relationship at time t is $\theta_t^a(i) < \theta_t^b(i) < \theta_t^c(i)$ then the same relationship is maintained for the time horizon. This is a reasonable assumption as long as the sampling duration and the horizon time are not large.

5.7 Stability Analysis on Nonlinear Control

In this section, we investigate the local stability conditions for our voltage/VAR support control formulation (5.21). Our analysis is based on standard Lyapunov stability results for uniform asymptotic stability of discrete time nonlinear systems. Further in this analysis, we assume that the control problem is always feasible, i.e., there always exists sufficient aggregate grid and DG injected reactive power for voltage/VAR support. Let $\mathscr{V}_{\mathbf{T}}^*(t, \mathbf{X}_t)$:

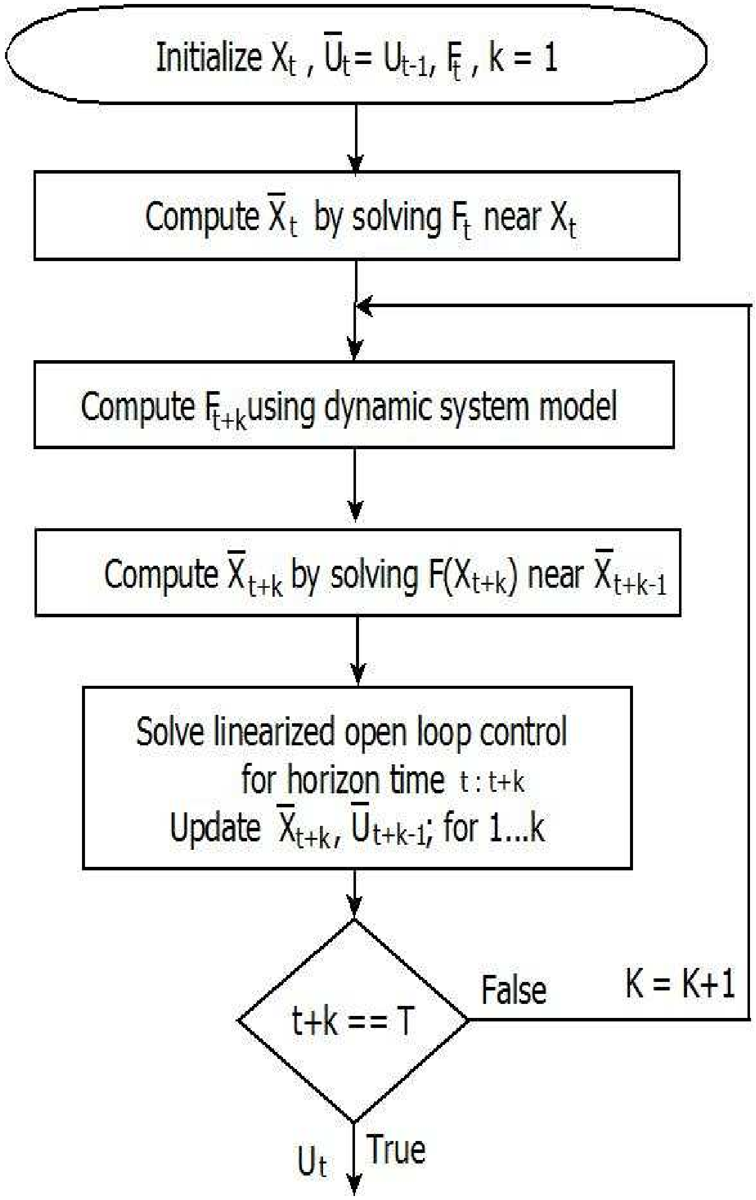

Figure 5.3: *STVL approx. Quasi-Infinite horizon NMPC*

$\mathbb{R}^+ \times \mathbb{R}^n \rightarrow \mathbb{R}$, represent Lyapunov function for our control problem. Then for local uniform asymptotic stability, the Lyapunov function $\mathscr{V}^*_{\mathbf{T}}(t, \mathbf{X}_t)$ is:

- locally positive definite function i.e., $\mathscr{V}^*_{\mathbf{T}}(t, \mathbf{0}) = 0$ and $\alpha(|\mathbf{X}|) \leq \mathscr{V}^*_{\mathbf{T}}(t, \mathbf{X}) \leq \beta(|\mathbf{X}|)$, $\forall \mathbf{X} \in$

Ω_X,

- locally decreasing function i.e., $\mathscr{V}^*_{\mathbf{T}}(t+1, \mathbf{X}) \leq \mathscr{V}^*_{\mathbf{T}}(t, \mathbf{X})$

  where, $\alpha(\cdot)$, $\beta(\cdot)$ are $\mathscr{K}$ class function; Ω_X is n dimensional space containing all feasible phasor voltage vectors (constraint C_4).

Generally, for model predictive control algorithms, cost functions is selected as Lyapunov function, i.e.,

$$\begin{aligned} \mathscr{V}^*_{\mathbf{T}}(t, \mathbf{X}_t) &= J(\mathbf{X}_t, \mathbf{Qg}_t) \\ &= \textstyle\sum_t^{t+T-1} (\mathbf{Qg}_t^T \mathbb{R}_t \mathbf{Qg}_t + (\mathbf{X}_t - \mathbf{X_o})^T \mathbb{S}_t (\mathbf{X}_t - \mathbf{X_o})) \\ &\quad + (\mathbf{X}_{t+\mathbf{T}} - \mathbf{X_o})^T \mathbb{S}_f (\mathbf{X}_{t+\mathbf{T}} - \mathbf{X_o}) \\ &= [\mathbf{X}_t^T \mathbf{Qg}_t^{*T} \cdots \mathbf{Qg}_{t+\mathbf{T}}^{*T}] \mathbf{\Theta}_t [\mathbf{X}_t^T \mathbf{Qg}_t^{*T} \cdots \mathbf{Qg}_{t+\mathbf{T}}^{*T}]^T \end{aligned} \tag{5.23}$$

where, $\mathbf{Qg}_t^{*T} \cdots \mathbf{Qg}_{t+\mathbf{T}}^{*T}$ is the sub-optimal solution of problem (5.22), and $\mathbf{\Theta}_t$ is $(n + \mathbb{T}n)$x$(n + \mathbb{T}n)$ matrix. Elements of $\mathbf{\Theta}_t$ can be computed from $\mathbb{R}_t \cdots \mathbb{R}_{t+\mathbf{T}-1}$, $\mathbb{S}_t \cdots \mathbb{S}_{t+\mathbf{T}-1}$, $\mathbb{S}_f$, $\mathbf{J}_t^{\mathbf{F}} \cdots \mathbf{J}_{t+\mathbf{T}}^{\mathbf{F}}$, $\mathbf{A}_t^{\mathbf{F}} \cdots \mathbf{A}_{t+\mathbf{T}}^{\mathbf{F}}$ and $\mathbf{B}_t^F \cdots \mathbf{B}_{t+\mathbf{T}-1}^F$. For $\mathscr{V}^*_{\mathbf{T}}(t, \mathbf{X}_t)$ to be positive definite and bounded, $\mathbf{\Theta}_t$ needs to be bounded as, $\mathbf{Qg}_t^{*T}$ and $\mathbf{X}_t^T$ are always bounded by constraints C_3 and C_4 of (5.22). Since, $\mathbb{R}_t$, $\mathbb{S}_t$, $\mathbb{S}_f$, $\mathbf{A}_t^{\mathbf{F}}$ $\mathbf{B}_t^{\mathbf{F}}$ are bounded $\forall t$, for $\mathbf{\Theta}_t$ to be bounded, Jacobian $\mathbf{J}_t^{\mathbf{F}}$ must be bounded $\forall t$. As stated in stability conditions of state estimate (section IV.B), Jacobian is always bounded under normal operating conditions. Also, the cost function is always greater than zero. So, the Lyapunov function $\mathscr{V}^*_{\mathbf{T}}(t, \mathbf{X}_t)$ is always bounded and positive definite.

The decreasing condition for Lyapunov function is satisfied by quasi-infinite behavior of control problem (5.21). By setting higher weight on final state deviation and thus final state cost, the Lyapunov cost function decreases along the horizon period. Thus with the persistent feasibility condition and boundedness of Jacobian with time, the local uniform asymptotic stability can be guaranteed. It can be noticed that this stability assume as accurate estimate of state $\mathbf{X}_t$. Also linearization errors are neglected in this analysis. Stochastic stability and robustness analysis under linearization error and bounded disturbances will be analyzed as part of our future work.

5.8 Simulation

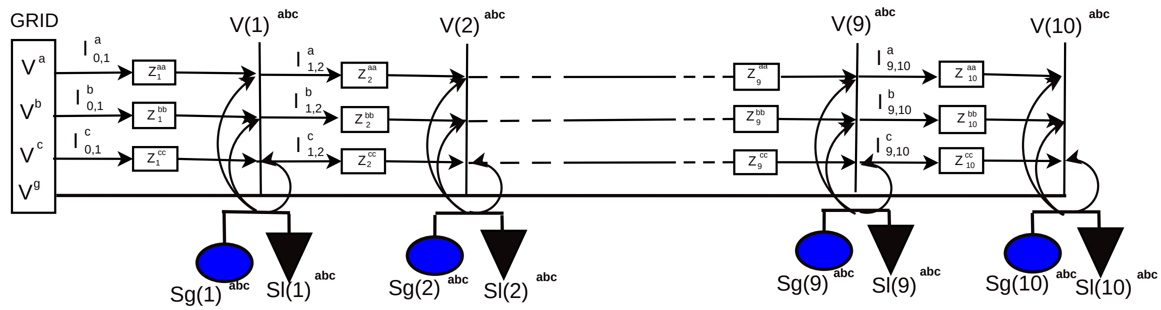

Figure 5.4: *Three phase radial distribution network with DG*

In this section, we apply the proposed estimation and control strategy on a three phase radial distribution network. The network model is shown in figure 5.4. Following is the simulation setup:

- System base values: 4.16kV and 100kVA

- Number of nodes: Grid + 10 nodes

- Inter node distance starting from grid:

  $\{800, 1200, 400, 1200, 800, 400, 1600, 800, 1200, 400\}ft.$

- Constant line impedance per mile:

$$\begin{bmatrix} 0.3465 + 1.0179i & 0.1560 + 0.5017 & 0.1580 + 0.4236i \\ 0.1560 + 0.5017i & 0.3375 + 1.0478 & 0.1535 + 0.3849i \\ 0.1580 + 0.4236i & 0.1535 + 0.3849i & 0.3414 + 1.0348i \end{bmatrix}$$

- Load distribution:

  $\{Sl_1^{abc}, Sl_2^{abc}, Sl_2^{abc}, Sl_3^{abc}, Sl_3^{abc}, Sl_3^{abc}, Sl_2^{abc}, Sl_3^{abc}, Sl_1^{abc}, Sl_3^{abc}\}$,

  where $Sl_{(\cdot)}^{abc} := Pl_{(\cdot)}^{abc} + Ql_{(\cdot)}^{abc}i$; $Pl_{(\cdot)}^{abc}$ and $Ql_{(\cdot)}^{abc}$ are the time series waveform.

- DG distribution:

  $\{0, Sg_1^{abc}, 0, 0, Sg_2^{abc}, 0, Sg_3^{abc}, 0, 0, Sg_4^{abc}\}$,

  where $Sg_{(\cdot)}^{abc}$ are the time series waveform.

- Phase imbalance tolerance: $\epsilon = 0.96$, i.e. phase difference between any two phases is between 115^o to 125^o.

- Reactive power injection constraint: $Qg_{max} \leq 0.6Sg_{max}$, i.e., upto only 60% of total power is avilable for reactive power supply by individual distributed generators.

- The time series waveforms are modeled by AR(1) process with following deterministic component:
  (for load) $D_t^{(\cdot)_1} = D + 0.05sin(6t/T + 0.1)\pi + 0.01sin\pi t/T$; $D_t^{(\cdot)_2} = D + 0.025sin(6t/T + 0.2)\pi + 0.1sin\pi t/T + 0.025sin(6t/T + 0.3)\pi$; $D_t^{(\cdot)_3} = D + 0.15sin(t/T)\pi$ where $D = 0.6\ for\ D_{\cdot}^{(Pl)\cdot}\ and\ 0.3\ for\ D_{\cdot}^{(Ql)\cdot}$.
  (for DG) $D_t^{(\cdot)_1} = D + 0.05sin(6t/T + 0.1)\pi + 0.01sin\pi t/T$; $D_t^{(\cdot)_2} = D + 0.025sin(6t/T + 0.2)\pi + 0.1sin\pi t/T + 0.025sin(6t/T + 0.3)\pi$, with $D = 0.35$;
  Setting a lower scalar constant (D) for distributed generators, relative to that of load ascertains that distributed generators are of low capacity, and they can't themselves support the distribution network. Time series waveforms are considered for 24 hours period, and with sampling time of 10mins, $T = 144$. The deterministic component are chosen to be sinusoidal to represent PV based DGs [112]. AR(1) coefficients for load and generator are assumed to be within the range $[0.6, 1.5]$ and $[0.6, 1]$, respectively.

- Measurements: Three phase inter node current phasor $I_{i,j}^{acb}$ between node $\{i, j\} = \{\{1, 2\}, \{3, 4\}, \{5, 6\}, \{7, 8\}, \{9, 10\}\}$; Voltage phasor $[V_i^{abc}; \theta_t^{abc}$ at node $i = \{2, 4, 6, 8, 10\}$

- Nonlinear process and measurement noise: zero mean i.i.d. Gaussian with covariance of order of 10^{-3} per unit values.

Firstly, we consider the state estimation analysis, and verify Lemma 1, relating critical packet drop rate with load AR(1) coefficients. To simplify the discussion, we assume only one phase is active over the network. The time invariant Jacobian condition ($\mathbb{J}^{\mathbf{F}}{}_{t+1} \approx \mathbb{J}^{\mathbf{F}}{}_t$) is satisfied by setting a small sampling duration of 10mins. Figure 5.5 shows estimated

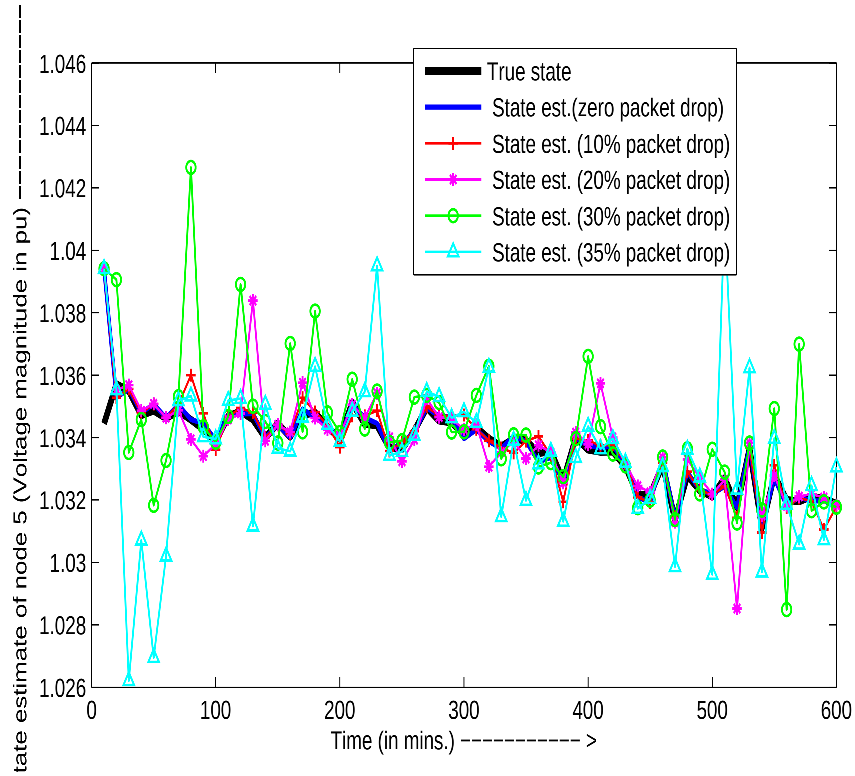

Figure 5.5: *Voltage magnitude estimate of node 5 with packet drop*

voltage magnitude of node 5 with four different rates of packet drop. When the drop rate is below 35%, voltage estimate closely track the true state. This behavior is typical of all nodes. However, at some sampling instants because of large packet drop rate there is large deviation. These intermittent large deviation can limit the operation of smart grid. In our simulation setup, the largest AR(1) coefficient for load is 1.5. According to Lemma 1, the critical probability for measurement update Λ_c for the bounded error covariance matrix must be greater that 0.555. Placing $\Lambda_c = 0.555$ in (5.16) gives $\lambda_c = 0.63$. This critical packet drop rate $(1 - \lambda_c)$ is 37%. This can be verified from figure 5.6, where the estimation starts getting unbounded around packet drop rate of 37%. This verifies the theoretical analysis.

Figure 5.7 shows tracking of voltage estimate with the sampling duration of 10mins and 20mins. The drop rate is set to 30%. This ensures that for 10mins sampling duration, $\mathbb{J}^{\mathbf{F}}{}_{t+1} \approx \mathbb{J}^{\mathbf{F}}{}_{t}$ and voltage estimate tracks true value without large deviations. For sampling duration set to 20mins, we cannot ensure $\mathbb{J}^{\mathbf{F}}{}_{t+1} \approx \mathbb{J}^{\mathbf{F}}{}_{t}$ for all time instants. This is shown in

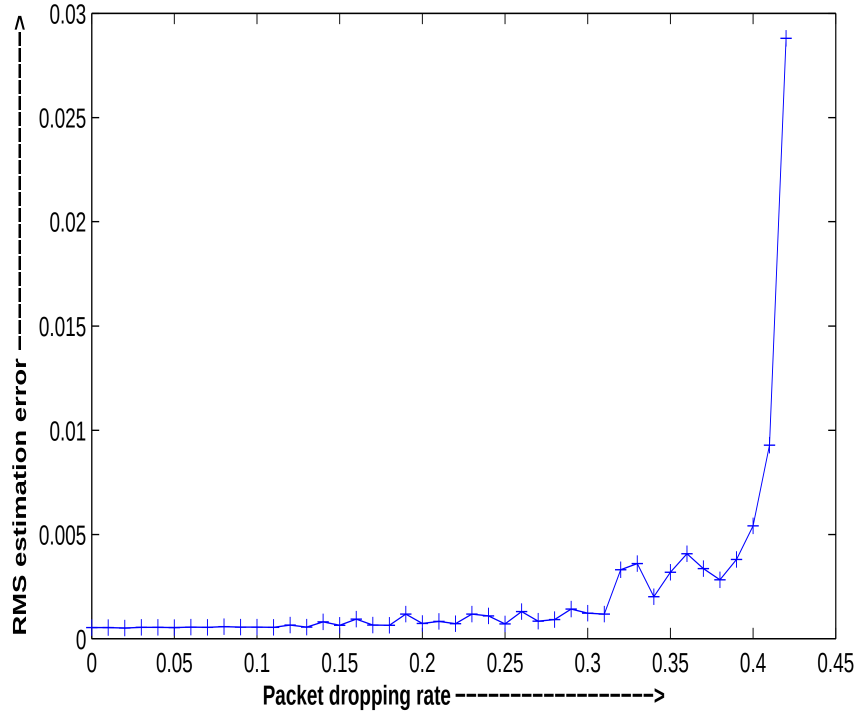

Figure 5.6: *RMS estimate error with different packet drop rates*

figure 5.8, where spectral radius of the state transition matrix exceeds 1.5 (maximum load AR(1) coefficients). This increse in spectral radius causes estimate to deviate from the true value as shown in figure 5.7. Thus sampling duration plays a crucial role in computing the critical packet drop rate.

Next, we consider the three phase distribution network for voltage/VAR support by DG. Figure 5.9, shows the aggregate reactive power injected by DG with different time horizons ($T = 1, 2, 3$, i.e., 10mins, 20mins and 30mins). It can be observed that by not computing control input myopically, we can better manage the reactive power resource. That is, with an increase in time horizon, the aggregate injected reactive power needed for meeting the distribution network constraints gets reduced. Also, the decremental improvement in reactive power requirement is more when horizon time is incremented from $T = 1$ to 2, compared to $T = 2$ to 3. Further, with increasing horizon time there is an increase in computational complexity and computation time. Hence, for a real time voltage/VAR

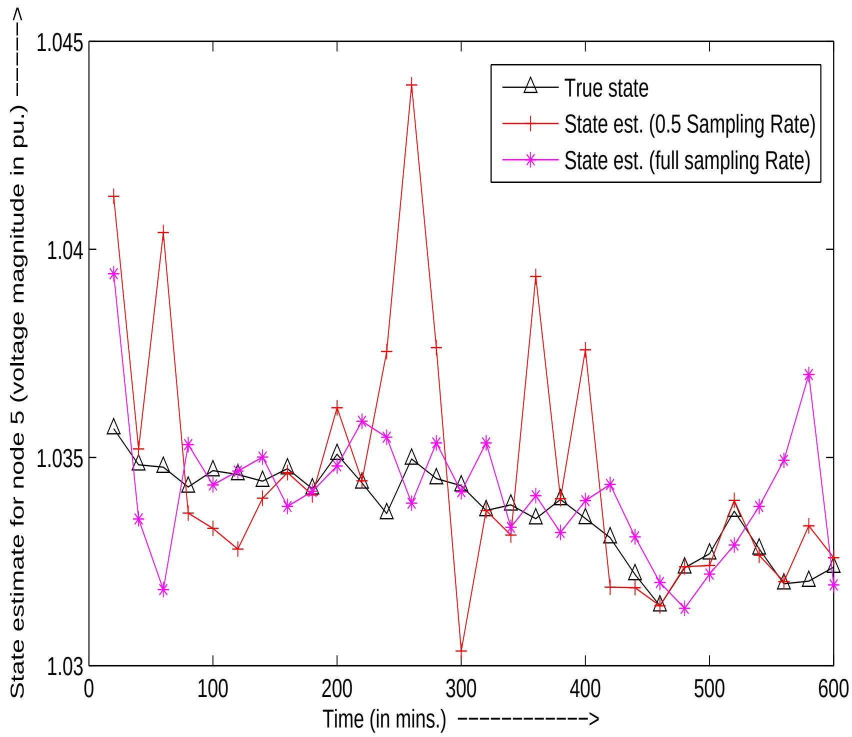

Figure 5.7: *State estimate with different sampling duration at drop rate of 30%*

control, a reasonable time horizon must be selected based on trade off in performance and computational complexity. Another observation from figure 5.9 is reduction in variability of required aggregate reactive power. With increase in time horizon, the reactive power requirement gets averaged over time. This is an important characteristic of model predictive control where, present control input is computed considering the prediction of future control inputs. Thus a sudden increase in reactive power requirement (at time step 12) is avoided by increasing the time horizon.

5.9 Summary

This chapter presents a CPS case study on control framework for voltage/VAR support via DGs in smart distribution networks. Firstly, a dynamic nonlinear input to state model is formulated for the control framework, which accommodates power flow equations along

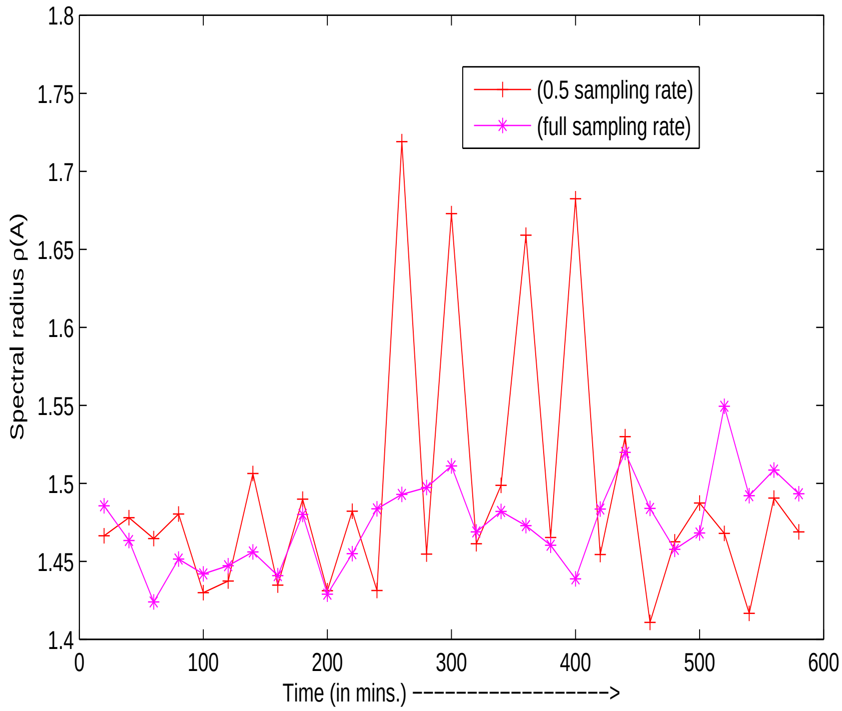

Figure 5.8: *Spectral radius with different sampling duration at drop rate of 30%*

with load and DG forecasts. Then, an EKF based dynamic state estimation approach is designed, followed by establishing the system conditions under which the stochastic stability can be ensured. The analysis considers communication network impact by modeling packet drops as independent Bernoulli random process. It is shown that under certain system conditions, a relation between the largest AR(1) coefficients of load and the critical packet drop rate can be established such that error covariance matrix is bounded. Finally, a NMPC problem is formulated for voltage/VAR support by DG injected reactive power. A successive time varying linear approximation strategy is proposed to linearize the nonlinear control problem with consideration of minimizing the linearization error. The proposed approach and analysis is validated by simulation of a radial distribution network.

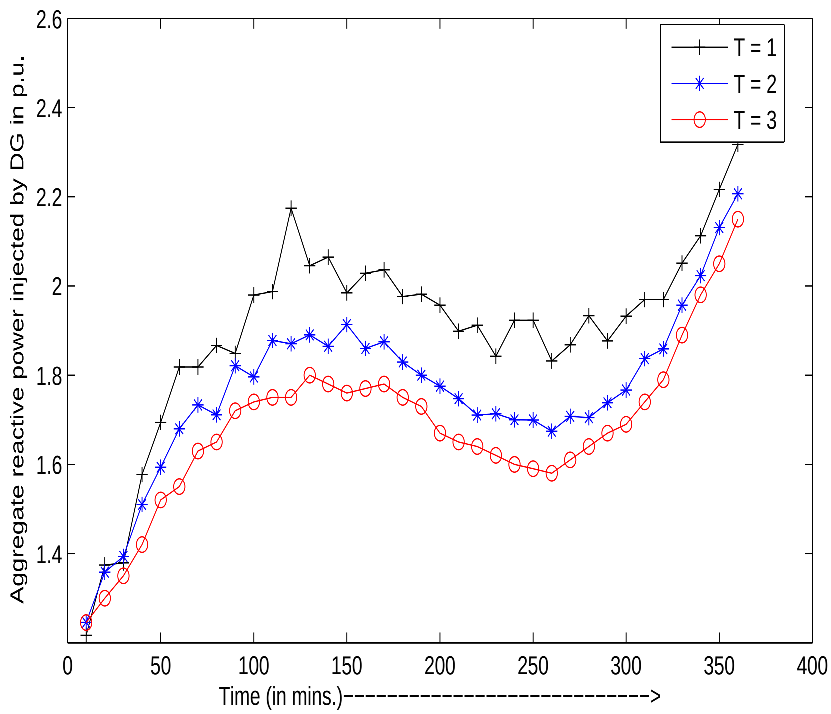

Figure 5.9: *Aggregate reactive power injection with different horizon time*

Chapter 6

Conclusion & Future Work

In this concluding chapter, we summarize the contributions of this dissertation and discuss future research directions.

6.1 Conclusion

This dissertation addresses estimation and control solutions for spatially distributed cyber physical systems (CPS). Spatially distributed CPS are physical systems such as smart distribution networks, smart highways and city transportation networks, smart irrigation networks, etc., where state of the underlying system is spatially distributed in physical space. Since such systems are typically large dynamical systems, we essentially consider the measurement scenario with multiple sensors arbitrarily deployed over physical space to jointly sense the complete system. The sensed measurements are collected at central estimation and control unit (ECU) via individual sensor to ECU communication links.

Similarly, for implementing control solution we consider multiple actuators arbitrarily deployed over physical space to jointly control of all state of the system. Further, the computed control solution at ECU is communicated to individual actuators via separate communication links. We denote these scenarios as *dispersed* sensor and *dispersed* actuator scenario. Since, in practice communication links are susceptible to random failures, the overall estimation and control process is subjected to: (1) partial observation updates in estimation process; and (2) partial actuator action implementation in control process. Thus, we study statistical properties of estimation error and Lyapunov function iteration over time, and establish necessary and sufficient network conditions for ensuring stability of overall ECU operation.

First addressing state estimation, we consider Kalman filter for state estimation in spatially distributed CPS. The measurements are sensed by *dispersed* sensors, and are encoded in packets to be sent to ECU over individual communication links. The random drop of packets over communication links result in: (1) random measurement loss; and (2) partial observation updates in Kalman filter. This in effect results in stochastic error covariance iteration over time, making offline stability analysis very difficult. Thus, we study statistical properties of error covariance iteration, and establish existence of critical probabilities on sensor communication links for ensuring convergence of error covariance matrix. Next, we use information theoretic concepts to establish the analogy in convergence with *gathered* measurement (measurements are first collected and then sent over single communication link) scenario. Using this analogy, we compute corresponding upper and lower bounds on critical probability of successful measurement reception from individual sensors by formulating a optimization / feasibility problem.

The analysis is further enhanced by exploiting spatially correlation between states in estimating lost measurements from received measurements. This eventually results in redefining new set of measurements for all possible measurement loss configurations, followed by conclusive analysis that a higher degree of information loss or poor network quality can be tolerated to archive a certain estimation accuracy. The analysis also accommodates correlated link failure scenario by placing constraints of joint probability mass function in computation of lower and upper bound on critical measurement loss rates.

Next, addressing control solution implementation, we consider linear quadratic regulator in spatially distributed CPS. The computed control solution is encoded in packets and is sent to respective actuators over separate communication links. The random drop of packets over network result in: (1) random actuator input loss; and (2) partial control solution implementation. We study Lyapunov stability of control process in this scenario. The Lyapunov function iteration over time is a stochastic process, making offline stability analysis very difficult. Thus, we study statistical properties of Lyapunov function iteration, and establish the existence of critical probabilities on individual actuator links for ensuring convergence of Lyapunov function. We utilize the stability results of *unified* actuator (all actuator actions are communicated over single link) scenario and compute upper and lower bounds on critical probabilities of individual actuator links, by formulating optimization/feasibility problem. The feasibility solution distributes the control action loss of *unified* actuator scenario to loss in individual communication links of *dispersed* actuators.

Finally, we present a case study on networked control framework for voltage/VAR support via distributed generation at distribution network level. Firstly, a dynamic nonlinear input to state model is formulated for the control framework, which accommodates power flow equations along with load and DG forecasts. Then, an EKF based dynamic state estimation approach is designed, followed by establishing the system conditions under which the stochastic stability can be ensured. The analysis considers communication network impact by modeling packet drops as independent Bernoulli random process. It is shown that under certain system conditions, a relation between the largest AR(1) coefficients of load and the critical packet drop rate can be established such that error covariance matrix is bounded. Finally, a NMPC problem is formulated for voltage/VAR support by DG injected reactive power. A successive time varying linear approximation strategy is proposed to linearize the nonlinear control problem with consideration of minimizing the linearization error. The proposed approach and analysis is validated by simulation of a radial distribution network. The overall case study illustrates how a CPS architecture can be effective within the distributed Smart Grid framework.

In summary, following open question on estimation and control in spatially distributed CPS are addressed in this dissertation:

- We analyze Kalman filter based state estimation process stability in spatially distributed CPS scenario, monitored by multiple sensors individually communicating the measurements to central estimation unit.

- We analyze LQR based control solution stability in spatially distributed CPS scenario, implemented over multiple actuators with control actions communicated over separate communication links from central control unit.

- We discuss CPS architecture for voltage/VAR support in smart distribution networks via distributed generation by formulating a dynamic nonlinear input to state model.

- We discuss extended Kalman filter based state estimation solution in smart distribution networks, with direct and indirect local measurements communicated to centralized state estimation unit via individual communication links.

- We discuss nonlinear model predictive control solution in smart distribution networks, with necessary reactive power injection input computed by linear time varying approximation strategy.

6.2 Future Work

In this section, we present possible future research direction in estimation and control for spatially distributed CPS. We first discuss some extensions to our work proposed in chapter 3-5.

- In our stability analysis in chapter 3-4, we assumed time homogeneous linear model as the dynamical system model of underlying spatially distributed CPS. Our analysis can be extended to time varying linear system model by: (1) performing worst case stability analysis; (2) perturbation analysis of eigen values of state transition matrix.

- Our stability analysis for spatially distributed CPS in chapter 3-4, can be extended for extended Kalman filter and nonlinear model predictive control considering nonlinear system model. In this case we have to consider the impact of linearization error along with maximum value of Jacobian matrix in error covariance iteration and Lyapunov function iteration, respectively. Similar to time varying system model, approaches like, (1) worst case stability analysis; and (2) eigen value perturbation analysis can be adopted.

- The linear quadratic control solution analyzed in chapter 4 can be extended for zero order hold condition in actuator implementation. In this configuration, whenever there is control action loss actuator continues to implement the same control action communicated to it in previous time steps. Thus, the system model needs to be modified appropriately followed by similar convergence analysis for Lyapunov function iteration.

- Another possible extension of our work is to exploit spatial correlation in estimating lost control action at the actuator. Here, we essentially require computation capability in actuators. This enables us to estimate lost control action by communication with neighboring actuators and spatial correlation model.

Next, we present some new areas of investigation in estimation and control for spatially distributed cyber physical systems. A subset of possible future research works is discussed below.

- *Compressed sensing*: Estimation and control solution in spatially distributed CPS can be efficiently implemented by exploiting concepts of compressed sensing [116],[117],[118]. Compressive sensing in state estimation is essentially use of l_1 regularization for reconstructing state vector from few random sample measurements. Compressive sensing for spatially distributed CPS architecture is still an unexplored area and is important to investigate estimation process stability in this configuration.

- *Network delay*: In our stability analysis on estimation and control, we assumed delayed measurements and control actions are not applicable for measurement updates in Kalman filter, and control updates in linear quadratic solution. However, delayed measurement and control inputs can be exploited with limited information, and can improve the estimation and control accuracy in poor network conditions [119], [120]. Thus, it is worth exploring inclusion of delayed measurements and control actions in stability analysis of spatially distributed CPS.

- *Quantization*: The physical system operates in analog domain, while digital signal processing occurs with quantized data. The quantization error in our analysis is accommodated as process noise, and measurement noise. However, some researchers have separately analyze design of quantizer in order to reduce quantization error [5], [121]. Thus, one can explore new designs in quantizers for spatial distributed CPS architectures, considering its impact on overall stability of estimation and control process.

- *Distributed/decentralized signal processing*: Our work in this dissertation considers centralized computation of state estimation and control solution. In future efforts, decentralized/distributed computation of estimation and control solution in spatially distributed CPS architecture can be investigated in order to address computational cost incurred in centralized computation [122], [123].

Bibliography

[1] R. Rajkumar, I. Lee, L. Sha, and J. Stankovic, "Cyber-physical systems: The next computing revolution," in *Design Automation Conference (DAC), 2010 47th ACM/IEEE*, 2010, pp. 731–736.

[2] L. Hu, N. Xie, Z. Kuang, and K. Zhao, "Review of cyber-physical system architecture," in *Object/Component/Service-Oriented Real-Time Distributed Computing Workshops (ISORCW), 2012 15th IEEE International Symposium on*, 2012, pp. 25–30.

[3] E. Lee, "Cyber physical systems: Design challenges," in *Object Oriented Real-Time Distributed Computing (ISORC), 2008 11th IEEE International Symposium on*, 2008, pp. 363–369.

[4] J. Bradley and E. Atkins, "Computational-physical state co-regulation in cyber-physical systems," in *Cyber-Physical Systems (ICCPS), 2011 IEEE/ACM International Conference on*, 2011, pp. 119–128.

[5] M. Fu, "Quantization for feedback control and estimation," in *Control Conference, 2008. CCC 2008. 27th Chinese*, 2008, pp. 751–756.

[6] P. Derler, E. Lee, and A.-S. Vincentelli, "Modeling cyber physical systems," *Proceedings of the IEEE*, vol. 100, no. 1, pp. 13–28, 2012.

[7] M. Ilic, L. Xie, U. Khan, and J. Moura, "Modeling future cyber-physical energy systems," in *Power and Energy Society General Meeting - Conversion and Delivery of Electrical Energy in the 21st Century, 2008 IEEE*, 2008, pp. 1–9.

[8] M. Lindberg and K. Arzen, "Feedback control of cyber-physical systems with multi resource dependencies and model uncertainties," in *Real-Time Systems Symposium (RTSS), 2010 IEEE 31st*, 2010, pp. 85–94.

[9] Y. Fallah and R. Sengupta, "A cyber-physical systems approach to the design of vehicle safety networks," in *Distributed Computing Systems Workshops (ICDCSW), 2012 32nd International Conference on*, 2012, pp. 324–329.

[10] D. Goswami, R. Schneider, and S. Chakraborty, "Co-design of cyber-physical systems via controllers with flexible delay constraints," in *Design Automation Conference (ASP-DAC), 2011 16th Asia and South Pacific*, 2011, pp. 225–230.

[11] A. Miloslavov and M. Veeraraghavan, "Sensor data fusion algorithms for vehicular cyber-physical systems," *IEEE Transactions on Parallel and Distributed Systems*, vol. 23, no. 9, pp. 1762–1774, 2012.

[12] R. Balani, L. Wanner, J. Friedman, M. Srivastava, K. Lin, and R. Gupta, "Programming support for distributed optimization and control in cyber-physical systems," in *Cyber-Physical Systems (ICCPS), 2011 IEEE/ACM International Conference on*, 2011, pp. 109–118.

[13] J. Cao and H. Li, "Energy-efficient structuralized clustering for sensor-based cyber physical systems," in *Ubiquitous, Autonomic and Trusted Computing, 2009. UIC-ATC '09. Symposia and Workshops on*, 2009, pp. 234–239.

[14] H. Li, L. Lai, and H. Poor, "Multicast routing for decentralized control of cyber physical systems with an application in smart grid," *Selected Areas in Communications, IEEE Journal on*, vol. 30, no. 6, pp. 1097–1107, 2012.

[15] F.-J. Wu, Y.-F. Kao, and Y.-C. Tseng, "From wireless sensor networks towards cyber physical systems," *Pervasive and Mobile Computing*, vol. 7, no. 4, pp. 397 – 413, 2011.

[16] F. Xia, L. Ma, J. Dong, and Y. Sun, "Network qos management in cyber-physical systems," in *Embedded Software and Systems Symposia, 2008. ICESS Symposia '08. International Conference on*, 2008, pp. 302–307.

[17] A. Cardenas, S. Amin, and S. Sastry, "Secure control: Towards survivable cyber-physical systems," in *Distributed Computing Systems Workshops, 2008. ICDCS '08. 28th International Conference on*, 2008, pp. 495–500.

[18] J. H. Seinfeld, "Optimal stochastic control of nonlinear systems," *AIChE Journal*, vol. 16, no. 6, pp. 1016–1022, 1970.

[19] H. J. Kappen, "Linear theory for control of nonlinear stochastic systems," *Phys. Rev. Lett.*, vol. 95, pp. 200 – 201, Nov 2005.

[20] L. Guo, "On critical stability of discrete-time adaptive nonlinear control," *Automatic Control, IEEE Transactions on*, vol. 42, no. 11, pp. 1488 –1499, nov 1997.

[21] T. Hayakawa, W. Haddad, and A. Leonessa, "A lyapunov-based adaptive control framework for discrete time nonlinear systems with exogenous disturbances," *International Journal of control*, vol. 77, no. 3, pp. 250 – 263, 2004.

[22] Y. Niu and D. Ho, "Design of sliding mode control for nonlinear stochastic systems subject to actuator nonlinearity," *Control Theory and Applications, IEE Proceedings -*, vol. 153, no. 6, pp. 737 –744, nov. 2006.

[23] M. Hovd and R. R. Bitmead, "Interaction between control and estimation in nonlinear MPC," *Modeling, Identification and Control*, vol. 26, no. 3, pp. 165–174, 2005.

[24] V. Sundarapandian, "A counterexample for the global separation principle for discrete-time nonlinear systems," *Applied Mathematics Letters*, vol. 18, no. 7, pp. 765 – 768, 2005.

[25] J. N. H. and S. J. H., “Local separation principle for non-linear systems,” *International Journal of Control*, vol. 73, no. 4, pp. 292–302, 2000.

[26] K. Veluvolu, Y. Soh, and W. Cao, “Robust discrete time nonlinear sliding model state estimation of uncertain discrete time systems,” *Robust and nonlinear Control, International Journal of*, vol. 17, pp. 803 – 828, nov. 2007.

[27] M. Xiao, “State estimation for nonlinear discrete time systems with input signals,” *Mathematical Control and Information, IMA Journal of*, vol. 26, pp. 141 – 150, april 2009.

[28] L. Scardovi, M. Baglietto, and T. Parisini, “Active state estimation for nonlinear systems: A neural approximation approach,” *Neural Networks, IEEE Transactions on*, vol. 18, no. 4, pp. 1172 –1184, july 2007.

[29] C. Rao, J. Rawlings, and D. Mayne, “Constrained state estimation for nonlinear discrete-time systems: stability and moving horizon approximations,” *Automatic Control, IEEE Transactions on*, vol. 48, no. 2, pp. 246 – 258, feb. 2003.

[30] S. Ungarala, E. Dolence, and K. Li, “Constrained extended kalman filter for nonlinear state estimation,” in *8th International Symposium on Dynamics and Control of Process Systems*, june 2007, pp. 66 – 68.

[31] S. Sarkka, “On unscented kalman filtering for state estimation of continuous-time nonlinear systems,” *Automatic Control, IEEE Transactions on*, vol. 52, no. 9, pp. 1631 –1641, sept. 2007.

[32] M. J. Kurtz and M. A. Henson, “State and disturbance estimation for nonlinear systems affine in the unmeasured variables,” *Computers and Chemical Engineering*, vol. 22, no. 10, pp. 1441 – 1459, 1998.

[33] K. Reif, S. Gunther, E. Yaz, and R. Unbehauen, "Stochastic stability of the discrete-time extended kalman filter," *Automatic Control, IEEE Transactions on*, vol. 44, no. 4, pp. 714 –728, apr 1999.

[34] R. Huang, S. Patwardhan, and L. Biegler, "Robust extended kalman filter based nonlinear model predictive control formulation," in *Decision and Control, 2009 held jointly with the 2009 28th Chinese Control Conference. CDC/CCC 2009. Proceedings of the 48th IEEE Conference on*, dec. 2009, pp. 8046 –8051.

[35] R. Huang, S. C. Patwardhan, and L. T. Biegler, "Robust stability of nonlinear model predictive control based on extended kalman filter," *Journal of Process Control*, vol. 22, no. 1, pp. 82 – 89, 2012.

[36] A. Jadbabaie and J. Hauser, "On the stability of receding horizon control with a general terminal cost," *Automatic Control, IEEE Transactions on*, vol. 50, no. 5, pp. 674 – 678, may 2005.

[37] A. Jadbabaie, J. Yu, and J. Hauser, "Unconstrained receding-horizon control of non-linear systems," *Automatic Control, IEEE Transactions on*, vol. 46, no. 5, pp. 776 –783, may 2001.

[38] P. Scokaert, D. Mayne, and J. Rawlings, "Suboptimal model predictive control (feasibility implies stability)," *Automatic Control, IEEE Transactions on*, vol. 44, no. 3, pp. 648 –654, mar 1999.

[39] L. zkan, M. V. Kothare, and C. Georgakis, "Model predictive control of nonlinear systems using piecewise linear models," *Computers and Chemical Engineering*, vol. 24, no. 27, pp. 793 – 799, 2000.

[40] P. Scokaert, J. Rawlings, and E. Meadows, "Discrete-time stability with perturbations: application to model predictive control," *Automatica*, vol. 33, no. 3, pp. 463 – 470, 1997.

[41] D. Marruedo, T. Alamo, and E. Camacho, "Input-to-state stable mpc for constrained discrete-time nonlinear systems with bounded additive uncertainties," in *Decision and Control, 2002, Proceedings of the 41st IEEE Conference on*, vol. 4, dec. 2002, pp. 4619 – 4624 vol.4.

[42] B. Sinopoli, L. Schenato, M. Franceschetti, K. Poolla, M. Jordan, and S. Sastry, "Kalman filtering with intermittent observations," *Automatic Control, IEEE Transactions on*, vol. 49, no. 9, pp. 1453 – 1464, sept. 2004.

[43] Z. Jin, C.-K. Ko, and R. Murray, "Estimation for nonlinear dynamical systems over packet-dropping networks," in *American Control Conference, 2007. ACC '07*, july 2007, pp. 5037 –5042.

[44] S. Kluge, K. Reif, and M. Brokate, "Stochastic stability of the extended kalman filter with intermittent observations," *Automatic Control, IEEE Transactions on*, vol. 55, no. 2, pp. 514 –518, feb. 2010.

[45] M. Huang and S. Dey, "Stability of kalman filtering with markovian packet loss," *Automatica*, vol. 43, pp. 598 – 607, 2007.

[46] M. Moayedi, Y. Foo, and Y. Soh, "Adaptive kalman filtering in networked systems with random sensor delays, multiple packet dropouts and missing measurements," *Signal Processing, IEEE Transactions on*, vol. 58, no. 3, pp. 1577 –1588, march 2010.

[47] S. Sun, L. Xie, and W. Xiao, "Optimal full-order and reduced-order estimators for discrete-time systems with multiple packet dropouts," *Signal Processing, IEEE Transactions on*, vol. 56, no. 8, pp. 4031 –4038, aug. 2008.

[48] M. Moayedi, Y. C. Soh, and Y. K. Foo, "Optimal kalman filtering with random sensor delays, packet dropouts and missing measurements," in *American Control Conference, 2009. ACC '09.*, june 2009, pp. 3405 –3410.

[49] H. Dong, Z. Wang, and H. Gao, "Optimal full-order and reduced-order estimators for discrete-time systems with multiple packet dropouts," *Signal Processing, IEEE Transactions on*, vol. 58, no. 4, pp. 1957 – 1966, april 2010.

[50] L. Schenato, "Optimal estimation in networked control systems subject to random delay and packet drop," *Automatic Control, IEEE Transactions on*, vol. 53, no. 5, pp. 1311 –1317, june 2008.

[51] I. G. Polushin, P. X. Liu, and C.-H. Lung, "On the model-based approach to nonlinear networked control systems," *Automatica*, vol. 44, no. 9, pp. 2409 – 2414, 2008.

[52] M. Liu, Q. Wang, and H. Li, "State estimation and stabilization for nonlinear networked control systems with limited capacity channel," *Journal of the Franklin Institute*, vol. 348, no. 8, pp. 1869 – 1885, 2011.

[53] S. Mastellone, C. Abdallah, and P. Dorato, "Model-based networked control for nonlinear systems with stochastic packet dropout," in *American Control Conference, 2005. Proceedings of the 2005*, june 2005, pp. 2365 – 2370 vol. 4.

[54] T. Matiakis, S. Hirche, and M. Buss, "Independent-of-delay stability of nonlinear networked control systems by scattering transformation," in *American Control Conference, 2006*, june 2006, p. 6 pp.

[55] M. Fei, J. Yi, and H. Hu, "Robust stability analysis of an uncertain networked control category," *International Journal of Control, Automation, and Systems*, vol. 4, no. 2, pp. 172–177, 2006.

[56] N. van de Wouw, D. Neic, and W. Heemels, "A discrete-time framework for stability analysis of nonlinear networked control systems," *Automatica*, no. 0, pp. –, 2012.

[57] B. Sinopoli, L. Schenato, M. Franceschetti, K. Poolla, M. Jordan, and S. Sastry, “Kalman filtering with intermittent observations,” *Automatic Control, IEEE Trans. on*, vol. 49, no. 9, pp. 1453 – 1464, sept. 2004.

[58] Y. Mo and B. Sinopoli, “A characterization of the critical value for kalman filtering with intermittent observations,” in *Decision and Control, 2008. CDC 2008. 47th IEEE Conference on*, dec. 2008, pp. 2692 –2697.

[59] X. Liu and A. Goldsmith, “Kalman filtering with partial observation losses,” in *Decision and Control, 2004. CDC. 43rd IEEE Conference on*, vol. 4, dec. 2004, pp. 4180 – 4186.

[60] M. Huang and S. Dey, “Stability of kalman filtering with markovian packet losses,” *Automatica*, vol. 43, no. 4, pp. 598 – 607, 2007.

[61] M. Moayedi, Y. Foo, and Y. Soh, “Adaptive kalman filtering in networked systems with random sensor delays, multiple packet dropouts and missing measurements,” *Signal Processing, IEEE Transactions on*, vol. 58, no. 3, pp. 1577 –1588, march 2010.

[62] L. Schenato, “Optimal sensor fusion for distributed sensors subject to random delay and packet loss,” in *Decision and Control, 2007 46th IEEE Conference on*, dec. 2007, pp. 1547 –1552.

[63] J. Gubner, *Probability and Random Processes for Electrical and Computer Engineers.* Cambridge University Press, 2006.

[64] S. Deshmukh, B. Natarajan, and A. Pahwa, “State estimation in spatially distributed cyber physical systems: Bounds on critical measurement drop rates,” in *Distributed Computing in Sensor Systems, IEEE International Conference on*, May 2013.

[65] ——, “State estimation over alossy network in spatially distributed cyber physical systems,” *Systems, Man and Cybernetics: Systems, IEEE Trans. on (under review).*

[66] ——, "Stochastic stability of linear quadratic controller over intermittent actuator inputs," in *Systems and Control, IEEE Multi-conference on (under review)*.

[67] ——, "Lqr controller over a lossy network in spatially distributed cyber-physical systems," *Automatic Control: IEEE Trans. on (under review)*.

[68] J. T. Spooner, M. Maggiore, R. Ordez, and K. M. Passino, *Stable Adaptive Control and Estimation for Nonlinear Systems*. John Wiley & Sons, Inc., 2002.

[69] J. N. H. and S. J. H., "Local separation principle for non-linear systems," *International Journal of Control*, vol. 73, no. 4, pp. 292–302, 2000.

[70] V. Sundarapandian, "A counterexample for the global separation principle for discrete-time nonlinear systems," *Applied Mathematics Letters*, vol. 18, no. 7, pp. 765 – 768, 2005.

[71] S. Deshmukh, B. Natarajan, and A. Pahwa, "Voltage/var control in distribution networks via reactive power injection through distributed generators," *Smart Grid, IEEE Transactions on*, vol. 3, no. 3, pp. 1226–1234, 2012.

[72] ——, "Stochastic state estimation for smart grids in the presence of intermittent measurements," in *Communications, LATINCOM 2012. IEEE Latin-American Conference on*, Nov. 2012.

[73] ——, "State estimation and voltage/var control in distribution networks with intermittent measurements," *Smart Grid, IEEE Transactions on (under review)*.

[74] B. D. O. Anderson, *Optimal Control: Linear Quadratic Methods*. Prentice Hall Information and System Science Series, 1990.

[75] D. Bertsekas, *Dynamic Programming and Optimal Control*. Athena Scientific; 4th edition, 2007.

[76] S. Boyd, "http://www.stanford.edu/class/ee363/lectures.html," Stanford University, 2008-09.

[77] E. F. Camacho, *Model Predictive Control*. Springer, 2nd edition, 2007.

[78] R. L. Eubank, *A Kalman Filter Primer*. Chapman and Hall/CRC, 2005.

[79] D. Simon, "Kalman filtering with state constraints: a survey of linear and nonlinear algorithms," *Control Theory Applications, IET*, vol. 4, no. 8, pp. 1303–1318, 2010.

[80] B. Teixeira, J. Chandrasekar, H. Palanthandalam-Madapusi, L. Torres, L. Aguirre, and D. Bernstein, "Gain-constrained kalman filtering for linear and nonlinear systems," *Signal Processing, IEEE Transactions on*, vol. 56, no. 9, pp. 4113–4123, 2008.

[81] C. Yang and E. Blasch, "Kalman filtering with nonlinear state constraints," in *Information Fusion, 2006 9th International Conference on*, 2006, pp. 1–8.

[82] X. Fu, Y. Jia, J. Du, and F. Yu, "Kalman filtering with multiple nonlinear-linear mixing state constraints," in *Decision and Control (CDC), 2010 49th IEEE Conference on*, 2010, pp. 340–345.

[83] L. Magni, *Nonlinear Model Predictive Control: Towards New Challenging Applications*. Springer, 2009.

[84] P. S. Maybeck, *Stochastic Models Estimation and Control*, ser. Mathematics in Science and Engineering. New York: Academics, 1979.

[85] P. Matisko and V. Havlena, "Cramer-rao bound for estimation of linear system noise covariance," *Jr. of Mechanical Engg. and Automation*, vol. 2, no. 2, pp. 6–11, 2012.

[86] R. F. Stengel, *Optimal Control and Estimation*. Dover publications, 1994.

[87] R. Horn and C. Johnson, *Matrix Analysis*. Cambridge University Press, 1990.

[88] P. P. Barker and R. W. De-Mello, "Determining the impact of distributed generation on power systems: Part 1 - Radial distribution systems," in *Power Engineering Society Summer Meeting*, vol. 3, July 2000, pp. 1645–1656.

[89] G. Pepermansa, J. Driesenb, D. Haeseldonckxc, R. Belmansc, and W. D'haeseleer, "Distributed generation: definition, benefits and issues," in *Energy Policy, ELSEVIER*, 2005.

[90] G. Joos, B. T. Ooi, D. McGillis, F. D. Galiana, and R. Marceau, "The potential of distributed generation to provide ancillary services," in *Power Engineering Society Summer Meeting, IEEE*, vol. 3, 2000, pp. 1762–1767.

[91] F. Li, J. D. Kueck, D. T. Rizy, and T. King, "A Preliminary Analysis of the Economics of Using Distributed Energy as a Source of Reactive Power Supply," in *Oak Ridge National Laboratory (ORNL), Oak Ridge, TN, Tech. Rep. (ORNL/TM-2006/014)*, April 2006.

[92] H. Willis, "Analytical methods and rules of thumb for modeling DG-distribution interaction," in *Power Engineering Society Summer Meeting, IEEE*, vol. 3, July 2000, pp. 1643–1644.

[93] M. Thomson and D. Infield, "Network power-flow analysis for a high penetration of distributed generation," *Power Systems, IEEE Transactions on*, vol. 22, no. 3, pp. 1157 –1162, aug. 2007.

[94] B. Mao, B. Zhang, J. Wang, Y. Chen, X. Zheng, Y. Gao, B. Wu, and Y. Liu, "Dynamic modeling for distribution networks containing dispersed generations and energy storage devices," in *Power System Technology (POWERCON), 2010 International Conference on*, oct. 2010, pp. 1 –6.

[95] C.-L. Su, "Stochastic evaluation of voltages in distribution networks with distributed generation using detailed distribution operation models," *Power Systems, IEEE Transactions on*, vol. 25, no. 2, pp. 786 –795, may 2010.

[96] A. Ishchenko, A. Jokic, J. Myrzik, and W. Kling, "Dynamic reduction of distribution networks with dispersed generation," in *Future Power Systems, 2005 International Conference on*, nov. 2005, pp. 7 pp. –7.

[97] K. Rogers, R. Klump, H. Khurana, A. Aquino-Lugo, and T. Overbye, "An authenticated control framework for distributed voltage support on the smart grid," *Smart Grid, IEEE Transactions on*, vol. 1, no. 1, pp. 40 –47, june 2010.

[98] J. Momoh, "Smart grid design for efficient and flexible power networks operation and control," in *Power Systems Conference and Exposition, 2009. PSCE '09. IEEE/PES*, march 2009, pp. 1 –8.

[99] A. Monticelli, *State Estimation in Electric Power Systems.* Springer, 2000.

[100] E. Blood, B. Krogh, and M. Ilic, "Electric power system static state estimation through kalman filtering and load forecasting," in *Power and Energy Society General Meeting - Conversion and Delivery of Electrical Energy in the 21st Century, 2008 IEEE*, july 2008, pp. 1 –6.

[101] G. Valverde and V. Terzija, "Unscented kalman filter for power system dynamic state estimation," *Generation, Transmission Distribution, IET*, vol. 5, no. 1, pp. 29 –37, jan. 2011.

[102] I. Dzafic, S. Henselmeyer, and H.-T. Neisius, "High performance state estimation for smart grid distribution network operation," in *Innovative Smart Grid Technologies (ISGT), 2011 IEEE PES*, jan. 2011, pp. 1 –6.

[103] P. Du, Z. Huang, Y. Sun, R. Diao, K. Kalsi, K. Anderson, Y. Li, and B. Lee, "Distributed dynamic state estimation with extended kalman filter," in *North American Power Symposium (NAPS), 2011*, aug. 2011, pp. 1 –6.

[104] A. Aquino-Lugo, R. Klump, and T. Overbye, "A Control Framework for the Smart Grid for Voltage Support Using Agent-Based Technologies," *IEEE Transactions on Smart Grid*, vol. 2, pp. 173–180, Mar 2011.

[105] H. Li, F. Li, Y. Xu, D. Rizy, and J. Kueck, "Dynamic voltage regulation using distributed energy resources," in *19th International Conference on Electricity Distribution, CIRED, Vienna*, May 2007.

[106] M. Triggianese, J. Morren, S. de Haan, and P. Marino, "Improved and extended DG capability in voltage regulation by reactive and active power," in *International Conference on Power Engineering, Energy and Electrical Drives,POWERENG 2007*, April 2007, pp. 583–588.

[107] P. Hrisheekesha and J. Sharma, "Evolutionary Algorithm Based Optimal Control Distribution System Dispersed Generation," *International Journal of Computer Applications*, pp. 31–37, Feb 2010.

[108] T. Niknam, "A new approach based on ant colony optimization for daily Volt/Var control in distribution networks considering distributed generators," *International Journal of Computer Applications*, vol. 49, pp. 3417 – 3424, 2008.

[109] F. Viawan and D. Karlsson, "Coordinated voltage and reactive power control in the presence of distributed generation," in *Power and Energy Society General Meeting - Conversion and Delivery of Electrical Energy in the 21st Century, 2008 IEEE*, july 2008, pp. 1 –6.

[110] K. Rogers, R. Klump, H. Khurana, A. Aquino-Lugo, and T. Overbye, "An Authenticated Control Framework for Distributed Voltage Support on the Smart Grid ," *IEEE Transactions on Smart Grid*, vol. 1, pp. 40–47, June 2010.

[111] S. Deshmukh, B. Natarajan, and A. Pahwa, "Voltage/var control in distribution network via reactive power injection through distributed generators," *Smart Grid, IEEE Transactions on*, (in press).

[112] P. Bacher, H. Madsen, and H. A. Nielsen, "Online short-term solar power forecasting," *Solar Energy*, vol. 83, no. 10, pp. 1772 – 1783, 2009.

[113] P. Ailliot, V. Monbet, and M. Prevosto, "An autoregressive model with time-varying coefficients for wind fields," 2005.

[114] Z. Jin, C.-K. Ko, and R. Murray, "Estimation for nonlinear dynamical systems over packet-dropping networks," in *American Control Conference, 2007. ACC '07*, july 2007, pp. 5037 –5042.

[115] S. Kluge, K. Reif, and M. Brokate, "Stochastic stability of the extended kalman filter with intermittent observations," *Automatic Control, IEEE Transactions on*, vol. 55, no. 2, pp. 514 –518, feb. 2010.

[116] Z. Li, Y. Zhu, H. Zhu, and M. Li, "Compressive sensing approach to urban traffic sensing," in *Distributed Computing Systems (ICDCS), 2011 31st International Conference on*, 2011, pp. 889–898.

[117] L. Mathelin, L. Pastur, and O. Le Matre, "A compressed-sensing approach for closed-loop optimal control of nonlinear systems," *Theoretical and Computational Fluid Dynamics*, vol. 26, no. 1-4, pp. 319–337, 2012.

[118] D. Kanevsky, A. Carmi, L. Horesh, P. Gurfil, B. Ramabhadran, and T. Sainath, "Kalman filtering for compressed sensing," in *Information Fusion (FUSION), 2010 13th Conference on*, 2010, pp. 1–8.

[119] S. Yuksel and T. Basar, "State estimation and control for linear systems over communication networks," in *Control Applications, 2003. CCA 2003. Proceedings of 2003 IEEE Conference on*, vol. 1, 2003, pp. 409–414 vol.1.

[120] V. Gupta, "On effect of communication delay and packet reordering on estimation and control."

[121] J. Baras, X. Tan, and W. Xi, "Jointly optimal quantization, estimation, and control of hidden markov chains," in *Decision and Control, 2003. Proceedings. 42nd IEEE Conference on*, vol. 1, 2003, pp. 1098–1103 Vol.1.

[122] R. Olfati-Saber and P. Jalalkamali, "Coupled distributed estimation and control for mobile sensor networks," *Automatic Control, IEEE Transactions on*, vol. 57, no. 10, pp. 2609–2614, 2012.

[123] P. Yang, R. Freeman, G. Gordon, K. Lynch, S. Srinivasa, and R. Sukthankar, "Decentralized estimation and control of graph connectivity in mobile sensor networks," in *American Control Conference, 2008*, 2008, pp. 2678–2683.

Appendix A

Proofs of Chapter 3

A.1 Proof of lemma 3.1

Consider two matrices $\mathbf{X}, \mathbf{Y} \succeq \mathbf{0}$ and let $\mathbf{Z} = \alpha\mathbf{X} + (1-\beta)\mathbf{Y}$, where $\beta \in [0,1]$, then

$$\begin{aligned}
\mathbf{g}_\alpha(\mathbf{Z}) &= \phi(\mathcal{K}_{\mathbf{Z},1}, \cdots, \mathcal{K}_{\mathbf{Z},2^k-1}, \mathbf{Z}) = \phi(\mathcal{K}_{\mathbf{Z},1}, \cdots, \mathcal{K}_{\mathbf{Z},2^k-1}, \beta\mathbf{X} + (1-\beta)\mathbf{Y}) \\
&=^{(a)} \beta\phi(\mathcal{K}_{\mathbf{Z},1}, \cdots, \mathcal{K}_{\mathbf{Z},2^k-1}, \mathbf{X}) + (1-\beta)\phi(\mathcal{K}_{\mathbf{Z},\mathbf{1}}, \cdots, \mathcal{K}_{\mathbf{Z},2^k-1}, \mathbf{Y}) \\
&\succeq^{(b)} \beta\phi(\mathcal{K}_{\mathbf{X},1}, \cdots, \mathcal{K}_{\mathbf{X},2^k-1}, \mathbf{X}) + (1-\beta)\phi(\mathcal{K}_{\mathbf{Y},1}, \cdots, \mathcal{K}_{\mathbf{Y},2^k-1}, \mathbf{Y}) \\
&= \beta\mathbf{g}_\alpha(\mathbf{X}) + (1-\beta)\mathbf{g}_\alpha(\mathbf{Y})
\end{aligned}$$

where, (a) follows due to auxiliary function $\phi(\mathcal{K}_{\mathbf{X},1}, \cdots, \mathcal{K}_{\mathbf{X},2^k-1}, \mathbf{X})$ being affine in $\mathbf{X}$, and (b) is due to equation (3.10). Thus, $\mathbf{g}_\alpha(\mathbf{X})$ is a concave function of $\mathbf{X} \succeq \mathbf{0}$.

A.2 Proof of lemma 3.2

Consider two matrices such that $\mathbf{0} \preceq \mathbf{X} \preceq \mathbf{Y}$, then $\mathbf{g}_\alpha(\mathbf{X}) = \phi(\mathcal{K}_{\mathbf{X},1}, \cdots, \mathcal{K}_{\mathbf{X},2^k-1}, \mathbf{X}) \preceq \phi(\mathcal{K}_{\mathbf{Y},1}, \cdots, \mathcal{K}_{\mathbf{Y},2^k-1}, \mathbf{X}) \preceq \phi(\mathcal{K}_{\mathbf{Y},1}, \cdots, \mathcal{K}_{\mathbf{Y},2^k-1}, \mathbf{Y}) = \mathbf{g}_\alpha(\mathbf{Y})$ where, first inequality is due to equation (3.10) and second inequality is due to quadratic form of auxiliary function $\phi(\mathcal{K}_{\mathbf{X},1}, \cdots, \mathcal{K}_{\mathbf{X},2^k-1}, \mathbf{X})$ with $\mathbf{X} \succeq \mathbf{0}$. Thus, $\mathbf{g}_\alpha(\mathbf{X})$ is monotonously nondecreasing function of $\mathbf{X} \succeq \mathbf{0}$.

A.3 Proof of lemma 3.3

Here, we prove lemma 3.3 for control solution implementation via two actuators, and then extend it for generality. let fix λ_2 then,

$$\begin{aligned}
\mathbf{g}_{\lambda_1^1\lambda_2}(\mathbf{X}) &= -(\lambda_1^1-\lambda_1^2)\lambda_2\left(\mathbf{AXC}'\left(\mathbf{CXC}'+\mathbf{R}\right)^{-1}\mathbf{CXA}'\right) \\
&\quad (\lambda_1^1-\lambda_1^2)\left(\mathbf{AXC}_1'\left(\mathbf{C}_1\mathbf{XC}_1'+\mathbf{R}_{11}\right)^{-1}\mathbf{C}_1\mathbf{XA}'\right) \\
&\quad +\lambda_2(\lambda_1^1-\lambda_1^1)\left(\mathbf{AXC}_2'\left(\mathbf{C}_2\mathbf{XC}_2'+\mathbf{R}_{22}\right)^{-1}\mathbf{C}_2\mathbf{XA}'\right) \\
&= (\lambda_1^2-\lambda_1^1)\lambda_2\left[\mathbf{AXC}'\left(\mathbf{CXC}'+\mathbf{R}\right)^{-1}\mathbf{CXA}'\right. \\
&\quad \left.-\mathbf{AXC}_1'\left(\mathbf{C}_1\mathbf{XC}_1'+\mathbf{R}_{11}\right)^{-1}\mathbf{C}_1\mathbf{XA}'\right] \\
&\quad +(\lambda_1^2-\lambda_1^2)(1-\lambda_2)\left(\mathbf{AXC}_2'\left(\mathbf{C}_2\mathbf{XC}_2'+\mathbf{R}_{22}\right)^{-1}\mathbf{C}_2\mathbf{XA}'\right)
\end{aligned}$$

Now, given $\lambda_1^1 \leq \lambda_1^2$, we have $(\lambda_1^2-\lambda_1^1)(1-\lambda_2)(\mathbf{AXC}_2'\left(\mathbf{C}_2\mathbf{XC}_2'+\mathbf{R}_{22}\right)^{-1}\mathbf{C}_2\mathbf{XA}') \succeq \mathbf{0}$. Also,

$$\begin{aligned}
&\mathbf{AXC}'\left(\mathbf{CXC}'+\mathbf{R}\right)^{-1}\mathbf{CXA}'-\mathbf{AXC}_1'\left(\mathbf{C}_1\mathbf{XC}_1'+\mathbf{R}_{11}\right)^{-1}\mathbf{C}_1\mathbf{XA}' \\
&= \mathbf{AXC}'\left(\mathbf{CXC}'+\mathbf{R}\right)^{-1}\mathbf{CXA}'-\mathbf{AXC}'\left(\mathbf{CXC}+\tilde{\mathbf{R}}\right)^{-1}\mathbf{CXA}' \\
&= \mathbf{AXC}'\left[\left(\mathbf{CXC}+\mathbf{R}\right)^{-1}-\left(\mathbf{CXC}'+\tilde{\mathbf{R}}\right)^{-1}\right]\mathbf{CXA}'
\end{aligned}$$

where, $\tilde{\mathbf{R}} = \mathbf{R} + \begin{bmatrix}\mathbf{0} & \mathbf{0}\\ \mathbf{0} & \sigma^2\mathbf{I}\end{bmatrix}$ with $\sigma \to \infty$. Clearly,

$$\begin{aligned}
&\left(\mathbf{R}+\mathbf{CXC}'\right)^{-1} \succeq \left(\mathbf{CXC}'+\tilde{\mathbf{R}}\right)^{-1} \\
&\to \left(\mathbf{CXC}'+\mathbf{R}\right)^{-1} \succeq \left(\mathbf{CXC}'+\tilde{\mathbf{R}}\right)^{-1}
\end{aligned}$$

and equivalently,

$\mathbf{AXC}'\left[\left(\mathbf{CXC}+\mathbf{R}\right)^{-1}-\left(\mathbf{C}_1\mathbf{XC}_1'+\mathbf{R}_{11}\right)^{-1}\right]\mathbf{C}_1\mathbf{XA}' \succeq \mathbf{0}$.

Thus, $\mathbf{g}_{\lambda_1^1\lambda_2}(\mathbf{X}) - \mathbf{g}_{\lambda_1^2\lambda_2}(\mathbf{X}) \succeq \mathbf{0}$, for $\lambda_1^1 \preceq \lambda_1^2$.

A.4 Proof of lemma 3.4

(1). Since, $\exists \mathcal{Y} \succeq \mathbf{0}$ such that $\mathcal{Y} \succ \mathcal{L}(\mathcal{Y})$ (by selecting proper λ for individual actuator communication links), we can select a scalar $0 \leq r < 1$ such that $\mathcal{L}(\mathcal{Y}) \prec r\mathcal{Y}$. Next, $\forall \mathcal{W} \succeq \mathbf{0}$, we can select $m \geq 0$ such that $\mathbf{0} \preceq \mathcal{W} \preceq mr\mathcal{Y}$. Further, $\mathcal{L}(\mathcal{Y})$ being monotonically nondecreasing linear function of $\mathcal{Y}$ we get, $\mathbf{0} \preceq \mathcal{L}(\mathcal{W}) \preceq \mathcal{L}(m\mathcal{Y}) = m\mathcal{L}(\mathcal{Y}) \preceq mr\mathcal{Y}$. After N iterations we get, $0 \preceq \mathcal{L}^N(\mathcal{W}) \preceq mr^N\mathcal{Y}$. As, $N \to \infty$, $r^N \to 0$, $\Rightarrow \mathcal{L}^N(\mathcal{W}) \to \mathbf{0}$ for any

$\mathcal{W} \succeq \mathbf{0}$.

$$\begin{aligned}\mathcal{Y}_N &= \mathcal{L}(\mathcal{Y}_{N-1}) + \mathcal{V} = \mathcal{L}^N(\mathcal{Y}_0) + \textstyle\sum_{t=0}^{N-1} \mathcal{L}^t(\mathcal{V}) \\ &\preceq m_0 r^N \mathcal{Y} + \textstyle\sum_{t=0}^{N-1} m_v r^N \mathcal{Y} = (m_0 r^N + m_v \frac{1-r^N}{1-r})\mathcal{Y} \\ &\preceq (m_0 + \frac{m_v}{1-r})\mathcal{Y}\end{aligned}$$

Thus, the recursion of $\mathcal{Y}_t$ is bounded.

A.5 Proof of lemma 3.5

Consider the matrices, $\bar{\mathbf{F}}_i = \mathbf{A} + \bar{\mathcal{K}}_1 \mathbf{C}$ and the auxiliary function $\mathcal{L}(\bar{\mathbf{P}}) = \alpha_0(\mathbf{A}\bar{\mathbf{P}}\mathbf{A}') + \sum_{k=1}^{2^k-1} \alpha_i(\bar{\mathbf{F}}_i \bar{\mathbf{P}} \bar{\mathbf{F}}_i')$. Notice that, $\bar{\mathbf{P}} \succ \phi(\bar{\mathcal{K}}_1, \cdots, \mathcal{K}_{2^k-1}, \bar{\mathbf{P}}) = \mathcal{L}(\bar{\mathbf{P}}) + \sum_{k=1}^{2^k-1} \bar{\mathcal{K}}_i \mathbf{R}_i \bar{\mathcal{K}}_i' \succeq \mathcal{L}(\bar{\mathbf{P}})$. Thus, by lemmas 3.4 and 3.1 we have,

$$\mathbf{P}_{t+1} = \mathbf{g}_\alpha(\mathbf{P}_t) \preceq \phi(\bar{\mathcal{K}}_1, \cdots, \bar{\mathcal{K}}_{2^k-1}, \mathbf{P}_t) = \mathcal{L}(\mathbf{P}_t) + \sum_{k=1}^{2^k-1} \bar{\mathcal{K}}_i \mathbf{R}_i \bar{\mathcal{K}}_i'$$

and we conclude that the sequence $\mathbf{P}_t$ is bounded.

A.6 Proof of theorem 3.1

Let MARE (4.12) be initialized at matrix $\mathbf{X}_0 \succeq \mathbf{0}$. Then, $\mathbf{X}_t = \mathbf{g}_\alpha^t(\mathbf{X}_0)$. Following the lemma 4.2, we deduce $\mathbf{X}_0 \preceq \mathbf{X}_1 \preceq \mathbf{X}_2 \cdots \mathbf{M}_{\mathbf{X}_0}$. Here we use lemma 4.6 to show that the trajectory converges and is bounded, i.e. $lim_{t\to\infty} \mathbf{X}_t = \bar{\mathbf{X}}$. We also notice that, $\bar{\mathbf{X}}$ is a fixed point in MARE iteration and is solution of MARE at steady state.

Next we show that MARE initialized at $\mathbf{Y}_0 \succeq \bar{\mathbf{X}}$ also converges, and also to same limit $\bar{\mathbf{X}}$. Let,

$$\begin{aligned}&\bar{\mathcal{K}}_i = -\mathbf{A}\bar{\mathbf{X}}\mathbf{H}_i'(\mathbf{H}_i \bar{\mathbf{X}} \mathbf{H}_i' + \mathbf{R}_i)^{-1} \;\&\; \bar{\mathbf{F}}_i = \mathbf{A} + \bar{\mathcal{K}}_i \mathbf{H}_i \\ &\hat{\mathcal{L}}(\mathbf{Y}) = \alpha_0(\mathbf{A}\mathbf{Y}\mathbf{A}') + \textstyle\sum_{k=1}^{2^k-1} \bar{\mathbf{F}}_i \mathbf{Y} \bar{\mathbf{F}}_i'\end{aligned}$$

Observe that, $\bar{\mathbf{X}} = \mathbf{g}_\alpha(\bar{\mathbf{X}}) = \mathcal{L}(\bar{\mathbf{X}}) + \sum_{k=1}^{2^k-1} \bar{\mathcal{K}}_i \mathbf{R}_i \bar{\mathcal{K}}_i' \succ \hat{\mathcal{L}}(\bar{\mathbf{X}})$. Thus, $\hat{\mathcal{L}}$ meets condition of lemma 3.4, i.e. $lim_{t\to\infty} \hat{\mathcal{L}}^t(\mathbf{Y}) = \mathbf{0}$. Now suppose, $\mathbf{Y}_0 \succeq \bar{\mathbf{X}}$, then $\mathbf{Y}_t = \mathbf{g}_\alpha^t(\mathbf{Y}_0) \succeq \bar{\mathbf{X}}\ \forall\ t$ as

$\mathbf{g}_\alpha(.)$ is non decreasing function. Additionally, we can notice $\mathbf{0} \preceq$

$$\begin{aligned}(\mathbf{Y}_{t+1}-\bar{\mathbf{X}}) &= \mathbf{g}_\alpha(\mathbf{Y}_t)-\mathbf{g}_\alpha(\bar{\mathbf{X}}) = \phi(\mathcal{K}_{\mathbf{Y}_t,1},\cdots,\mathcal{K}_{\mathbf{Y}_t,2^k-1},\mathbf{Y}_t)\\ &-\phi(\mathcal{K}_{\bar{\mathbf{X}},1},\cdots,\mathcal{K}_{\bar{\mathbf{X}},2^k-1},\bar{\mathbf{X}})\\ &\preceq \phi(\mathcal{K}_{\bar{\mathbf{X}},1},\cdots,\mathcal{K}_{\bar{\mathbf{X}},2^k-1},\mathbf{Y}_t)-\phi(\mathcal{K}_{\bar{\mathbf{X}},1},\cdots,\mathcal{K}_{\bar{\mathbf{X}},2^k-1},\bar{\mathbf{X}})\\ &= \alpha_0\mathbf{A}(\mathbf{Y}_t-\bar{\mathbf{X}})\mathbf{A}'+\sum_{i=1}^{2^k-1}\mathbf{F}_{\bar{\mathbf{X}},i}(\mathbf{Y}_t-\bar{\mathbf{X}})\mathbf{F}'_{\bar{\mathbf{X}},i}\\ &= \hat{\mathcal{L}}(\mathbf{Y}_t-\bar{\mathbf{X}})\end{aligned}$$

Thus, $\mathbf{0} \preceq \lim_{t\to\infty}(\mathbf{Y}_t-\bar{\mathbf{X}}) \to \mathbf{0}$, proving the unique convergence to $\bar{\mathbf{X}}$.

A.7 Proof of theorem 3.2

Let all sensor probabilities be set at $\{\lambda_1^c,\cdots,\lambda_k^c\}$ except for sensor j, such that $\mathbf{X} = g_\alpha(\mathbf{X})$ is unbounded when $\lambda_j = 0$ and bounded when $\lambda_j = 1$. Since, g_α is monotonically nondecreasing function in λ_j (Lemma 4.3), one can choose $\lambda_j^c = \{inf.\lambda_j^* : \lambda_j > \lambda_j^*\} \Rightarrow \mathbb{E}[\mathbf{P}_t]$ is bounded $\forall \mathbf{P}_0 \succeq 0$.

A.8 Proof of lemma 3.6

$\mathbf{X} \succeq \mathbf{0} \Rightarrow \mathbf{F}_i\mathbf{X}\mathbf{F}'_i \succeq \mathbf{0}$; Similarly, $\mathbf{R} \succeq \mathbf{0} \Rightarrow \mathcal{K}_i\mathbf{R}\mathcal{K}'_i \succeq \mathbf{0}$, $\forall i = 1,\cdots,2^k-1$. Thus,
$\mathbf{g}_\alpha(\mathbf{X}) = \phi(\mathcal{K}_{X,1},\cdots,\mathcal{K}_{X,2^k-1},\mathbf{X}) \succeq \alpha_0\mathbf{A}\mathbf{X}\mathbf{A}'+\sum_{i=1}^{2^k-2}\alpha_i\mathbf{A}'\mathbf{X}\mathcal{F}(\mathbf{H}_i,\mathbf{G}_i,\mathbf{X})\mathbf{X}\mathbf{A}$.

A.9 Proof of lemma 3.7

Taking expectation over both sides of (3.21) and following Lemma 3.1, we can get (3.22).

Appendix B

Proofs of Chapter 4

B.1 Proof of lemma 4.1

Consider two matrices $\mathbf{X}, \mathbf{Y} \succeq \mathbf{0}$ and let $\mathbf{Z} = \alpha\mathbf{X} + (1-\beta)\mathbf{Y}$, where $\beta \in [0,1]$, then

$$\begin{aligned}
\mathbf{g}_\alpha(\mathbf{Z}) &= \phi(\mathcal{K}_{\mathbf{Z},1}, \cdots, \mathcal{K}_{\mathbf{Z},2^k-1}, \mathbf{Z}) = \phi(\mathcal{K}_{\mathbf{Z},1}, \cdots, \mathcal{K}_{\mathbf{Z},2^k-1}, \beta\mathbf{X} + (1-\beta)\mathbf{Y}) \\
&=^{(a)} \beta\phi(\mathcal{K}_{\mathbf{Z},1}, \cdots, \mathcal{K}_{\mathbf{Z},2^k-1}, \mathbf{X}) + (1-\beta)\phi(\mathcal{K}_{\mathbf{Z},\mathbf{1}}, \cdots, \mathcal{K}_{\mathbf{Z},2^k-1}, \mathbf{Y}) \\
&\succeq^{(b)} \beta\phi(\mathcal{K}_{\mathbf{X},1}, \cdots, \mathcal{K}_{\mathbf{X},2^k-1}, \mathbf{X}) + (1-\beta)\phi(\mathcal{K}_{\mathbf{Y},1}, \cdots, \mathcal{K}_{\mathbf{Y},2^k-1}, \mathbf{Y}) \\
&= \beta\mathbf{g}_\alpha(\mathbf{X}) + (1-\beta)\mathbf{g}_\alpha(\mathbf{Y})
\end{aligned}$$

where, (a) follows due to auxiliary function $\phi(\mathcal{K}_{\mathbf{X},1}, \cdots, \mathcal{K}_{\mathbf{X},2^k-1}, \mathbf{X})$ being affine in $\mathbf{X}$, and (b) is due to equation (4.14). Thus, $\mathbf{g}_\alpha(\mathbf{X})$ is a concave function of $\mathbf{X} \succeq \mathbf{0}$.

B.2 Proof of lemma 4.2

Consider two matrices such that $\mathbf{0} \preceq \mathbf{X} \preceq \mathbf{Y}$, then $\mathbf{g}_\alpha(\mathbf{X}) = \phi(\mathcal{K}_{\mathbf{X},1}, \cdots, \mathcal{K}_{\mathbf{X},2^k-1}, \mathbf{X}) \preceq \phi(\mathcal{K}_{\mathbf{Y},1}, \cdots, \mathcal{K}_{\mathbf{Y},2^k-1}, \mathbf{X}) \preceq \phi(\mathcal{K}_{\mathbf{Y},1}, \cdots, \mathcal{K}_{\mathbf{Y},2^k-1}, \mathbf{Y}) = \mathbf{g}_\alpha(\mathbf{Y})$ where, first inequality is due to equation (4.14) and second inequality is due to quadratic form of auxiliary function $\phi(\mathcal{K}_{\mathbf{X},1}, \cdots, \mathcal{K}_{\mathbf{X},2^k-1}, \mathbf{X})$ with $\mathbf{X} \succeq \mathbf{0}$. Thus, $\mathbf{g}_\alpha(\mathbf{X})$ is monotonously nondecreasing function of $\mathbf{X} \succeq \mathbf{0}$.

B.3 Proof of lemma 4.3

Here, we prove lemma 4.3 for control solution implementation via two actuators, and then extend it for generality. Firstly, notice that $\mathcal{F}_{\mathbf{H}_i,\mathbf{X}} := 2\mathbf{I} - \mathbf{H}_i'\mathbf{X}\mathbf{H}_i\left(\mathbf{R}_i + \mathbf{H}_i'\mathbf{X}\mathbf{H}_i\right)^{-1} \succeq \mathbf{0}$, $\Rightarrow$ $\mathbf{A}'\mathbf{X}\mathbf{H}_i\left(\mathbf{R}_i + \mathbf{H}_i'\mathbf{X}\mathbf{H}_i\right)^{-1}\mathcal{F}_{\mathbf{H}_i,\mathbf{X}}\mathbf{H}_i'\mathbf{X}\mathbf{A} \succeq \mathbf{0}$. Next, let fix λ_2 then,

$$\begin{aligned}
\mathbf{g}_{\lambda_1^1\lambda_2}(\mathbf{X}) &= -(\lambda_1^1-\lambda_1^2)\lambda_2\left(\mathbf{A}'\mathbf{X}\mathbf{B}\left(\mathbf{R}+\mathbf{B}'\mathbf{X}\mathbf{B}\right)^{-1}\mathcal{F}_{\mathbf{B},\mathbf{X}}\mathbf{B}'\mathbf{X}\mathbf{A}\right)\\
&\quad(\lambda_1^1-\lambda_1^2)\left(\mathbf{A}'\mathbf{X}\mathbf{B}_1\left(\mathbf{R}_{11}+\mathbf{B}_1'\mathbf{X}\mathbf{B}_1\right)^{-1}\mathcal{F}_{\mathbf{B}_1,\mathbf{X}}\mathbf{B}_1'\mathbf{X}\mathbf{A}\right)\\
&\quad+\lambda_2(\lambda_1^1-\lambda_1^1)\left(\mathbf{A}'\mathbf{X}\mathbf{B}_2\left(\mathbf{R}_{22}+\mathbf{B}_2'\mathbf{X}\mathbf{B}_2\right)^{-1}\mathcal{F}_{\mathbf{B}_2,\mathbf{X}}\mathbf{B}_2'\mathbf{X}\mathbf{A}\right)\\
&= (\lambda_1^2-\lambda_1^1)\lambda_2\left[\mathbf{A}'\mathbf{X}\mathbf{B}\left(\mathbf{R}+\mathbf{B}'\mathbf{X}\mathbf{B}\right)^{-1}\mathcal{F}_{\mathbf{B},\mathbf{X}}\mathbf{B}'\mathbf{X}\mathbf{A}\right.\\
&\quad\left.-\mathbf{A}'\mathbf{X}\mathbf{B}_1\left(\mathbf{R}_{11}+\mathbf{B}_1'\mathbf{X}\mathbf{B}_1\right)^{-1}\mathcal{F}_{\mathbf{B}_1,\mathbf{X}}\mathbf{B}_1'\mathbf{X}\mathbf{A}\right]\\
&\quad+(\lambda_1^2-\lambda_1^2)(1-\lambda_2)\left(\mathbf{A}'\mathbf{X}\mathbf{B}_2\left(\mathbf{R}_{22}+\mathbf{B}_2'\mathbf{X}\mathbf{B}_2\right)^{-1}\mathcal{F}_{\mathbf{B}_2,\mathbf{X}}\mathbf{B}_2'\mathbf{X}\mathbf{A}\right)
\end{aligned}$$

Now, given $\lambda_1^1 \leq \lambda_1^2$, we have $(\lambda_1^2-\lambda_1^1)(1-\lambda_2)(\mathbf{A}'\mathbf{X}\mathbf{B}_2\left(\mathbf{R}_{22}+\mathbf{B}_2'\mathbf{X}\mathbf{B}_2\right)^{-1}\mathcal{F}_{\mathbf{B}_2,\mathbf{X}}\mathbf{B}_2'\mathbf{X}\mathbf{A}) \succeq \mathbf{0}$. Also,

$$\begin{aligned}
&\mathbf{A}'\mathbf{X}\mathbf{B}\left(\mathbf{R}+\mathbf{B}'\mathbf{X}\mathbf{B}\right)^{-1}\mathcal{F}_{\mathbf{B},\mathbf{X}}\mathbf{B}'\mathbf{X}\mathbf{A} - \mathbf{A}'\mathbf{X}\mathbf{B}_1\left(\mathbf{R}_{11}+\mathbf{B}_1'\mathbf{X}\mathbf{B}_1\right)^{-1}\mathcal{F}_{\mathbf{B}_1,\mathbf{X}}\mathbf{B}_1'\mathbf{X}\mathbf{A}\\
&= \mathbf{A}'\mathbf{X}\mathbf{B}\left(\mathbf{R}+\mathbf{B}'\mathbf{X}\mathbf{B}\right)^{-1}\mathcal{F}_{\mathbf{B},\mathbf{X}}\mathbf{B}'\mathbf{X}\mathbf{A} - \mathbf{A}'\mathbf{X}\mathbf{B}\left(\tilde{\mathbf{R}}+\mathbf{B}'\mathbf{X}\mathbf{B}\right)^{-1}\mathcal{F}_{\mathbf{B},\mathbf{X}}\mathbf{B}'\mathbf{X}\mathbf{A}\\
&= \mathbf{A}'\mathbf{X}\mathbf{B}\left[\left(\mathbf{R}+\mathbf{B}'\mathbf{X}\mathbf{B}\right)^{-1}\mathcal{F}_{\mathbf{B},\mathbf{X}} - \left(\tilde{\mathbf{R}}+\mathbf{B}'\mathbf{X}\mathbf{B}\right)^{-1}\mathcal{F}_{\mathbf{B},\mathbf{X}}\right]\mathbf{B}'\mathbf{X}\mathbf{A}
\end{aligned}$$

where, $\tilde{\mathbf{R}} = \mathbf{R} + \begin{bmatrix}\mathbf{0} & \mathbf{0}\\ \mathbf{0} & \sigma^2\mathbf{I}\end{bmatrix}$ with $\sigma \to \infty$. Clearly,

$$\begin{aligned}
&\left(\mathbf{R}+\mathbf{B}'\mathbf{X}\mathbf{B}\right)^{-1} \succeq \left(\tilde{\mathbf{R}}+\mathbf{B}'\mathbf{X}\mathbf{B}\right)^{-1}\\
&\to \left(\mathbf{R}+\mathbf{B}'\mathbf{X}\mathbf{B}\right)^{-1}\mathcal{F}_{\mathbf{B},\mathbf{X}} \succeq \left(\tilde{\mathbf{R}}+\mathbf{B}'\mathbf{X}\mathbf{B}\right)^{-1}\mathcal{F}_{\mathbf{B},\mathbf{X}}
\end{aligned}$$

and equivalently,

$\mathbf{A}'\mathbf{X}\mathbf{B}\left[\left(\mathbf{R}+\mathbf{B}'\mathbf{X}\mathbf{B}\right)^{-1}\mathcal{F}_{\mathbf{B},\mathbf{X}} - \left(\mathbf{R}_{11}+\mathbf{B}_1'\mathbf{X}\mathbf{B}_1\right)^{-1}\mathcal{F}_{\mathbf{B}_1,\mathbf{X}}\right]\mathbf{B}_1'\mathbf{X}\mathbf{A} \succeq \mathbf{0}$.

Thus, $\mathbf{g}_{\lambda_1^1\lambda_2}(\mathbf{X}) - \mathbf{g}_{\lambda_1^2\lambda_2}(\mathbf{X}) \succeq \mathbf{0}$, for $\lambda_1^1 \preceq \lambda_1^2$.

B.4 Proof of lemma 4.4

$\mathbf{X} \succeq \mathbf{0} \Rightarrow \mathbf{F}_i'\mathbf{X}\mathbf{F}_i \succeq \mathbf{0}$; Similarly, $\mathbf{R} \succeq \mathbf{0} \Rightarrow \mathcal{K}_i\mathbf{R}\mathcal{K}_i' \succeq \mathbf{0}$. Thus, $\mathbf{g}_\alpha(\mathbf{X}) = \phi(\mathcal{K}_{X,1}, \cdots, \mathcal{K}_{X,2^k-1}, \mathbf{X}) \succeq \alpha_0\mathbf{A}'\mathbf{X}\mathbf{A} + \sum_{i=1}^{2^k-2}\alpha_i\mathbf{A}'\mathbf{X}\mathcal{Z}\left(\mathbf{H}_i, \mathbf{G}_i, \mathbf{X}\right)\mathbf{X}\mathbf{A}$.

B.5 Proof of lemma 4.5

Taking expectation over both sides of (4.18) and following Lemma 4.1, we can get (4.19).

B.6 Proof of lemma 4.6

(1). Since, $\exists \mathcal{Y} \succeq \mathbf{0}$ such that $\mathcal{Y} \succ \mathcal{L}(\mathcal{Y})$ (by selecting proper λ for individual actuator communication links), we can select a scalar $0 \leq r < 1$ such that $\mathcal{L}(\mathcal{Y}) \prec r\mathcal{Y}$. Next, $\forall \mathcal{W} \succeq \mathbf{0}$, we can select $m \geq 0$ such that $\mathbf{0} \preceq \mathcal{W} \preceq mr\mathcal{Y}$. Further, $\mathcal{L}(\mathcal{Y})$ being monotonically nondecreasing linear function of $\mathcal{Y}$ we get, $\mathbf{0} \preceq \mathcal{L}(\mathcal{W}) \preceq \mathcal{L}(m\mathcal{Y}) = m\mathcal{L}(\mathcal{Y}) \preceq mr\mathcal{Y}$. After N iterations we get, $0 \preceq \mathcal{L}^N(\mathcal{W}) \preceq mr^N\mathcal{Y}$. As, $N \to \infty$, $r^N \to 0$, $\Rightarrow \mathcal{L}^N(\mathcal{W}) \to \mathbf{0}$ for any $\mathcal{W} \succeq \mathbf{0}$.

$$\begin{aligned}\mathcal{Y}_N &= \mathcal{L}(\mathcal{Y}_{N-1}) + \mathcal{V} = \mathcal{L}^N(\mathcal{Y}_0) + \textstyle\sum_{t=0}^{N-1} \mathcal{L}^t(\mathcal{V}) \\ &\preceq m_0 r^N \mathcal{Y} + \textstyle\sum_{t=0}^{N-1} m_v r^N \mathcal{Y} = (m_0 r^N + m_v \frac{1-r^N}{1-r})\mathcal{Y} \\ &\preceq (m_0 + \frac{m_v}{1-r})\mathcal{Y}\end{aligned}$$

Thus, the recursion of $\mathcal{Y}_t$ is bounded.

B.7 Proof of lemma 4.7

Consider the matrices, $\bar{\mathbf{F}}_i = \mathbf{A} + \mathbf{B}\bar{\mathcal{K}}_1'$ and the auxiliary function $\mathcal{L}(\bar{\mathbf{P}}) = \alpha_0(\mathbf{A}'\bar{\mathbf{P}}\mathbf{A}) + \sum_{k=1}^{2^k-1} \alpha_i(\bar{\mathbf{F}}_i'\bar{\mathbf{P}}\bar{\mathbf{F}}_i)$. Notice that, $\bar{\mathbf{P}} \succ \phi(\bar{\mathcal{K}}_1, \cdots, \mathcal{K}_{2^k-1}, \bar{\mathbf{P}}) = \mathcal{L}(\bar{\mathbf{P}}) + \sum_{k=1}^{2^k-1} \bar{\mathcal{K}}_i \mathbf{R}_i \bar{\mathcal{K}}_i' \succeq \mathcal{L}(\bar{\mathbf{P}})$. Thus, by lemmas 4.6 and 4.1 we have,

$$\mathbf{P}_{t+1} = \mathbf{g}_\alpha(\mathbf{P}_t) \preceq \phi(\bar{\mathcal{K}}_1, \cdots, \bar{\mathcal{K}}_{2^k-1}, \mathbf{P}_t) = \mathcal{L}(\mathbf{P}_t) + \sum_{k=1}^{2^k-1} \bar{\mathcal{K}}_i \mathbf{R}_i \bar{\mathcal{K}}_i'$$

and we conclude that the sequence $\mathbf{P}_t$ is bounded.

B.8 Proof of theorem 4.1

Let MARE (4.12) be initialized at matrix $\mathbf{X}_0 \succeq \mathbf{0}$. Then, $\mathbf{X}_t = \mathbf{g}_\alpha^t(\mathbf{X}_0)$. Following the lemma 4.2, we deduce $\mathbf{X}_0 \preceq \mathbf{X}_1 \preceq \mathbf{X}_2 \cdots \mathbf{M}_{\mathbf{X}_0}$. Here we use lemma 4.6 to show that the trajectory converges and is bounded, i.e. $lim_{t\to\infty}\mathbf{X}_t = \bar{\mathbf{X}}$. We also notice that, $\bar{\mathbf{X}}$ is a fixed point in MARE iteration and is solution of MARE at steady state.

Next we show that MARE initialized at $\mathbf{Y}_0 \succeq \bar{\mathbf{X}}$ also converges, and also to same limit $\bar{\mathbf{X}}$. Let,

$$\bar{\mathcal{K}}_i = -\mathbf{A}'\bar{\mathbf{X}}\mathbf{H}_i(\mathbf{R}_i + \mathbf{H}_i'\bar{\mathbf{X}}\mathbf{H}_i)^{-1} \;\&\; \bar{\mathbf{F}}_i = \mathbf{A} + \mathbf{H}_i\bar{\mathcal{K}}_i'$$
$$\hat{\mathcal{L}}(\mathbf{Y}) = \alpha_0(\mathbf{A}'\mathbf{Y}\mathbf{A}) + \sum_{k=1}^{2^k-1}\bar{\mathbf{F}}_i'\mathbf{Y}\bar{\mathbf{F}}_i$$

Observe that, $\bar{\mathbf{X}} = \mathbf{g}_\alpha(\bar{\mathbf{X}}) = \mathcal{L}(\bar{\mathbf{X}}) + \sum_{k=1}^{2^k-1}\bar{\mathcal{K}}_i\mathbf{R}_i\bar{\mathcal{K}}_i' \succ \hat{\mathcal{L}}(\bar{\mathbf{X}})$. Thus, $\hat{\mathcal{L}}$ meets condition of lemma 4.6, i.e. $lim_{t\to\infty}\hat{\mathcal{L}}^t(\mathbf{Y}) = \mathbf{0}$. Now suppose, $\mathbf{Y}_0 \succeq \bar{\mathbf{X}}$, then $\mathbf{Y}_t = \mathbf{g}_\alpha^t(\mathbf{Y}_0) \succeq \bar{\mathbf{X}}\ \forall\ t$ as $\mathbf{g}_\alpha(.)$ is non decreasing function. Additionally, we can notice $\mathbf{0} \preceq$

$$\begin{aligned}
(\mathbf{Y}_{t+1} - \bar{\mathbf{X}}) \quad &= \mathbf{g}_\alpha(\mathbf{Y}_t) - \mathbf{g}_\alpha(\bar{\mathbf{X}}) = \phi(\mathcal{K}_{\mathbf{Y}_t,1}, \cdots, \mathcal{K}_{\mathbf{Y}_t,2^k-1}, \mathbf{Y}_t) \\
&-\phi(\mathcal{K}_{\bar{\mathbf{X}},1}, \cdots, \mathcal{K}_{\bar{\mathbf{X}},2^k-1}, \bar{\mathbf{X}}) \\
&\preceq \phi(\mathcal{K}_{\bar{\mathbf{X}},1}, \cdots, \mathcal{K}_{\bar{\mathbf{X}},2^k-1}, \mathbf{Y}_t) - \phi(\mathcal{K}_{\bar{\mathbf{X}},1}, \cdots, \mathcal{K}_{\bar{\mathbf{X}},2^k-1}, \bar{\mathbf{X}}) \\
&= \alpha_0\mathbf{A}'(\mathbf{Y}_t - \bar{\mathbf{X}})\mathbf{A} + \sum_{i=1}^{2^k-1}\mathbf{F}'_{\bar{\mathbf{X}},i}(\mathbf{Y}_t - \bar{\mathbf{X}})\mathbf{F}_{\bar{\mathbf{X}},i} \\
&= \hat{\mathcal{L}}(\mathbf{Y}_t - \bar{\mathbf{X}})
\end{aligned}$$

Thus, $\mathbf{0} \preceq \lim_{t\to\infty}(\mathbf{Y}_t - \bar{\mathbf{X}}) \to \mathbf{0}$, proving the unique convergence to $\bar{\mathbf{X}}$.

B.9 Proof of theorem 4.2

Let all actuator probabilities be set at $\{\lambda_1^c, \cdots, \lambda_k^c\}$ except for actuator j, such that $\mathbf{X} = g_\alpha(\mathbf{X})$ is unbounded when $\lambda_j = 0$ and bounded when $\lambda_j = 1$. Since, g_α is monotonically nondecreasing function in λ_j (Lemma 4.3), one can choose $\lambda_j^c = \{inf.\lambda_j^* : \lambda_j > \lambda_j^*\} \Rightarrow \mathbb{E}[\mathbf{P}_t]$ is bounded $\forall \mathbf{P}_0 \succeq 0$.

B.10 Derivation of equation (4.15)

Let $\mathbf{B} = \begin{bmatrix} H & G \end{bmatrix}$, then $\mathbf{B}(\mathbf{R} + \mathbf{B}'\mathbf{X}\mathbf{B})^{-1}$ can be expanded as,

$$\begin{aligned}
&= \begin{bmatrix} H & G \end{bmatrix}\left(\begin{bmatrix} \mathbf{R}_H & \mathbf{R}_{HG} \\ \mathbf{R}_{GH} & \mathbf{R}_G \end{bmatrix} + \begin{bmatrix} \mathbf{H}' \\ \mathbf{G}' \end{bmatrix}\mathbf{X}\begin{bmatrix} H & G \end{bmatrix}\right)^{-1} \\
&= \begin{bmatrix} \mathbf{H}A + \mathbf{G}C & \mathbf{H}B + \mathbf{G}D \end{bmatrix}
\end{aligned}$$

where, if $K = \mathbf{R}_H + \mathbf{H}'\mathbf{X}\mathbf{H}$; $L = \mathbf{R}_{HG} + \mathbf{H}'\mathbf{X}\mathbf{G}$; $M = \mathbf{R}_{GH} + \mathbf{G}'\mathbf{X}\mathbf{H}$; and $N = \mathbf{R}_G + \mathbf{G}'\mathbf{X}\mathbf{G}'$ then

$$
\begin{aligned}
A &= K^{-1} + K^{-1}L\left(N - MK^{-1}L\right)^{-1}MK^{-1} \\
B &= -K^{-1}L\left(N - MK^{-1}L\right)^{-1} \\
C &= -N^{-1}M\left(K - LN^{-1}M\right)^{-1} \\
D &= N^{-1} + N^{-1}M\left(K - LN^{-1}M\right)^{-1}LN^{-1}.
\end{aligned}
$$

Next, $\mathcal{F}(\mathbf{B},\mathbf{R},\mathbf{X}) \;=\; 2\mathbf{I} - \mathbf{B}'\mathbf{X}\mathbf{B}\left(\mathbf{R} + \mathbf{B}'\mathbf{X}\mathbf{B}\right)^{-1}$ is expressed as,

$$
\mathcal{F}(\mathbf{B},\mathbf{R},\mathbf{X}) = \begin{bmatrix} 2\mathbf{I} - \mathbf{H}'\mathbf{X}\mathbf{H}A - \mathbf{H}'\mathbf{X}\mathbf{G}C & -\mathbf{H}'\mathbf{X}\mathbf{H}B - \mathbf{H}'\mathbf{X}\mathbf{G}D \\ -\mathbf{G}'\mathbf{X}\mathbf{H}A - \mathbf{G}'\mathbf{X}\mathbf{G}C & 2\mathbf{I} - \mathbf{G}'\mathbf{X}\mathbf{H}B - \mathbf{G}'\mathbf{X}\mathbf{G}D \end{bmatrix}
$$

Similarly, $\mathbf{B}\left(\mathbf{R} + \mathbf{B}'\mathbf{X}\mathbf{B}\right)^{-1}\mathcal{F}(\mathbf{B},\mathbf{R},\mathbf{X})\mathbf{B}'$ is expressed as,

$$
\begin{aligned}
&\left(\mathbf{H}A + \mathbf{G}C\right)\left(2\mathbf{I} - \mathbf{H}'\mathbf{X}\mathbf{H}A - \mathbf{H}'\mathbf{X}\mathbf{G}C\right)\mathbf{H}' && (a) \\
&+\left(\mathbf{H}B + \mathbf{G}D\right)\left(-\mathbf{G}'\mathbf{X}\mathbf{H}A - \mathbf{G}'\mathbf{X}\mathbf{G}C\right)\mathbf{H}' && (b) \\
&+\left(\mathbf{H}A + \mathbf{G}C\right)\left(-\mathbf{H}'\mathbf{X}\mathbf{H}B - \mathbf{H}'\mathbf{X}\mathbf{G}D\right)\mathbf{G}' && (c) \\
&+\left(\mathbf{H}B\mathbf{G}D\right)\left(2\mathbf{I} - \mathbf{G}'\mathbf{X}\mathbf{H}B - \mathbf{G}'\mathbf{X}\mathbf{G}D\right)\mathbf{G}' && (d)
\end{aligned}
$$

Lastly, expanding part (a) and substituting expression of A and K we get,

$$
\begin{aligned}
&\mathbf{H}\left(\mathbf{R}_H + \mathbf{H}'\mathbf{X}\mathbf{H}\right)^{-1}\left(2\mathbf{I} - \mathbf{H}'\mathbf{X}\mathbf{H}\left(\mathbf{R}_H + \mathbf{H}'\mathbf{X}\mathbf{H}\right)^{-1}\right)\mathbf{H}' \\
&+\mathbf{H}K^{-1}L\left(N - MK^{-1}L\right)^{-1}MK^{-1}\left(2\mathbf{I} - \mathbf{H}'\mathbf{X}\mathbf{H}K^{-1}\right)\mathbf{H}' && (e) \\
&+\mathbf{H}K^{-1}\left(2\mathbf{I} - \mathbf{H}'\mathbf{X}\mathbf{H}K^{-1}L\left(N - MK^{-1}L\right)^{-1}MK^{-1}\right)\mathbf{H}' && (f)
\end{aligned} \tag{B.1}
$$

Thus, we can finally express

$$
\begin{aligned}
&\mathbf{H}\left(\mathbf{R}_H + \mathbf{H}'\mathbf{X}\mathbf{H}\right)^{-1}\left(2\mathbf{I} - \mathbf{H}'\mathbf{X}\mathbf{H}\left(\mathbf{R}_H + \mathbf{H}'\mathbf{X}\mathbf{H}\right)^{-1}\right)\mathbf{H}' = \\
&\mathbf{B}\left(\mathbf{R} + \mathbf{B}'\mathbf{X}\mathbf{B}\right)^{-1}\left(2\mathbf{I} - \mathbf{B}'\mathbf{X}\mathbf{B}\left(\mathbf{R} + \mathbf{B}'\mathbf{X}\mathbf{B}\right)^{-1}\right)\mathbf{B}' - \mathcal{Z}\left(\mathbf{H},\mathbf{G},\mathbf{X}\right)
\end{aligned} \tag{B.2}
$$

where, $\mathcal{Z}\left(\mathbf{H},\mathbf{G},\mathbf{X}\right) = (b) + (c) + (d) + (e) + (f)$.